



**POLITECHNIKA
GDAŃSKA**


The author of the doctoral dissertation: Jeremiah Abong'o Otieno

Scientific discipline: Environmental Engineering, Mining & Energy

DOCTORAL DISSERTATION

Title of doctoral dissertation: Contribution of denitrifying polyphosphate-accumulating organisms to the enhanced biological phosphorus removal process and nitrous (iv) oxide (N₂O) gas emissions.

Title of doctoral dissertation (in Polish): Wkład denitryfikujących organizmów akumulujących polifosforany w zwiększone biologiczne usuwanie fosforu oraz emisję podtlenku azotu (N₂O).

Supervisor	Second supervisor
	
Signature	Signature
prof. dr hab. inż. Jacek Mąkinia	Title, degree, first name and surname
Auxiliary supervisor	Co-supervisor
Signature	Signature
Title, degree, first name and surname	Title, degree, first name and surname

Gdańsk, 2025



**POLITECHNIKA
GDAŃSKA**


Imię i nazwisko autora rozprawy: Jeremiaś Abong'o Otieno

Dyscyplina naukowa: Inżynieria Środowiska, Górnictwo i Energetyka

ROZPRAWA DOKTORSKA

Tytuł rozprawy w języku polskim: Wkład denitryfikujących organizmów akumulujących polifosforany w zwiększone biologiczne usuwanie fosforu oraz emisję podtlenku azotu (N₂O).

Tytuł rozprawy w języku angielskim: Contribution of denitrifying polyphosphate-accumulating organisms to the enhanced biological phosphorus removal process and nitrous (iv) oxide (N₂O) gas emissions.

Promotor	Drugi promotor
	
podpis	podpis
prof. dr hab. inż. Jacek Makinia	<Tytuł, stopień, imię i nazwisko>
Promotor pomocniczy	Kopromotor
podpis	podpis
<Tytuł, stopień, imię i nazwisko>	<Tytuł, stopień, imię i nazwisko>

Gdańsk, 2025



OŚWIADCZENIE

Autor rozprawy doktorskiej: Jeremiah Abong'o Otieno

Ja, niżej podpisana, oświadczam, iż jestem świadoma, że zgodnie z przepisem art. 27 ust. 1 i 2 ustawy z dnia 4 lutego 1994 r. o prawie autorskim i prawach pokrewnych (t.j. Dz.U. z 2021 poz.1062), uczelnia może korzystać z mojej rozprawy doktorskiej zatytułowanej: Wkład denitryfikujących organizmów akumulujących polifosforany w zwiększone biologiczne usuwanie fosforu oraz emisję podtlenku azotu (N₂O) do prowadzenia badań naukowych lub w celach dydaktycznych.¹

Świadoma odpowiedzialności karnej z tytułu naruszenia przepisów ustawy z dnia 4 lutego 1994 r. o prawie autorskim i prawach pokrewnych i konsekwencji dyscyplinarnych określonych w ustawie Prawo o szkolnictwie wyższym i nauce (Dz.U.2021.478 t.j.), a także odpowiedzialności cywilnoprawnej oświadczam, że przedkładana rozprawa doktorska została napisana przeze mnie samodzielnie.

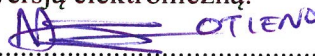
Oświadczam, że treść rozprawy opracowana została na podstawie wyników badań prowadzonych pod kierunkiem i w ścisłej współpracy z promotorem prof. dr hab. inż. Jacek Mąkinia.

Niniejsza rozprawa doktorska nie była wcześniej podstawą żadnej innej urzędowej procedury związanej z nadaniem stopnia doktora.

Wszystkie informacje umieszczone w ww. rozprawie uzyskane ze źródeł pisanych i elektronicznych, zostały udokumentowane w wykazie literatury odpowiednimi odnośnikami, zgodnie z przepisem art. 34 ustawy o prawie autorskim i prawach pokrewnych.

Potwierdzam zgodność niniejszej wersji pracy doktorskiej z załączoną wersją elektroniczną.

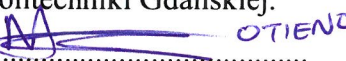
Gdańsk, dnia 28.08.2025

 OTIENO

podpis doktoranta

Ja, niżej podpisana, wyrażam zgodę na umieszczenie ww. rozprawy doktorskiej w wersji elektronicznej w otwartym, cyfrowym repozytorium instytucjonalnym Politechniki Gdańskiej.

Gdańsk, dnia 28.08.2025

 OTIENO

podpis doktoranta

¹ Art. 27. 1. Instytucje oświatowe oraz podmioty, o których mowa w art. 7 ust. 1 pkt 1, 2 i 4–8 ustawy z dnia 20 lipca 2018 r. – Prawo o szkolnictwie wyższym i nauce, mogą na potrzeby zilustrowania treści przekazywanych w celach dydaktycznych lub w celu prowadzenia działalności naukowej korzystać z rozpowszechnionych utworów w oryginale i w tłumaczeniu oraz zwielokrotnić w tym celu rozpowszechnione drobne utwory lub fragmenty większych utworów.

² W przypadku publicznego udostępniania utworów w taki sposób, aby każdy mógł mieć do nich dostęp w miejscu i czasie przez siebie wybranym korzystanie, o którym mowa w ust. 1, jest dozwolone wyłącznie dla ograniczonego kręgu osób uczących się, nauczających lub prowadzących badania naukowe, zidentyfikowanych przez podmioty wymienione w ust. 1.



STATEMENT

The author of the doctoral dissertation: Jeremiah Abong'o Otieno

I, the undersigned, declare that I am aware that in accordance with the provisions of Art. 27 (1) and of the Act of 4th February 1994 on Copyright and Related Rights (Journal of Laws of 2021, item 1062), the university may use my doctoral dissertation entitled: Contribution of denitrifying polyphosphate-accumulating organisms to the enhanced biological phosphorus removal process and nitrous (iv) oxide (N₂O) gas emissions for scientific or didactic purposes.¹

Gdańsk, 28.08.2025

 OTIENO

signature of the PhD student

Aware of criminal liability for violations of the Act of 4th February 1994 on Copyright and Related Rights and disciplinary actions set out in the Law on Higher Education and Science (Journal of Laws 2021, item 478), as well as civil liability, I declare, that the submitted doctoral dissertation is my own work.

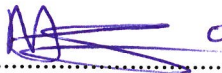
I declare, that the submitted doctoral dissertation is my own work performed under and in cooperation with the supervision of prof. dr hab. inż. Jacek Małkinia.

This submitted doctoral dissertation has never before been the basis of an official procedure associated with the awarding of a PhD degree.

All the information contained in the above thesis which is derived from written and electronic sources is documented in a list of relevant literature in accordance with Art. 34 of the Copyright and Related Rights Act.

I confirm that this doctoral dissertation is identical to the attached electronic version.


Gdańsk, 28.08.2025

 OTIENO

signature of the PhD student

I, the undersigned, agree to include an electronic version of the above doctoral dissertation in the open, institutional, digital repository of Gdańsk University of Technology.

Gdańsk, 28.08.2025

 OTIENO

signature of the PhD student

¹Art 27. 1. Educational institutions and entities referred to in art. 7 sec. 1 points 1, 2 and 4–8 of the Act of 20 July 2018 – Law on Higher Education and Science, may use the disseminated works in the original and in translation for the purposes of illustrating the content provided for didactic purposes or in order to conduct research activities, and to reproduce for this purpose disseminated minor works or fragments of larger works.

² If the works are made available to the public in such a way that everyone can have access to them at the place and time selected by them, as referred to in para. 1, is allowed only for a limited group of people learning, teaching or conducting research, identified by the entities listed in paragraph 1.



OPIS ROZPRAWY DOKTORSKIEJ

Autor rozprawy doktorskiej: Jeremia Abong'o Otieno

Tytuł rozprawy doktorskiej w języku polskim: Wkład denitryfikujących organizmów akumulujących polifosforany w zwiększone biologiczne usuwanie fosforu oraz emisję podtlenku azotu (N_2O).

Tytuł rozprawy w języku angielskim: Contribution of denitrifying polyphosphate-accumulating organisms to the enhanced biological phosphorus removal process and nitrous (iv) oxide (N_2O) gas emissions.

Język rozprawy doktorskiej: angielski

Promotor rozprawy doktorskiej: prof. dr hab. inż. Jacek Mąkinia

Data obrony: <dzień, miesiąc, rok>

Słowa kluczowe rozprawy doktorskiej w języku polskim: DPAO; EBPR; Produkcja N_2O , źródła węgla, glukoza; akceptor elektronów

Słowa kluczowe rozprawy doktorskiej w języku angielskim: DPAO; EBPR; N_2O emissions, carbon sources, electron acceptor

Streszczenie rozprawy w języku polskim: Proces pogłębionego biologicznego usuwania fosforu (ang. EBPR) podlega stopniowej przemianie w kierunku bardziej innowacyjnych metod z uwzględnieniem efektywności ekonomicznej i zrównoważonego rozwoju. Proces ten opiera się przede wszystkim na zdolności organizmów akumulujących polifosforany (ang. PAO) do pobierania i magazynowania zwiększonych ilości fosforu (P), szczególnie w naprzemiennych warunkach beztlenowych i anoksycznych. Warunkiem efektywnego usuwania P jest dostępność oraz wykorzystanie źródeł węgla wraz z akceptorami elektronów, takimi jak tlen lub azotany (NO_3^-)/azotyny (NO_2^-). Odkrycie denitryfikujących organizmów akumulujących fosforany (ang. DPAO), zdolnych do przeprowadzania anoksycznego poboru fosforanów (PO_4^{3-}), zmieniło początkową wiedzę na temat procesu EBPR.

Zastosowanie DPAO w układach z EBPR umożliwi zrównoważone podejście do zintegrowanego usuwania fosforu (P) i azotu (N) w oczyszczalniach ścieków. W warunkach

anoksydacyjnych DPAO wykorzystują NO_3^- lub NO_2^- jako akceptory elektronów, co prowadzi do bardziej efektywnego zużycia węgla, oszczędności energii oraz zmniejszenia produkcji osadów. Warunki beztlenowo-anoksydacyjne mają kluczowe znaczenie dla usuwania P z wykorzystaniem DPAO. Z uwagi na ograniczoną zawartość węgla w ściekach, istnieje potrzeba wykorzystania zewnętrznych źródeł węgla, takich jak glukoza i octan w procesie EBPR. Rola octanu jest dobrze opisana w literaturze. Z kolei glukoza jest powszechnie uważana za mniej preferowane źródło węgla dla procesu EBPR, jednak ostatnie doniesienia literaturowe wskazują na możliwość wykorzystania glukozy przez DPAO o wysokiej zawartości bakterii *Tetrasphaera*. Poza tym, aktywność DPAO w warunkach anoksydacyjnych może powodować zwiększone emisje podtlenku azotu (N_2O), które dotychczas nie zostały wystarczająco poznane.

Celem pracy było zbadanie zachowania się osadu o wysokiej zawartości bakterii *Tetrasphaera* w obecności glukozy jako potencjalnego substratu dla DPAO. W tym celu wykonano serię dwufazowych (beztlenowych/anoksydacyjnych) laboratoryjnych testów wsadowych z wykorzystaniem glukozy i octanu jako źródeł węgla oraz NO_2^- lub NO_3^- jako akceptorów elektronów. Do badań wykorzystano osad czynny z oczyszczalni ścieków Debogorze w Gdyni. Badania wykonywano przy stężeniach biomasy w zakresie (2-5 g smo/L). Glukoza i octan były dawkiowane w różnych ilościach przy zmiennych proporcjach ChZT:P (>2,5 lub <2,5). Właściwości osadu o wysokiej zawartości bakterii *Tetrasphaera* badano na podstawie pomiarów szybkości uwalniania/poboru fosforanów (ang. PRR i PUR) oraz szybkości zużycia azotanów/azotynów (ang. NUR/NiUR). Dodatkowo, w niektórych eksperymentach, monitorowano produkcję N_2O . Zadana temperatura procesu wynosiła 20°C , a pH utrzymywano na poziomie zbliżonym do neutralnego.

Uzyskane wyniki wykazały, że octan znacznie zwiększał aktywność DPAO w porównaniu do glukozy, osiągając nawet 25-krotnie wyższe wartości PRR. W obecności NO_3^- , testy z octanem osiągały wartość PUR do $1,5 \pm 0,6$ mg P / (gsmo·h) oraz NUR do $2,9 \pm 0,9$ mg N / (gsmo·h). Produkcję N_2O obserwowano głównie w obecności NO_2^- . Pomimo wysokich wartości NUR, nie zaobserwowano akumulacji N_2O elektronów obecności NO_3^- . DPAO były odpowiedzialne

głównie za redukcję NO_3^- do NO_2^- , a ich udział w produkcji N_2O był mniej znaczący. Produkcja N_2O była wynikiem aktywności innych bakterii heterotroficznych.

W eksperymentach serii I nie zidentyfikowano dokładnego procentowego udziału DPAO. Jednak w serii II było to możliwe w oparciu o obliczone wartości NUR po zastosowaniu chemicznego strącania $\text{PO}_4\text{-P}$. Około 26-32% całkowitego NUR było związane z aktywnością DPAO, podczas gdy 68-74% było związane z denitryfikacją z udziałem innych bakterii heterotroficznych.

Streszczenie rozprawy w języku angielskim: Enhanced biological phosphorus removal (EBPR) is gradually transitioning from conventional approaches to more innovative methods, largely driven by cost efficiency and sustainability considerations. This process primarily relies on the ability of polyphosphate-accumulating organisms (PAOs) to take up and store phosphorus (P) beyond their growth requirements, particularly under alternating anaerobic and anoxic conditions. The availability and utilization of carbon sources and electron acceptors, such as dissolved oxygen or nitrate (NO_3^-)/nitrite (NO_2^-), are essential for effective P removal. The discovery of denitrifying phosphate-accumulating organisms (DPAOs) capable of carrying out anoxic phosphate (PO_4^{3-}) uptake reshaped the understanding of EBPR.

The application of DPAOs in EBPR systems offers a sustainable approach for combined phosphorus (P) and nitrogen (N) removal in wastewater treatment plants (WWTPs). Under anoxic conditions, DPAOs use NO_2^- or NO_3^- as an electron acceptor instead of dissolved oxygen, leading to improved carbon use, energy saving, and reduced sludge production. The anaerobic-anoxic conditions are critical for the novel role of DPAOs in P removal. However, due to the limitation of carbon in the influent wastewater, there is a high motivation to use external carbon sources, such as glucose and acetate for the EBPR processes. The role of acetate in EBPR is well understood in literature. In contrast, glucose is traditionally considered a less-preferred carbon source for EBPR, but recent reports suggested its use by *Tetrasphaera*-rich DPAOs. Moreover, the denitrification activity of DPAOs under anoxic conditions has equally raised concerns about nitrous oxide (N_2O) emissions, which remain insufficiently understood.

The aim of this study was to investigate the behavior of *Tetrasphaera*-rich sludge in the presence of glucose as a potential substrate for DPAO-driven EBPR. A series of two-phase laboratory batch tests (anaerobic/anoxic) was carried out, using glucose and acetate as carbon sources under either NO_2^- or NO_3^- as electron acceptor conditions. Activated sludge was sourced from Debogorze WWTP in Gdynia (northern Poland), with biomass concentrations ranging between (2-5 g MLVSS/L) (adjusted for cuvette-based tests). Glucose and acetate were supplied in variable amounts based on the COD:P ratios (>2.5 vs. <2.5). The functional performance of the *Tetrasphaera*-rich sludge was evaluated by measuring phosphate release/uptake rates (PRRs and PURs), and nitrate utilization rates (NURs/NiURs), while also monitoring N_2O production in some experiments. The process temperature was set to 20°C and pH was kept closely to the neutral conditions.

The results showed that acetate greatly enhanced DPAO activity compared to glucose, achieving PRR values up to 25 times higher. Under NO_3^- conditions, acetate-fed tests reached PURs up to $1.5 \pm 0.6 \text{ mg P / (gMLVSS}\cdot\text{h)}$ and NURs up to $2.9 \pm 0.9 \text{ mg N / (gMLVSS}\cdot\text{h)}$. N_2O production was primarily observed with the use of NO_2^- electron acceptor. Despite high NUR values, no N_2O production was observed with the use of NO_3^- electron acceptor. DPAOs were associated with the observed reduction of NO_3^- to NO_2^- and not directly to N_2O production. N_2O production was primarily linked to ordinary heterotrophic organisms (OHOs).

In Series I experiments, the exact percentage contribution of DPAOs was not explicitly identified. However, in Series II experiments, N removal rates before and after chemical precipitation of $\text{PO}_4\text{-P}$ provided clearer insight into the activity of *Tetrasphaera*-rich sludge under modified anoxic conditions. Based on the calculated NUR values, approximately 26-32% of the total NUR was attributed to DPAO-driven PHA utilization linked to PO_4^{3-} uptake, whereas 68-74% was attributed to denitrifying OHOs

DESCRIPTION OF DOCTORAL DISSERTATION

The author of the doctoral dissertation: Jeremiah Abong'o Otieno

Title of doctoral dissertation in English : Contribution of denitrifying polyphosphate-accumulating organisms to the enhanced biological phosphorus removal process and nitrous (iv) oxide (N₂O) gas emissions

Title of doctoral dissertation in Polish: Wkład denitryfikujących organizmów akumulujących polifosforany w zwiększone biologiczne usuwanie fosforu oraz emisję podtlenku azotu (N₂O).

Language of Doctoral Dissertation: English

Supervisor: prof. dr hab. inż. Jacek Mąkinia

Date of doctoral defense: <day, month, year>

Keywords of doctoral dissertation in Polish: DPAO; EBPR; Produkcja N₂O, źródła węgla, glukoza; akceptor elektronów

Keywords of doctoral dissertation in English:DPAO; EBPR; N₂O production, carbon sources, glucose; electron acceptor

Summary of doctoral dissertation in Polish: Proces pogłębionego biologicznego usuwania fosforu (ang. EBPR) podlega stopniowej przemianie w kierunku bardziej innowacyjnych metod z uwzględnieniem efektywności ekonomicznej i zrównoważonego rozwoju. Proces ten opiera się przede wszystkim na zdolności organizmów akumulujących polifosforany (ang. PAO) do pobierania i magazynowania zwiększonych ilości fosforu (P), szczególnie w naprzemiennych warunkach beztlenowych i anoksycznych. Warunkiem efektywnego usuwania P jest dostępność oraz wykorzystanie źródeł węgla wraz z akceptorami elektronów, takimi jak tlen lub azotany (NO₃⁻)/azotyny (NO₂⁻). Odkrycie denitryfikujących organizmów akumulujących fosforany (ang. DPAO), zdolnych do przeprowadzania anoksycznego poboru fosforanów (PO₄³⁻), zmieniło początkową wiedzę na temat procesu EBPR.

Zastosowanie DPAO w układach z EBPR umożliwia zrównoważone podejście do zintegrowanego usuwania fosforu (P) i azotu (N) w oczyszczalniach ścieków. W warunkach anoksydacyjnych DPAO wykorzystują NO_3^- lub NO_2^- jako akceptory elektronów, co prowadzi do bardziej efektywnego zużycia węgla, oszczędności energii oraz zmniejszenia produkcji osadów. Warunki beztlenowo-anoksydacyjne mają kluczowe znaczenie dla usuwania P z wykorzystaniem DPAO. Z uwagi na ograniczoną zawartość węgla w ściekach, istnieje potrzeba wykorzystania zewnętrznych źródeł węgla, takich jak glukoza i octan w procesie EBPR. Rola octanu jest dobrze opisana w literaturze. Z kolei glukoza jest powszechnie uważana za mniej preferowane źródło węgla dla procesu EBPR, jednak ostatnie doniesienia literaturowe wskazują na możliwość wykorzystania glukozy przez DPAO o wysokiej zawartości bakterii *Tetrasphaera*. Poza tym, aktywność DPAO w warunkach anoksydacyjnych może powodować zwiększone emisje podtlenku azotu (N_2O), które dotychczas nie zostały wystarczająco poznane.

Celem pracy było zbadanie zachowania się osadu o wysokiej zawartości bakterii *Tetrasphaera* w obecności glukozy jako potencjalnego substratu dla DPAO. W tym celu wykonano serię dwufazowych (bztlenowych/anoksydacyjnych) laboratoryjnych testów wsadowych z wykorzystaniem glukozy i octanu jako źródeł węgla oraz NO_2^- lub NO_3^- jako akceptorów elektronów. Do badań wykorzystano osad czynny z oczyszczalni ścieków Debogorze w Gdyni. Badania wykonywano przy stężeniach biomasy w zakresie (2-5 g smo/L). Glukoza i octan były dawkiowane w różnych ilościach przy zmiennych proporcjach ChZT:P (>2,5 lub <2,5). Właściwości osadu o wysokiej zawartości bakterii *Tetrasphaera* badano na podstawie pomiarów szybkości uwalniania/poboru fosforanów (ang. PRR i PUR) oraz szybkości zużycia azotanów/azotynów (ang. NUR/NiUR). Dodatkowo, w niektórych eksperymentach, monitorowano produkcję N_2O . Zadana temperatura procesu wynosiła 20°C, a pH utrzymywano na poziomie zbliżonym do neutralnego.

Uzyskane wyniki wykazały, że octan znacznie zwiększał aktywność DPAO w porównaniu do glukozy, osiągając nawet 25-krotnie wyższe wartości PRR. W obecności NO_3^- , testy z octanem osiągały wartość PUR do $1,5 \pm 0,6$ mg P / (gsmo·h) oraz NUR do $2,9 \pm 0,9$ mg N / (gsmo·h).

Produkcję N_2O obserwowano głównie w obecności NO_2^- . Pomimo wysokich wartości NUR, nie zaobserwowano akumulacji N_2O elektronów obecności NO_3^- . DPAO były odpowiedzialne głównie za redukcję NO_3^- do NO_2^- , a ich udział w produkcji N_2O był mniej znaczący. Produkcja N_2O była wynikiem aktywności innych bakterii heterotroficznych.

W eksperymentach serii I nie zidentyfikowano dokładnego procentowego udziału DPAO. Jednak w serii II było to możliwe w oparciu o obliczone wartości NUR po zastosowaniu chemicznego strącania $\text{PO}_4\text{-P}$. Około 26-32% całkowitego NUR było związane z aktywnością DPAO, podczas gdy 68-74% było związane z denitryfikacją z udziałem innych bakterii heterotroficznych.

Summary of doctoral dissertation in English: Enhanced biological phosphorus removal (EBPR) is gradually transitioning from conventional approaches to more innovative methods, largely driven by cost efficiency and sustainability considerations. This process primarily relies on the ability of polyphosphate-accumulating organisms (PAOs) to take up and store phosphorus (P) beyond their growth requirements, particularly under alternating anaerobic and anoxic conditions. The availability and utilization of carbon sources and electron acceptors, such as dissolved oxygen or nitrate (NO_3^-)/nitrite (NO_2^-), are essential for effective P removal. The discovery of denitrifying phosphate-accumulating organisms (DPAOs) capable of carrying out anoxic phosphate (PO_4^{3-}) uptake reshaped the understanding of EBPR.

The application of DPAOs in EBPR systems offers a sustainable approach for combined phosphorus (P) and nitrogen (N) removal in wastewater treatment plants (WWTPs). Under anoxic conditions, DPAOs use NO_2^- or NO_3^- as an electron acceptor instead of dissolved oxygen, leading to improved carbon use, energy saving, and reduced sludge production. The anaerobic-anoxic conditions are critical for the novel role of DPAOs in P removal. However, due to the limitation of carbon in the influent wastewater, there is a high motivation to use external carbon sources, such as glucose and acetate for the EBPR processes. The role of acetate in EBPR is well understood in literature. In contrast, glucose is traditionally considered a less-preferred carbon source for EBPR, but recent reports suggested its use by *Tetrasphaera*-rich DPAOs. Moreover, the denitrification

activity of DPAOs under anoxic conditions has equally raised concerns about nitrous oxide (N₂O) emissions, which remain insufficiently understood.

The aim of this study was to investigate the behavior of *Tetrasphaera*-rich sludge in the presence of glucose as a potential substrate for DPAO-driven EBPR. A series of two-phase laboratory batch tests (anaerobic/anoxic) was carried out, using glucose and acetate as carbon sources under either NO₂⁻ or NO₃⁻ as electron acceptor conditions. Activated sludge was sourced from Debogorze WWTP in Gdynia (northern Poland), with biomass concentrations ranging between (2-5 g MLVSS/L) (adjusted for cuvette-based tests). Glucose and acetate were supplied in variable amounts based on the COD:P ratios (>2.5 vs. <2.5). The functional performance of the *Tetrasphaera*-rich sludge was evaluated by measuring phosphate release/uptake rates (PRRs and PURs), and nitrate utilization rates (NURs/NiURs), while also monitoring N₂O production in some experiments. The process temperature was set to 20°C and pH was kept closely to the neutral conditions.

The results showed that acetate greatly enhanced DPAO activity compared to glucose, achieving PRR values up to 25 times higher. Under NO₃⁻ conditions, acetate-fed tests reached PURs up to 1.5 ± 0.6 mg P / (gMLVSS·h) and NURs up to 2.9 ± 0.9 mg N / (gMLVSS·h). N₂O production was primarily observed with the use of NO₂⁻ electron acceptor. Despite high NUR values, no N₂O production was observed with the use of NO₃⁻ electron acceptor. DPAOs were associated with the observed reduction of NO₃⁻ to NO₂⁻ and not directly to N₂O production. N₂O production was primarily linked to ordinary heterotrophic organisms (OHOs).

In Series I experiments, the exact percentage contribution of DPAOs was not explicitly identified. However, in Series II experiments, N removal rates before and after chemical precipitation of PO₄-P provided clearer insight into the activity of *Tetrasphaera*-rich sludge under modified anoxic conditions. Based on the calculated NUR values, approximately 26-32% of the total NUR was attributed to DPAO-driven PHA utilization linked to PO₄³⁻ uptake, whereas 68-74% was attributed to denitrifying OHOs.



**Contribution of denitrifying Polyphosphate Accumulating Organisms to the
Enhanced Biological Phosphorus Removal Process and Nitrous (iv) oxide Gas
Emissions**

Doctoral Thesis

mgr inż. Jeremiah Abong'o Otieno

Scientific Supervisor:

prof. dr hab. inż Jacek Małkinia

Gdańsk, 2025

TABLE OF CONTENTS

Abstract.....	18
Streszczenie.....	21
List of Figures.....	24
List of Tables.....	27
List of Abbreviations.....	29
List of Symbols.....	32
Acknowledgments.....	33
1. INTRODUCTION.....	34
1.1 Background.....	34
1.2 Motivation, objectives, and scope.....	39
1.3 Dissertation structure.....	42
2. LITERATURE REVIEW.....	44
2.1 Phosphorus occurrences in the WWTPs.....	44
2.2 Basic principles of phosphorus removal from wastewater.....	47
2.3 Enhanced Biological Phosphorus Removal (EBPR).....	51
2.3.1 Evolution of EBPR.....	51
2.3.2 Mechanism of EBPR.....	53
2.3.3 DPAO in EBPR systems.....	57
2.3.4 Implication of external carbon sources and EBPR performance.....	59
2.3.5 Configurations of the EBPR systems.....	61
2.3.6 Implications of DPAOs on EBPR configuration and operation.....	63
2.4 Factors affecting the occurrence and DPAO in EBPR systems.....	66
2.4.1 Temperature.....	67
2.4.2 pH and DO.....	69
2.4.3 Influent wastewater characteristics.....	72
2.4.4 Presence of DO and NO ₂ ⁻	73
2.5 Nitrous oxide (N ₂ O) gas emissions in EBPR processes.....	75
3. MATERIAL AND METHODS.....	80
3.1 Preliminary study and selection of case study WWTP.....	80

3.2	Dębogórze WWTP – case study facility	82
3.3	Experimental setup.....	86
3.4	Experimental design.....	88
3.5	Experimental series I.....	91
3.5.1	Scenario 1.1—COD-limiting conditions COD:P ratio < 2.5	92
3.5.2	Scenario 1.2 – COD non-limiting conditions COD:P ratio > 2.5	93
3.6	Experimental series II	95
3.6.1	The anaerobic phase test in the CCT.....	97
3.6.2	Modified anoxic tests	98
3.6.2.1	Scenario 2.1: Reference test (“standard” as in scenario 1.1)	100
3.6.2.2	Scenario 2.2: PO ₄ ³⁻ precipitated anoxic conditions	101
3.6.2.3	Scenario 2.3: PHA-depleted anoxic conditions	102
3.7	Evaluation framework.....	102
3.8	Analytical methods.....	103
3.9	Polyhydroxyalkanoates (PHA) measurements.....	104
3.10	Microbiological analyses: DNA extraction and high throughput 16S rDNA sequencing	105
3.10.1	DNA extraction	106
3.10.2	Amplification and sequencing of 16S rRNA Gene V3–V4 region.....	106
3.10.3	Bioinformatics workflow and taxonomic classification	106
3.10.4	Data submission and further analysis	107
3.11	Process rate calculations	107
3.11.1	Nitrate and nitrite utilization rates (NUR and NiUR).....	108
3.11.2	Phosphate release and uptake rates (PRR and PUR)	111
3.11.3	COD consumption rate	112
4.	RESULTS.....	113
4.1	Microbial community	113
4.1.1	Results of preliminary study in four WWTPs in the Pomeranian region, Poland	113
4.1.2	Microbial characterization of the biomass in Gdynia Debogórze (GD)-Case study WWTP	115

4.2	Results of experimental series I	117
4.2.1	Scenario 1.1—COD-limiting conditions (COD:P ratio < 2.5).....	117
4.2.2	Scenario 1.2 – COD non-limiting conditions COD:P ratio > 2.5	122
4.2.2.1	Phosphate release and uptake rates (PRR and PUR).....	123
4.2.2.2	Nitrate and nitrite utilization rates (NUR and NiUR).....	127
4.2.2.3	Polyhydroxyalkanoates (PHA) production.....	128
4.3	Results of experimental series II.....	130
4.3.1	The anaerobic phase test in CCT	131
4.3.2	The modified anoxic phase tests (in three scenarios)	132
4.3.2.1	Scenario 2.1: Reference tests (as in Scenario 1.1).....	133
4.3.2.2	Scenario 2.2: PO ₄ -P anoxic precipitated condition.....	135
4.3.2.3	Scenario 2.3 : PHA-depleted conditions.....	139
4.3.3	Denitrification share by microbial groups based on NURs and NiUR.....	141
4.4	N ₂ O production and DPAO activities	144
4.4.1	N ₂ O production under COD non-limiting conditions :Series I.....	145
4.4.2	N ₂ O production in dynamic anoxic conditions - Series II	148
4.4.2.1	N ₂ O production profiles under series II , Trial 1 (ST1).....	149
4.4.2.2	N ₂ O production profiles under series II , Trial 2 (ST2).....	153
5.	DISCUSSION	159
5.1	Microbial Community Structure the four WWTPs in the Pomeranian region, Poland	159
5.1.1	Dominance of <i>Tetrasphaera</i>	159
5.1.2	Abundance of <i>Ca. Microthrix</i>	161
5.1.3	Low abundance of <i>Ca. Accumulibacter</i> and <i>Dechloromonas</i>	161
5.2	Microbial characterization of the case study WWTPs - GD.....	163
5.3	Impact of COD:P ratios on the DPAO metabolism (glucose and acetate as substrates and NO ₃ ⁻ or NO ₂ ⁻ as electron acceptors).....	165
5.3.1	Phosphorus release and uptake rate (PRR and PUR).....	166
5.3.2	Nitrate and nitrite utilization rates (NUR and NiUR).....	171
5.3.3	Polyhydroxyalkanoates (PHA) production	173



5.4	DPAO metabolism under modified anoxic conditions.	175
5.4.1	DPAOs metabolism under anoxic standard conditions.....	175
5.4.2	PO ₄ ³⁻ anoxic precipitation on DPAO metabolism.....	176
5.4.3	PHA depleted anoxic on DPAO metabolism.....	179
5.5	N ₂ O production and denitrifying PAO activity.....	181
5.5.1	Electron acceptor type on N ₂ O production.....	181
5.5.2	Pulse dosage of NO ₂ ⁻ strategy effect on N ₂ O.....	182
5.5.3	Internal reserves (PHA, poly-P) on N ₂ O production.....	182
5.5.4	Effect of carbon source on N ₂ O production.....	184
6.	CONCLUSIONS.....	187
6.1	Challenges and future research directions.....	189
	REFERENCES.....	191
	APPENDICES.....	221

ABSTRACT

Enhanced biological phosphorus removal (EBPR) is gradually transitioning from conventional approaches to more innovative methods, largely driven by cost efficiency and sustainability considerations. This process primarily relies on the ability of polyphosphate-accumulating organisms (PAOs) to take up and store phosphorus (P) beyond their growth requirements, particularly under alternating anaerobic and anoxic conditions. The availability and utilization of carbon sources and electron acceptors, such as dissolved oxygen or nitrate (NO_3^-)/nitrite (NO_2^-), are essential for effective P removal. The discovery of denitrifying phosphate-accumulating organisms (DPAOs) capable of carrying out anoxic phosphate (PO_4^{3-}) uptake reshaped the understanding of EBPR.

The application of DPAOs in EBPR systems offers a sustainable approach for combined phosphorus (P) and nitrogen (N) removal in wastewater treatment plants (WWTPs). Under anoxic conditions, DPAOs use NO_2^- or NO_3^- as an electron acceptor instead of dissolved oxygen, leading to improved carbon use, energy saving, and reduced sludge production. The anaerobic-anoxic conditions are critical for the novel role of DPAOs in P removal. However, due to the limitation of carbon in the influent wastewater, there is a high motivation to use external carbon sources, such as glucose and acetate for the EBPR processes. The role of acetate in EBPR is well understood in literature. In contrast, glucose is traditionally considered a less-preferred carbon source for EBPR, but recent reports suggested its use by *Tetrasphaera*-rich DPAOs. Moreover, the denitrification activity of DPAOs under anoxic conditions has equally raised concerns about nitrous oxide (N_2O) emissions, which remain insufficiently understood.

The aim of this study was to investigate the behavior of *Tetrasphaera*-rich sludge in the presence of glucose as a potential substrate for DPAO-driven EBPR. A series of two-phase laboratory batch tests (anaerobic/anoxic) was carried out, using glucose and acetate as carbon sources under either NO_2^- or NO_3^- as electron acceptor conditions. Activated sludge was sourced from Debogorze WWTP in Gdynia (northern Poland), with biomass concentrations ranging between (2-5 g MLVSS/L) (adjusted for cuvette-based tests). Glucose and acetate were supplied in variable amounts based on the COD:P ratios (>2.5 vs. <2.5). The functional performance of the *Tetrasphaera*-rich sludge was evaluated by measuring phosphate release/uptake rates (PRRs and PURs), and nitrate utilization rates (NURs/NiURs), while also monitoring N_2O production in some experiments. The process temperature was set to 20°C and pH was kept closely to the neutral conditions.

The results showed that acetate greatly enhanced DPAO activity compared to glucose, achieving PRR values up to 25 times higher. Under NO_3^- conditions, acetate-fed tests reached PURs up to 1.5 ± 0.6 mg P / (gMLVSS·h) and NURs up to 2.9 ± 0.9 mg N / (gMLVSS·h). N_2O production was primarily observed with the use of NO_2^- electron acceptor. Despite high NUR values, no N_2O production was observed with the use of NO_3^- electron acceptor. DPAOs were associated with the observed reduction of NO_3^- to NO_2^- and not directly to N_2O production. N_2O production was primarily linked to ordinary heterotrophic organisms (OHOs).

In Series I experiments, the exact percentage contribution of DPAOs was not explicitly identified. However, in Series II experiments, N removal rates before and after chemical precipitation of $\text{PO}_4\text{-P}$ provided clearer insight into the activity of *Tetrasphaera*-rich sludge under modified anoxic conditions. Based on the calculated NUR values, approximately 26-32% of the total NUR was

attributed to DPAO-driven PHA utilization linked to PO_4^{3-} uptake, whereas 68-74% was attributed to denitrifying OHOs.

Keywords: DPAO; EBPR; N_2O production, carbon sources, glucose; electron acceptor

STRESZCZENIE

Proces pogłębionego biologicznego usuwania fosforu (ang. EBPR) podlega stopniowej przemianie w kierunku bardziej innowacyjnych metod z uwzględnieniem efektywności ekonomicznej i zrównoważonego rozwoju. Proces ten opiera się przede wszystkim na zdolności organizmów akumulujących polifosforany (ang. PAO) do pobierania i magazynowania zwiększonych ilości fosforu (P), szczególnie w naprzemiennych warunkach beztlenowych i anoksydacyjnych. Warunkiem efektywnego usuwania P jest dostępność oraz wykorzystanie źródeł węgla wraz z akceptorami elektronów, takimi jak tlen lub azotany (NO_3^-)/azotyny (NO_2^-). Odkrycie denitryfikujących organizmów akumulujących fosforany (ang. DPAO), zdolnych do przeprowadzania anoksydacyjnego poboru fosforanów (PO_4^{3-}), zmieniło początkową wiedzę na temat procesu EBPR.

Zastosowanie DPAO w układach z EBPR umożliwia zrównoważone podejście do zintegrowanego usuwania fosforu (P) i azotu (N) w oczyszczalniach ścieków. W warunkach anoksydacyjnych DPAO wykorzystują NO_3^- lub NO_2^- jako akceptory elektronów, co prowadzi do bardziej efektywnego zużycia węgla, oszczędności energii oraz zmniejszenia produkcji osadów. Warunki beztlenowo-anoksydacyjne mają kluczowe znaczenie dla usuwania P z wykorzystaniem DPAO. Z uwagi na ograniczoną zawartość węgla w ściekach, istnieje potrzeba wykorzystania zewnętrznych źródeł węgla, takich jak glukoza i octan w procesie EBPR. Rola octanu jest dobrze opisana w literaturze. Z kolei glukoza jest powszechnie uważana za mniej preferowane źródło węgla dla procesu EBPR, jednak ostatnie doniesienia literaturowe wskazują na możliwość wykorzystania glukozy przez DPAO o wysokiej zawartości bakterii *Tetrasphaera*.. Poza tym, aktywność DPAO w warunkach anoksydacyjnych może powodować zwiększone emisje podtlenku azotu (N_2O), które dotychczas nie zostały wystarczająco poznane.

Celem pracy było zbadanie zachowania się osadu o wysokiej zawartości bakterii *Tetrasphaera* w obecności glukozy jako potencjalnego substratu dla DPAO. W tym celu wykonano serię dwufazowych (beztlenowych/anoksydacyjnych) laboratoryjnych testów wsadowych z wykorzystaniem glukozy i octanu jako źródeł węgla oraz NO_2^- lub NO_3^- jako akceptorów elektronów. Do badań wykorzystano osad czynny z oczyszczalni ścieków Debogorze w Gdyni. Badania wykonywano przy stężeniach biomasy w zakresie (2-5 g smo/L). Glukoza i octan były dawkiowane w różnych ilościach przy zmiennych proporcjach ChZT:P (>2,5 lub <2,5). Właściwości osadu o wysokiej zawartości bakterii *Tetrasphaera* badano na podstawie pomiarów szybkości uwalniania/poboru fosforanów (ang. PRR i PUR) oraz szybkości zużycia azotanów/azotynów (ang. NUR/NiUR). Dodatkowo, w niektórych eksperymentach, monitorowano produkcję N_2O . Zadana temperatura procesu wynosiła 20°C , a pH utrzymywano na poziomie zbliżonym do neutralnego.

Uzyskane wyniki wykazały, że octan znacznie zwiększał aktywność DPAO w porównaniu do glukozy, osiągając nawet 25-krotnie wyższe wartości PRR. W obecności NO_3^- , testy z octanem osiągały wartość PUR do $1,5 \pm 0,6$ mg P / (gsmo·h) oraz NUR do $2,9 \pm 0,9$ mg N / (gsmo·h). Produkcję N_2O obserwowano głównie w obecności NO_2^- . Pomimo wysokich wartości NUR, nie zaobserwowano akumulacji N_2O elektronów obecności NO_3^- . DPAO były odpowiedzialne głównie za redukcję NO_3^- do NO_2^- , a ich udział w produkcji N_2O był mniej znaczący. Produkcja N_2O była wynikiem aktywności innych bakterii heterotroficznych.

W eksperymentach serii I nie zidentyfikowano dokładnego procentowego udziału DPAO. Jednak w serii II było to możliwe w oparciu o obliczone wartości NUR po zastosowaniu chemicznego

strącania $\text{PO}_4\text{-P}$. Około 26-32% całkowitego NUR było związane z aktywnością DPAO, podczas gdy 68-74% było związane z denitryfikacją z udziałem innych bakterii heterotroficznych.

Słowa kluczowe: DPAO; EBPR; Produkcja N_2O , źródła węgla, glukoza; akceptor elektronów

LIST OF FIGURES

Figure 1-1: General overview of the metabolic pathways in EBPR (A) Conventional PAO activity, (B) novel DPAO activity with associated N ₂ O emissions (adapted from Otieno et al., (2022)) ..	39
Figure 2-1: Detrimental effects of eutrophication on water resources due to excess P	45
Figure 2-2: Overview of phosphorus removal processes (adapted from Ruzhitskaya & Gogina, 2017)).....	48
Figure 2-3: Chemical dosing points where chemicals are introduced into wastewater stream systems (1) immediately upstream of primary clarification, (2) immediately in the aeration tank before final clarification, and (3) at both points simultaneously (adopted from Graziani, 2006).	49
Figure 2-4: Struvite precipitation process and associated technology for phosphorus removal (adapted from Nadagouda et al., 2024).....	50
Figure 2-5: Early configurations of EBPR systems (a) Phoredox and (b) PhoStrip (adapted from Makinia & Zaborowska, 2020).....	52
Figure 2-6: Timeline of the potential microbial community of PAOs at the genus level (adapted from Diaz et al., 2022)	53
Figure 2-7: Metabolic pathways and biochemical transformation of phosphorus DPAOs in full-scale EBPR (Barnard et al., 2017; Mąkinia & Zaborowska, 2020).....	54
Figure 2-8: Comparative mechanism pathways of DPAOs, PAOs, and OHO interactions in anaerobic, anoxic, and aerobic zones (Barnard et al., 2017a; Mąkinia & Zaborowska, 2020)	55
Figure 2-9: A summary overview of the global abundance of the DPAOs within the general microbial community in the EBPR system according to data from MIDAS in comparison to Poland's WWTPs as the case study (Dueholm et al., 2024; Wu et al., 2019).	59
Figure 2-10: The pH and dissolved oxygen (DO) variance to EBPR performance.....	72
Figure 2-11: N ₂ O production pathways (Al-Hazmi et al., 2023).....	78
Figure 3-1: Geographic location and key characteristics of the four surveyed WWTPs in the Pomeranian region of Poland.....	81
Figure 3-2: Aerial view of “ Dębogórze” WWTP as the selected case study.	84
Figure 3-3: (a) Schematic diagram of the laboratory-scale batch reactor system (b) Actual image of the two parallel bioreactors and the connected control unit.	88

Figure 3-4:Schematic diagram of the series II experimental setup of the CCT (anaerobic phase) and batch reactor (anoxic phase)..... 97

Figure 3-5:NUR calculations for specific carbon sources and microbial activities in the anoxic phases..... 110

Figure 4-1:Relative percentages of dominant DPAO genera in bacterial communities from mixed liquor samples across four large WWTPs in the Pomeranian region, Poland: Gdynia Dębogórze (GD), Gdańsk Wschód (GW), Słupsk (SL), and Swarzewo (SW). Error bars represent standard deviation of duplicate samples..... 114

Figure 4-3:Mean relative abundance (\pm SD) of key functional bacterial groups in the GD WWTP activated sludge. Data is averaged from four sampling events over six months. Functional groups include :Ammonia-oxidizing bacteria (AOB), Nitrite-oxidizing bacteria (NOB),Polyphosphate-accumulating organisms (PAO/DPAO), Glycogen-accumulating organisms (GAO), and Heterotrophic denitrifiers (DEN HET). Taxonomic classification is shown at the genus level. 116

Figure 4-4:Results of the batch experiments with acetate as a carbon source under COD limiting conditions with anoxic addition of NO_3^- (a) and NO_2^- (b)..... 120

Figure 4-5:Results of the batch experiments with as a carbon source under COD-limiting conditions with anoxic addition of NO_3^- (a) and NO_2^- (b)..... 121

Figure 4-6:Results of the batch experiments with acetate as a carbon source under COD non-limiting conditions with anoxic addition of NO_3^- (a) and NO_2^- (b)..... 124

Figure 4-7:Results of the batch experiments with glucose as a carbon source under COD non-limiting conditions with anoxic addition of NO_3^- (a) and NO_2^- (b)..... 125

Figure 4-8:Results of the batch experiments with glucose as a carbon source under COD non-limiting conditions with anoxic addition of NO_2^- in pulse dosage..... 126

Figure 4-9:Comparison of NUR and NiUR values in acetate- and glucose-fed tests..... 128

Figure 4-10:PHB and PHV production profiles in the bacterial cell COD non-limiting conditions (a) acetate with nitrate. (b) acetate with nitrite, and (c) glucose with nitrite 130

Figure 4-11:Results of the anaerobic phase in the common cultivation reactor (CCT) with the profiles of PO_4^{3-} release and COD consumption in (a) Trial 1 (ST1) and (b) Trial 2 (ST2)..... 132

Figure 4-12:The profiles of COD, $\text{NO}_3\text{-N}$, $\text{NO}_2\text{-N}$, and $\text{PO}_4\text{-P}$ concentrations (mg. L^{-1}) under the modified anoxic **scenario 2.1**: reference tests without addition of glucose on the 6th hour. 134

Figure 4-13:The profiles of COD, NO₃-N, NO₂-N, and PO₄-P concentrations (mg. L⁻¹) under the modified anoxic **scenario 2.2:** PO₄³⁻ precipitated with the addition of glucose on the 6th hour. 137

Figure 4-14:The profiles of COD, NO₃-N, NO₂-N, and PO₄-P concentrations (mg. L⁻¹) under the anaerobic-anoxic PHA absence conditions. Glucose addition on the 6th hour..... 140

Figure 4-15:Percentage contribution of DPAOs and HET to NUR under modified anoxic conditions..... 144

Figure 4-16:N₂O production profiles in experimental series I , scenario 1.2 COD non-limiting conditions under NO₃⁻ as the electron acceptor. 146

Figure 4-17:N₂O production profiles in experimental series I , scenario 1.2 COD non-limiting conditions with NO₂⁻ as the electron acceptor. 147

Figure 4-18:N₂O production profiles under dynamic anoxic conditions in series II – Trial 1 (ST1) using NO₂⁻ as electron acceptor across scenarios (a) 2.1 (reference) ,(b) 2.2 (PO₄³⁻-precipitated), and (c) 2.3 (PHA-depleted)..... 150

Figure 4-19:N₂O production profiles under dynamic anoxic conditions in series II – Trial 1 (ST1) using NO₃⁻ as electron acceptor across scenarios (a) 2.1 (reference) ,(b) 2.2 (PO₄³⁻-precipitated), and (c) 2.3 (PHA-depleted)..... 152

Figure 4-20:N₂O production profiles under dynamic anoxic conditions in series II – Trial 2 (ST2) using NO₂⁻ as electron acceptor across scenarios (a) 2.1 (reference) ,(b) 2.2 (PO₄³⁻-precipitated), and (c) 2.3 (PHA-depleted)..... 155

Figure 4-21: N₂O production profiles under dynamic anoxic conditions in series II – Trial 2 (ST2) using NO₃⁻ as electron acceptor across scenarios (a) 2.1 (reference) ,(b) 2.2 (PO₄³⁻-precipitated), and (c) 2.3 (PHA-depleted)..... 157

LIST OF TABLES

Table 2-1: European Union Urban Wastewater Phosphorus Limits in WWTP (Council Directive of 21 May 1991 - 91/271/EEC - 2014 and new Urban Wastewater Treatment Directives vs (EU 2024/3019)	47
Table 2-2: The functional clades of PAO distinguished based on distinct biochemical properties.	57
Table 2-3: Summary of preferable electron acceptors by the main functional bacterial groups involved in EBPR.	65
Table 2-4: Temperature dependent abundance trends of PAOs and GAOs in EBPR Systems	68
Table 2-5: Influence of pH and Dissolved Oxygen on EBPR Performance	71
Table 2-6: Impact on P- removal under different NO_2^- levels (mg N/L) (Zekker et al., 2021; Zeng et al., 2014)	74
Table 3-1: The four WWTPs in the Pomeranian region of Poland by location , size , and configuration	81
Table 3-2: Concentrations and degrees of reduction of basic pollutant indicators in treated sewage from “Dębogórze” in 2015–2023 (Source: https://pewik.gdynia.pl).....	85
Table 3-3: General schedule and description of the work carried out in the study on EBPR by Tetrasphaera-rich activated sludge.....	90
Table 3-4: Summary of dosages of electron acceptors (NO_3^- vs. NO_2^-) and carbon sources (acetate vs. glucose) for the COD limiting conditions (COD:P ratio < 2.5).	93
Table 3-5: Summary of dosage amounts of electron acceptors (NO_3^- vs. NO_2^-) and carbon sources (acetate vs. glucose) for the high COD:P ratio > 2.5.	94
Table 3-6: Experimental series II activities: anaerobic phase in the CCT and modified anoxic phase scenarios in batch reactors	100
Table 3-7: Summary of dosages of electron acceptors (nitrate vs. nitrite) and carbon sources (acetate vs. glucose) in R1 and R2 under each of the trial (ST1 and ST2).....	101
Table 4-1: Comprehensive overview of the anaerobic process rates, i.e., PRR and COD values, under COD-limiting conditions.	118
Table 4-2: Comprehensive overview of the anoxic process rate, i.e., PUR, NUR, and NiUR values, under COD-limiting conditions.	118

Table 4-3: Comprehensive overview of the anaerobic process rates and other parameters under COD non-limiting conditions COD:P ratio > 2.5.	122
Table 4-4: Comprehensive overview of the anoxic process rates and other parameters under COD non-limiting conditions COD:P ratio > 2.5.....	123
Table 4-5: Summary of the most important EBPR performance indicators in comparing tests with acetate at COD non-limiting conditions in different NO ₂ ⁻ dosage strategies.	126
Table 4-6: The process rates under modified anoxic reference conditions in trials 1 and 2.	135
Table 4-7: Denitrification rates under different carbon sources and electron acceptors in anaerobic-anoxic experiments with PO ₄ -P precipitated conditions.....	139
Table 4-8: Summary of denitrification rates under different carbon sources and electron acceptors in anaerobic-anoxic experiments with PHA-depleted conditions.....	141
Table 4-9: NUR and NiUR rates and estimated microbial group contributions under modified anoxic conditions for Trial 1 (ST1) and Trial 2 (ST2).	142
Table 4-10: Estimated microbial group share proportions in total NUR and their corresponding percentage contributions to denitrification activity (ST1 and ST2).	143

LIST OF ABBREVIATIONS

WWTPs	Wastewater treatment plants
EBPR	Enhanced Biological Phosphorus Removal
BNR	Biological Nutrient Removal
DPAOs	Denitrifying Polyphosphate-Accumulating Organisms
PHA	Polyhydroxyalkanoates
PHB	Polyhydroxybutyrate
COD	Chemical Oxygen Demand
VFA	Volatile Fatty Acids
R ² value	Ratio of nitrite or nitrate correlation
Poly-P	Polyphosphate
Ortho-P	Orthophosphate
RbCOD	Biodegradable Chemical Oxygen Demand
BOD ₅	Biochemical Oxygen Demand over 5 days
rbCOD	Readily Biodegradable COD
PHA	polyhydroxyalkanoates
Poly- P	Polyphosphate
TCA	Tricarboxylic acid cycle
<i>CphA</i>	Cyanophycin synthesis gene
PCR-DGGE	Polymerase Chain Reaction - Denaturing Gradient Gel Electrophoresis
rDNA	Ribosomal Deoxyribonucleic Acid
ASM	Activated sludge models



GAO	Glycogen accumulating organisms
ATP	Adenosine Triphosphate
TCA	Tricarboxylic acid cycle
RAS	Recirculated activated sludge
C/P	Carbon to Phosphorus ratio
gMLVSSL ⁻¹	Grams of mixed liquor volatile suspended solids per liter
C/N	Carbon to Nitrogen ratio
DO	Dissolved oxygen
GHG	Greenhouse gas
NUR	Nitrate utilization rate.
NiUR	Nitrite utilization rate
PUR	Phosphate utilization rate
DNA	Deoxyribonucleic Acid
SD	Standard deviation
SRT	Solids retention time
AOB	Ammonia-Oxidizing Bacteria
AOB	Ammonia-Oxidizing Archaea
Nor	Nitric oxide reductase
Nar	Nitrate reductase
Nir	Nitrite reductase
GD	Gdynia Debogórze Wastewater Treatment Plant



GW	Gdańsk Wschód Wastewater Treatment Plant
SL	Słupsk Wastewater Treatment Plant
SW	Swarzewo Wastewater Treatment Plant
TN	Total nitrogen
TP	Total phosphorus
PE	Population Equivalent
OHOs	Ordinary Heterotrophic Organisms
CCT	Common Cultivation Tank
R1	Reactor 1
R2	Reactor 2
ST1	Trial 1
ST2	Trial 2
<i>Ca.</i>	<i>Candidatus</i>

LIST OF SYMBOLS

N	Nitrogen
P	Phosphorus
CO ₂	Carbon dioxide
Fe(III) or Fe ³⁺	Ferric iron
Fe(II) or Fe ²⁺	Ferrous iron
NH ₄ -N or NH ₄ ⁻	Ammonia
N ₂ O	Nitrous (iv) oxide
NO	Nitric oxide
NO ₂ -N or NO ₂ ⁻	Nitrite
NO ₃ -N or NO ₃ ⁻	Nitrate
O ₂	Oxygen
C ₆ H ₅ Na ₃ O ₇	Sodium citrate
H ₂ SO ₄	sulfuric acid
MgO	Magnesium oxide
Mg(OH) ₂	Magnesium hydroxide
NaOH	Sodium hydroxide
<i>pH</i>	Measure of hydrogen ion activity (acidity/alkalinity)
CH ₄	Methane
N ₂	Molecular nitrogen (dinitrogen)
NH ₂ OH	Hydroxylamine
kW	Kilowatt - unit of power
MWh	Megawatt hour – unit of energy
PO ₄ ³⁻ or PO ₄ -P	Orthophosphate
FeCl ₃	Ferric chloride

ACKNOWLEDGMENTS

I would like to express my deep gratitude to my supervisor Professor Jacek Mąkinia for allowing me to do a PhD. His support, guidance, patience, assistance, and encouragement during this research kept me on course. I am forever grateful and fortunate to have such a professional mentor during my research.

Special thanks to my co-supervisor dr inż. Przemysław Kowal for his patience and guidance and for being there in support during the field sampling, logistics, laboratory set-up, and in-depth guidance during the experimental sessions. Besides, I am grateful for other academic colleagues from our department, who have helped me in different stages of this journey. Last but not least, I express my thanks to my family and siblings for their love, patience, and understanding of my absence life while preparing this research. Without any of them, this research work would not have been possible.

Funding and research

This research has been financially supported by the doctoral program at the Gdansk University of Technology, Poland. Moreover, I acknowledge the support from the Polish National Agency for Academic Exchange (NAWA) by providing me with the Ignacy Łukasiewicz scholarship program a step that led to this chapter in my life. I also express my gratitude to the Erasmus program for enabling a short internship at the University of Palermo, Italy.

1. INTRODUCTION

1.1 Background

Nutrient removal, particularly nitrogen (N), and phosphorus (P), from wastewater treatment plants (WWTPs) is primarily aimed at reducing eutrophication in receiving water bodies. In recent years, there has been a growing focus on P and N removal and recovery, due to the urgent need to reduce dependency on non-renewable reserves and also to foster sustainable nutrient recycling, utilization, and circularity (X. Li et al., 2024; Roy et al., 2025).

P can be removed through chemical and biological processes (Akinawo, 2023). The chemical P removal processes involve phosphate precipitation and coagulation/flocculation using metal salts of calcium, aluminum, or iron (Owodunni et al., 2023). However, the use of chemicals for P removal has limitations, including high costs and greater sludge production, which in turn raise sludge handling and disposal expenses. In contrast, biological P removal offers a cost-effective alternative to the chemical treatment methods with reduced sludge production (Zhang et al., 2023).

Enhanced biological phosphorus removal (EBPR) is the most effective P-removal process in WWTPs (Zhang et al., 2024). As one of the most complex processes in biological nutrient removal activated sludge systems, EBPR demonstrates advantages in cost, reliability, and sustainability (Izadi & Andalib, 2023). Recent research has expanded knowledge and improved efficiency by identifying key pathways and microorganisms involved. The EBPR process involves the metabolic activities of polyphosphate-accumulating organisms (PAOs), which function under alternating anaerobic-aerobic/anoxic conditions (Nielsen et al., 2019; Xie et al., 2024). Initially, it was believed that PAOs could not accumulate phosphate (PO_4^{3-}) under anoxic conditions (Tchobanoglous & Burton, 1991). However, subsequent studies, conducted in both lab-scale and

full-scale WWTPs, have changed that hypothesis, demonstrating anoxic P-uptake (Bai et al., 2024; Barnard et al., 2017; Li et al., 2024). Denitrifying polyphosphate accumulating organisms (DPAOs) have been identified as responsible for this process, enabling simultaneous denitrification and P removal (Zhao et al., 2024).

The dual benefit of DPAOs in removing both N and P enhances the overall efficiency and sustainability of EBPR in WWTPs by reducing carbon source consumption, energy saving from aeration, and minimizing sludge production (Li et al., 2020; Li et al., 2024). EBPR can save up to 30% in aeration costs and address 50% of carbon limitations related to COD, while also reducing sludge production (Kuba et al., 1996; Wang et al., 2015). DPAOs utilize alternative electron acceptors, such as nitrite (NO_2^-) or nitrate (NO_3^-), for denitrification instead of oxygen (O_2) enabling P uptake under anoxic conditions (Li et al., 2022; Zekker et al., 2021). Oehmen et al., (2010) categorized DPAOs into two types based on their denitrification capabilities: Type I (DPAOs I), which reduce both NO_3^- and NO_2^- , and Type II (DPAOs II), which can only reduce NO_2^- . However, ongoing debate exists, regarding whether DPAOs I can directly use NO_3^- for anoxic phosphate uptake or DPAOs I rely on secondary NO_2^- generated (Rubio-Rincón et al., 2019a). Expanding the understanding of DPAO activity has been demonstrated in both lab-scale and full-scale EBPR systems with several recent studies (Chen et al., 2022; Li et al., 2020; Mukherjee et al., 2019; Shoji et al., 2003). For example, Bai et al., (2023) observed that DPAOs optimize nutrient removal in WWTPs, especially when organic substrates for EBPR and denitrification are limited. In addition, recent research has reported the DPAO account for up to 80% of the entire PAO population in EBPR systems (Małkinia & Zaborowska, 2020; Nielsen et al., 2019). Furthermore, DPAO have been identified as the dominant bacteria responsible for P

removal (Dueholm et al., 2024). Li et al., (2020) reported that DPAOs can achieve 76% P removal efficiency, while Gao et al., (2023) reported an even higher efficiency of up to 84 %.

The denitrification process due to anoxic P-uptake by DPAOs has raised concerns about increased nitrous oxide (N₂O) emissions, contributing to global warming (Hou et al., 2022). Recent laboratory experiments have found notable N₂O production due to DPAO activity in EBPR systems (Marques et al., 2018a; Ribera-Guardia et al., 2016; Wisniewski et al., 2018). Liu et al. (2015) observed that N₂O could be produced and accumulated as an important intermediate of denitrification since portions of N (NO₃⁻ or NO₂⁻) are converted into N₂O. This disrupts net zero carbon emissions and contributes to 3.3-10% of total N₂O emissions in WWTPs (Asadi & McPhedran, 2021; Maktabifard et al., 2023). Nielsen et al., (2019) reported that *Tetrasphaera* possesses partial denitrification pathways and may be involved in N₂O production. Moreover, Ribera-Guardia et al., (2016) found that DPAOs exhibit higher denitrification capacity and N₂O accumulation. The proportion of N₂O produced in denitrifying P removal systems ranges from 2.3% to 21.6% of the influent N load (Liu et al., 2015). Although literature suggests that N₂O emissions account for up to 75% of the total carbon footprint of WWTPs, it is believed to be underestimated globally at full-scale levels. Therefore, understanding N₂O production and accumulation related to DPAO activity in EBPR is crucial. The metabolic mechanism of DPAOs is illustrated in **Figure 1-1**.

Despite concerns over N₂O emissions from DPAO activity, interest in implementing P removal under anaerobic-anoxic conditions has continued. Special attention has been directed towards microbial community members responsible for the process, particularly the DPAOs group. Recent molecular investigations have highlighted *Candidatus (Ca.) Accumulibacter* and *Tetrasphaera* as

the primary genera responsible for EBPR (Close et al., 2021; Mukherjee et al., 2019; Nielsen et al., 2019). In early studies from the 1970s and 1980s, *Acinetobacter* species were considered key players in EBPR due to their high affinity for acetate as a carbon source (Tchobanoglous & Burton, 1991). Later, a bacterial group phylogenetically close to *Rhodocyclus tenuis* in the *Betaproteobacteria*, named '*Candidatus Accumulibacter phosphatis*' (hereafter referred to as *Accumulibacter*), was identified as a primary PAO in acetate or propionate enriched laboratory scale reactors (Bond et al., 1995; Crocetti et al., 2000; Hesselmann et al., 1999) as well as in the full scale WWTPs (Kong et al., 2004). For over three decades since identification, *Accumulibacter*, have been generally assumed to be the main functional PAOs in EBPR (Seviour & McIlroy, 2008). Kong et al., (2005) demonstrated the aerobic P-uptake of genus *Tetrasphaera* with their identity later verified as putative PAOs (Kristiansen et al., 2013) and their detection in higher abundance (H. T. T. Nguyen et al., 2015a; Stockholm-Bjerregaard et al., 2017).

Of particular interest is the ability of *Tetrasphaera* to perform denitrification under varying environmental conditions in alternate between aerobic respiration and denitrification (R. Liu et al., 2019a). All identified isolates are known to reduce nitrate (NO_3^-) to nitrite (NO_2^-), with EBPR-related strains possessing the additional capability to reduce nitrate to nitrous oxide (N_2O) (Marques et al., 2018a). Despite this prevalence, the specific role of *Tetrasphaera* in bulk P removal and its broader impact on EBPR remain unclear. The presence of *Tetrasphaera* varies by plant-specific factors and geographic regions. For example, Fernando et al. (2019) observed the coexistence of *Ca. Accumulibacter* and *Tetrasphaera* in Danish WWTPs designed for EBPR. Their findings revealed that *Tetrasphaera* contributed more significantly to P removal than *Ca. Accumulibacter*. Conversely, Farmer et al., (2023) identified the presence of the cyanophycin

synthesis gene (*cphA*) in both *Ca. Accumulibacter* and *Tetrasphaera*, highlighting their potential for simultaneous N and P removal. Additionally, Nielsen et al., (2019) reported the presence of other bacteria genus, including *Dechloromonas*, *Ca. Holomonas* and *Ca. Microthrix* with substantial polyphosphate (poly-P) reserves, further emphasizing the collaborative nature of microbial communities in P removal processes. Zhao et al., (2022) identified *Tetrasphaera* and *Dechloromonas* as members of the DPAO group, while Chen et al., (2021) emphasized the dominance of *Dechloromonas* within this community. Surveys across numerous WWTPs worldwide confirm the widespread abundance of *Ca. Accumulibacter* and *Tetrasphaera* (Dueholm et al., 2024).

The metabolic pathways of DPAOs present a complex yet critical research area, with evidence suggesting deviations from traditional PAO processes. Through the macrogenomics analysis of Kristiansen et al, (2013) on *Tetrasphaera* and *Accumulibacter*, some genes related to glucose and amino acid can be transported in *Tetrasphaera* and not in *Accumulibacter* placing *Tetrasphaera* to have a wider substrate utilization profile and can directly absorb and utilize glucose or amino acids as a carbon source for metabolism. Barnard et al., (2017) reported that DPAOs can ferment high-carbon compounds like glucose, releasing P without poly-hydroxy-alkanoates (PHA) cycling- where PAOs in the anaerobic phase, take up volatile fatty acids (VFAs) and store them as PHAs by using energy from breaking down polyphosphate while in an aerobic phase, PAOs consume the stored PHAs to generate energy and restore polyphosphate and glycogen levels (Marques et al., 2017). This pathway also produces volatile fatty acids (VFAs), which serve as substrates for other PAOs and facilitate P uptake under aerobic or anoxic conditions. To meet anaerobic energy demands, these bacteria hydrolyze and release aerobically stored polyphosphate but appear to lack

the capacity for glycogen storage, despite the potential to do so. Instead, glucose is stored as glycogen rather than PHA, as indicated by (Zhang et al., 2023).

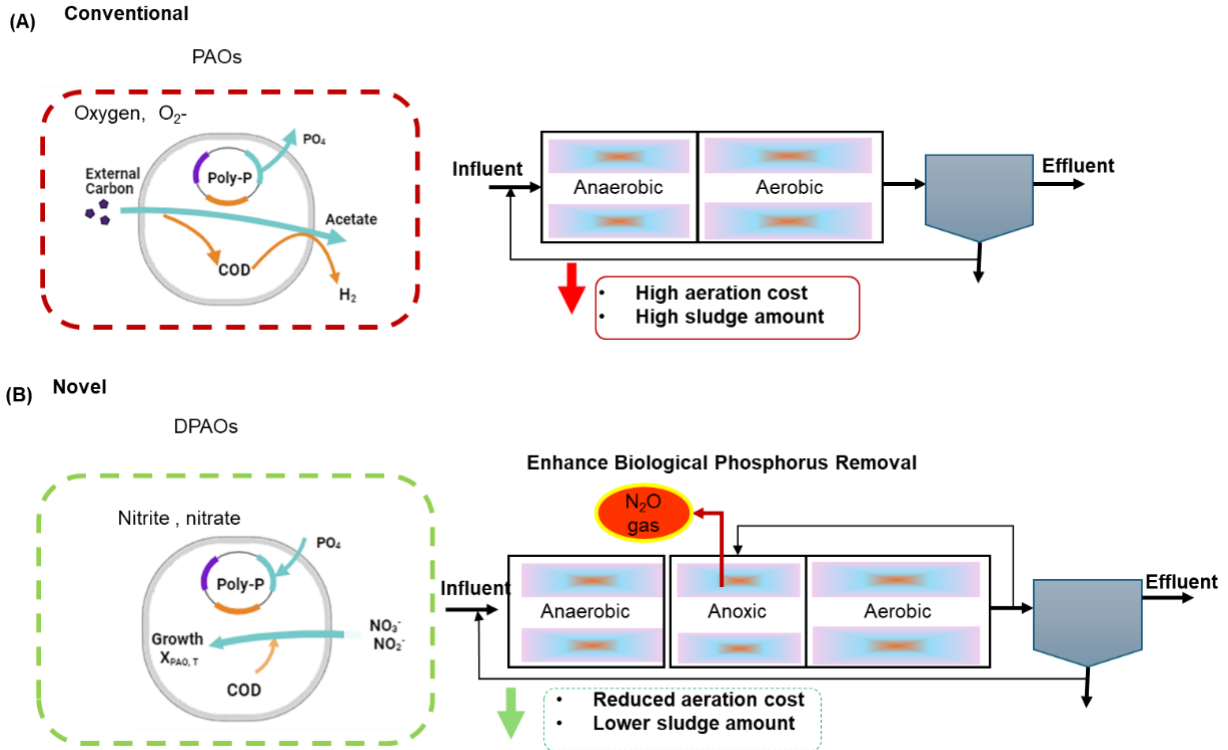


Figure 1-1: General overview of the metabolic pathways in EBPR (A) Conventional PAO activity, (B) novel DPAO activity with associated N_2O emissions (adapted from Otieno et al., (2022))

1.2 Motivation, objectives, and scope

The limitation of carbon is a well-established factor influencing both nutrient removal and microbial activity. In the case of DPAOs, carbon serves as the electron donor in their metabolic pathways, making it a key determinant of their function (Gao et al., 2023). This is particularly significant when compared to the conventional PAOs, whose carbon utilization and metabolic processes differ from those of novel DPAOs, underscoring the importance of tailored carbon management to optimize P removal (Barnard et al., 2017).

Traditionally, acetate has been recognized as one of the most prevalent VFA and the typical carbon source for EBPR in laboratory studies and full-scale WWTPs (Chen et al., 2015). However, recent studies have increasingly explored glucose and other alternative carbon sources for EBPR (Aghilinasrollahabadi et al., 2024; Petriglieri et al., 2021; Y. Tian et al., 2022). While VFAs, such as acetate and propionate, are generally considered more effective for P removal (Oehmen, Yuan, et al., 2005a), Zhang et al. (2020) suggested that glucose can support EBPR under specific conditions. Conversely, conflicting reports exist regarding using glucose as an external carbon for EBPR (Izadi et al., 2021). Zhang et al. (2023) observed that EBPR could occur with a peptone-glucose mix or glucose alone. Additionally, Fernando et al., (2019) found that glucose stimulated the growth of DPAOs, including the recently discovered *Tetrasphaera*. Furthermore, He et al. (2024) reported glucose uptake and activity by *Tetrasphaera*, highlighting its potential role in EBPR.

The influence of external carbon sources on P removal by the DPAOs has been widely studied, with varying results. Yu et al., (2023) found that acetate was the most effective carbon source, leading to superior P removal compared to glucose and glycerol. However, research EBPR systems with a high abundance of DPAOs, such as *Tetrasphaera*, remains limited. In contrast, *Ca. Accumulibacter*, a key organism in conventional EBPR, has limited capacity to utilize glucose for P removal due to the lower expression of glucose uptake genes compared to its strong preference for VFAs (Begum & Batista, 2012). This aligns with the findings of Wang et al.,(2010), where glucose as the primary carbon source led to sub optimal EBPR performance.

In full-scale WWTPs, internal sludge recirculation from aerobic to anaerobic zones can lead to simultaneous exposure to carbon and electron acceptors like NO_3^- and NO_2^- . Understanding how

these conditions influence EBPR and microbial community dynamics is crucial for improving operational efficiency. The impact of varying carbon sources, such as glucose and acetate, on P removal in DPAO-enriched sludge in full-scale EBPR systems has not yet been fully understood.

This dissertation aims to investigate the behavior of *Tetrasphaera*-rich sludge in the presence of glucose as a potential substrate for DPAO-driven EBPR processes. The metabolic responses of DPAOs to external addition carbon sources (acetate vs glucose) and electron acceptors (NO_3^- vs. NO_2^-), focusing on their roles in denitrification, P removal, and N_2O emissions under anoxic conditions was investigated. It was hypothesized that glucose will enhance EBPR activity in *Tetrasphaera*-rich sludge, particularly when paired with efficient denitrification. Through series of two-phase laboratory batch tests (anaerobic/anoxic) glucose and acetate were supplied in variable amounts based on the COD:P ratios (>2.5 vs. <2.5) under either NO_2^- or NO_3^- as electron acceptor conditions using activated sludge sourced from Debogorze WWTP in Gdynia (northern Poland), with biomass concentrations ranging between (2-5 g MLVSS/L). Through measuring phosphate release/uptake rates (PRRs and PURs), and nitrate utilization rates (NURs/NiURs), the functional performance of the *Tetrasphaera*-rich sludge was evaluated by while also monitoring N_2O production in some experiments. The interactions between these factors under anoxic conditions will provide insights into the contribution of DPAOs to EBPR. Furthermore, microbial community dynamics were analyzed using 16S rDNA PCR-DGGE (Polymerase Chain Reaction - Denaturing Gradient Gel Electrophoresis) to examine microbial diversity and its relationship with internal carbon storage. The analysis focused on microbial composition under varying conditions of orthophosphate and PHA availability.

To achieve these objectives, the following research questions were formulated:

- i. To investigate the impact of glucose as a potential substrate on DPAO driven EBPR processes in *Tetrasphaera*-enriched sludge under anaerobic-anoxic conditions compared to acetate.
- ii. To evaluate the influence of carbon source variability (including COD:P ratio) and electron acceptor dosage on $\text{NO}_3^- / \text{NO}_2^-$ removal rates and overall EBPR efficiency.

1.3 Dissertation structure

This doctoral dissertation is presented in six chapters, as follows:

Chapter 1 introduces the document, establishes the context of the research by presenting a comprehensive introduction to EBPR processes, with particular emphasis on the emerging significance of DPAOs. It outlines the key knowledge gaps, defines the research problem, and formulates the objectives and hypotheses that underpin the study.

Chapter 2 provides an in-depth literature review, synthesizing current scientific knowledge on the physiology, ecology, and metabolic versatility of DPAOs in EBPR systems. This chapter critically evaluates the role of DPAOs in simultaneous nitrogen and phosphorus removal under anaerobic-anoxic conditions. Additionally, it addresses the implications of DPAO activity for system performance, N_2O gas emissions, and eutrophication control, thereby framing the relevance of this research within both operational and environmental contexts.

Chapter 3 describes the methodology where freshly collected mixed liquor rich in *Tetrasphaera* from the Gdynia Dębogórze (GD) WWTP was used to conduct the series I and series II of the anaerobic-anoxic phases batch experiments. Different COD:P ratios (limiting >2.5 and non-

limiting < 2.5 conditions) were tested to evaluate their impact on DPAO's activity and the overall performance of the EBPR. Additionally, the N_2O emissions as a result of the activities of the DPAOs were investigated and measured.

Chapter 4 presents the results while *chapter 5* gives robust discussion derived from all the experimental series (I, II and preliminary studies) of the anaerobic – anoxic batch tests described in *chapter 3*. The last *chapter 6* provides a summary of the conclusions drawn from the present dissertation and the gaps and outlines some directions for further research.

Additionally, list of tables, figures and abbreviations are presented at the beginning of the document.

2. LITERATURE REVIEW

This section provides an expanded review of the occurrence of P in WWTPs and the common P removal pathways, including both chemical and biological pathways. The key microorganisms involved in EBPR are discussed, along with their metabolic processes and P removal mechanisms. The factors that influence these processes are also considered. The functionality and configurations of EBPR systems are explored, focusing on their design and operational aspects. Additionally, the literature highlights N₂O emissions associated with denitrification activities within EBPR. The detailed literature review is included as part of this work, with the review paper attached for reference.

2.1 Phosphorus occurrences in the WWTPs

P in WWTPs occurs primarily as orthophosphates (ortho-P, PO₄³⁻) and polyphosphate (Poly-P), with the latter able to undergo hydrolysis to PO₄³⁻ (Park et al., 2016; Tang et al., 2023). Numerous past and recent research findings have highlighted the critical role of P as a limiting nutrient for plant growth and an essential component of living organisms (Chen et al., 2023; Vollenweider, 1992). Although P is a vital element, its excessive presence in natural water bodies can lead to severe environmental issues, such as eutrophication (Akinnawo, 2023; Preisner, 2023). By definition, eutrophication is a phenomenon where excessive nutrient levels, especially nitrogen (N) and P, lead to uncontrolled algal blooms, degrading water quality in aquatic environments (Bali & Gueddari, 2019; Lemley et al., 2022).

WWTPs are significant point sources of P discharges, but their contribution to surface water P levels varies by region, wastewater treatment efficiency, and the presence of other sources, such as agricultural runoff (Venhauerova et al., 2022). The cumulative effect of excessive P from

WWTPs and runoff has led to the loss of resilience in aquatic ecosystems (Huser et al., 2016). Influent P concentrations in WWTPs typically range from 6 to 12 mgP L⁻¹, depending on the wastewater source and treatment plant characteristics (Capua et al., 2022). Conversely, P discharge limits ranging from 0.005 to 15 mgP L⁻¹ have been reported and can vary depending on the size of the WWTPs, environmental and geographic characteristics, the original use of the wastewater, and the assimilation capacity of the receiving water body (Carrillo et al., 2024) see **Table 2-1**. The USEPA has recommended total P (TP) limits of 0.05 mgP L⁻¹ for streams entering lakes and 0.1 mgP L⁻¹ for rivers and flowing waters to prevent eutrophication (U.S. Environmental Protection Agency, 2002). The P cycle leading to eutrophication due to excessive P in water resources has been highlighted in **Figure 2-1**.

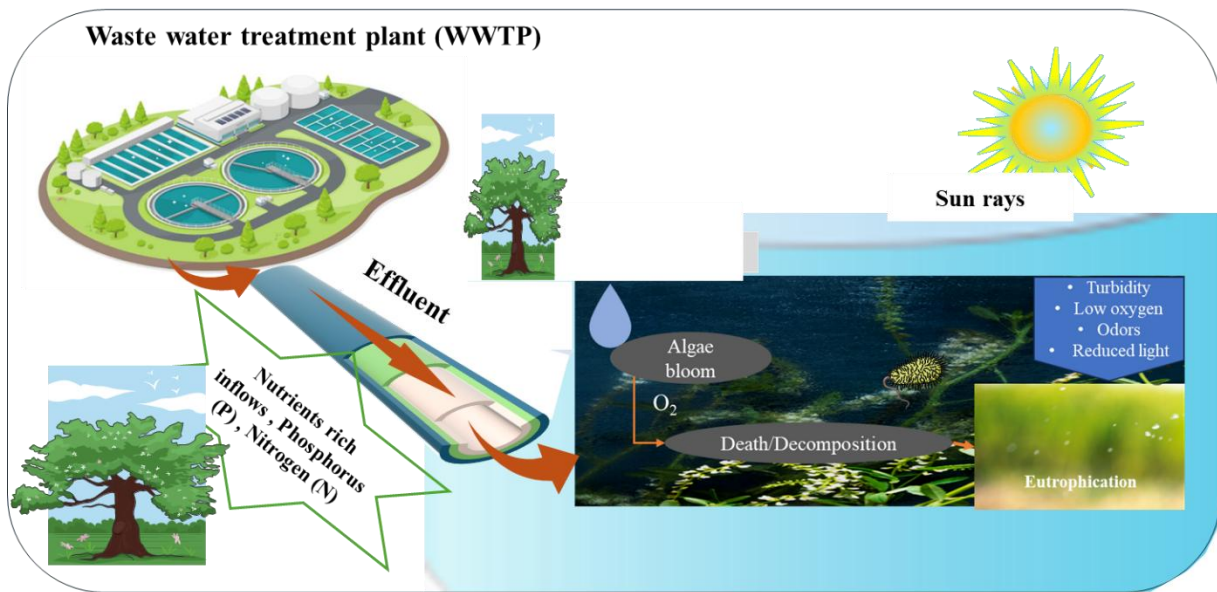


Figure 2-1:Detrimental effects of eutrophication on water resources due to excess P

Over the past three decades, the integration of P removal systems, including EBPR, has been increasingly recognized as essential for mitigating eutrophication (Otieno et al., 2022). This justification is supported by the findings that inhibiting levels to the growth of algae are below 0.5 mgP L^{-1} (Ren et al., 2017). Andersen et al., (2009) estimated that WWTPs contribute a significant proportion of the P load in the Baltic Sea region, accounting for approximately 37,000 tons P annually. Increasing P discharges from WWTPs and agricultural fields have raised concerns among policymakers and environmental authorities (Abdoli et al., 2024). Concerted efforts and pressures on governments and regional unions, e.g. the European Union (EU), to enact and implement policies and regulations in their respective environmental protection plans to reduce P load released from WWTPs discharges into the water bodies are on the rise (Di Capua et al., 2022). Recently, EU Council Directive of 21 May 1991 Concerning Urban Waste Water Treatment (91/271/EEC), 2014) was replaced with 2024, P removal and recovery have become mandatory in countries such as Germany, the Netherlands, and Austria before wastewater discharge. As a result, most installations in these countries have replaced outdated treatment plants with modern technologies that enable both effective phosphorus removal and its recovery for use in fertilizer production. However, in many other countries, the high costs associated with implementing these advanced technologies remain a major financial barrier to adoption. Moreover, the new EU regulation comes with even more strict circumstances for water quality requirements as illustrated in **Table 2-1**:

Table 2-1:European Union Urban Wastewater Phosphorus Limits in WWTP (Council Directive of 21 May 1991 - 91/271/EEC - 2014 and new Urban Wastewater Treatment Directives vs (EU 2024/3019)

Parameter	Size of plant by Population Equivalent	EU 2014 Directive On concentration limits	EU 2024 Directive on concentration limits
Total phosphorus (TP)	10000-150000	2 mg L ⁻¹	1 mg L ⁻¹
	≥150000	1 mg L ⁻¹	0.5 mg L ⁻¹

In Germany, Netherlands, and Austria P-removal and recovery has become mandatory before discharge and most installations replacing the old WWTP embracing the with the new technology for fertilizer production (Bannert et al., 2021). Moreover, in Poland for instance, thermal treatments are embraced in newer installations and at times under pilot plants in some regions like Gdynia (Kacprzak & Kupich, 2023; Smol et al., 2016, 2020). According to Preisner, (2020) , about 1575 WWTPs were modernized and 403 new ones built with the support of the European funding. Additionally, key legislation has been enacted into laws outlining discharge conditions for wastewater and substances harmful to aquatic ecosystems, for instance the 2001 Water Law and its subsequent amendments, set limits on effluent P concentrations. However , for many countries , the cost of technologies presents a new financial barrier.

2.2 Basic principles of phosphorus removal from wastewater

The selection of the P removal method has a critical impact on the further possibilities of P recovery. There are many ways to remove P from activated sludge systems. According to Ruzhitskaya & Gogina, (2017), P removal from WWTPs takes various forms including chemical,

biological, and hybrid as in **Figure 2-2**. For many years, chemical methods like coagulation have been used for P removal, while struvite precipitation has gained attention as a P recovery technique.

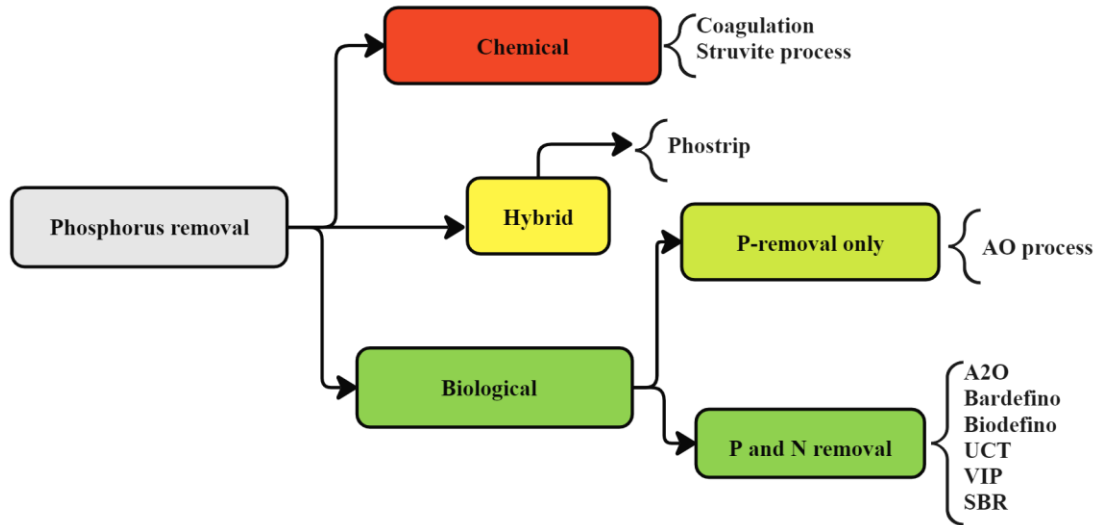


Figure 2-2: Overview of phosphorus removal processes (adapted from Ruzhitskaya & Gogina, 2017)).

P removal has been accomplished conventionally by chemical precipitation using coagulating chemicals, such as lime, aluminum, and iron salts (Wu et al., 2023). The commonly used salts are aluminum sulfate (alum), sodium aluminate, poly-aluminum chloride, ferric chloride, ferrous chloride, and ferrous sulfate which are dosage during the treatment process as in **Figure 2-3**.

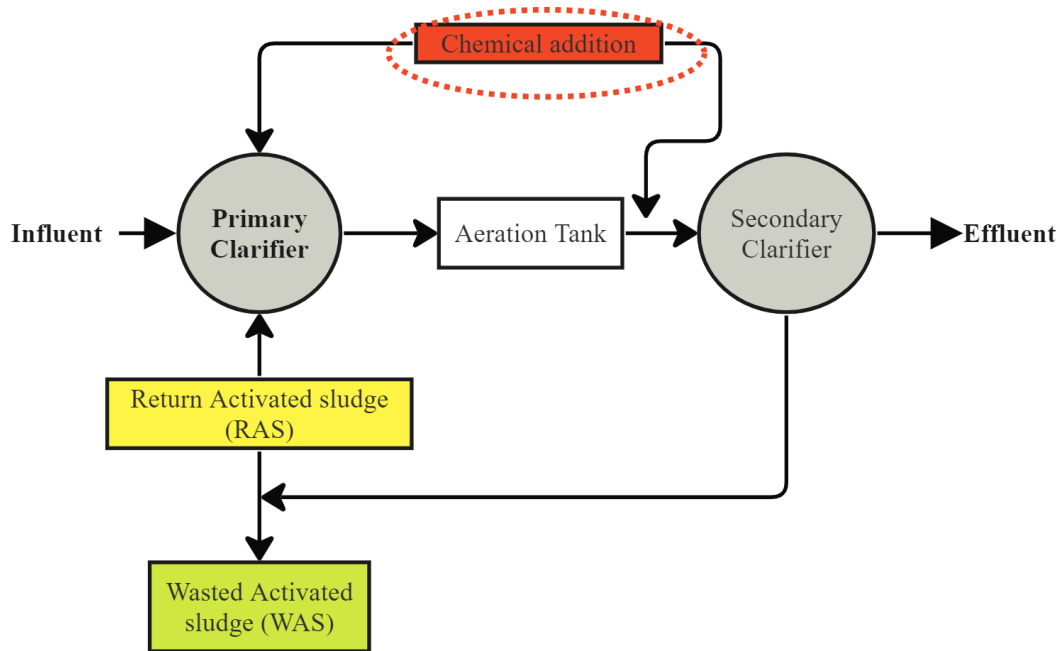
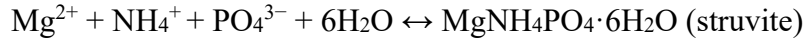


Figure 2-3: Chemical dosing points where chemicals are introduced into wastewater stream systems (1) immediately upstream of primary clarification, (2) immediately in the aeration tank before final clarification, and (3) at both points simultaneously (adopted from Graziani, 2006).

Furthermore, struvite technology to recover and recycle P from WWTPs as a slow-release fertilizer despite the constraining economic and environmental costs that come with its operation (Śniatała et al., 2024). Struvite P recovery occurs through a precipitation-crystallization reaction that depends on the availability of magnesium (Mg), ammonium (NH_4^+), and phosphate (PO_4^{3-}) in appropriate molar ratios, as well as optimal pH conditions (typically 8.0 - 9.5) (Nadagouda et al., 2024). Struvite is a white crystalline compound with an orthorhombic pattern, composed of Mg, NH_4^+ , and PO_4^{3-} and often used as a raw product for the fertilizer industries (Acelas et al., 2014). During the anaerobic phase in EBPR, PAOs release stored poly P into the liquid phase. With the increased concentration of P in the liquid phase and NH_4^+ alongside, depending on the pH, struvite precipitation takes the pathway indicated in the chemical reaction equation:



Molar ratio:

1 (Mg^{2+}): 1 (NH_4^+): 1 (PO_4^{3-}) (Acelas et al., 2014; Achilleos et al., 2022)

The flowchart below indicates the chemical stages followed in the phosphorus removal as struvite crystals.

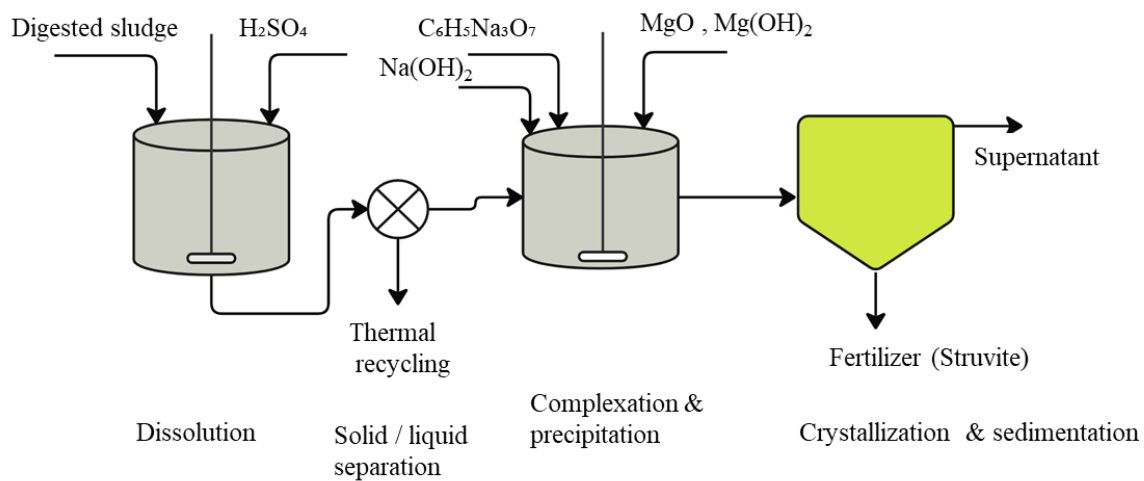


Figure 2-4: Struvite precipitation process and associated technology for phosphorus removal (adapted from Nadagouda et al., 2024)

For many years, attention has been focused on biological P removal based on an anaerobic-aerobic/anoxic sequence treatment, which resulted in excess P uptake by the microorganisms capable of storing P beyond their normal microbial growth requirements. This dissertation centers on EBPR.

2.3 Enhanced Biological Phosphorus Removal (EBPR)

EBPR is recognized for its potential cost-effectiveness and environmental sustainability (Izadi & Andalib, 2023). EBPR performance relies on sequential anaerobic and aerobic/anoxic conditions, while its effectiveness depends on the availability of volatile fatty acids (VFAs) and stable operational conditions, including temperature, pH, DO, and many other factors that may upset operations (Lu et al., 2021; Otieno et al., 2022). Through cycling between anaerobic and aerobic/anoxic conditions, PAOs can leverage stored poly-P as an energy source (Comeau et al., 1987; Zhang et al., 2023).

Conventionally, P removal through PAO activity is achieved by triggering anaerobic-aerobic conditions, which considerably increase operational costs related to energy consumption due to aeration (Lv et al., 2023) necessitating the novel denitrification by DPAOs pathway (Nielsen et al., 2019).

2.3.1 Evolution of EBPR

The biological P removal process was first observed in the 1970s, with most findings derived from laboratory-scale (Levin & Shapiro, 1965) and to a lesser extent, from full-scale plants (Srinath et al., 1959). Barnard (1974) through experimental work, formulated the principles of P removal technology, which justifies the need for anaerobic contact between activated sludge and influent wastewater before aerobic treatment to accomplish P removal. Subsequently, Barnard,(1975) introduced the term Phoredox to represent any process with an anaerobic/aerobic sequence to promote the biological P removal technology concept. The Phoredox concept includes an anaerobic chamber upstream of an aerated bioreactor, which emphasizes the requirement of low redox conditions to properly initiate BPR metabolism (Barnard, 2006). The first full-scale

Phoredox system was implemented in 1973, demonstrating the feasibility of biological P removal in WWTPs (Levin., 1975). Simultaneously, an alternative side-stream P removal technology was developed based on the separation of the enriched side-stream liquor treated with lime called PhoStrip (Levin & Sala, 1987) as illustrated in **Figure 2-5**.

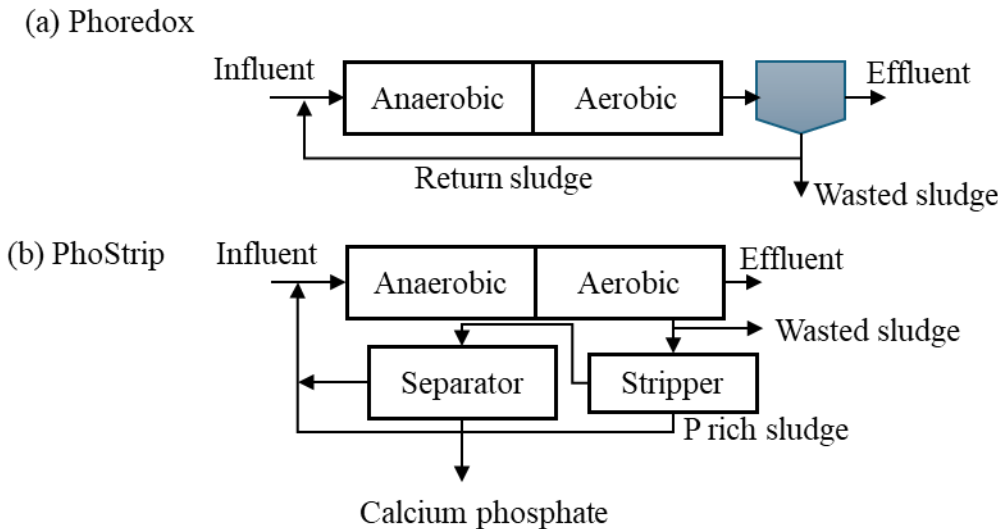


Figure 2-5:Early configurations of EBPR systems (a) Phoredox and (b) PhoStrip (adapted from Makinia & Zaborowska, 2020)

P removal was initially believed to occur primarily through chemical mechanisms; however, Fuhs & Chen (1975), challenged this notion by identifying *Acinetobacter* as a key organism responsible for P removal in the PhoStrip process. Under anaerobic conditions, *Acinetobacter* utilized VFAs in the influent wastewater, leading to the release of stored phosphorus. Since then, several studies have discovered more. Wagner et al., (1994) determined *Betaproteobacteria* as the dominant bacterial group in P-removal as well as detecting a high abundance of *Actinobacteria* in EPBR systems. Bond et al., (1999) identified *Rhodocyclus*-related as key players in EBPR. Subsequent

studies confirmed that *Ca. Accumulibacter* is the primary PAO and clarified that PAOs are primarily responsible for EBPR (Stewart et al., 2024; X. Xie et al., 2024).

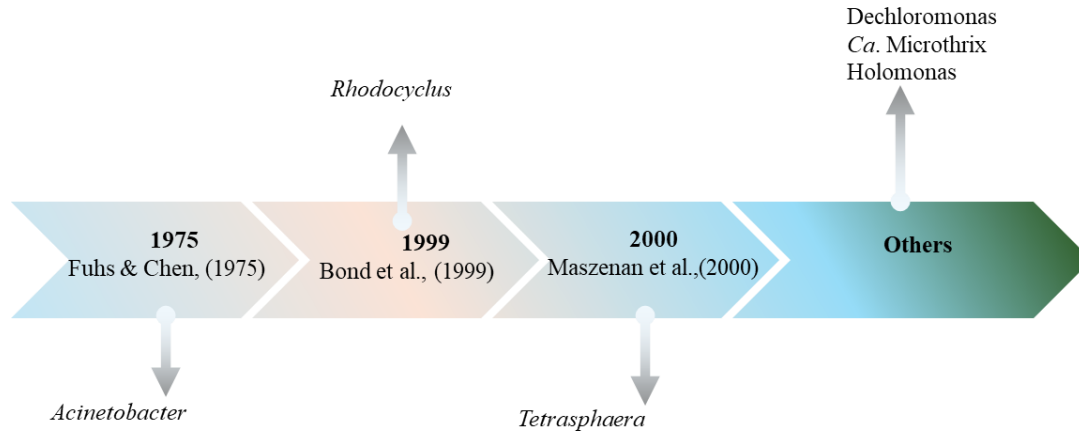


Figure 2-6: Timeline of the potential microbial community of PAOs at the genus level (adapted from Diaz et al., 2022)

Further insights into the history and evolution of EBPR, including a discussion on *Tetrasphaera*: morphology, physiology, and phylogeny, are provided in the review paper (Otieno et al., 2022).

2.3.2 Mechanism of EBPR

Basic metabolic models assume that DPAOs exhibit intracellular P storage as poly-P and energy storage as PHAs, under appropriate environmental conditions, particularly in the presence of NO_3^- / NO_2^- as alternative electron acceptors (Jenkins & Wanner, 2014). The stored PHA reserves provided energy used for the growth of DPAOs when exposed to anoxic conditions, due to the capability of simultaneous denitrification and P uptake. Initially, P removal has not been linked with denitrification activity, as was modelled in Activated Sludge Model no. 2 (ASM2) (Gujer et al., 1999, p. 3, 1999, p. 3; Henze et al., 1999). However, Vlekke et al., (1988) demonstrated the capacity of the DPAOs, leading to an update of ASM2d (Henze et al., 1999). Characterization of

the DPAO metabolism, especially regarding the capability of complex carbon compounds utilization, provided further insights into the potential pathways within EBPR, as presented in **Figure 2-7**.

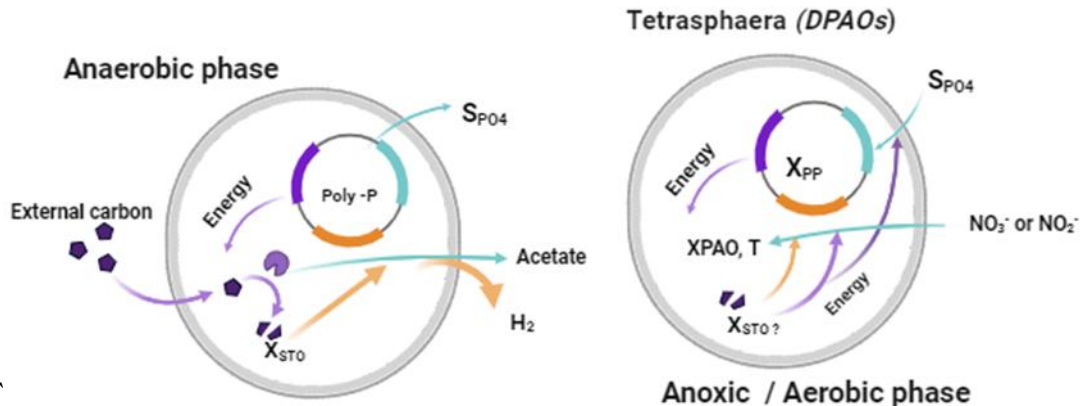


Figure 2-7:Metabolic pathways and biochemical transformation of phosphorus DPAOs in full-scale EBPR (Barnard et al., 2017; Małkinia & Zaborowska, 2020)

DPAOs predominantly function in the anoxic phase due to their denitrification capabilities, but they also exhibit anaerobic activity where they store VFAs as PHAs (Luo et al., 2024). The traditional understanding of PAO interactions under anaerobic, anoxic, and aerobic conditions and the interactions and symbiotic behavior of OHOs, where they produce VFA through fermentation of influent readily biodegradable COD (rbCOD) derived from hydrolysis of particulate biodegradable COD are illustrated in different chambers as highlighted in **Figure 2-8** for a comprehensive comparison.

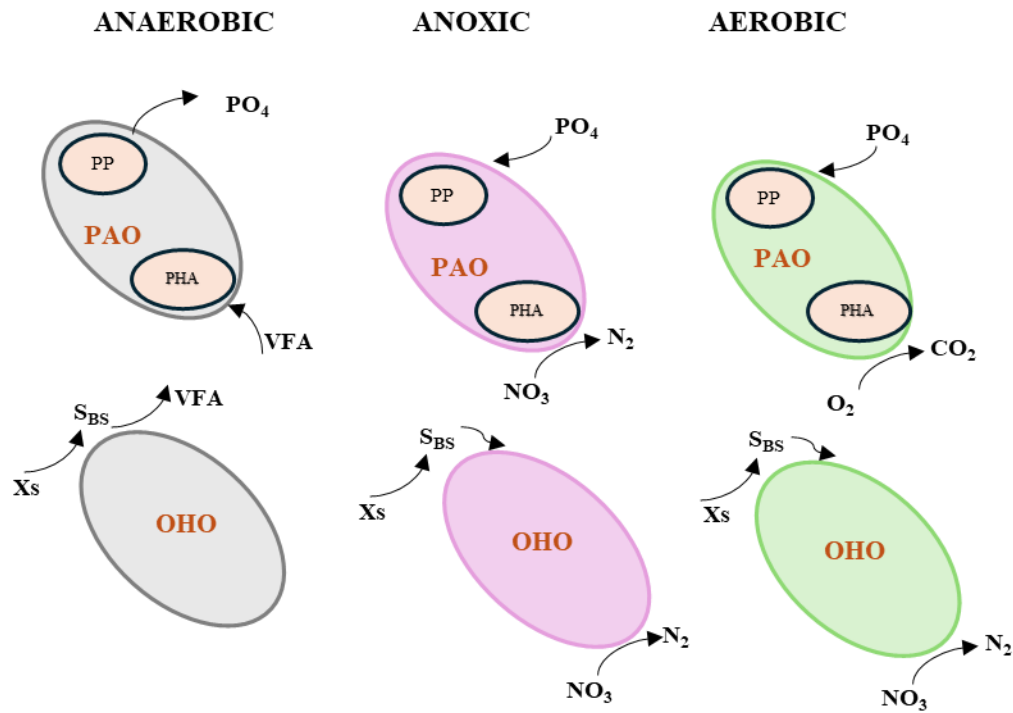


Figure 2-8:Comparative mechanism pathways of DPAOs, PAOs, and OHO interactions in anaerobic, anoxic, and aerobic zones (Barnard et al., 2017a; Mąkinia & Zaborowska, 2020)

During the anaerobic phase, PAOs, such as *Ca. Accumulibacter*, primarily take up VFAs (e.g., acetate, propionate), whereas some PAOs, like *Tetrasphaera*, can metabolize complex carbon compounds, such as glucose (Roy et al., 2021). The energy required for glycogen synthesis is supplied by fermentation and/or polyphosphate decomposition to orthophosphate. In the aerobic-anoxic phase, the stored glycogen is degraded, supplying energy for growth and enhanced P uptake, followed by replenishing the polyphosphate storage.

Various studies based on experimental results have highlighted proposed metabolic models regarding the P-removal of DPAOs (Kristiansen et al., 2013; Marques et al., 2017; Nguyen et al., 2015a). The majority of the proposed models have been based on applied carbon sources and microbial cultures (mixed or pure culture), the mass flow varied a lot regarding the storage

compounds and flow direction (Izadi et al., 2021b). Kristiansen et al., (2013) proposed a model describing the metabolism of *Tetrasphaera* in EBPR, highlighting its ability to utilize glucose as a substrate. Under anaerobic conditions, *Tetrasphaera* takes up glucose using poly-P as an energy source and glucose can be stored as glycogen. In subsequent aerobic conditions, the stored glycogen can be used for growth and for replenishing supplies of poly-P. Nguyen et al., (2015) demonstrated that certain PAOs, such as *Tetrasphaera*, can accumulate intracellular amino acids (e.g., glycine, glutamine, serine, alanine) under anaerobic conditions.. These intracellular metabolites can then be used to support the P-uptake aerobically. Moreover, *Tetrasphaera* shares some key metabolic pathways with *Ca. Accumulibacter*, such as tricarboxylic acid cycle (TCA) and poly-P degradation. Overall, representatives of *Tetrasphaera* are extremely versatile, capable of surviving in highly dynamic environments, and occur in substantial numbers in WWTPs. Therefore, the reliable, generic model is still missing, and there is no consensus on accepted biochemical transformation models for the *Tetrasphaera* within EBPR. Metabolic modelling through biochemical transformation characteristics based on microbial metabolism and prediction of bacterial activity can help provide useful information for optimization and design purposes (Oehmen et al., 2007a). Research has characterized the ability of *Tetrasphaera* to metabolize complex carbon sources and store glycogen in the anaerobic phase, however, further studies are needed to refine metabolic models for this group (Izadi et al., 2021).

Tetrasphaera models are directly relevant to models in EBPR processes, namely activated sludge models (ASM) and metabolic models (Lopez-Vazquez, Hooijmans, et al., 2009) . Oehmen et al. (2010) found that the anaerobic stoichiometry is identical for all PAO subgroups (PAO I and PAO II) but also noted key distinctions between PAOs and glycogen accumulating organisms (GAOs)

in their carbon storage mechanisms. Smolders et al. (1994) expanded the model of (Mino et al. (1998) and developed a detailed mechanistic model of PAO anaerobic metabolism with acetate as a single carbon source. According to this theory, PAO transports acetate across the cell membrane and converts it into acetyl-coa with the process energy of cleaving poly-P and releasing phosphate from the cell. The parameter represents the ATP required for the transport of 1 C-mmol acetate across the cell membrane (Filipe et al., 2001; Smolders et al., 1994). Acetylcoa formation in PAOs is influenced by pH but also depends on redox conditions and enzymatic activity. The origin of the reducing power (i.e., Nicotinamide adenine dinucleotide NADH) required for PHA synthesis has been debated by many authors, with Mino et al. (1998) supporting that it comes from internal glycolysis. Based on distinct biochemical properties, four independent clades of PAO have been identified using molecular techniques, as presented in **Table 2-2**.

Table 2-2:The functional clades of PAO distinguished based on distinct biochemical properties.

PAO type	Method of identification	Electron acceptors	Reference
PAO I	Electron acceptor	DO, NO ₃ > N ₂	Oehmen et al., 2010
PAO II	Electron acceptor	DO, NO ₂ > N ₂	Oehmen et al., 2010
PAO III	Electron acceptor	DO	Oehmen et al., 2010
PAO IV	Fermentation	DO	Oehmen et al., 2010

2.3.3 *DPAO in EBPR systems*

Various members classified as DPAOs have been identified and studied for their prevalence in laboratory-scale and full-scale plants. In full-scale EBPR plants, diverse microbial communities are present with key PAOs and DPAOs, including *Ca. Accumulibacter* (Qiu et al., 2019), *Halomonas* (H. Nguyen et al., 2012), *Tetrasphaera* (Liu et al., 2019; Zhao et al., 2022),

Dechloromonas (Petriglieri et al., 2021), *Ca. Microthrix* (Nierychlo et al., 2021). At the same time, the existence of competition groups of microbial communities such as GAOs, whose members include *Ca. Competibacter* (Rubio-Rincón et al., 2017), *Defluviicoccus* (Chen et al., 2022) have been reported.

Among the key microorganisms studied, *Tetrasphaera* has gained considerable attention in these recent studies due to its high abundance (Liu et al., 2019b; Sun et al., 2021; Zhang & Kinyua, 2020). In full-scale EBPR systems, *Tetrasphaera* has been reported to reach up to 30% abundance in some plants (Muszyński et al., 2015; Ong et al., 2014; Onnis-Hayden et al., 2020). However, its dominance relative to *Ca. Accumulibacter* varies depending on operational conditions, influent composition, and plant configuration. Stockholm-Bjerregaard et al. (2017) reported a high abundance of *Tetrasphaera*, constituting up to 35% of the biomass. Similarly, Herbst et al., (2019) identified *Tetrasphaera* using 16S rRNA in situ hybridization (FISH) to be the most abundant genus in Danish WWTP accounting for up to 30% of the activated sludge community. These findings were confirmed by a survey of 32 full-scale EBPR plants in 12 countries, where a higher abundance of *Tetrasphaera* in most plants was noted by 16S rRNA high-throughput gene sequencing (Dueholm et al., 2024). In the range from 1.3% to 11.9%. The recent MIDAS project, which surveyed EBPR bacterial communities across 12 countries and 5 continents, found *Tetrasphaera* to constitute approximately 4.60% of the microbial community. This suggests its significance in EBPR, prevailing other DPAOs like the *Dechloromonas* (2.84%), *Ca. Accumulibacter* (1.19%), *Ca. Microthrix* at 0.85% and *Halomonas* at 0.01% (Dueholm et al., 2024; Wu et al., 2019). However, the PAO community structure varies widely among EBPR plants, and the role of each organism is influenced by plant-specific factors. The use of Raman spectroscopy

technology for in-situ intracellular compound quantification detected a higher abundance of *Tetrasphaera*, *Ca. Accumulibacter*. in full-scale WWTPs in Denmark (Fernando et al., 2019a). Poland, for instance, exhibits a notably higher abundance of *Tetrasphaera*, as illustrated in the global summary in **Figure 2-9**- chosen for the case study.

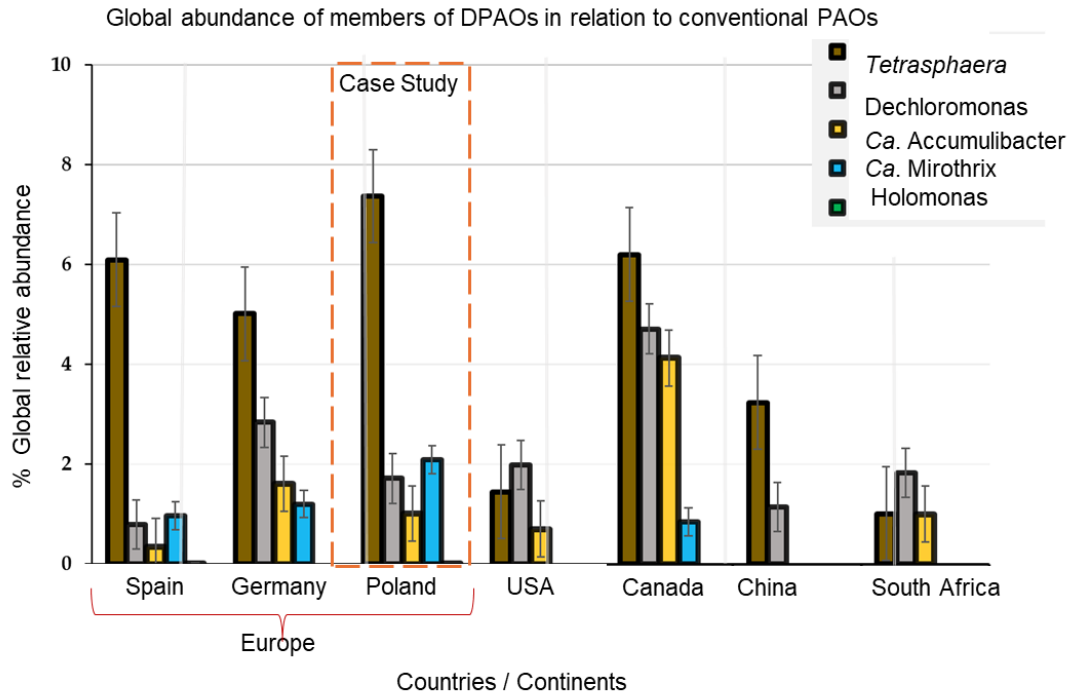


Figure 2-9:A summary overview of the global abundance of the DPAOs within the general microbial community in the EBPR system according to data from MIDAS in comparison to Poland’s WWTPs as the case study (Dueholm et al., 2024; Wu et al., 2019).

2.3.4 Implication of external carbon sources and EBPR performance

The limitation of biodegradable organic compounds in influent wastewater impedes EBPR performance due to competition among microorganisms (Ma et al., 2024). GAOs can concurrently grow in EBPR systems, competing with PAOs for carbon sources, while not contributing to P

removal (Izadi et al., 2021). To overcome this limitation, the application of alternative commercial carbon sources such as methanol, ethanol, acetic acid, sodium acetate, and glucose are being explored for the efficiency of the P-removal in EBPR (Tuszynska et al., 2019). Currently, the research community has focused on the identification of the carbon sources that can be metabolized by DPAOs i.e. *Tetrasphaera* to release P. The most frequently tested substrates were acetate, glucose, glutamate, glycine, and lactate. Moreover, *Tetrasphaera* exhibits the ability to assimilate a wider range of carbon sources including amino acids, sugars, and higher VFAs under anaerobic conditions (Kong et al., 2008; Kristiansen et al., 2013; Nguyen et al., 2011). Fermentation of amino acids and sugars, subsequent storage of either amino acids or glycogen anaerobically and use of internally stored substrates as an energy source for aerobic P uptake by *Tetrasphaera* has been demonstrated in numerous studies (Kristiansen et al., 2013; Marques et al., 2017; Nguyen et al., 2015). For instance, the laboratory results of an experiment with a *Tetrasphaera-enriched* culture fed only with casein hydrolysate as the carbon source showed that the *Tetrasphaera* metabolized amino acids and was responsible for most of the aerobic removal of phosphorus (Marques et al., 2017). Additionally, P uptake and release have been realized in acetate for the aerobic P-uptake as opposed to the glucose and other organics including formic acid, propionate, butyric acid, pyruvate, lactate, ethanol, glucose, oleic acid, aspartic acid, glutamic acid, leucine, glycine, thymidine, and mixed amino acids (Kong et al., 2005). In some cases, *Tetrasphaera* showed different preferences for the consumption of carbon sources in their different isolates in achieving P release/uptake. The use of glucose and glutamic acid utilization was performed under anaerobic conditions by Tet3-19 isolates despite no P uptake (Nguyen et al., 2015). Species *T. Australiensis*, *T. Japonica* and *T. Elongate* responded positively to acetate, while propionate in addition to acetate favored species *T. Jenkinsii*, *T. Vanveenii*, and *T. Veronensis* (Maszenan et al.,

2000). In the studies by Marques et al., (2017) glucose, aspartate, glutamate, and glycine were explored with an enriched *Tetrasphaera* culture. The results from FISH-MAR showed that *Tetrasphaera* presented P-uptake anaerobically with each of these four carbons solely. In terms of intracellular compounds, glycogen has been considered regarded one important energy storage compound in *Tetrasphaera* (Kristiansen et al., 2013). Kong et al. (2005) and Nguyen et al. (2011) demonstrated that mixed culture with predominance of *Tetrasphaera* was able to consume glucose anaerobically to promote P uptake aerobically. The experiments conducted in a pure culture of *Tetrasphaera elongata*, demonstrated its ability to utilize glucose as a carbon source and its P uptake mechanism differs from that of classical PAOs like *Ca. Accumulibacter* (Kristiansen et al., 2013). Moreover, glycogen production in the anaerobic phase was also observed in another study not only with glucose, but also glutamate, and aspartate supplied as an external carbon source (Marques et al., 2017).

To summarize, *Tetrasphaera* differs from *Ca. Accumulibacter* in its metabolism; while some *Tetrasphaera* species do not primarily rely on PHA accumulation, others have been shown to store small amounts of PHA under certain conditions. Instead, *Tetrasphaera* can ferment amino acids and sugars and store intracellular glycogen or other energy reserves anaerobically, which it utilizes during P uptake under aerobic conditions.

2.3.5 Configurations of the EBPR systems

To address carbon limitations and other operation efficiency the configurations of the EBPR systems have been under evolution both in the main and side streams (Cheng et al., 2024). The common feature of conventional side-stream configurations was the sole treatment of return sludge anaerobically combined with chemical precipitation, while in main-stream configurations all

mixed liquors flow through a sequence of anaerobic, anoxic, and/or aerobic conditions for P removal (Egle et al., 2016). Modern mainstream EBPR systems by design, are meant to avail conditions that sustain the parallel processes of N and P removal (D. Wang et al., 2019). Achieving optimal operating conditions for the biological processes, such as P release and uptake, nitrification, and denitrification, requires consideration of specific environmental conditions within anaerobic, aerobic, and anoxic zones. Due to the limited resources and stricter operational regulations, continuous modernization, and reevaluation of the BNR configurations have been observed (Izadi et al., 2020). A successful EBPR process is dependent on the presence of readily biodegradable organic carbon and P, an anaerobic zone prior to the aerobic zone, and enough nutrients since it relies on the growth and selection of PAOs which can store orthophosphate in excess.

Earlier configurations achieved P removal with > 90% efficiency by changing the sequential steps in the specific configuration, a low P removal efficiency was achieved, leading to an understanding of the necessary conditions of EBPR (J. Barnard, 1974). The availability of COD favors heterotrophic activities (PAO, denitrifies) under aerobic/anoxic conditions, while nitrification takes place in the aerobic zone. P removal depends on several conditions that are essential for the microbial metabolism of PAO (Alasino et al., 2008) . However, simultaneous N and P removal presents challenges because the anaerobic zone primarily selects for PAOs by promoting P release. However, the presence of enables P uptake to occur under anoxic conditions, facilitating concurrent N and P removal (Guerrero et al., 2011). In general, nitrification and denitrification may cause detrimental impact on EBPR due to the presence of NO_2^- and NO_3^- in the external recycle stream which enters the anaerobic zone, leading to a competition from denitrifying

heterotrophic bacteria growth which outcompete PAO. However, DPAOs can couple denitrification with P uptake, mitigating this impact under specific conditions. As indicated by (Conidi et al., 2018), the most common cause of instability in EBPR systems is the underestimated size of anaerobic zones, often less than 10% by mass of solids, whereas 15-25 % is recommended for a stable operation.

Currently, the main direction toward increasing EBPR stability is the implementation of the novel sidestream EBPR (S2EBPR) configurations. With respect to the existing bioreactor configurations, providing a side stream fermentation zone (S2EBPR reactor) of recirculated activated sludge (RAS) or mixed liquor fermentation has emerged as a prospective solution to solve this issue. The main potential advantages offered by these solutions are increased anaerobic mass fraction and the potential for selective GAO suppression (Onnis-Hayden et al., 2020).

Due to its metabolic versatility, including the ability to ferment various organic compounds and denitrify while simultaneously taking up P, *Tetrasphaera* has been identified as a significant contributor in some S2EBPR systems (Bi et al., 2025). However, it should be noted that currently available data from the S2EBPR operations are limited, due to a narrow range of the operational conditions studied to date. As pointed by Wang et al.,(2019) more extensive data are highly required to develop models specifically dedicated to S2EBPR systems. Makinia & Zaborowska, (2020) and Tooker et al., (2017) highlight a more comprehensive description of the mainstream systems while examples of S2EBPR configurations have also been presented (Otieno et al., 2022).

2.3.6 Implications of DPAOs on EBPR configuration and operation

The identification and characterization of DPAOs play a vital role in optimizing EBPR in WWTPs (R. Liu et al., 2019a). Maximizing the P removal fraction achieved in anoxic conditions can

significantly reduce the operational costs of EBPR systems. Several different process configurations are available, in which both P and N removal are combined (Oehmen et al., 2007a). The early studies by Barker & Dold (1996) and (Meinhold et al., 1999) highlighted two diverse groups of PAOs, including aerobic PAOs (aPAOs) and denitrifying PAOs (DPAOs) and reported their differences. DPAOs differ from aPAOs by their ability to use NO_3^- and/or NO_2^- as electron acceptors under anoxic conditions, whereas aPAOs rely solely on DO.

Later, Oehmen et al., (2010) postulated that DPAOs have different denitrification capabilities and can be classified based on their reduction abilities towards NO_2^- or NO_3^- . Different PAO types, such as Type I and II *Accumulibacter* and various *Tetrasphaera* species, show distinct preferences for electron acceptors and carbon sources, impacting their metabolic roles in EBPR systems (Camejo et al., 2016). Type I primarily reduces NO_3^- to NO_2^- , while Type II further reduces NO_2^- to N_2 gas.

The representatives of *Tetrasphaera* reflect differential preferences for electron donors and acceptors. While genera *T. Australiensis*, *T. Japonica*, *T. Elongata* show similar metabolic properties to Type I with acetate as the key carbon source, whereas the aerobic pathway and preference of propionate are specific features of *T. Jenkinsii*, *T. Vanveenii* and *T. Veronensis* (R. Liu et al., 2019a). **Table 2-3** summarizes these preferences, showing the metabolic versatility and ecological roles of key microbial groups.

Table 2-3:Summary of preferable electron acceptors by the main functional bacterial groups involved in EBPR.

Bacterial functional group	Electron acceptors
APAO	DO
DPAO (I)	$\text{NO}_3^- \rightarrow \text{NO}_2^- \rightarrow \text{N}_2\text{O} \rightarrow \text{N}_2$
DPAO (II)	$\text{NO}_2^- \rightarrow \text{N}_2\text{O} \rightarrow \text{N}_2$
GAO	$\text{NO}_3^- \rightarrow \text{NO}_2^- \rightarrow \text{N}_2\text{O} \rightarrow \text{N}_2$ $\text{NO}_3^- \rightarrow \text{NO}_2$
<i>T. Australiensis</i> <i>T. Japonica</i> <i>T. Elongata</i>	$\text{NO}_3^- \rightarrow \text{NO}_2^- \rightarrow \text{N}_2\text{O} \rightarrow \text{N}_2$
<i>T. Jenkinsii</i> , <i>T. Vanveenii</i> , <i>T. Veronensis</i>	DO

* Reduction abilities towards NO_2^- and NO_3^- of the EBPR microbes.

Mino et al., (1998) highlights that the denitrification potential of PAOs is vital when designing activated sludge systems. In this context, two-stage anaerobic - anoxic configurations have gained attention, as they aim to enhance DPAO activity in EBPR processes by supporting P uptake under anoxic conditions and improving carbon use for denitrification (Izadi et al., 2020). These systems are typically designed with larger anoxic zones than aerobic ones. Nevertheless, DPAOs showed variable performance, contributing 0 - 25% to denitrification and 0-62% to P removal. This may be due to their reduced ability to metabolize intracellular carbon sources like PHA or glycogen compared to aerobic PAOs (Z. Hu et al., 2002; Tuszynska et al., 2019).

The presence of other microorganisms, like GAO, in EBPR systems is an additional, prominent issue that can affect EBPR performance (Meng et al., 2020). *Defluviicoccus* and *Candidatus Competibacter* are recognized as the most dominant GAOs in WWTPs, with relative abundances ranging from 36.0–42.6% and 15.3–24.9%, respectively (Maszenan et al., 2022; Song et al., 2022). The predominance of *Defluviicoccus* is strongly associated with a higher propionate to

acetate ratio in the feed. While *Defluviicoccus* exhibits a preference for propionate, its uptake rates are lower than those of *Ca. Accumulibacter*, but higher than those of *Ca. Competibacter* (Song et al., 2022). Notably, it remains unclear which factors govern the changes in the known GAO community composition as well as competition with PAOs, including solids retention time (SRT) (Onnis-Hayden et al., 2020), C to P ratios (J. Li, Zhu, Lv, Hu, et al., 2024) and available carbon sources (Shen et al., 2017; W. Tian et al., 2010), which have been evidenced to be associated with GAO shifts.

The challenge of identifying PAO and GAO metabolisms is merely based on the functional genes related to phenotype characteristics, such as the ability to cycle P, polyhydroxyalkanoates (PHA), and/or glycogen, as intracellular storage materials within bacterial cells (Roy et al., 2021). GAO's prevalence might have been overestimated in some studies due to laboratory conditions favoring acetate-based enrichment (Aghilinasrollahabadi et al., 2024). Numerous microbial characterizations had been conducted in a laboratory or pilot scale, where a widespread practice was the application of enormous concentrations of acetate, which favored the growth of GAO. Similar suppositions have been formulated (Nielsen et al., 2019).

2.4 Factors affecting the occurrence and DPAO in EBPR systems.

Although certain factors affecting DPAO occurrence remain poorly understood, environmental and operational parameters - namely influent composition (Nguyen et al., 2023; Schuler & Jenkins, 2002), dissolved oxygen (DO), pH, and temperature (Chen et al., 2017; Onnis-Hayden et al., 2020) are recognized as key influencers (Chen et al., 2023; Zheng et al., 2014).

2.4.1 *Temperature*

Temperature plays a critical role in determining microbial growth, influencing the structure of microbial communities and the rates of enzyme catalyzed reactions, thereby affecting the operational efficiency of EBPR (Tsertou et al., 2024). Temperature range of 25 to 32 °C has been reported suitable for the tropical EBPR and effective in achieving P removal efficiencies above 95% Ong et al., (2014). It is hypothesized that PAOs are less competitive than GAOs at higher temperatures (Ong et al., 2016). Moreover, PAO is deemed to have important advantages over GAO at low and moderate temperatures (below 20 °C), while temperatures higher than 20 °C are more beneficial for GAO (Lopez-Vazquez, Hooijmans, et al., 2009; Ong et al., 2016). Increasing temperatures to 24°C are generally considered optimal for EBPR efficiency (Sayi-Ucar et al., 2015). Chan et al., (2020) reported higher (86%) P removal efficiency at 20 °C in EBPR systems, but performance declined to 71% at 15 °C and is completely lost at 10 °C. Below 10 °C, microbial activity, including DPAO function, becomes significantly inhibited (Lopez-Vazquez, Oehmen, et al., 2009).

Several studies have demonstrated that EBPR can be optimized at tropical temperatures through acclimatization and operational modifications (Bertanza et al., 2020; Gebremariam et al., 2011; Nielsen et al., 2019; Winkler et al., 2011; Zheng et al., 2014). Conversely, other research indicates that high temperatures (35°C to 40°C) may lead to a decline in EBPR performance (Poh et al., 2021). Qiu et al., (2019) and Wang et al., (2020) reported the possibility of operating the EBPR at higher temperatures (28 °C - 32 °C), in line with a previous study by (Ong et al., 2014), where high efficiency of the EBPR was realized. Similarly, (Law et al., 2016) reported effective EBPR in full-scale tropical WWTPs predominant with *Accumulibacter* populations. In addition, (Shen et

al., 2017) also described an efficient laboratory-scale EBPR system operated at 30 °C to 32 °C, using acetate as the only carbon source, having a community with high *Ca. Accumulibacter* abundance. Qiu et al., (2019) highlighted that the three tropical treatment plants tested in Singapore exhibited high in situ EBPR activity, with *Ca. Accumulibacter* being the main active PAO among the diverse PAO community at temperatures above 28 °C. Poh et al., (2021) indicated that a brief excess of 35 °C will not adversely affect the performance of the EBPR. **Table 2-4** below summarizes typical abundance patterns of PAOs (*Accumulibacter*) and GAOs (*Competibacter* and *Defluviicoccus*) under various temperature conditions in EBPR systems.

Table 2-4: Temperature dependent abundance trends of PAOs and GAOs in EBPR Systems

Temperature	<i>Accumulibacter</i> (PAO)	GAOs (e.g., <i>Competibacter</i> , <i>Defluviicoccus</i>)	Comments	Reference
10–15°C	Moderate to Low	Low to Moderate	Slower kinetics for both; PAOs may still dominate if acclimated.	(Erdal et al., 2006; Otieno et al., 2022)
20–25°C	High	Moderate	Optimal for PAOs; EBPR most efficient in this range.	(Guo et al., 2018)
25–30°C	Declining	Increasing	Shift begins; GAOs begin to outcompete PAOs.	(Guo et al., 2018; Poh et al., 2021)
>30°C	Low	High	GAOs dominate; risk of EBPR failure if system isn't controlled.	(Qiu et al., 2022)

2.4.2 *pH and DO*

pH and dissolved oxygen (DO) are critical factors influencing the performance of EBPR systems. Although microorganisms in WWTPs can grow over a wide range of pH 6-9, the microbial community compositions are remarkably affected by variation control is a promising strategy in increasing the reliability of biological P removal systems (Filipe et al., 2001). Studies consistently show that higher pH values, typically around 7.5 to 8.5, favor the growth and activity of PAOs, leading to improved P removal (Guo et al., 2017; Oehmen, Teresa Vives, et al., 2005), while lower pH encourages the proliferation of GAOs, which can reduce EBPR efficiency. A controlled laboratory study investigated the P removal capabilities of *Tetrasphaera*-enriched polyphosphate-accumulating cultures under varying pH conditions. The results demonstrated that at pH 8.0, P release and uptake rates were over three and two times higher, respectively, compared to pH 6.0. P uptake peaked at 15.4 mg P/g-MLVSS at 25°C, pH 7, and DO 2.0 mg/L. These findings suggest that alkaline conditions significantly enhance the metabolic activity and EBPR performance of *Tetrasphaera* populations (P. Y. Nguyen et al., 2023). In an enriched *Tetrasphaera*-rich sludge study on pH factor, an increase between the pH 6 to 8 was reported to favor P-release and P-uptake (Nguyen et al., 2023). Higher pH levels (above 8.2) have been associated with a reduction in P-uptake (Serralta et al., 2006). Additionally, Wang et al. (2013) reported P removal increased with the increase of pH from 6.6 to 7.8 whereas higher levels of pH increase from 7.8 to 8.2 slowed down the P-removal. The pH of 7.8 equally recorded an elevated abundance of the PAOs, justifying the 1.7 times higher P removal compared to the pH of 6.6 in the same research. In the study of Filipe et al. (2001), PAOs removed acetate faster than GAOs at pH greater than 7.5 with increased P removal.

Other studies confirmed that higher pH values (7.5–8.5) generally favor PAO activity and can inhibit GAO proliferation under certain conditions (Lopez-Vazquez et al., 2009; Oehmen et al., 2007; Schuler and Jenkins, 2003). However, the extent of GAO inhibition is influenced by other factors such as carbon source and system configuration (Lopez-Vazquez, Oehmen, et al., 2009). There is now strong evidence that the stability of EBPR systems can be improved by increasing the pH of the anaerobic zone, thus creating conditions under which PAOs can uptake acetate faster than GAOs. Recently, (Kang et al., 2019) found that a pH greater than or equal to 7.5 improved P removal from 90.8% to 99.6%, while a pH below 7.0 realized only about 63.1%. Further research on the inhibition of GAO proliferation known competitors to the PAOs on alkaline conditions has been reported (Izadi et al., 2021a; Weissbrodt et al., 2017). GAO activity has been observed within a pH range of 7.0–8.0, which partially overlaps with the favorable range for PAOs (Mao et al., 2016; Weissbrodt et al., 2017; Filipe et al., 2001).

Dissolved oxygen also plays a role, with studies indicating that moderate DO concentrations (around 2.0 mg L⁻¹) under aerobic conditions support effective P uptake by PAOs, while too low or too high DO can negatively impact EBPR performance and equally P uptake peaked at 15.4 mg P/gMLVSS at 25°C, pH 7, and DO 2.0 mg L⁻¹ (Nittami et al., 2011). The **table 2-5** below summarizes the influence of pH and dissolved oxygen (DO) on EBPR performance.

Table 2-5: Influence of pH and Dissolved Oxygen on EBPR Performance

Parameter	Optimal range	Effect on PAOs	Effect on GAOs	EBPR performance	Reference
pH	7.0–7.5	promotes PAO activity; balanced VFA uptake and phosphate cycling	inhibits GAO competition slightly	optimal P removal	(Mino et al., 1998b)
	<6.5	suppresses PAO metabolism and poly-P synthesis	favors GAO growth	reduced EBPR efficiency; risk of failure	(Serralta et al., 2006)
	>8.0	can enhance <i>Tetrasphaera</i> PAO activity	varies; may inhibit some GAO species	Enhanced P removal in some cases, but system-dependent	(W.-T. Liu et al., 1996)
DO	1.5–2.5 mg/L	supports aerobic P uptake by PAOs	limited impact	Efficient EBPR with low energy use	(Nittami et al., 2011)
	<0.5 mg/L (low DO)	Inhibits aerobic PAO activity; favors DPAOs in anoxic zones	some GAOs tolerate low DO; possible shift in competition	Potential EBPR instability unless DPAOs are active	(X. Yu et al., 2021)
	>3.0 mg/L (high DO)	Enhances PAO aerobic uptake but increases energy costs	minor effect	stable EBPR but less energy-efficient	(Qin et al., 2023)

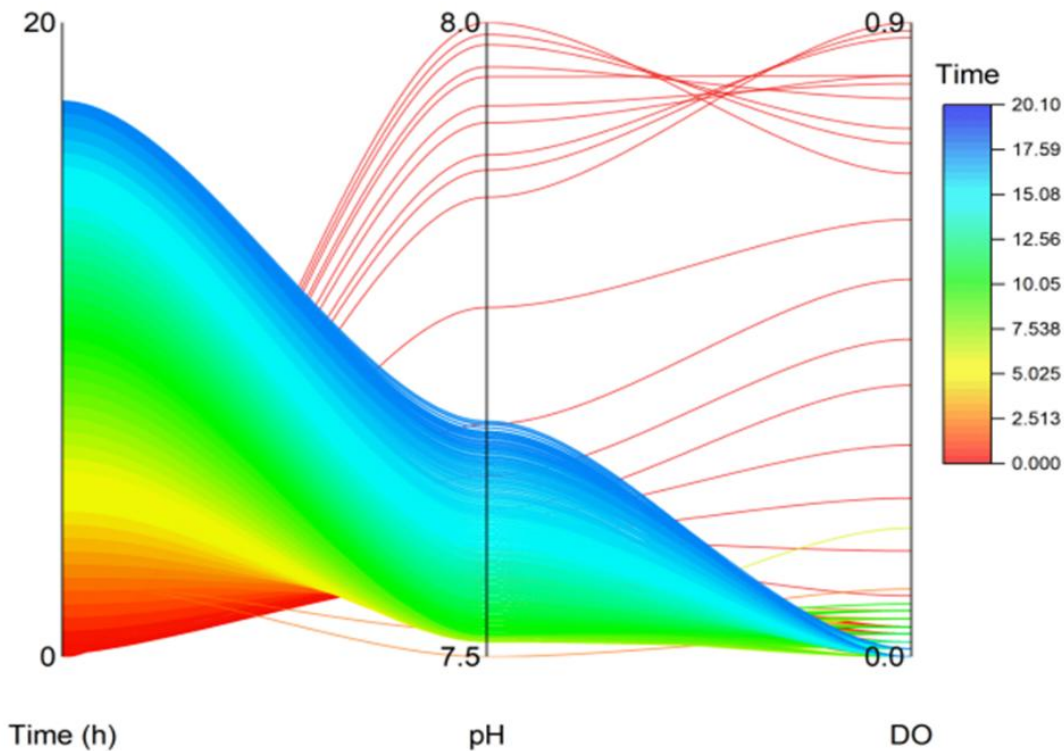


Figure 2-10: The pH and dissolved oxygen (DO) variance to EBPR performance.

2.4.3 *Influent wastewater characteristics*

Organic substrates are important constituents of influent wastewater characteristics that potentially boost the growth and metabolism of DPAOs. External carbon sources provide the required VFAs vital to the EBPR performance due to the limited substrate for microbial activities (Xie et al., 2017; Zeng et al., 2016). Due to this carbon limitation, the high cost of VFAs, and the need for a stable EBPR, alternative applications of industrial VFAs that are cost-friendly are attracting attention. The availability of diverse organic carbon sources, rather than specific electron acceptors, plays a crucial role in promoting the P removal activity of *Tetrasphaera* (J. Chen et al., 2025; Shen & Zhou, 2016). While a study of Kong et al. (2005) suggested that *Tetrasphaera* may be more

adaptable in certain industrial WWTPs, the long-term study of Mielczarek et al. (2013) indicated only weak correlations between its abundance and the proportion of industrial wastewater in influent streams. . That study was focused on the correlation of the abundance of *Tetrasphaera* and wastewater characteristics, process design, and operation. The data of over 3 years from 28 Danish WWTPs showed weak correlations with the increased amount of industrial wastewater in the feeding. A balanced acetate-to-propionate ratio (e.g., 75-25% or 50-50%) can create favorable conditions for PAO activity over GAOs. However, additional factors such as temperature, pH, and operational parameters also significantly influence PAO-GAO competition, and elevated temperatures (30°C) do not universally ensure PAO dominance (Lopez-Vazquez et al., 2009).

The capability to metabolize and internally store many carbon compounds provides *Tetrasphaera* enormous adaptability to the dynamic conditions of substrate availability specified for the WWTPs (F. A. Herbst et al., 2019). Such physiological plasticity, may gain *Tetrasphaera* advantage over *Ca. Accumulibacter*, which is highly dependent on acetate availability under anaerobic conditions (Schuler & Jenkins, 2002a).

2.4.4 Presence of DO and NO_2^-

NO_2^- as an intermediate product of nitrification and denitrification processes, can accumulate in the bioreactor chambers (Vargas et al., 2011). Numerous studies on NO_2^- utilization have been mainly focused on its inhibitory effect on aerobic and anoxic P uptake rather than on the potential use of NO_2^- as an electron acceptor (Hou et al., 2024; Rey-Martínez et al., 2021; Sin et al., 2008; Zhou et al., 2012). (Zekker et al., 2021) investigated nitrite inhibition for the DPAOs and noted that indeed NO_2^- production negatively affects anoxic P uptake. The inhibitory effect of NO_2^- on P removal in enriched DPAO culture systems and bioreactors has been previously reported

depending on the concentrations amounts of NO_2^- . Meinhold et al., (1999) reported that nitrite concentrations up to 5 mg N L^{-1} had no significant impact on anoxic P uptake. However, at 8 mg N L^{-1} , partial inhibition was observed, while at concentrations above 60 mg N L^{-1} , P-uptake was almost completely suppressed (Guisasola et al., 2009). (X. Wang et al., 2024) concurred that only a small amount of NO_2^- in anoxic P uptake improves P uptake efficiency and only through the use of polyhydroxyalkanoates (PHA) oxidation, which is accompanied by biomass growth and glycogen regeneration. Furthermore, Zeng et al. (2014) reported that while high NO_2^- concentrations ($>10 \text{ mg N L}^{-1}$) suppress DPAO activity, moderate levels ($2.25 - 5 \text{ mg N L}^{-1}$) can still support denitrifying P removal. Excessive NO_2^- accumulation can lead to a decline in DPAO performance, but complete inhibition occurs only at substantially higher concentrations.

Table 2-6: Impact on P- removal under different NO_2^- levels (mg N L^{-1}) (Zekker et al., 2021; Zeng et al., 2014)

Conc. of NO_2^- (mg N/L)	Level	Impact on P-removal	Reference
$>5 \text{ mg N. L}^{-1}$	high	inhibition	(Coma et al., 2012)
$<5 \text{ mg N. L}^{-1}$	low	non-inhibition	
2 mg N.L^{-1}	high	severe inhibition	(Saito et al., 2004)
$> 6 \text{ mg N.L}^{-1}$	high	complete inhibition	
$0.00047 \text{ mg N.L}^{-1}$	Low	inhibition	(W. Zeng et al., 2014)
2.25 mg N.L^{-1}	high	suppressed P- removal	
$5 \text{ mg NO}_2\text{-N.L}^{-1}$	Low	no inhibition	(Meinhold et al., 1999)
$8 \text{ mg NO}_2\text{-N.L}^{-1}$	high	severe inhibition	
$60 \text{ mg NO}_2\text{-N.L}^{-1}$	high	inhibition	(Guisasola et al., 2009)

At the same time, the concentration of DO, as an operational factor, has been found highly impactful on EBPR performance and PAO dominance. Izadi et al., (2021) achieved effective P-removal at low DO concentrations ($0.5\text{-}0.8\text{ mg O}_2\text{L}^{-1}$) suggesting that PAOs can maintain activity under these conditions. However, the selective advantage of PAOs over GAOs at low DO levels depends on additional factors such as carbon source availability and competition dynamics. The presence of DO or NO_2^- or NO_3^- can compete with PAOs for available VFAs, potentially impacting P removal (Zuthi et al., 2013). However, effective system design, such as optimized anaerobic-aerobic cycling, can mitigate this competition and sustain PAO activity. At low DO levels, PAOs and GAOs can exhibit varying competitive dynamics. While PAOs can remain active under limited DO, certain GAOs (*Ca. Competibacter*) also persist under microaerobic conditions, depending on substrate availability and operational parameters (Oehmen, Yuan, et al., 2005a). Excessive aeration can contribute to instability in P removal by promoting GAO competition, particularly in systems with imbalanced carbon availability. Oehmen et al. (2010) and Chen et al. (2014) observed that maintaining DO at $0.5\text{ mg O}_2\text{L}^{-1}$ allowed for EBPR activity, but excessively low DO can also risk incomplete P uptake.

2.5 Nitrous oxide (N_2O) gas emissions in EBPR processes

Greenhouse gases (GHG) emanating from WWTP i.e nitrous oxide (N_2O), carbon dioxide (CO_2), and methane (CH_4) in WWTP are as a result either emitted directly or by indirect means (Koutsou et al., 2018; Mannina et al., 2016; Shang et al., 2024). Direct emissions in WWTPs are primarily driven by CH_4 from anaerobic digestion or sewer systems, and N_2O from nitrification and denitrification in the bioreactors. CO_2 emissions are associated with microbial respiration and they are considered biogenic and are not typically classified as direct GHG emissions (Valenzuela et al.,

2021; Zhu et al., 2022). While both N_2O and CH_4 are produced during biological treatment, the emissions do not necessarily occur only from these biological treatment processes. Indirect emissions are associated with energy consumption, physical - chemical treatment processes, and other additional handling operations (Khalil et al., 2024). The share of direct emissions from biological processes in WWTPs often surpasses energy-related indirect emissions, though the exact proportions depend on site-specific factors (Maktabifard et al., 2023). N_2O emissions often constitute a significant proportion of direct GHG emissions from nitrogen removal processes, while CH_4 emissions dominate in systems with anaerobic digestion or poorly managed sewer networks (Valenzuela et al., 2021; Khalil et al., 2024). However, the exact ratios depend on site-specific conditions. Globally, N_2O emissions from WWTPs are estimated to contribute between 3.0–10.2% of total WWTP GHG emissions. However, emissions may rise in the future due to increased treatment demand and insufficient mitigation measures (Maktabifard et al., 2023; Zhang et al., 2024). This higher contribution of the N_2O direct emission has raised greater concern among researchers and stakeholders with efforts towards its mitigation. The adversities associated to N_2O emissions pose a significant challenge to the net effect in global warming and climate change (Solís et al., 2022). In the EBPR, the management measures and control for N_2O production are largely based on the optimization of operating parameters during biological processes (nitrification and denitrification) that dictate the pathways to the emitted gas. The nitrification process is commonly regarded as a two-step process of oxidation of $\text{NH}_4\text{-N}$ to $\text{NO}_3\text{-N}$ by two groups of aerobic autotrophic bacteria and one group of archaea. In the first step nitrification, autotrophic bacteria and archaea from the dominate of the AOB and AOA are responsible for the oxidation of $\text{NH}_4\text{-N}$ to $\text{NO}_2\text{-N}$ (Fernandes et al., 2013). Dominant AOB genera include can be found among the *Betaproteobacteria*, such as *Nitrosomonas*, *Nitrosospira*, and *Nitrosovibrio*, and

Gammaproteobacteria, such as *Nitrosococcus*. Dominant AOA genera, including *Nitrosopumilus*, *Nitrososphaera*, *Nitrosotalea*, *Nitrososphaera* and *Nitrosocaldus*, belong to the *Thaumarchaeota* phylum (Pester et al., 2012; Daebeler et al., 2018)

On the other hand, denitrification is defined as the microbial reduction of inorganic nitrogen forms (NO_3^- , NO_2^- , NO , N_2O) into (N_2) gaseous (Kowal et al., 2022). Green et al., (2010) found that five genera of converting $\text{NO}_3\text{-N}$ to N_2 gas. Most denitrifying bacteria present in the environment are heterotrophic organisms, such as *Paracoccus denitrificans* and various *Pseudomonads* that use organic carbon in anoxic conditions with either NO_3^- or NO_2^- as the final electron acceptor (Gong et al., 2013). Moreover, autotrophic denitrifiers have also been identified as *Thiobacillus denitrificans* (Harry R. Beller et al., 1977). In other cases, some autotrophic microorganisms use inorganic compounds, such as thiosulfate or thiocyanate, as electron donors to reduce NO_3^- to NO_2^- then to N_2 gas (Broman et al., 2017). Ji et al., (2015) observed that nitrate reductase is vital for aerobic denitrifiers and *NapA* gene could be the proof of aerobic denitrifiers, mainly belonging to *Alpha*, *Beta*, and *Gamma-Proteobacteria*.

Broadly, the pathways to N_2O emissions in BNR systems are defined by actions of microbial activities in aerobic or anoxic conditions where nitrification and heterotrophic denitrification biological processes take place respectively. This far there are three main biological N_2O emissions pathways documented in many research namely: nitrifier nitrification pathway, nitrifier denitrification pathway, and heterotrophic denitrification pathway (Kampschreur et al., 2009).

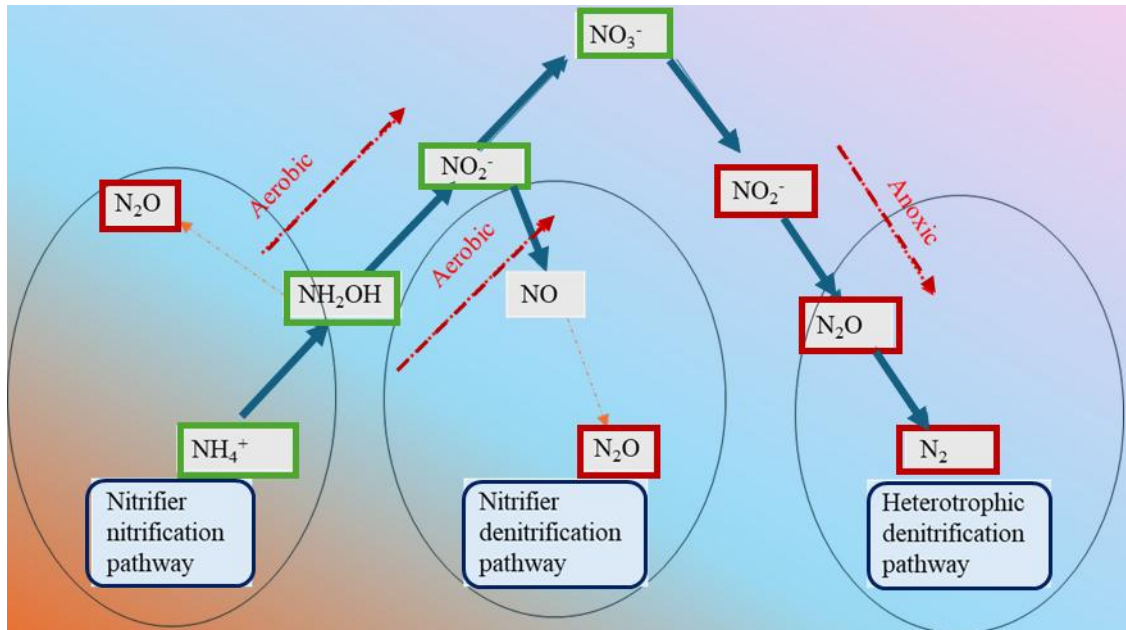
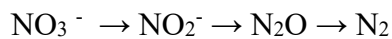


Figure 2-11: N₂O production pathways (Al-Hazmi et al., 2023).

The latter involves four reduction steps from nitrate (NO₃⁻) to molecular nitrogen (N₂) via nitrite (NO₂⁻), nitric oxide (NO), and nitrous oxide (N₂O), (Al-Hazmi et al., 2023b; Wang et al., 2021).



The process involves the enzymes nitrate reductase (Nar), nitrite reductase (Nir), nitric oxide reductase (Nor), and nitrous oxide reductase (Nos) (Hallin et al., 2018), and it is regulated to maintain the two toxic compounds, NO₂⁻ and NO, at low levels (Wang et al., 2021). It is the nitrous oxide reductase (Nos) that is the only enzyme known to reduce N₂O and the lack of its genome in some organisms leads to the emission of the intermediate N₂O as the end-product of the denitrification rather than N₂ (Carvalho et al., 2007).

The NH₂OH oxidation pathway is largely catalyzed by the autotrophic ammonia-oxidizing bacteria (AOB) and ammonia-oxidizing archaea (AOA) (Al-Hazmi et al., 2023). Bioreactors can be responsible for 90% of N₂O production in WWTPs, but the actual contribution varies depending

on process configurations and operational parameters (Campos et al., 2016). The driving determinants for the denitrification enzymes and the process kinetic rates are limiting (dissolved) oxygen concentrations (DO) and the availability of anoxic (NO_3^- , NO_2^- , and NO) terminal electron acceptors (Vieira et al., 2018). The type of nitrogen electron acceptor available strongly affect the N_2O to N_2 production ratio and consequently the emissions of N_2O from WWTPs. For instance, Ribera-Guardia et al. (2016) highlighted NO_2^- accumulation as a factor influencing N_2O production by GAO.

3. MATERIAL AND METHODS

3.1 Preliminary study and selection of case study WWTP

The Pomeranian region of Poland, located along the Baltic Sea belt, is home to a diverse range of WWTPs with varying capacities, configuration, and operational practices. To identify a suitable case study for in-depth investigation of microbial dynamics and EBPR performance, four major biological nutrient removal (BNR) facilities were screened: Gdynia Debogórze (GD), Gdańsk Wschód (GW), Słupsk (SL), and Swarzewo (SW) (**Figure 3-1**). All the WWTPs are in compliance with the effluent criteria of the European Union Urban Wastewater Directive (91/271) for large WWTPs, including a total nitrogen (TN) concentration of 10 mgN L^{-1} and a total phosphorus (TP) concentration of 1 mgP L^{-1} . The goal was to select a representative facility exhibiting a strong denitrifying polyphosphate-accumulating organism (DPAO) presence for subsequent laboratory-scale experimentation.

Detailed technical and operational parameters for each plant are summarized in **Figure 3-1**.

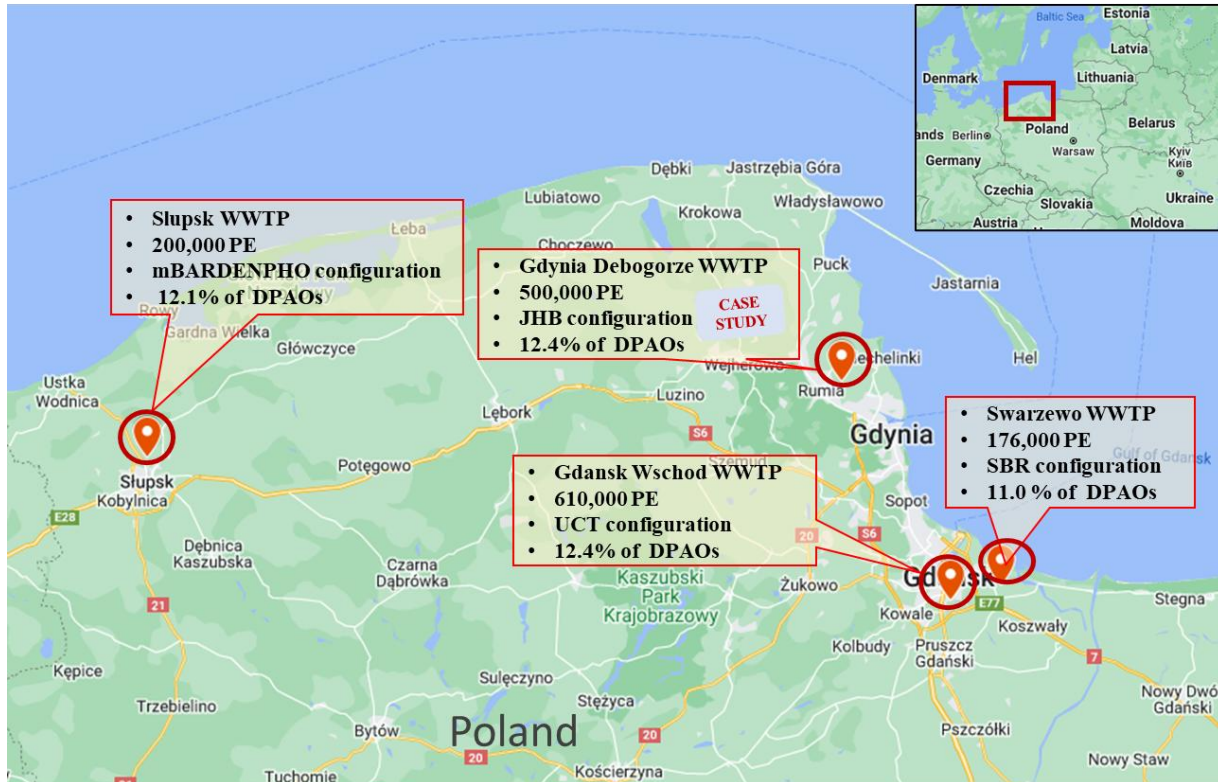


Figure 3-1:Geographic location and key characteristics of the four surveyed WWTPs in the Pomeranian region of Poland.

Table 3-1: The four WWTPs in the Pomeranian region of Poland by location , size , and configuration

WWTPs	Size [PE]	System configuration	Location [Latitude ; Longitude]
Gdansk Wschod(GW)	610,000	UCT	Poland [54.34 N, 18.75 E]
Gdynia Debogorze (GD)	550,000	JHB	Poland [54.58 N, 18.43 E]
Słupsk (SL)	200,000	mBARDENPHO	Poland [54.49 N, 17.03 E]
Swarzewo(SW)	176,800	SBR	Poland [54.49 N, 17.03 E]

To evaluate the microbial communities at each plant, mixed liquor samples (approximately 50–100 mL) were periodically collected over a one-year period from the bioreactors. Total genomic DNA was extracted from these samples, followed by high-throughput sequencing of the 16S rDNA gene fragment to characterize microbial community composition.

Among the four surveyed facilities, GD exhibited the highest relative abundance of DPAOs in relation to ordinary heterotrophic organisms (OHOs), indicating favorable operational conditions for P removal processes. This microbial profile, combined with its operational scale and system configuration, provided a strong rationale for selecting GD as the case study site for subsequent laboratory experiments and process optimization analyses. The microbial results for the selection are outlined in the results section (**Figure 4.1**).

3.2 Dębogórze WWTP – case study facility

The biomass used in the laboratory-scale experiments was obtained from the selected case study facility. “Dębogórze” WWTP. The plant serves a major catchment area comprising the cities of Gdynia, Rumia, Reda, Wejherowo, and surrounding municipalities including Puck, Kosakowo, Szemud. The treated wastewater is ultimately discharged into the Puck Bay, part of the Baltic Sea, through a 9 km long collector, which emphasizes the environmental importance of maintaining high treatment standards to protect marine ecosystems.

First commissioned in 1964 for mechanical treatment, the plant was upgraded with the addition of biological treatment using the activated sludge process. A major upgrade in 1997 implemented four biological reactors, employing the Johannesburg (JHB) process configuration for advanced N and P removal. In 2009, the facility expanded its capacity and upgraded its sludge management system by adding two new secondary clarifiers and bioreactors as part of efforts to modernize its

processes and comply with the requirements of EU Directive 91/271/EEC.

As part of further modernization and expansion to enhance the stability and effectiveness of wastewater treatment processes and improve the efficiency of sewage sludge management, new infrastructures were constructed, including

- New anaerobic digesters with the capacity of 19,200 m³ anaerobic sludge stabilization. As a result, the sludge retention time was extended from 15 to approximately 25 days, leading to a 26% increase in biogas production. This biogas is now used for electricity and heat generation, significantly improving the energy balance of the facility. By 2023, over 60% of the WWTP's electricity demand was met by renewable energy sources, marking a more than 20% increase from the previous year.
- Enhanced sludge stabilization for dewatering, drying, and incineration. This has improved downstream processes, reducing polyelectrolyte consumption by approximately 13% and enhancing energy (biogas consumption) efficiency.
- Sewage sludge dewatering supernatant treatment installation utilizing AnitaMox technology, which allows for Anammox metabolic pathways for nitrogen removal under minimal aeration achieving the reduced pollutant load by nearly 80%, with an overall 10% decreased energy consumption for aeration.

To support the energy goals of the plant, a photovoltaic system with a capacity of 400 kW was installed and became operational in March 2022. In 2023, this system generated 448 MWh, covering approximately 3.1% of WWTP's total electricity consumption. **Figure 3-2** shows an aerial view of the plant while **Table 3-2** shows the results of the quality of discharged sewage in

recent years.



Figure 3-2: Aerial view of “ Dębogórze” WWTP as the selected case study.

Currently , the plant treats approximately 62,000 m³/day of wastewater, with a design load of 543,000 PE. Wastewater enters through large-diameter (Polyethylene High-Density) PEHD pipelines and undergoes preliminary treatment in mechanical screens, grit chambers, and fat separators. It then passes through primary settling tanks before entering the biological reactors. The treatment sequence uses simultaneous denitrification, nitrification, and biological phosphorus removal via the BARDENPHO® and CAROUSEL systems. Sludge is thickened, digested anaerobically, and reused or composted. High-quality effluent is ensured with nitrogen levels below 10 mg/L and phosphorus under 1 mg/L.

Table 3-2: Concentrations and degrees of reduction of basic pollutant indicators in treated sewage from “Dębogórze” in 2015–2023

(Source: <https://pewik.gdynia.pl>)

Parameter / Year	COD		BOD ₅		Total suspended solids		Total N		Total P	
	mgO ₂ /d m ³	reduction (%)	mgO ₂ /dm ³	reduction (%)	mg/dm ³	reduction (%)	mgN/dm ³	reduction (%)	mgP/dm ³	reduction (%)
2015	30.5	97.2	0.1	99.9	0.1	99.9	7.4	92.2	0.64	94.6
2016	31.2	97.1	1.2	99.7	0.0	99.9	7.7	91.9	0.64	94.4
2017	31.5	96.9	0.4	99.9	0*	99.9	7.3	92.2	0.65	93.9
2018	33.8	97.0	0.3	99.9	1.3	99.7	6.9	92.8	0.66	94.3
2019	34.4	96.8	0.4	99.9	0.7	99.9	6.7	92.9	0.62	94.7
2020	33.3	97.1	0.8	99.9	1.2	99.8	6.6	93.4	0.55	95.5
2021	30.9	97.3	2.3	99.6	2.7	99.5	6.2	93.8	0.58	95.1
2022	28.5	97.6	1.4	99.7	3.0	99.4	5.7	94.6	0.60	95.4
2023	31.8	97.4	0.4	99.9	2.1	99.6	7.3	92.7	0.68	93.9
Process / Line limits	125		15		35		10		1	

3.3 Experimental setup

Laboratory-scale experiments were conducted using a system consisting of two identical batch reactors, each with a working volume of 3.0 L. The reactors were specifically designed to facilitate controlled biological processes under variable operational conditions relevant to BNR. The experimental setup was located in the laboratory facilities of the Faculty of Civil and Environmental Engineering at Gdańsk University of Technology (54.37 N, 18.61 E). The system configuration enabled independent control of operational conditions in each reactor, facilitating parallel experiments under varying scenarios.

The batch reactors were constructed from Plexiglas and positioned in parallel on a laboratory bench arrangement. A centralized computer control unit equipped with a display interface was mounted above the reactors to regulate mixing conditions, as well as adjust and monitor critical operational parameters. Each reactor was fitted with manual check valves at the base to enable full drainage between experimental cycles.

Both reactors were equipped with an online monitoring system, including two Inolab Multi 740 multifunction meters (WTW, Munich, Germany) for temperature, pH and dissolved oxygen (DO) concentrations. The temperature was maintained using water bath Labart Julabo F-12 (Seelbach, Germany) connected to the reactor's water jackets. Online pH monitoring was provided using a SenTix 41 pH electrode (WTW, Munich, Germany). Aeration in each reactor was monitored and controlled using a system consisting of an air pump (Mistral 200, Aqua Medic, Germany), a Cellox® 325 DO sensor (WTW, Munich, Germany), and an electromagnetic valve.

N₂O measurements in the liquid phase were performed using modified Clark-type N₂O-R microsensors with mounted caps connected to the dedicated monometer (Unisense, Aarhus,

Denmark). Prior each experimental trial, N₂O-R microsensors were polarized and calibrated according to the manufacturer's specifications detailed in the Unisense "*Nitrous oxide sensor user manual*." Data acquisition was facilitated through Free Sensor Trace BASIC software (Unisense, Aarhus, Denmark).

Homogeneous mixing was achieved using mechanical stirrers (Heidolph RZR 2021, Heidolph Instruments GmbH, Schwabach, Germany) equipped with 5 cm diameter paddles operating at approximately 200 rpm during all experimental phases. Mixing regime provided adequate mass transfer while minimizing mechanical stress on the microbial biomass.

All measured parameters, including pH, DO, temperature, and N₂O, were continuously transmitted to a central control unit for real-time monitoring and automated adjustment of operational conditions. Data were simultaneously archived for subsequent analysis and interpretation, ensuring comprehensive documentation of system performance throughout each experimental cycle. A schematic representation of the batch reactor configuration and continuous measurement systems is illustrated in **Figure 3-3a**, while **Figure 3-3b** presents photographic documentation of the actual experimental setup, including the two parallel bioreactors, control unit, and display screen connected to the bioreactors.

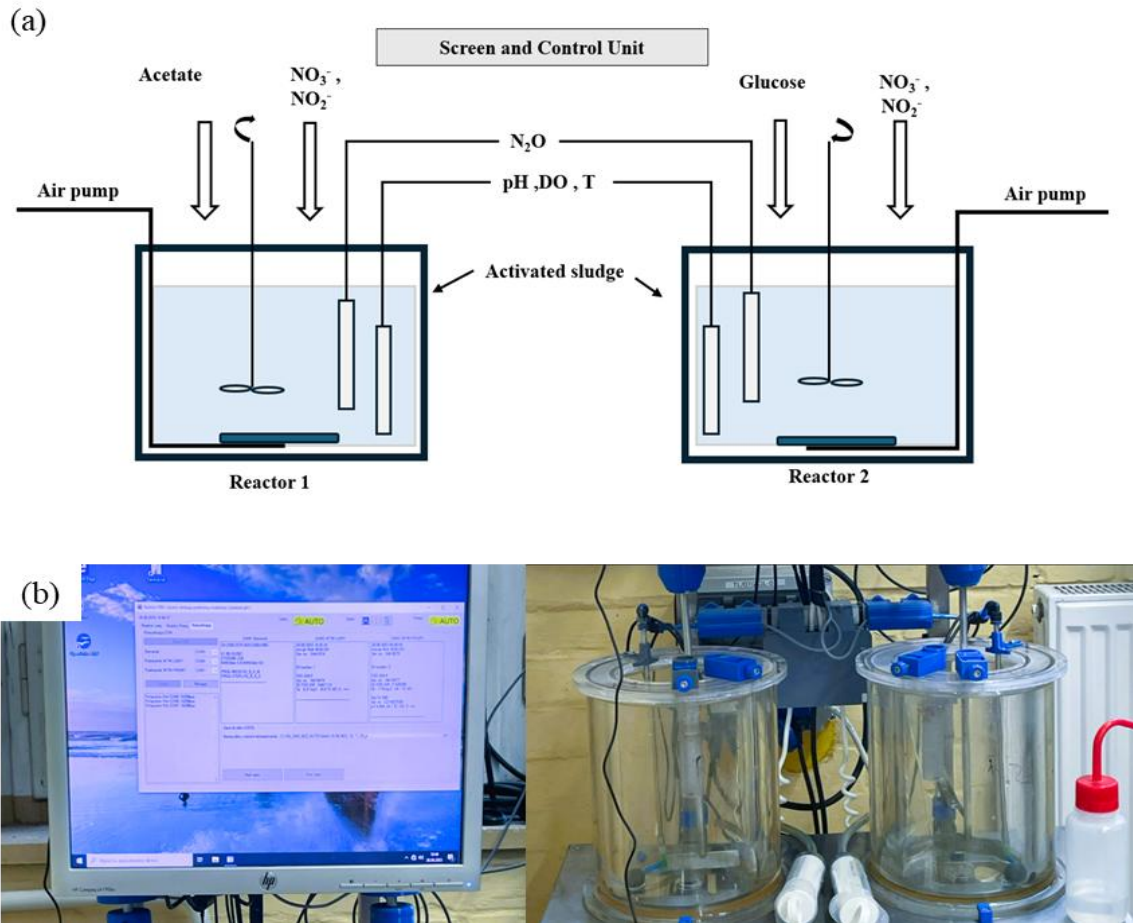


Figure 3-3: (a) Schematic diagram of the laboratory-scale batch reactor system (b) Actual image of the two parallel bioreactors and the connected control unit.

3.4 Experimental design

This study was designed to evaluate the metabolic activity of DPAOs under controlled laboratory conditions simulating EBPR environments. The primary objective was to assess how variations in external carbon source, COD:P ratio, and electron acceptor type (NO_3^- vs. NO_2^-) influence DPAO-driven denitrification, PO_4^{3-} uptake, and N_2O productions. To systematically examine these factors, the experiments were divided into two distinct series, I & II, each addressing environmental and

metabolic scenarios. A detailed overview of the experimental schedule and setup is provided in

Table 3-3.

Table 3-3: General schedule and description of the work carried out in the study on EBPR by *Tetrasphaera*-rich activated sludge

Timeline	Year I	Year II	Year III	Years IV & V
Series	Theoretical	Experimental (Series I)	Experimental (Series II)	Reporting
Approach	Comprehensive literature review on EBPR focused on the role of <i>Tetrasphaera</i>	<p>Preliminary anaerobic-anoxic batch experiments under varying external carbon sources (glucose and acetate) and electron acceptors (NO_3^- and NO_2^-):</p> <ul style="list-style-type: none"> – Scenario 1.1: COD-limiting (COD:P ratio < 2.5) – Scenario 1.2: COD non-limiting (COD:P ratio > 2.5) 	<p>Anaerobic-anoxic batch experiments under modified anoxic conditions:</p> <ul style="list-style-type: none"> – Scenario 2.1: Reference tests (“standard” COD-limiting, as in Scenario 1.1) – Scenario 2.2: PO_4^{3-}-precipitated conditions – Scenario 2.3: PHA-depleted conditions 	Manuscript preparation for submission and defense
Aim	Preparation of a review paper on EBPR performance by <i>Tetrasphaera</i> -rich activated sludge	Investigation of the effect of glucose and acetate addition on DPAO metabolism and N_2O production with NO_3^- and NO_2^- as electron acceptors	Investigation of the effect of modified anoxic conditions on DPAO activity and its implications for EBPR performance and N_2O production	Completion of the doctoral requirements
Outcome	Publication of the review paper	Understanding of substrate specific DPAO behavior and related N_2O production profiles under “standard” EBPR conditions	Determination of the impact of modified conditions on EBPR performance and N_2O production profiles	Dissertation submission and defense

3.5 Experimental series I

Experimental series I involved conventional anaerobic-anoxic batch tests using freshly collected activated sludge from the GD WWTP. Two key experimental scenarios were designed based on the initial COD:P mass ratio at the beginning of the anaerobic phase:

Scenario 1.1 - COD-limiting conditions: COD:P ratio < 2.5

Scenario 1.2 - COD non-limiting conditions: COD:P ratio > 2.5

Each test followed a two-phase anaerobic-anoxic sequence:

- Anaerobic phase (2.5 h): External carbon addition (acetate or glucose) was added to promote the uptake of VFA or sugars, leading to intracellular storage (e.g. PHA or glycogen) and PO_4^{3-} release.
- Anoxic phase (≥ 4 h): Electron acceptors (NO_3^- or NO_2^-) were introduced to initiate denitrification and observe subsequent PO_4^{3-} uptake under oxygen-free conditions.

The effects of different dosages of external carbon sources (acetate or glucose) on DPAO activity were investigated based on these two scenarios as preliminary tests in determining the type and proportion of the external carbon for efficient EBPR processes in experimental series II. All experiments were conducted at $20.0 \pm 0.5^\circ\text{C}$, with pH maintained at 7.0 ± 0.5 through manual NaOH dosing. The mixed liquor biomass concentration in MLVSS values was up to 2.38 g L^{-1} in series I, while in Series II, the biomass concentration, MLVSS values of 4.1 g L^{-1} without dilution. The variation in biomass concentration was due to the effect of seasonal fluctuations in influent characteristics at the WWTP at different sampling and experimental seasons. N_2O production was continuously monitored throughout the anoxic phase to evaluate the environmental implications of incomplete denitrification and to distinguish DPAO activity from other denitrifiers (OHOs).

This experimental series specifically targeted the evaluation of metabolic differences between *Tetrasphaera*-like and *Accumulibacter*-type DPAOs in response to the carbon source (glucose and acetate) under two electron acceptors (NO_3^- or NO_2^-).

3.5.1 Scenario 1.1—COD-limiting conditions COD:P ratio < 2.5

This experimental scenario focused on investigating DPAO performance under carbon-limiting conditions, simulating operational challenges in BNR plants with restricted carbon availability. Decreasing the COD:P ratio below 2.5 allowed to evaluate how external carbon scarcity constrains intracellular storage, denitrification efficiency, and PO_4^{3-} uptake, particularly when coupled with varying nitrogen electron acceptors.

Sodium acetate and glucose were used as carbon sources, but the initial COD equivalent mass was restricted to 70 mg COD L^{-1} (**Table 3-4**), representing approximately half the carbon load of the non-limiting tests. This reduction was meant to limit PHA or glycogen synthesis during the anaerobic phase and thereby suppress DPAO activity during the subsequent anoxic phase and that of denitrifying activity of OHOs during the anoxic phase.

During the anaerobic phase, carbon was added at the beginning to promote limited internal carbon storage. The anaerobic release of PO_4^{3-} was used as an indicator of successful uptake of external substrate and microbial readiness for anoxic P removal. In the anoxic phase, NO_3^- or NO_2^- was added at fixed concentrations (approximately 20 mg N L^{-1} equivalent mass) as seen in(**Table 3-4**).

Key evaluation points included:

- Nitrate/nitrite utilization rates in COD-limiting condition.
- Phosphorus release and uptake rates under COD limiting conditions.

- N₂O accumulation trends, hypothesized to increase due to impaired electron donor availability, particularly under NO₂⁻-based denitrification.

Table 3-4: Summary of dosages of electron acceptors (NO₃⁻ vs. NO₂⁻) and carbon sources (acetate vs. glucose) for the COD limiting conditions (COD:P ratio < 2.5).

Scenario 1.1: Tests with COD limiting conditions (COD:P ratio < 2.5)					
Electron acceptor	Units	NO ₃ ⁻	NO ₃ ⁻	NO ₂ ⁻	NO ₂ ⁻
External carbon added		Acetate	Glucose	Acetate	Glucose
Initial mass of carbon anaerobic	mg	462.0	290.5	462.0	290.5
Equivalent mass	mg COD L ⁻¹	70.0	70.0	70.0	70.0
Mass of N added -anoxic	mg	548.3	548.3	374.6	356.8
Equivalent mass	mg N L ⁻¹	20.0	20.0	20.0	20.0
Phosphate	mg P L ⁻¹	3.9	1.8	4.9	3.5
COD	mg COD L ⁻¹	195.0	151.0	198.0	195.0

This set of experiments formed the baseline reference for subsequent tests for COD non-limiting conditions and helped identify optimal carbon – nitrogen pairing strategies for minimizing productions while maximizing EBPR performance.

3.5.2 Scenario 1.2 – COD non-limiting conditions COD:P ratio > 2.5

This scenario was designed to evaluate the impact of excess external carbon on the metabolic dynamics of DPAOs, focusing on their PO₄³⁻ uptake, denitrification capacity, and N₂O production profiles. A high COD:P ratio condition (greater than 2.5) was applied to simulate scenarios where carbon dosing is not a limiting factor, reflecting the EBPR systems supplemented with external carbon sources.

Prior to each test, DO was stripped from the reactors using nitrogen gas to establish strictly anaerobic conditions. At the beginning of each anaerobic phase, either sodium acetate or glucose was added to promote intracellular storage compound synthesis (PHA or glycogen) and initiate PO_4^{3-} release. The initial organic carbon concentration was increased by approximately 120 or 150 mg COD L^{-1} , depending on the type of substrate used (**Table 3-5**), ensuring the establishment of a carbon-rich environment to extend external carbon availability for the anoxic phase.

Table 3-5: Summary of dosage amounts of electron acceptors (NO_3^- vs. NO_2^-) and carbon sources (acetate vs. glucose) for the high COD:P ratio > 2.5 .

Scenario 1.2: Tests with COD non-limiting conditions (COD:P ratio > 2.5)						
Electron acceptor	Units	NO_3	NO_3^-	NO_2^-	NO_2^-	NO_2^- Pulse
External carbon		Acetate	Glucose	Glucose	Acetate	Acetate
Initial mass of carbon anaerobic	mg	990.1	622.4	622.4	792.1	792.1
Equivalent COD	mg COD L^{-1}	150.0	150.0	150.0	120.0	120.0
Mass of N-anoxic	mg	685.4	374.6	374.6	468.2	18.0
Equivalent mass	mgN L^{-1}	25.0	20.0	20.0	25.0	5.0
Phosphate	mg P L^{-1}	3.0	3.1	2.4	3.1	1.5

The anoxic phase in all the tests was initiated with the addition of an electron acceptor, NO_3^- or NO_2^- . A special test, incorporating anoxic NO_2^- pulse dosage, was carried out, as indicated in **Table 3-5**. The inclusion of anoxic NO_2^- pulse additions allowed for time-resolved profiling of denitrification kinetics and N_2O accumulation dynamics under transient NO_2^- availability conditions.

Each test configuration was carefully constructed to maintain balanced carbon and nitrogen inputs, with PO_4^{3-} levels held near 3.0 mg P L^{-1} to ensure representative DPAO activity (**Table 3-2**). The five experimental scenarios incorporated variations in both carbon source variations (acetate vs. glucose) and electron acceptor forms, enabling evaluation of DPAO metabolic responses.

Key evaluation points included:

1. NO_3^- and NO_2^- utilization rates, identifying differences in electron acceptor utilization rates.
2. PO_4^{3-} uptake rates during the anoxic phase, linked to the nature and availability of intracellular storage pools.
3. Continuous monitoring of N_2O production to evaluate the potential trade-offs between effective denitrification and greenhouse gas release under carbon-rich conditions.

The results of experimental **series I** were critical to determine the dosages of carbon and electron acceptors in experimental **series II**, aiming to enhance EBPR performance.

3.6 Experimental series II

The experimental **series II** was carried out with the anaerobic phase performed in a common cultivation tank (CCT) and modified anoxic phases performed in two parallel batch reactors (R1 and R2) (**Figure 3-4**). Based on the results obtained in **Series I, Scenario 1.1**, COD-limiting conditions demonstrated improved EBPR performance, with no observable delay in anoxic PO_4^{3-} uptake. Consequently, COD-limiting conditions were adopted for all experiments in **Series II** to maintain consistent denitrification dynamics and optimize P removal under modified anoxic phases. The experimental **series II** was designed to distinguish and assess the actual role of DPAOs in denitrification and PO_4^{3-} uptake under more specialized and constrained anoxic conditions. Tests

examined the availability of key intracellular PHA and extracellular PO_4^{3-} that influence DPAO metabolism.

Three anoxic experimental scenarios were implemented using sludge preconditioned in the CCT under anaerobic conditions with acetate enrichment: These anoxic scenarios are as outlined.

- **Scenario 2.1:** Reference tests (“standard” COD-limiting, as in Scenario 1.1): Sludge directly from the anaerobic tank (referred to CCT) without further treatment.
- **Scenario 2.2:** PO_4^{3-} -precipitated conditions: PO_4^{3-} was chemically precipitated using FeCl_3 (PIX113) to assess denitrification in the absence of extracellular P.
- **Scenario 2.3:** PHA-depleted conditions: PHA was metabolically depleted via overnight aeration before the anoxic phase to examine the role of intracellular stored PHA on denitrification and PO_4^{3-} uptake.

The design and sequencing of these tests are presented in **Figure 3-4**. A detailed description of preparation steps and operational runs for each test scenario, **2.1**, **2.2**, and **2.3**, is described in **sections 3.6.1**, **3.6.2**, and **3.6.3** respectively.

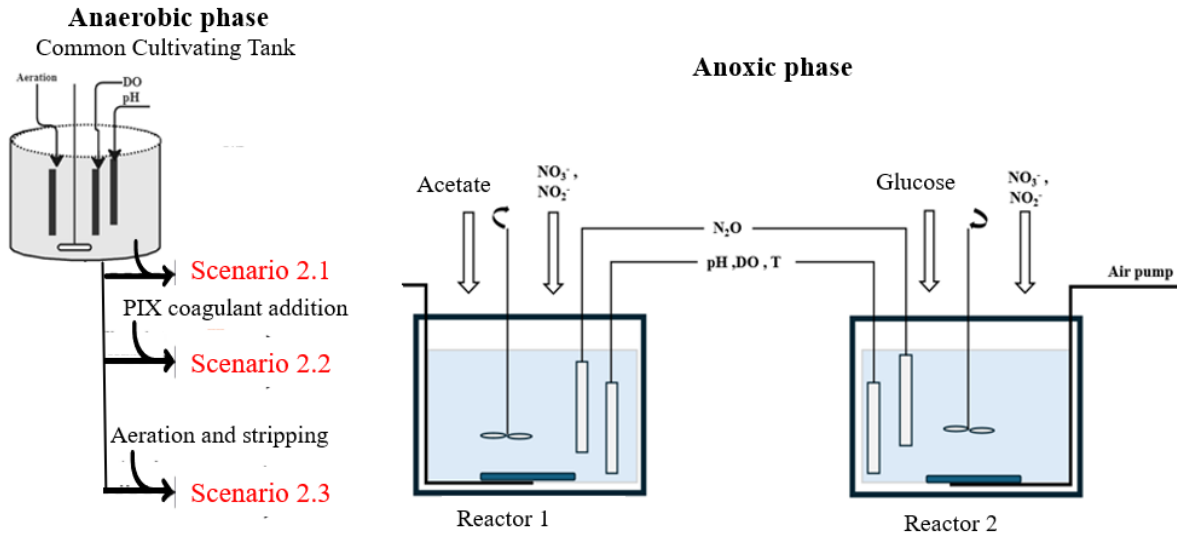


Figure 3-4: Schematic diagram of the series II experimental setup of the CCT (anaerobic phase) and batch reactor (anoxic phase).

The anaerobic phase of the tests was performed in the CCT (see in section 3.6.1). The modified anoxic tests were performed in parallel 3 L batch reactors. Data were collected at 11 defined time points over a 7-hour anoxic period, including concentrations of PO_4^{3-} , NO_3^- , NO_2^- , PHA, and real-time N_2O production. Both NO_3^- and NO_2^- were used as electron acceptors, and glucose was added at specified time points during the anoxic phase.

The design of **series II** allowed for a comparative evaluation of DPAO activity vs. OHO percentage contributions to denitrification under varying substrate availability.

3.6.1 The anaerobic phase test in the CCT

Anaerobic preconditioning was conducted in a CCT of a working volume of 20 L, where fresh activated sludge ($\text{MLVSS} = 4.0 - 5.0 \text{ g}\cdot\text{L}^{-1}$) was dosed with 2528 mg of sodium acetate as the external carbon source. This resulted in a COD:P ratio of $2.4 \text{ mg COD:mg P}^{-1}$, sufficient to induce

anaerobic P release and stimulate PHA synthesis by DPAOs. Glucose was excluded in this series due to its previously observed limited impact on anaerobic release and anoxic uptake of PO_4^{3-} in **series I** experiments. A total of 2528 mg of sodium acetate was administered.

DO was stripped using nitrogen gas until the DO concentration of $\leq 0.01 \text{ mg}\cdot\text{L}^{-1}$ was achieved, verified using DO sensors connected to the portable meter (WTW, Munich, Germany). Sampling for soluble PO_4^{3-} and COD was performed at 2, 20, 40, 60, 90, 120, and 150 minutes. Biomass samples for PHA quantification were collected at 2, 60, and 150 minutes, then immediately frozen to prevent post-sampling PHA degradation. Following the anaerobic phase, the bulk sludge was subjected to overnight mixing (without aeration) in preparation for the subsequent anoxic phase, ensuring metabolic stabilization and stratified preparation for three divergent test scenarios.

3.6.2 *Modified anoxic tests*

The anoxic phase tests were conducted in 3.0 L glass batch reactors (R1 and R2), the same configuration used in Series I, operated under controlled environmental conditions, with temperature maintained at $20.0 \pm 0.5^\circ\text{C}$, pH at 7.0 ± 0.2 , and DO kept at $0.0 \text{ mg}\cdot\text{L}^{-1}$ by continuous N_2 gas stripping. For each anoxic experimental scenario, two reactors were run in parallel, as illustrated in **Figure 3.4**. **R1** was dosed with 432.86 mg KNO_3 , corresponding to $22 \text{ mg NO}_3^- \cdot \text{N}\cdot\text{L}^{-1}$, while **R2** received 295.71 mg NaNO_2 , corresponding to $16 \text{ mg NO}_2^- \cdot \text{N}\cdot\text{L}^{-1}$. In both reactors, a single pulse of 126 mg glucose was added as an external carbon administered after 210 minutes into the anoxic phase, except for **Scenario 2.1**, i.e., reference test. At the beginning of the anoxic phase, the respective reactors were dosed with a source of electron acceptors in the amounts outlined:

- **R1** dosed with 432.86 mg KNO₃ (equivalent to (NO₃⁻-N = 22 mg·L⁻¹),
- **R2** dosed with 295.71 mg NaNO₂ (equivalent to (NO₂⁻-N = 16 mg·L⁻¹).

Sampling for soluble PO₄⁻³, NO₂⁻-N, NO₃⁻-N and COD was performed at 180, 195, 240, 300 and 360th minutes. Biomass samples for PHA quantification were collected at 180, 240, and 360th, then immediately frozen to prevent post-sampling PHA degradation.

Experimental trials (ST1 vs. ST2)

Two experimental trials were conducted under the same operational procedure, differing only in the timing of sampling and experimental analysis as summarized in (**Table 3.6**) below. August is considered as late summer, with warmer ambient temperatures typically ranging from 18–28°C and longer daylight hours while November is considered late autumn, with cooler temperatures ranging from 2–10°C and significantly reduced daylight. These seasonal differences are characteristic of Poland's temperate climate and can subtly influence wastewater treatment characteristics for instance biomass concentration and others, even under controlled laboratory conditions. In real-world settings, higher temperatures in summer generally enhance microbial activity, improve biological nutrient removal efficiency, and increase reaction rates, whereas lower temperatures in autumn and winter may slow down microbial metabolism, affect substrate uptake (e.g., carbon, nitrogen), and alter the composition or behavior of microbial communities. Although the reactors in this study were temperature-controlled, factors such as the source sludge characteristics, microbial acclimation, or the timing of sludge collection and storage could still reflect seasonal influences. As such, potential differences in N₂O production, denitrification performance, or substrate utilization between the August and November trials may partially reflect

these broader seasonal effects on microbial community structure and function within the wastewater treatment plant.

Table 3-6: Experimental series II activities: anaerobic phase in the CCT and modified anoxic phase scenarios in batch reactors

Series II experimental dates		Activities carried out
ST1	ST2	Biomass collection at Debogórze WWTP
21-08-2023	17-11-2023	Biomass collection at Debogórze WWTP N ₂ O sensor calibration and laboratory setup
22-08-2023	18-11-2023	Anaerobic phase tests in the CCT
23-08-2023	19-11-2023	Scenario 2.1: Reference conditions (standard anoxic phase) in two batch reactors
24-08-2023	20-11-2023	Scenario 2.2: PO ₄ ³⁻ -depleted condition in two batch reactors
25-08-2023	21-11-2023	Scenario 2.3: PHA-depleted conditions in two batch reactors
26-08-2023	22-11-2023	Clearing tables and data analysis

3.6.2.1 Scenario 2.1: Reference test (“standard” as in scenario 1.1)

Scenario 2.1 in both trials (ST1 and ST2) was conducted under the same procedure as **Scenario 1.1**. It enabled direct comparison with **Scenarios 2.2** and **2.3** to assess the specific effects of phosphate precipitation and PHA depletion on N₂O production and nutrient dynamics under modified anoxic conditions. A summary of the dosages is presented in **Table 3-7**.

Table 3-7: Summary of dosages of electron acceptors (nitrate vs. nitrite) and carbon sources (acetate vs. glucose) in R1 and R2 under each of the trial (ST1 and ST2)

Parameters	Units	Anaerobic phase	Anoxic phase
External carbon		Acetate	Glucose
Sludge volume	Liters (L)	20	3
COD mass added	mg COD	1517.0	131.6
COD:P ratio	mg COD /mg P	2.4	27
Nitrogen mass added	mg	-	432.86 mg of KNO ₃ (R1) 295.71 mg of NaNO ₂ (R2)
Biomass concentration	g MLVSS·L ⁻¹	4.0 - 5.0	4.0 - 5.0

3.6.2.2 Scenario 2.2: PO₄³⁻ precipitated anoxic conditions

This scenario examined the role of intracellular carbon (PHA) in driving denitrification and PO₄³⁻ uptake under carbon-stressed conditions. After anaerobic acetate uptake, the residual 8 L of sludge in the CCT was aerated overnight to deplete stored PHA reserves, followed by nitrogen gas stripping to re-establish anoxic conditions. Subsequently, 3 L were transferred to reactors R1 and R2, with NO₃⁻/NO₂⁻ additions as above.

The lack of intracellular carbon pools (PHA) was hypothesized to:

- Impair anoxic PO₄³⁻ uptake,
- Alter denitrification kinetics,
- Increase dependency on external glucose for electron supply.

Sampling and glucose dosing were the same as in the previous **Scenario 2.2**. During the test, the pH drop was monitored and adjusted using NaOH solution.

3.6.2.3 *Scenario 2.3: PHA-depleted anoxic conditions*

This critical condition examined the role of intracellular carbon reserves in driving denitrification and PO_4^{3-} uptake under carbon-limited stress. After anaerobic acetate uptake, the residual 8 L of CCT sludge was aerated overnight to oxidize and deplete PHA reserves, followed by nitrogen stripping to re-establish anoxic conditions. Subsequently, 3 L were transferred to R1 and R2, with $\text{NO}_3^-/\text{NO}_2^-$ additions as above.

The lack of intracellular carbon pools (PHA) was hypothesized to:

- Impair anoxic PO_4^{3-} uptake,
- Alter denitrification kinetics,
- Increase dependency on external glucose for electron supply.

Sampling and glucose dosing mirrored the prior scenarios. PHA samples confirmed intracellular depletion. During the test, the pH drop was monitored and adjusted by the addition of NaOH solution.

3.7 Evaluation framework

The two-phase structure of the experimental program enabled a systematic assessment of microbial function, from general denitrifying behavior under controlled EBPR conditions to targeted metabolic responses under selective stress conditions (e.g., PO_4^{3-} precipitated, PHA depletion).

This structured approach provided insights into:

1. The metabolic flexibility of DPAOs under varying COD:P ratios (<2.5 and >2.5 for COD limiting and non-limiting conditions respectively).
2. Electron acceptor-specific responses, particularly in terms of N₂O production patterns.
3. Quantitative differentiation of DPAO and OHO contributions to total N and P removal.

Environmental implications of operational parameters (e.g., carbon type, COD:P ratio) on N₂O production.

3.8 Analytical methods

To accurately monitor the dynamics of key process parameters during the batch experiments, a rigorous sampling and analytical protocol was employed. For each batch test, 30 mL samples of mixed liquor were withdrawn at specified time points and immediately subjected to filtration under vacuum. The filtration process utilized sequential nitrocellulose membrane filters with pore sizes of 1.2 µm and 0.45 µm (Millipore, USA) to ensure effective removal of biomass and colloidal material, thus providing clear filtrates suitable for spectrophotometric analysis.

Sampling for the anaerobic phase was done in the intervals of 2, 20, 40, 60, 90, 120, 150 mins. In each of the **reactors 1** and **2** of the anoxic phase sampling was done in the intervals of 2, 20, 40, 60, 120, 180, 240, 270, 300, 360 and 420 mins and parameters PO₄-P, COD, NO₃-N, NO₂-N and N₂O concentration. Shorter intervals were applied during phases of rapid biochemical transformation, such as the initial series of denitrification. The quantitative determination of chemical species (PO₄-P, COD, NO₃-N, NO₂-N) in the filtered samples was carried out using standard cuvette-based colorimetric test kits in conjunction with a Xion 500 spectrophotometer (Dr. Lange GmbH, Germany). The parameters analyzed and corresponding methodologies included:

- Chemical Oxygen Demand (COD): measured using LCI 400 cuvette tests (ISO 15705), suitable for a working range of 0–1000 mg·L⁻¹ O₂.
- Nitrate (NO₃⁻-N): quantified with LCK 340 cuvette kits, with a measurement range of 5–35 mg·L⁻¹ NO₃⁻-N.
- Nitrite (NO₂⁻-N): analyzed using LCK 343 cuvette tests, with a detection range of 2–90 mg·L⁻¹ NO₂⁻-N.
- Orthophosphate (PO₄³⁻-P): determined via LCK 350 kits, designed for 6–60 mg·L⁻¹ PO₄-P. This included measurement of both PO₄³⁻ and total phosphate when required.
- All photometric analyses adhered to quality control protocols and were conducted following DIN 38405 D9-2 and ISO 23696-1.

Additionally, solid-phase parameters, such as mixed liquor suspended solids (MLSS) and their volatile fraction (MLVSS), were measured gravimetrically. The determination followed the standard procedure outlined in Polish Norm PN-72/C-04559, based on oven drying at 105°C and ignition at 550°C. These values were essential for calculating specific rates of denitrification and phosphorus uptake.

3.9 Polyhydroxyalkanoates (PHA) measurements

The quantification and characterization of intracellular PHAs were performed to assess the metabolic activity of DPAOs under varying operational conditions. The analysis targeted the two primary PHA monomers commonly accumulated in activated sludge systems: 3-hydroxybutyrate (3HB) and 3-hydroxyvalerate (3HV). Prior to analysis, PHAs were extracted from the biomass and converted into their corresponding methyl esters following the methanolysis protocol described by (Comeau et al., 1987). This method involved acid-catalyzed esterification of intracellular PHA

polymers in the presence of methanol and chloroform, effectively converting the biopolymers into volatile methyl esters of the constituent hydroxy acids. This procedure allows for efficient extraction and subsequent quantification of PHA monomers in complex biological matrices. The resulting methyl esters were analyzed using a CP-3800 gas chromatograph (Varian, USA) equipped with a split/spitless injector and a flame ionization detector (FID). Chromatographic separation was achieved using a VF-5ms capillary column (30 m length, 0.25 mm inner diameter, 0.25 μm film thickness), which enabled high-resolution separation of the target analytes. The oven temperature program and injector conditions were optimized based on the methodology of Oehmen et al. (2005) to ensure optimal peak resolution and reproducibility.

A commercial PHA copolymer standard consisting of 3-hydroxybutyrate-co-12% 3-hydroxyvalerate (Sigma-Aldrich, USA) was used for calibration and quantification purposes. Peak identification was confirmed by comparing retention times with those of authentic standards. The total PHA content in the biomass was calculated as the sum of 3HB and 3HV concentrations, expressed in terms of mg PHA per gram of mixed liquor volatile suspended solids ($\text{mg PHA} \cdot \text{g}^{-1}$ MLVSS).

3.10 Microbiological analyses: DNA extraction and high throughput 16S rDNA sequencing

To characterize the microbial community structure and assess the diversity of DPAOs across different operational regimes, comprehensive microbiological analyses were performed using high-throughput sequencing of the 16S rRNA gene fragment. Mixed liquor sub-samples (50 mL each) were collected in triplicate from four full-scale biological nutrient removal (BNR) facilities, encompassing a range of environmental and operational conditions relevant to EBPR systems.

3.10.1 DNA extraction

Total genomic DNA was extracted from each sample using the FastDNA™ SPIN Kit for Soil (MP Biomedicals, USA), which is optimized for the efficient lysis of microbial cells in complex matrices such as activated sludge. DNA isolation was conducted in duplicate to ensure consistency and reproducibility. Following extraction, replicate DNA samples were pooled, and the resulting DNA extracts were subjected to quality and concentration assessment via spectrophotometry (NanoDrop ND-1000, Thermo Scientific), with absorbance ratios at A260/A280 and A260/A230 used as indicators of purity.

3.10.2 Amplification and sequencing of 16S rRNA Gene V3–V4 region

The V3–V4 hypervariable region of the bacterial 16S rRNA gene was amplified using the universal primer set 341F/785R as described by Klindworth et al. (2013). Amplicon libraries were prepared according to Illumina's recommended workflow and sequenced on the Illumina MiSeq platform using the MiSeq Reagent Kit V2 (2 × 250 bp paired-end reads). A target sequencing depth of >60,000 reads per sample was achieved to ensure adequate representation of microbial taxa, including low-abundance functional groups.

3.10.3 Bioinformatics workflow and taxonomic classification

Raw sequencing reads were initially processed using the USEGalaxy web platform (<https://usegalaxy.org>), where paired-end reads were merged using the fastq-join tool. Quality filtering was then applied, retaining sequences with a Phred quality score ≥ 20 and a minimum read length ≥ 100 bp to remove low-quality and truncated reads. Chimeric sequences—a common

artifact in PCR amplification — were identified and removed using the DECIPHER FindChimeras tool (<https://www2.decipher.codes/FindChimeras.html>).

Taxonomic classification of high-quality reads was performed against the SILVA rRNA gene database (www.arb-silva.de) using a confidence threshold of 80% for assignment, ensuring reliable identification of microbial lineages. Community composition data were interpreted in the context of known functional roles, particularly focusing on taxa such as *Ca. Microthrix*, *Tetrasphaera*, *Accumulibacter*, and *Dechloromonas*, which are recognized for their involvement in denitrification and P accumulation.

3.10.4 Data submission and further analysis

All processed datasets were submitted to the MetaGenome Rapid Annotation using Subsystem Technology (MG-RAST) server (Keegan et al., 2016), a publicly accessible platform for metagenomic data storage and annotation. Functional annotation and diversity metrics were derived from MG-RAST pipelines to supplement taxonomic insights with ecosystem-level information on gene abundances and metabolic pathways.

3.11 Process rate calculations

To quantitatively assess the performance of DPAOs and OHOs under varying operational conditions, specific process rates were calculated based on substrate concentration changes during anaerobic and anoxic phases. These rates include nitrate utilization rates (NURs), nitrite utilization rates (NiURs), phosphate release and uptake rates (PRR and PUR), and COD consumption rates.

All rate calculations were normalized to the concentration of biomass (measured as mixed liquor volatile suspended solids, MLVSS) to express results as mg / gMLVSS·h.

3.11.1 Nitrate and nitrite utilization rates (NUR and NiUR)

Denitrification rates were derived by monitoring the concentration decline of NO_3^- and NO_2^- during the anoxic phase. Linear regression slopes from the concentration profiles over time were used to calculate specific reduction rates as follows:

$$\mathbf{NUR} = \frac{\text{slope}(S_{\text{NO}_3,t})}{\Delta t \cdot X} \quad [\text{mg N}/(\text{gMLVSS} \cdot \text{h})] \dots \dots \dots (1)$$

$$\mathbf{NiUR} = \frac{\text{slope}(S_{\text{NO}_2,t})}{\Delta t \cdot X} \quad [\text{mg N}/(\text{gMLVSS} \cdot \text{h})] \dots \dots \dots (2)$$

Where:

- Slope $S_{\text{NO}_3,t}$ the concentrations of nitrate nitrogen between times t_1 and t_2 [mg N L^{-1}], and calculated in MS Excel.
- Δt is the time interval between t_1 and t_2 [h].
- X is the MLVSS concentration [g L^{-1}].

The values of NUR from modified anoxic tests (reference, PO_4^{3-} precipitated and PHA- depleted conditions) allowed differentiation between the activities of DPAOs and OHOs, depending on the availability of specific carbon source (acetate or glucose) and the type of electron acceptor (NO_3^- or NO_2^-). According to (Tuszynska et al., 2019) whose experiments were validated by extended Activated Sludge Model no 2d (ASM2d) as a support tool, chemical precipitation of PO_4^{3-} and PHA- depleted conditions lead to DPAOs reduced metabolism, resulting in lower NURs,

necessary for respiration and intracellular transformation . Accordingly, it can be assumed that the difference between the N removal values before and after chemical precipitation of PO_4^{3-} could be related to the activity of DPAOs (storage of PO_4^{3-} at the expense of PHA)(Tuszynska et al., 2019).The relative contributions (percentage) of different metabolic pathways to the observed denitrification activity (NUR_1 , NUR_2 , NUR_3) were further analyzed and presented in **Figure 3-5**. Similar calculation was also performed for the NiUR rates.

NITRITE UTILIZATION RATE COMPONENT

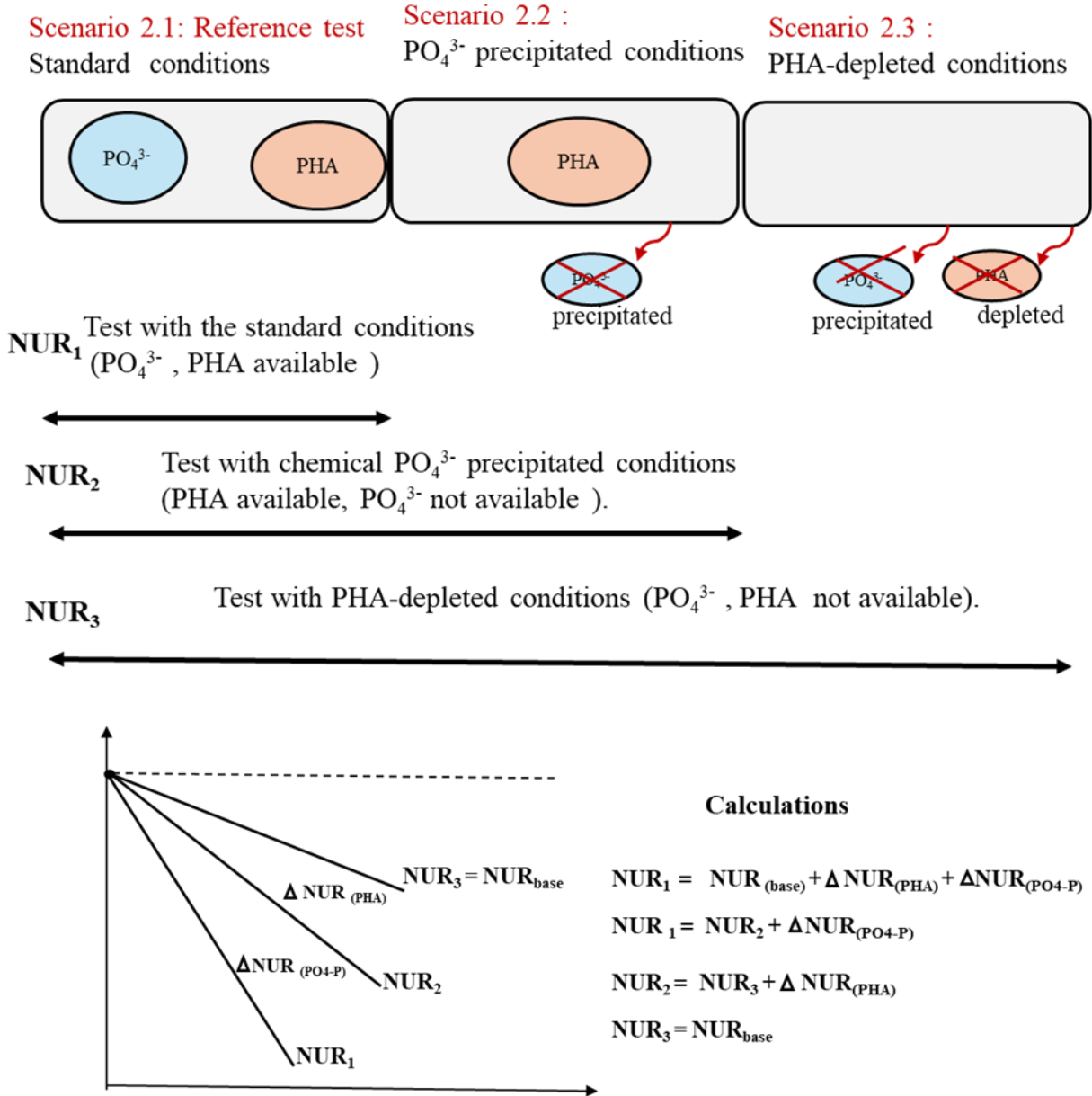


Figure 3-5: NUR calculations for specific carbon sources and microbial activities in the anoxic phases.

3.11.2 Phosphate release and uptake rates (PRR and PUR)

Phosphate turnover was monitored during both anaerobic and anoxic phases to quantify DPAO-related P cycling. Phosphate release rates were measured during the first hour of the anaerobic phase, whereas phosphate uptake rates were determined over the anoxic period. The following equations were applied:

$$\mathbf{PRR} = \frac{\text{slope}(S_{\text{PO}_4,t})}{\Delta t \cdot X} \text{ [mg P/(gMLVSS} \cdot \text{h)]} \dots\dots\dots(3)$$

$$\mathbf{PUR} = \frac{\text{slope}(S_{\text{PO}_4,t})}{\Delta t \cdot X} \text{ [mg P/(gMLVSS} \cdot \text{h)]} \dots\dots\dots(4)$$

Where:

- Slope S_{PO_4} is the phosphate concentration at time points times t [mg P L⁻¹] and calculated in MS Excel.
- Δt is the time interval between t_1 and t_2 [h].
- X is the MLVSS concentration [g L⁻¹].

The PRR reflects polyphosphate release linked to internal carbon storage under anaerobic conditions, while PUR quantifies phosphate uptake as a function of denitrification and polyphosphate uptake in the presence of NO_3^- or NO_2^- .

3.11.3 *COD consumption rate*

The degradation of external carbon sources was assessed by calculating COD consumption rates during both anaerobic and anoxic phases. COD utilization was used to infer overall microbial activity and substrate preference (glucose vs. acetate), as described by the following equation:

$$\text{COD}_{\text{CR}} = \frac{\text{slope } (S_{\text{COD},t})}{\Delta t \cdot X} [\text{mg COD}/(\text{gMLVSS} \cdot \text{h})] \dots\dots\dots(5)$$

Where:

- Slope $S_{\text{COD},t}$ represents the measured COD concentration at t [mg COD L^{-1}], and calculated in MS Excel
- Δt is the time interval between t_1 and t_2 [h].
- X is the MLVSS concentration [g L^{-1}].

COD degradation dynamics, in combination with NURs and PURs, provided insights into carbon utilization efficiency and the balance between storage and energy production under the tested conditions.

4. RESULTS

4.1 Microbial community

4.1.1 *Results of preliminary study in four WWTPs in the Pomeranian region, Poland*

In order to identify the WWTP with the highest *Tetrasphaera* -enrichment , a preliminary study was conducted across four major WWTPs in the Pomeranian region - Gdynia Dębogórze (GD), Gdańsk Wschód (GW), Słupsk (SL), and Swarzewo (SW).The relative abundance and composition characterizing the microbial communities with emphasis on key DPAO members , are presented in the **Figure 4-1**. While the total relative abundance of DPAOs was comparable across the four WWTPs, ranging from $11.0\% \pm 2.1\%$ to $12.4\% \pm 2.0\%$, the composition of the DPAO subpopulation varied notably. Among the four plants, GD exhibited the highest cumulative proportion of DPAO members (12.4%), with *Tetrasphaera* representing the dominant genus. This justified the selection of GD as the primary case study plant for this dissertation.

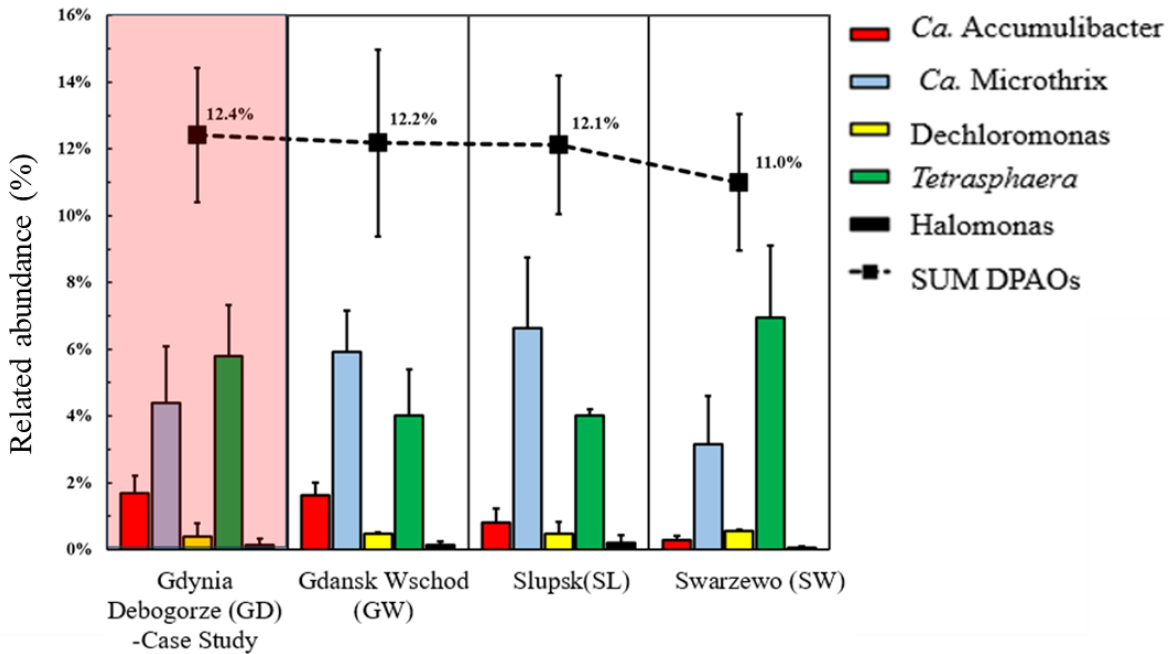


Figure 4-1:Relative percentages of dominant DPAO genera in bacterial communities from mixed liquor samples across four large WWTPs in the Pomeranian region, Poland: Gdynia Dębogórze (GD), Gdańsk Wschód (GW), Słupsk (SL), and Swarzewo (SW). Error bars represent standard deviation of duplicate samples.

Across all analyzed plants, the genus *Tetrasphaera* was the dominant DPAO, with an average relative abundance of 7.0% (SD \pm 2.2%). *Candidatus* *Microthrix* (henceforth referred as *Ca. Microthrix*), a filamentous bacterium often associated with sludge bulking, was also abundant at avg. 6.6% (SD \pm 2.1%). In contrast, *Ca. Accumulibacter* showed lower relative abundance (1.7% \pm 0.5%), although it is well recognized for high metabolic in P removal.

The distribution of dominant DPAO was similar across the three largest WWTPs, including GD (550,000 PE), GW (760,000 PE), and SL (250,000 PE), with average abundances of 4.6% \pm 1.0% for *Tetrasphaera*, 5.6% \pm 1.1% for *Ca. Microthrix*, and 1.4% \pm 0.5% for *Ca. Accumulibacter*. In

contrast, mixed liquor from SW, the smallest WWTP (176,000 PE), revealed a distinct microbial composition. Notably, *Tetrasphaera* was the dominant genera at ($7.0\% \pm 2.2\%$), surpassing *Ca. Microthrix* ($3.1\% \pm 1.5\%$) and showing reduced abundances of *Ca. Accumulibacter* ($0.3\% \pm 0.1\%$). Other less prevalent DPAO taxa, such as *Dechloromonas* and *Halomonas*, remained at stable, low abundances across all four WWTPs, averaging $0.5\% \pm 0.1\%$ and $0.14\% \pm 0.1\%$, respectively.

4.1.2 Microbial characterization of the biomass in Gdynia Debogórze (GD)-Case study WWTP

To assess a representative characterization of major functional bacterial groups, with special attention to the DPAOs in the GD WWTP, four mixed-liquor samples were collected and analyzed over a six-month period by Illumina sequencing of the 16S rRNA gene. The community composition was observed to be highly stable across the sampling points, justifying the use of averaged data to describe the core microbiome at both the phylum and genus levels.

At the phylum level, the community was dominated by *Proteobacteria* ($23.27\% \pm 0.03\%$), *Actinobacteriota* ($21.70\% \pm 0.03\%$), *Chloroflexi* ($15.28\% \pm 0.02\%$) and *Bacteroidota* ($14.98\% \pm 0.04\%$). Less abundant but notable phyla included *Patescibacteria* ($7.15\% \pm 0.02\%$), *Acidobacteriota* ($4.10\% \pm 0.01\%$) and *Firmicutes* ($2.95\% \pm 0.01\%$). The remaining phyla contributed less than 2%. The phylum-level composition was typical for activated sludge systems (L. Wu et al., 2019).

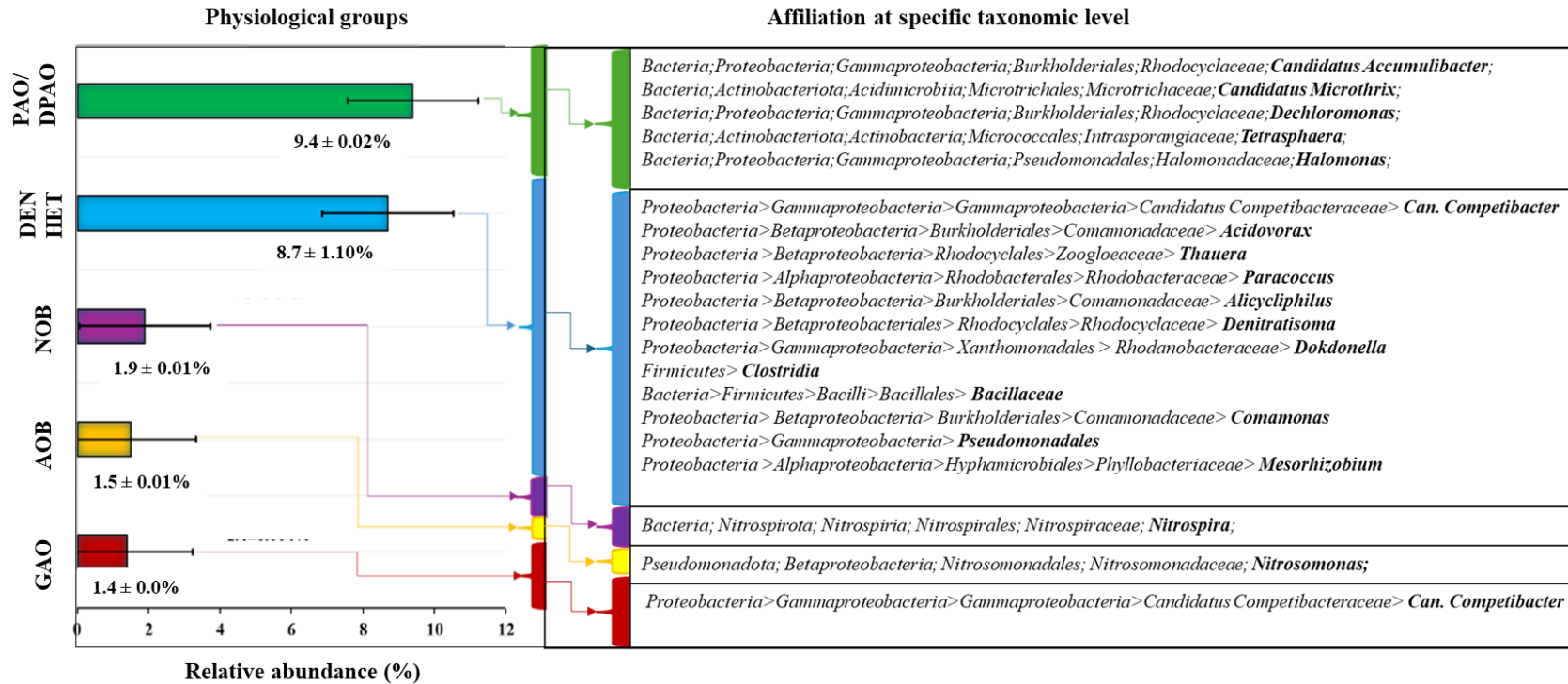


Figure 4-2: Mean relative abundance (\pm SD) of key functional bacterial groups in the GD WWTP activated sludge. Data is averaged from four sampling events over six months. Functional groups include Ammonia-oxidizing bacteria (AOB), Nitrite-oxidizing bacteria (NOB), Polyphosphate-accumulating organisms (PAO/DPAO), Glycogen-accumulating organisms (GAO), and Heterotrophic denitrifiers (DEN HET). Taxonomic classification is shown at the genus level.

The bacterial community composition and relative abundance of the key functional groups is shown in **Figure 4-2**. Total PAOs, including DPAOs, constituted the largest functional group, accounting for 9.4% (SD \pm 0.02%) of the total microbiome. Within this group, members of the genus *Tetrasphaera* (4.73% \pm 0.69%) and the filamentous *Candidatus* Microthrix (4.08% \pm 1.06%) were co-dominant. The abundances of the conventional PAO, *Candidatus* Accumulibacter (0.51% \pm 0.15%) and the DPAO *Dechloromonas* (0.05% \pm 0.01%) were substantially lower.

Heterotrophic denitrifiers were the second most abundant functional group, with an averaged relative abundance of 8.7% \pm 1.10%. Nitrifying bacteria were present at lower contribution; the ammonia-oxidizing bacteria (AOB), represented by *Nitrosomonas*, and the nitrite-oxidizing bacteria (NOB), represented by *Nitrospira*, had mean abundances of 1.5% \pm 0.01% and 1.9% \pm 0.01%, respectively. Finally, glycogen-accumulating organisms (GAOs), potential competitors to PAOs, were detected at a low abundance of 1.4% \pm 0.01%, represented by *Candidatus* Competibacter.

4.2 Results of experimental series I

To investigate the effects of glucose and acetate addition on DPAO metabolism and N₂O production with NO₃⁻ and NO₂⁻ as electron acceptors, **Series I** included two scenarios: **Scenario 1.1** under COD-limiting conditions and **Scenario 1.2** under COD non-limiting conditions discussed in sections (4.2.1 and 4.2.2).

4.2.1 Scenario 1.1—COD-limiting conditions (COD:P ratio < 2.5)

The results of measurement of key process rates, PRR, PUR, NUR, NiUR, and COD:P ratios, during this test scenario under COD-limiting conditions were summarized in **Tables 4-1** and **4-**

2, whereas the individual PO₄-P, COD, NO₃-N, NO₂-N, and N₂O profiles are presented in **Figures 4-3 and 4-4**.

Table 4-1:Comprehensive overview of the anaerobic process rates, i.e., PRR and COD values, under COD-limiting conditions.

Parameter	Units	COD-limiting conditions			
		NO ₃ ⁻	NO ₃ ⁻	NO ₂ ⁻	NO ₂ ⁻
Electron acceptor		NO ₃ ⁻	NO ₃ ⁻	NO ₂ ⁻	NO ₂ ⁻
External carbon		Acetate	Glucose	Acetate	Glucose
PRR	mg P /gMLVSS·h	7.3 ± 1.1	0.3 ± 0.02	6.3 ± 0.4	0.4 ± 0.05
COD _{anaerobic}	mg COD /gMLVSS·h	32.1 ± 3.2	13.1 ± 0.1	25.2 ± 4.1	15.9 ± 1.5
ΔCOD _{uptake} /ΔP _{release}	mg COD /mg P	4.4 ± 0.0	39.3 ± 1.0	4.1 ± 0.5	40.2 ± 4.0

Table 4-2:Comprehensive overview of the anoxic process rate, i.e., PUR, NUR, and NiUR values, under COD-limiting conditions.

Parameter	Units	COD-limiting conditions			
		NO ₃ ⁻	NO ₃ ⁻	NO ₂ ⁻	NO ₂ ⁻
Electron acceptor		NO ₃ ⁻	NO ₃ ⁻	NO ₂ ⁻	NO ₂ ⁻
External carbon		Acetate	Glucose	Acetate	Glucose
PUR	mg P /gMLVSS·h	0.9 ± 0.1	*	0.8 ± 0.2	*
NUR	mg N /gMLVSS·h	0.9 ± 0.1	0.6 ± 0.0	*	*
NUiR	mg N /gMLVSS·h	*	*	0.6 ± 0.0	0.6 ± 0.0

*Not applicable

In the anaerobic phase, significantly higher PRR were observed when acetate was used as the external carbon source compared to glucose, regardless of whether NO_3^- or NO_2^- was applied in the anoxic phase. For instance, acetate with NO_3^- produced the highest PRR ($7.3 \pm 1.1 \text{ mg P / (g MLVSS} \cdot \text{h)}$), while glucose with NO_3^- yielded a significantly lower PRR ($0.3 \pm 0.02 \text{ mg P / (g MLVSS} \cdot \text{h)}$). Similarly, under NO_2^- conditions, acetate led to a PRR of $6.3 \pm 0.4 \text{ mg P / (g MLVSS} \cdot \text{h)}$, whereas glucose resulted in only $0.4 \pm 0.05 \text{ mg P / (g MLVSS} \cdot \text{h)}$. These findings indicate stronger metabolic activity and PO_4^{3-} release with acetate, suggesting that it is more readily assimilated and metabolized by PAOs under anaerobic conditions. This is corroborated by the higher COD removal efficiencies observed with acetate (32.1% and 25.2% for NO_3^- and NO_2^- , respectively) compared to glucose (13.1% and 15.9%, respectively), reflecting more substantial fermentation and uptake activity (**Table 4-1**).

In the anoxic phase, PUR, NUR, and NiUR further emphasize the efficiency of acetate as a carbon source. For both NO_3^- and NO_2^- electron acceptors, the PUR values were measurable only with acetate (0.9 ± 0.1 and $0.8 \pm 0.2 \text{ mg P / (g MLVSS} \cdot \text{h)}$, respectively), while they were negligible with glucose (**Table 4-2**). Similarly, NUR was higher with acetate ($0.9 \pm 0.1 \text{ mg N / (g MLVSS} \cdot \text{h)}$) than with glucose ($0.6 \pm 0.0 \text{ mg N / (g MLVSS} \cdot \text{h)}$) when NO_3^- was used as the electron acceptor. These outcomes suggest that acetate promotes denitrifying P removal more effectively than glucose under carbon-limited conditions. The R^2 values of the regression lines during the anoxic phase (**0.92–0.97**) reflect consistent nitrate or nitrite reduction, yet this reduction was not accompanied by significant PO_4^{3-} uptake in glucose tests, affirming the limited DPAO activity under such substrate conditions.

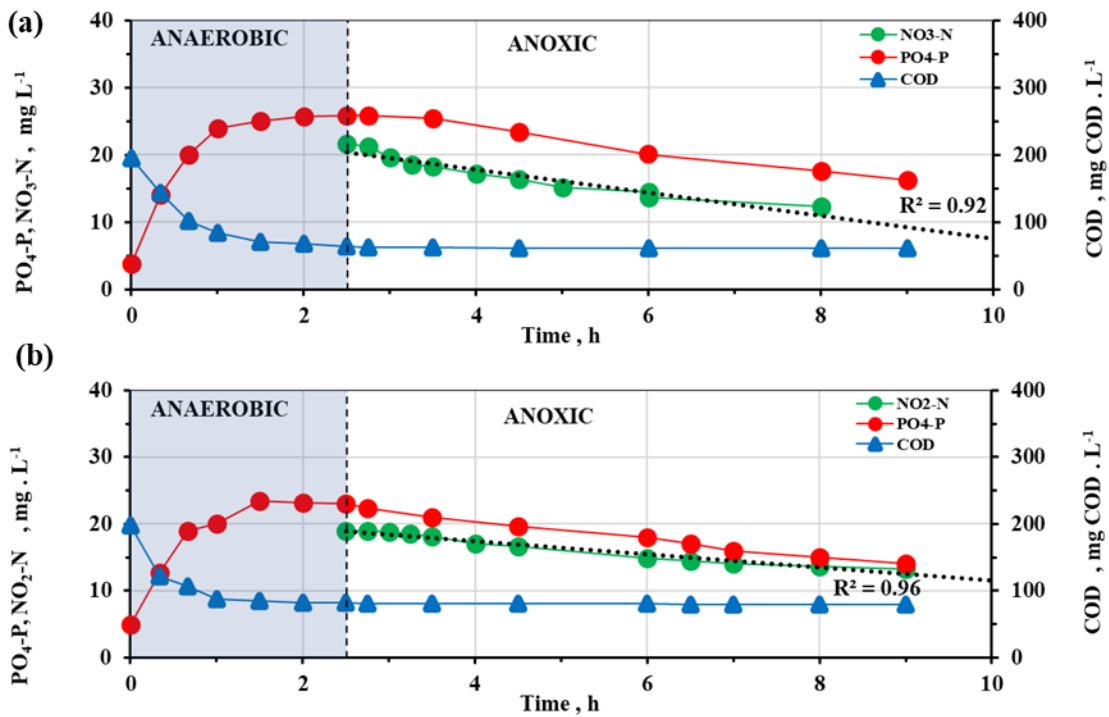


Figure 4-3: Results of the batch experiments with acetate as a carbon source under COD limiting conditions with anoxic addition of NO₃⁻ (a) and NO₂⁻ (b)

As seen in (Figure 4-3), substantial anaerobic PO₄³⁻ release was observed following the addition of NO₃⁻ (a) and NO₂⁻ (b), with rates of 7.3 ± 1.1 and 6.3 ± 0.4 mg P / (gMLVSS · h), respectively. In both cases, PO₄³⁻ release was confined to the anaerobic phase and did not extend into the anoxic phase, a clear contrast to the behavior under COD non-limiting conditions (Figure 4-5 (b)). These results suggest that, even under COD-limiting conditions, sufficient biodegradable substrate, particularly acetate was available to support efficient anaerobic PO₄³⁻ release.

Furthermore, anoxic PO₄³⁻ uptake (PUR) was recorded at 0.9 ± 0.0 mg P / (gMLVSS · h) with NO₃⁻ and 0.8 ± 0.2 mg P / (gMLVSS · h) with NO₂⁻. In addition, NUR with acetate and glucose were

0.9 ± 0.1 and 0.6 ± 0.0 mg N / (gMLVSS·h), respectively (Table 4-2), indicating that acetate supported more efficient denitrification activity compared to glucose under these conditions.

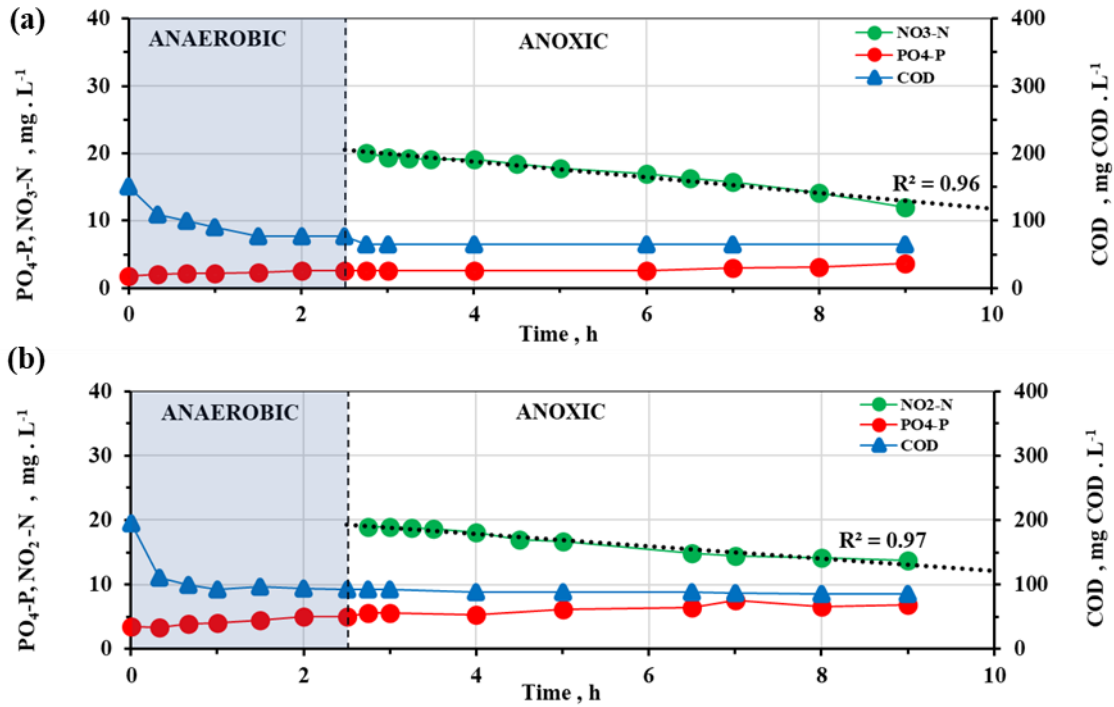


Figure 4-4: Results of the batch experiments with acetate as a carbon source under COD-limiting conditions with anoxic addition of NO_3^- (a) and NO_2^- (b)

As illustrated in **Figure 4-4**, the glucose-fed system exhibited negligible PO_4^{3-} release (PRR values of 0.4 ± 0.1 and 0.3 ± 0.02 mg P / (gMLVSS·h) with NO_3^- (a) and NO_2^- (b) respectively) under COD-limiting conditions, and continuous release was observed throughout the anoxic period. These observations underscore the crucial role of readily available VFAs, such as acetate, in activating EBPR functions while glucose proves to be complex substrate and requires additional processes to supply VFAs and sustain EBPR activity as per the findings by (Long et al.,

2021). Similar findings were reported for ethanol, which also necessitated fermentation into VFAs (X. Hu et al., 2018).

4.2.2 Scenario 1.2 – COD non-limiting conditions COD:P ratio > 2.5

The key process rates, PRR, PUR, NUR, NiUR, and COD:P ratios, during the 8.5-hour tests (2.5 h anaerobic + 6 h anoxic) are summarized in **Table 4-3** (anaerobic phase) and **Table 4-4** (anoxic phase). The results of the batch tests, including one special test with anoxic NO₂⁻ pulse dosage performed under this scenario, including PO₄-P, COD, NO₃-N, NO₂-N, and N₂O profiles, are presented in **Figures 4-5** and **4-6**.

Table 4-3: Comprehensive overview of the anaerobic process rates and other parameters under COD non-limiting conditions COD:P ratio > 2.5.

Parameter	Units	COD non-limiting conditions -anaerobic phase				
		NO ₃ ⁻	NO ₃ ⁻	NO ₂ ⁻	NO ₂ ⁻	NO ₂ ⁻ Pulse
Electron acceptor		NO ₃ ⁻	NO ₃ ⁻	NO ₂ ⁻	NO ₂ ⁻	NO ₂ ⁻ Pulse
External carbon		Acetate	Glucose	Acetate	Glucose	Acetate
PRR	mg P /gMLVSS · h	6.7±0.4	0.4± 0.1	7.4± 0.9	0.5 ±0.02	6.3±1.0
COD anaerobic	mg COD /gMLVSS · h	30.6± 2	33.4 ± 1.9	33.2 ±1.4	24.3 ± 0.9	19.1 ± 1.5
ΔCOD _{uptake} / ΔPrelease	mg COD /mg P	4.5 ± 0.1	91.3 ± 0.0	4.5 ± 0.1	88.3 ± 6.0	3.1± 0.03

Table 4-4: Comprehensive overview of the anoxic process rates and other parameters under COD non-limiting conditions COD:P ratio > 2.5

Parameter	Units	COD non-limiting conditions - anoxic phase				
		NO ₃ ⁻	NO ₃ ⁻	NO ₂ ⁻	NO ₂ ⁻	NO ₂ ⁻ Pulse
External carbon		Acetate	Glucose	Acetate	Glucose	Acetate
PUR	mg P /gMLVSS ·h	1.5± 0.6	*	0.7 ± 0.5	*	0.6 ± 0.1
NUR	mg N /gMLVSS ·h	2.9 ± 0.9	0.5 ± 0.2	*	*	*
NiUR	mg N/gMLVSS ·h	*	*	0.8 ± 0.4	0.1 ± 0.0	0.3 ± 0.1
PHBsyn(COD)		4.29	*	*	*	0.9
$\Delta P_{\text{uptake}} / \Delta \text{COD}_{\text{anoxic}}$	mg COD /mg P	0.07	0.002	0.6	0.08	0.09

4.2.2.1 Phosphate release and uptake rates (PRR and PUR)

Under acetate

The specific anaerobic PRRs measured when acetate was the external carbon source, the tests showed complete PO₄³⁻ release in the anaerobic phase, with PRR values between 6.3 and 7.4 mg P / (gMLVSS ·h) (**Table 4-3**). The anaerobic utilization of COD within 2.5 hours was accompanied by the PHA production (**see section 2.4.2**). In the presence of NO₃⁻ as an electron acceptor (**Figure 4-5a**), PO₄³⁻ release of 6.7±0.4 mg P / (gMLVSS ·h) continued into the anoxic phase when acetate

was still available, indicating high COD availability. Upon substrate (acetate) depletion, DPAOs resumed PO_4^{3-} uptake, reflecting a delayed anoxic PO_4^{3-} uptake. The observed anoxic PUR with NO_3^- was $1.5 \pm 0.6 \text{ mg P / (gMLVSS}\cdot\text{h)}$. Acetate tests with NO_3^- also demonstrated stable denitrification with a relatively high NUR of $2.9 \pm 0.9 \text{ mg N / (gMLVSS h)}$. On the other hand, acetate tests with NO_2^- (**Figure 4-5b**) depict a similar approach of PO_4^{3-} release as in **Figure 4-5a** but with a slightly PRR value of $7.4 \pm 0.9 \text{ mg N / (gMLVSS h)}$ without any observed delay of anoxic PO_4^{3-} uptake. Despite the presence of non-limiting COD, the COD removal coefficient was less pronounced in the test with acetate and NO_2^- with $R^2 = 0.95$ compared to acetate and NO_3^- with a strong linear correlation ($R^2 = 0.99$).

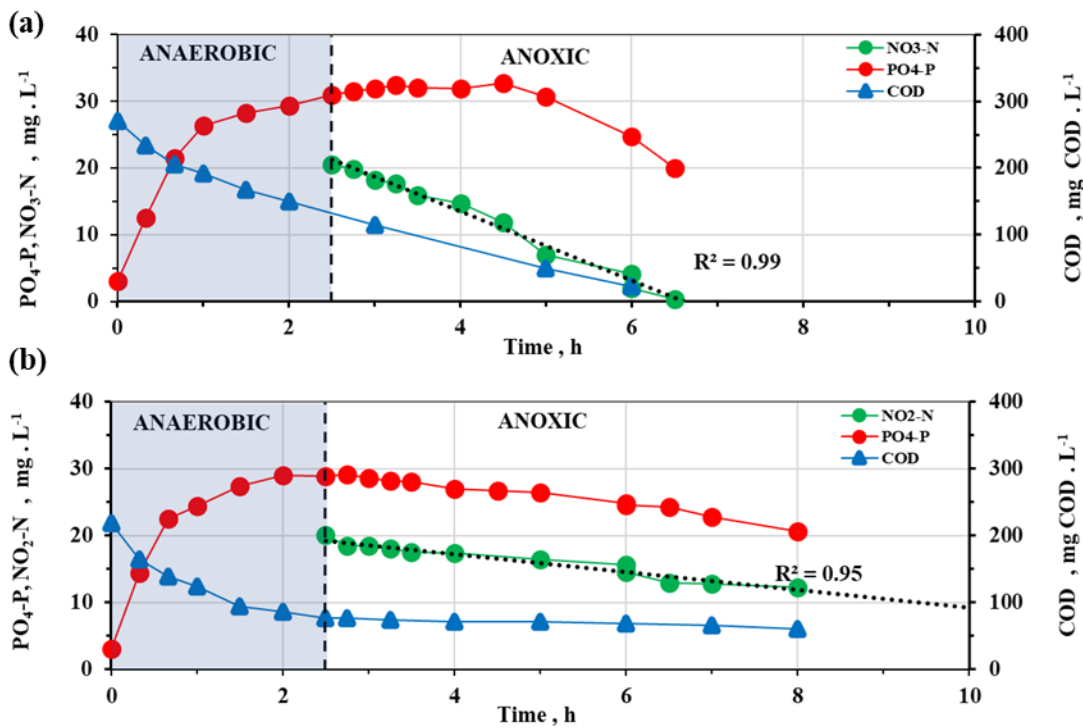


Figure 4-5: Results of the batch experiments with acetate as a carbon source under COD non-limiting conditions with anoxic addition of NO_3^- (a) and NO_2^- (b).

Under glucose

In contrast, the tests with glucose, negligible PO_4^{3-} release with low PRR values of 0.4 ± 0.1 and $0.5 \pm 0.02 \text{ mg P / (gMLVSS}\cdot\text{h)}$ (Table 4-3). Equally, the anoxic PO_4^{3-} uptake values were also negligible, regardless of electron acceptor type. However, higher COD consumption rates at 33.4 ± 1.9 and $24.3 \pm 0.9 \text{ mg COD / (gMLVSS}\cdot\text{h)}$ (Figure 4-6) account for up to < 4% compared to the tests under acetate. Glucose potentially stimulated other HETs rather than DPAOs, which is consistent with findings of Wang et al. (2019) and Echeverría et al. (2023), who reported that HETs can outcompete DPAOs under glucose-rich conditions. conditions.

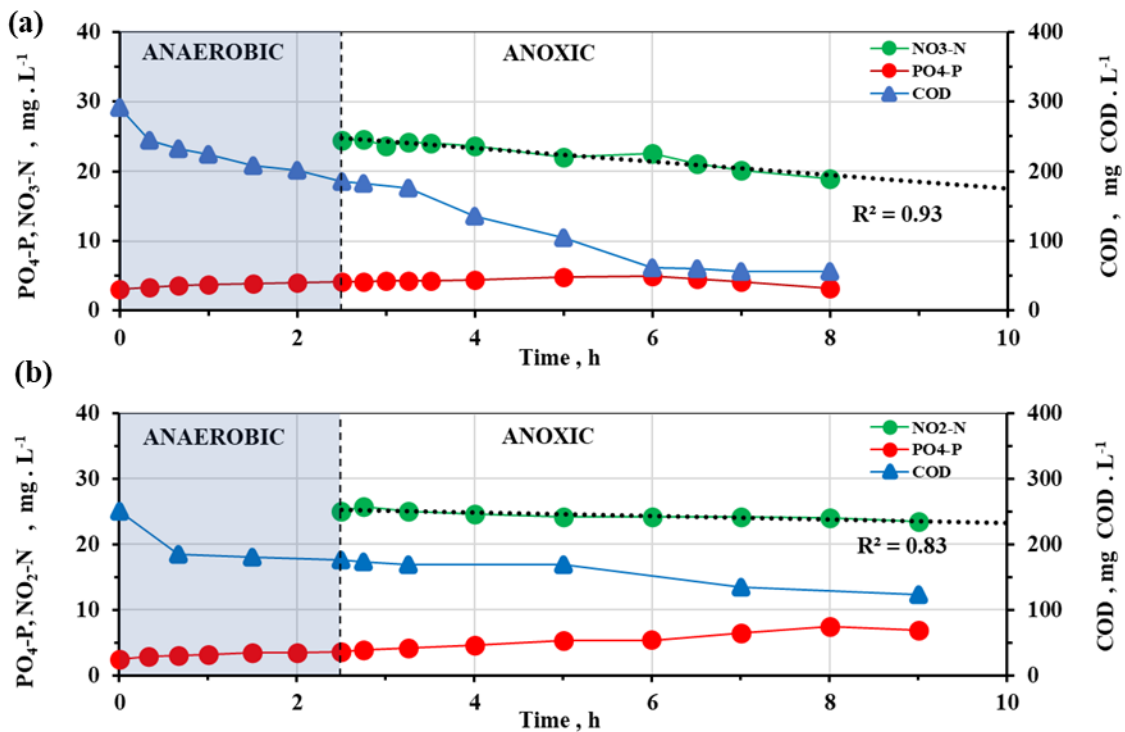


Figure 4-6:Results of the batch experiments with glucose as a carbon source under COD non-limiting conditions with anoxic addition of NO_3^- (a) and NO_2^- (b)

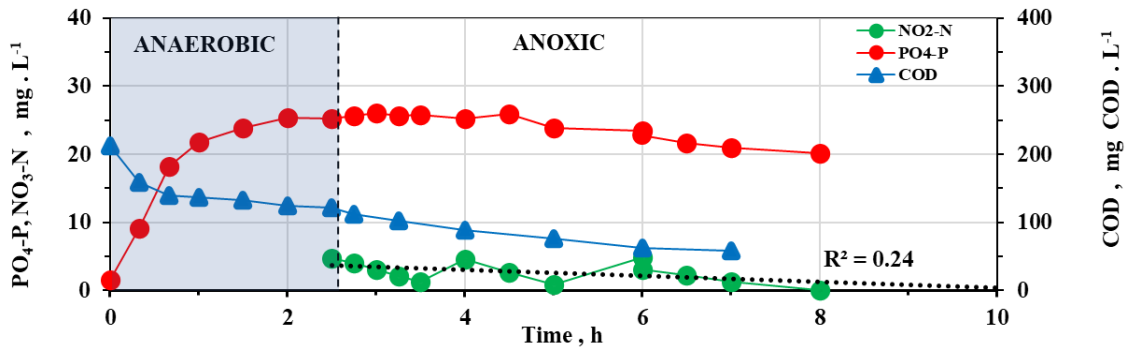


Figure 4-7: Results of the batch experiments with glucose as a carbon source under COD non-limiting conditions with anoxic addition of NO_2^- in pulse dosage.

Pulse dosing of NO_2^- under COD non-limiting conditions led to slightly improvement in PO_4^{3-} uptake as seen in (Figure 4-7). PUR values were comparable: 0.7 ± 0.5 vs. 0.6 ± 0.1 mg P / (gMLVSS·h) for the full and pulse dosage, respectively (Table 4-5).

Table 4-5: Summary of the most important EBPR performance indicators in comparing tests with acetate at COD non-limiting conditions in different NO_2^- dosage strategies.

Parameter	Unit	Single (Full)-dosage Figure 4-6 (b)	Pulse-dosage (Figure 4-7)
R^2 correlation	-	0.95	0.24
$\text{COD}_{\text{Anoxic}}$	mg O_2 / gMLVSS·h	1.2	7.4
PUR	mg P / gMLVSS·h	0.7 ± 0.5	0.6 ± 0.1
COD:P	mg COD/mg P	4.9	3.5
NiUR	mg N / gMLVSS·h	0.8 ± 0.4	0.3 ± 0.1
PHBsyn(COD)	-	n/a	0.92

n/a: not applicable

4.2.2.2 Nitrate and nitrite utilization rates (NUR and NiUR)

The availability of carbon source significantly influenced the total denitrification rates. Under COD-limiting conditions, acetate addition resulted in a NUR of 2.9 ± 0.9 mg N / (gMLVSS h) and a NiUR of 0.8 ± 0.4 mg N / (gMLVSS h). These rates were substantially higher than those measured with glucose, which were 0.5 ± 0.2 and 0.6 ± 0.0 mg N / (gMLVSS·h) for NUR and NiUR, respectively (**Table 4-4**). The NUR correlation values in acetate and glucose-fed tests ranged between $R^2 = 0.92 - 0.96$, while those of NiUR ranged at $R^2 = 0.96 - 0.97$ as can be seen in **Figures 4-3** and **4-4**, respectively.

Under COD non-limiting conditions, the NUR correlation range was $R^2 = 0.93-0.99$ while NiUR ranged at $R^2 = 0.83 - 0.95$. The corresponding NUR and NiUR correlation values in acetate- and glucose-fed tests showed comparable results of $R^2 = 0.92$ and $R^2 = 0.96$, and NiUR values of $R^2 = 0.96$ and $R^2 = 0.97$ in **Figures 4-5** and **4-6**. These findings suggest that DPAO activities are more dominant with acetate in the anoxic phase than with glucose. Thus, acetate proves to be the preferred carbon source for PO_4^{3-} uptake similar to findings reported in Yu et al. (2023), DPAOs response to acetate, glucose, and glycerol additions found that acetate induced effective P-removal, surpassing glucose and glycerol. Wang et al., (2010) equally reported unsatisfactory performance of glucose as the primary carbon source in EBPR. **Figure 4-8** compares NUR and NiUR values for acetate- and glucose-fed conditions, clearly demonstrating the enhanced denitrification performance associated with acetate as an external carbon source.

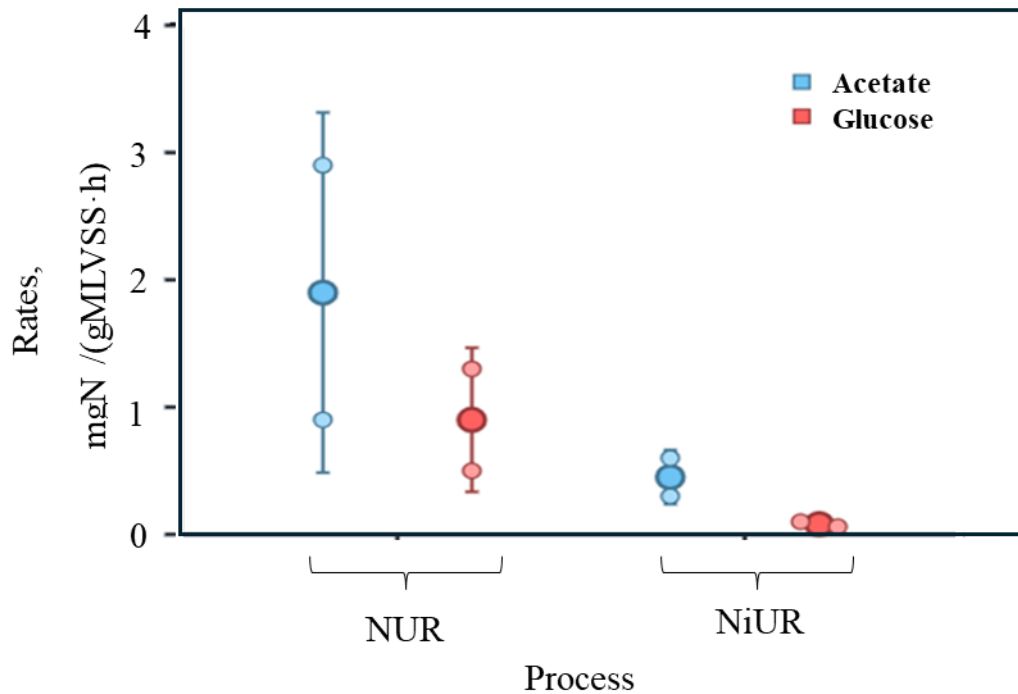


Figure 4-8: Comparison of NUR and NiUR values in acetate- and glucose-fed tests

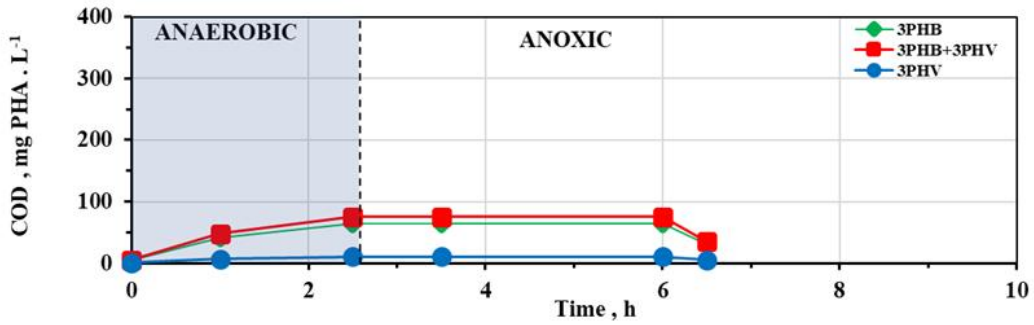
4.2.2.3 Polyhydroxyalkanoates (PHA) production

The synthesis of intracellular storage materials (polyhydroxybutyrate - 3PHB and polyhydroxy valerate - PHV) was analyzed under COD non-limiting conditions to understand the mechanisms of carbon uptake and relation to the EBPR. PHA production was fundamentally dependent on the type of carbon source supplied (**Figure 4-9**).

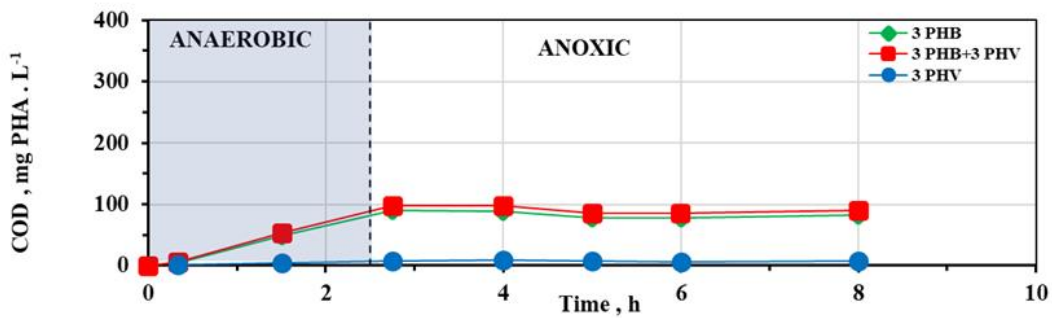
In the case of acetate, noticeable synthesis of 3PHB was observed during the initial 2.5-hour anaerobic phase (**Figure 4-9(a-b)**). These observations align with previous research by Bauhs et al. (2022) who identified 3PHB as the most abundant component in the polymer composition. The observed PHB formation coincided with phosphate release, which is consistent with canonical EBPR stoichiometry: ATP generated from poly-P hydrolysis supports the uptake of external acetate

and its storage as PHB during the anaerobic phase. During the subsequent anoxic phase, stored PHA served as the electron donor for denitrifying phosphate uptake. PHB accumulation appeared insensitive to whether NO_2^- or NO_3^- was used later as the electron acceptor but strongly dependent on the anaerobic carbon source (acetate vs glucose), as shown in **Figure 4-9(a–b)**, while no PHA production was observed with glucose (**Figure 4-9(c)**). When glucose was the substrate, no significant PHA production was detected during the anaerobic period (**Figure 4-9c**). This lack of carbon storage explains the failure of the glucose-fed biomass to perform anoxic phosphate uptake, as it had no internal electron donor available for the process.

(a) Acetate – NO₃⁻



(b) Acetate – NO₂⁻ pulse dosage



(c) Glucose – NO₂⁻

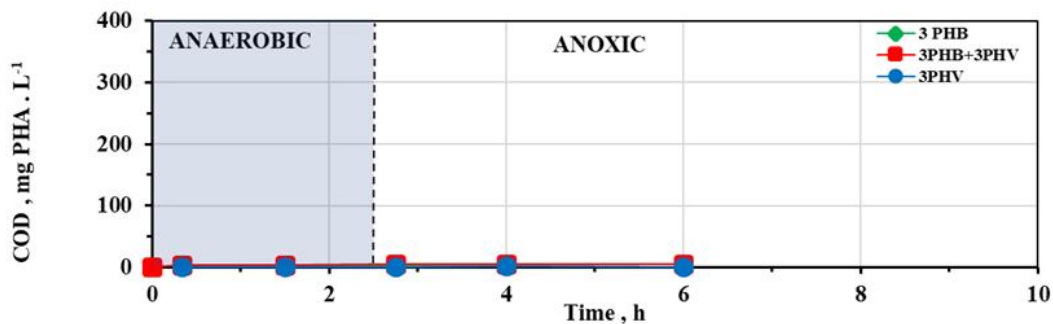


Figure 4-9:PHB and PHV production profiles in the bacterial cell COD non-limiting conditions (a) acetate with nitrate. (b) acetate with nitrite, and (c) glucose with nitrite

4.3 Results of experimental series II

The series II experiments were aimed at investigating the effect of modified anoxic conditions on DPAO activity and its implications for EBPR performance and N₂O production. The results of the

impact of modified conditions on EBPR performance and N_2O production profiles are presented largely under the anaerobic phase in CCT and three scenarios of modified anoxic with **Scenario 2.1** as a reference test similar to (“standard” COD-limiting, as was **series I Scenario 1.1** experiments), **Scenario 2.2**: PO_4^{3-} precipitated conditions and **Scenario 2.3**: PHA-depleted conditions.

4.3.1 The anaerobic phase test in CCT

The results of the anaerobic PO_4^{3-} release test with acetate for ST1 and ST2 are shown in **Figure 4-10**. In both trials, a nearly complete PO_4^{3-} release was obtained within 2.5 h, pointing to the high presence of an internal level of polyphosphate in the DPAO-rich biomass. The $\text{PO}_4\text{-P}$ concentration eventually reached a level of 23.8 mg PL^{-1} and 24.8 mg PL^{-1} , corresponding to the value of $12.53 \text{ mg P / (gMLVSS}\cdot\text{h)}$ and $13.05 \text{ mg P / (gMLVSS}\cdot\text{h)}$ for the ST1 and ST2, respectively, within the initial 60 minutes. This ratio provided sufficient external carbon that ensured polyphosphate depletion in the biomass by the activities of the DPAOs. The competing group, i.e., GAOs, to that of DPAOs, showed less and insignificant hindrance by the GAOs in the respective Trial. Glucose was not applied for the anaerobic PO_4^{3-} release in the **series II** experiments based on the previous findings that glucose insignificantly induced the anaerobic PO_4^{3-} release, i.e., $0.26 \text{ mg P / (gMLVSS}\cdot\text{h)}$, and therefore was not suitable carbon for the EBPR performance. Wisniewski et al. (2018) reported similar findings with acetate at $34.70 \text{ mg P / (gMLVSS}\cdot\text{h)}$ compared to another non-acclimated biomass.

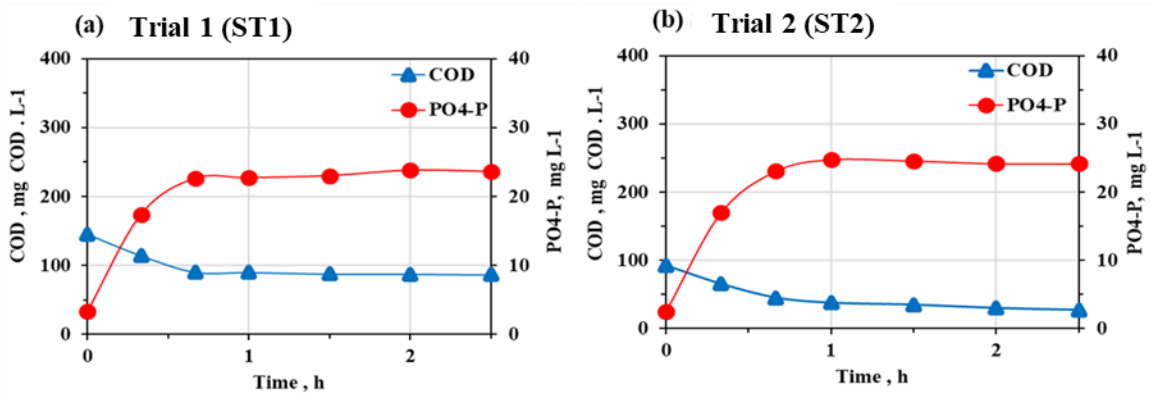


Figure 4-10: Results of the anaerobic phase in the common cultivation reactor (CCT) with the profiles of PO_4^{3-} release and COD consumption in (a) Trial 1 (ST1) and (b) Trial 2 (ST2).

In both batch experiments **Figure 4-10 (a and b)**, the anaerobic phase (0–2.5 hours) PO_4^{3-} release, alongside a significant uptake of COD, suggests that the organisms consumed the available carbon source for the synthesis of internal storage compounds such as PHAs. Most PO_4^{3-} release occurred within the first 60-90 minutes, attributed to sufficient availability of carbon and acetate at the average PRRs of $6.2 \pm 0.1 \text{ mg P / (g MLVSS} \cdot \text{h)}$ and $7.2 \pm 0.02 \text{ mg P / (g MLVSS} \cdot \text{h)}$ in ST1 and ST2, respectively.

4.3.2 *The modified anoxic phase tests (in three scenarios)*

To quantify the role of DPAOs in total anoxic nitrogen removal after reference scenario, two sequential scenarios were designed to selectively inhibit their metabolic pathway. **Scenario 2.2** blocked anoxic phosphate uptake via chemical precipitation, while **Scenario 2.3** eliminated the internal carbon source (PHA) required for DPAO-driven denitrification.

4.3.2.1 Scenario 2.1: Reference tests (as in Scenario 1.1)

The process rates and P-removal efficiencies of the anoxic reference test conditions are summarized in **Table 4-6**, while the individual observed profiles of the $\text{NO}_3\text{-N}$ or $\text{NO}_2\text{-N}$, COD, and $\text{PO}_4\text{-P}$ concentrations are presented in **Figure 4-11**.

In all the reference tests similar to the “standard” COD-limiting, as in **Scenario 1.1**, there was no addition of any external carbon source in the anoxic phase on the 6th hour. These tests served as a reference in the determination of the microbial share contribution to P-removal relative to denitrification rates. In both ST1 and ST2, the PO_4^{3-} uptake followed a similar trend, achieving the lowest $\text{PO}_4\text{-P}$ concentrations after 6.5 hours of the anoxic phase. The maximum NUR values obtained were $1.3 \text{ mg N / (gMLVSS}\cdot\text{h)}$ in ST1 and $1.0 \text{ mg N / (gMLVSS}\cdot\text{h)}$ (ST2) (**Table 4-7**). ST1 tests obtained PUR of 1.4 mg PL^{-1} and 0.5 mg PL^{-1} while in ST2, 1.1 mg PL^{-1} and 1.2 mg PL^{-1} of the same with NO_3^- and NO_2^- electron acceptors, respectively.

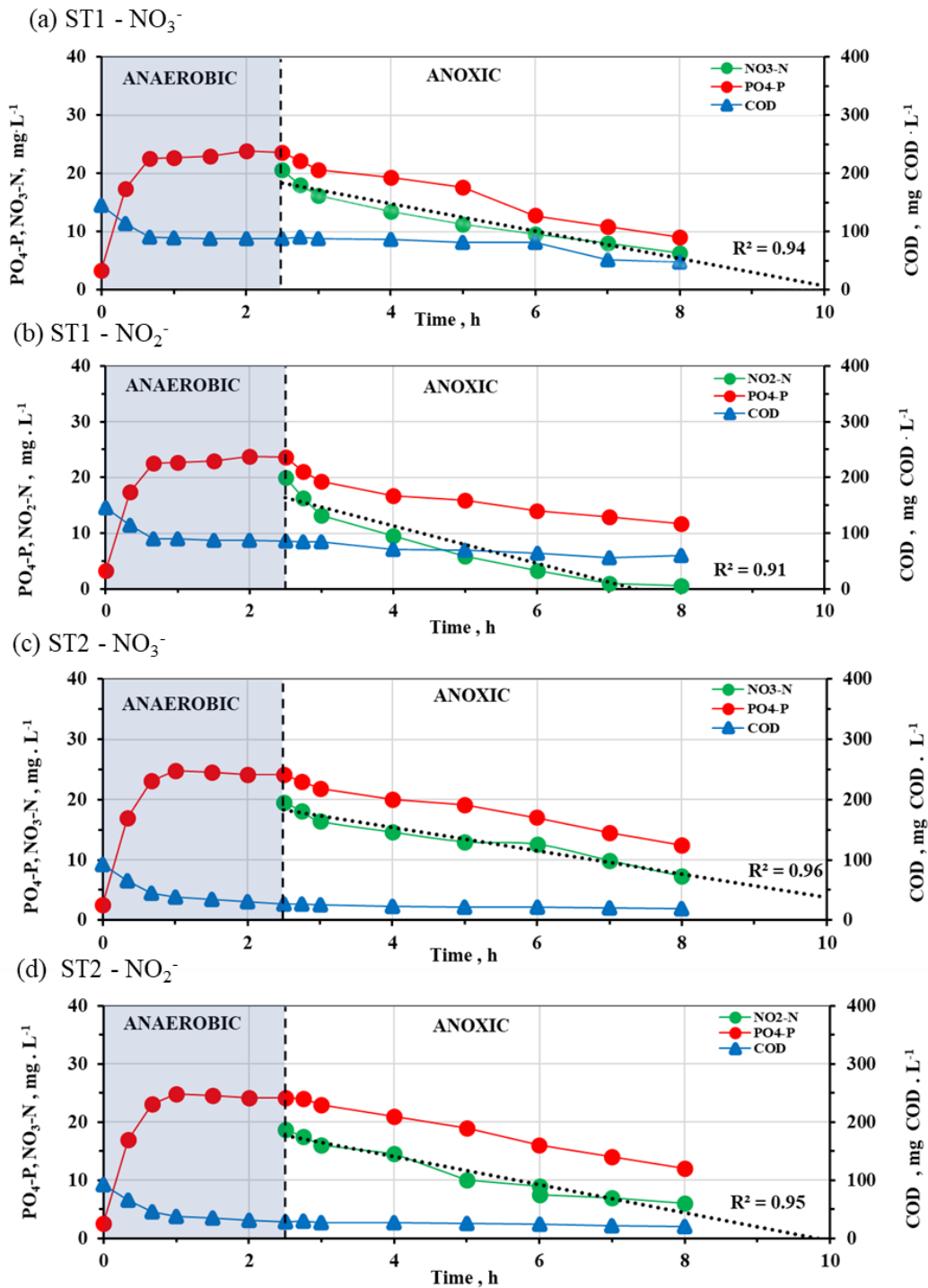


Figure 4-11: The profiles of COD, NO₃-N, NO₂-N, and PO₄-P concentrations (mg·L⁻¹) under the modified anoxic **scenario 2.1**: reference tests without addition of glucose on the 6th hour.

The PRR of 6.2 mg P / (gMLVSS·h) was higher than the subsequent anoxic PUR of 1.4 mg P / (gMLVSS·h). In all the tests, PO₄³⁻ release strictly occurred only within the anaerobic phase and did not continue into the anoxic phase (**Figure 4-11**), further pointing to the findings that COD-limiting conditions are sufficient for P-removal compared to the higher COD non-limiting conditions in **Series I** experiments.

Table 4-6: The process rates under modified anoxic reference conditions in trials 1 and 2.

Parameter		Scenario 2.1: modified anoxic reference conditions			
		ST1		ST2	
Parameter	Units	NO ₃ ⁻	NO ₂ ⁻	NO ₃ ⁻	NO ₂ ⁻
PUR	mg P / (gMLVSS·h)	1.4	0.5	1.1	1.2
NUR	mg N / (gMLVSS·h)	1.3	-	1.0	-
NiUR	mg N / (gMLVSS·h)	-	1.8	-	1.3
Carbon source		anaerobic-acetate,		anoxic – no glucose addition	

4.3.2.2 Scenario II: PO₄-P anoxic precipitated condition.

The application of the chemical precipitation of PO₄³⁻ resulted in lower NURs of 0.4 mg N / (gMLVSS·h) in both ST1 and ST2 (**Table 4-7**). This is a significant drop compared to the NURs in Scenario 2.1 (**Table 4-6**). The PO₄-P absence in the anoxic conditions as presented in **Figure 4-12** resulted in lower NURs depicting reduced denitrification and microbial metabolisms related to respiration and intracellular transformation (**Figure 4-12**). Accordingly, it can be assumed that the difference between the N removal values before and after chemical precipitation of PO₄-P could be related to the activity of DPAOs storage of PO₄-P at the expense of PHA. It is seen from the

result that both the chemical precipitation and PHA-depleted anoxic conditions significantly impacted DPAO activity.

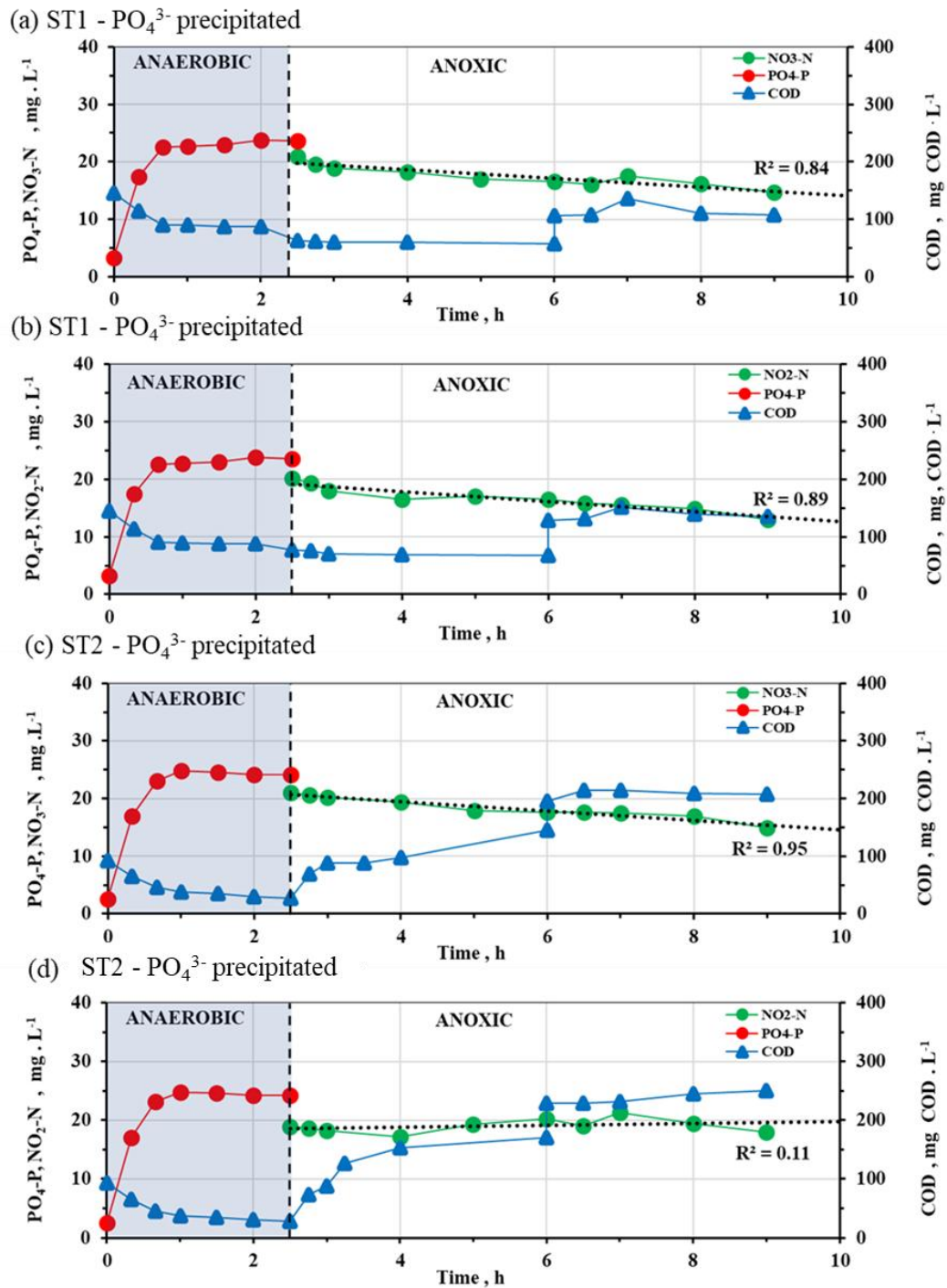


Figure 4-12: The profiles of COD, NO₃-N, NO₂-N, and PO₄-P concentrations (mg·L⁻¹) under the modified anoxic **scenario 2.2:** PO₄³⁻ precipitated with the addition of glucose on the 6th hour.

At the onset of the anoxic phase (post 2.5 hours), either $\text{NO}_3\text{-N}$ (**Figure 4-12a**) or $\text{NO}_2\text{-N}$ (**Figure 4-12b**) was introduced as the electron acceptor. Despite prior chemical precipitation of $\text{PO}_4\text{-P}$, a rapid decrease in PO_4^{3-} levels are observed after the transition to anoxic conditions, possibly indicating residual biological PO_4^{3-} uptake or incomplete precipitation. With NO_3^- as the electron acceptor, a gradual concentration decreases from approximately 22 mgN.L^{-1} was observed, and the regression analysis showed a good fit ($R^2 = 0.84$), indicating consistent NO_3^- reduction. A glucose pulse introduced at the 6th hour temporarily increases COD levels, enhancing NO_3^- reduction and indicating that denitrification may have been limited by the availability of readily biodegradable carbon. With NO_2^- , a steeper and more consistent decrease is observed, with a higher R^2 value of 0.89. This suggests that NO_2^- was utilized more efficiently, in line with previous findings that DPAOs often prefer NO_2^- over NO_3^- due to the lower energy requirements for its reduction. The COD profile mirrors this trend, with a similar response to glucose addition. The $\text{PO}_4\text{-P}$ concentration remains relatively stable after the anoxic phase begins, confirming the effect of chemical precipitation and limited biological PO_4^{3-} uptake thereafter.

Table 4-7: Denitrification rates under different carbon sources and electron acceptors in anaerobic-anoxic experiments with PO₄-P precipitated conditions

Parameter	Units	Scenario 2.2: PO ₄ -P precipitated conditions			
		ST1		ST2	
Electron acceptor		NO ₃ ⁻	NO ₂ ⁻	NO ₃ ⁻	NO ₂ ⁻
NUR	mg N / (gMLVSS·h)	0.4	-	0.4	-
NiUR	mg N / (gMLVSS·h)	-	0.5		0.3
COD _{anoxic} rate	mg O ₂ / (g MLVSS·h)	5.8	6.8	14.1	21.6
COD:N	g COD / g N	14.93	14.8	491.3	249.8
Carbon source	anaerobic-acetate anoxic-glucose addition				

Chemical precipitation of PO₄³⁻, residual biological activity, may persist, and the type of electron acceptor significantly affects the efficiency of denitrification. NO₂⁻ proved to be a more effective electron acceptor than NO₃⁻, and external carbon addition improved denitrification performance under potentially carbon-limited conditions.

4.3.2.3 Scenario 2.3 : PHA-depleted conditions

In the absence of PHA, the obtained values of the NUR further declined to 0.014 mg N / (gMLVSS·h) and 0.3 mg N / (gMLVSS·h) in ST1 and ST2, respectively (**Table 4-8**). This is a significant drop compared to those in scenario 2.1 (**Table 4-6**) and scenario 2.2 (**Table 4-7**). The denitrification is associated with the small portion of other groups of unidentified microorganisms with denitrifying capabilities potentially using intracellular stored lipids in g COD / g N.

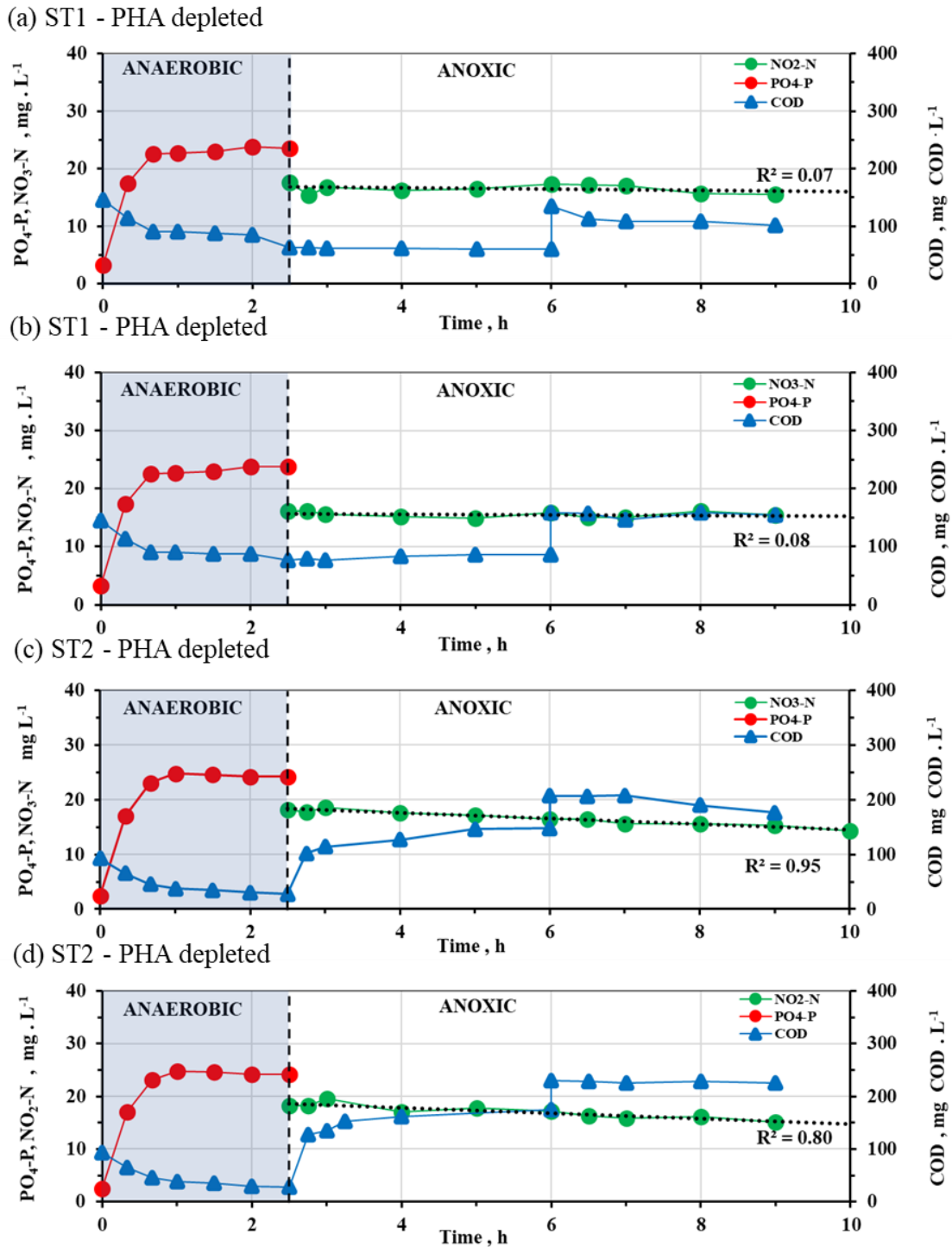


Figure 4-13: The profiles of COD, NO₃-N, NO₂-N, and PO₄-P concentrations (mg · L⁻¹) under the anaerobic-anoxic PHA absence conditions. Glucose addition on the 6th hour.

Table 4-8: Summary of denitrification rates under different carbon sources and electron acceptors in anaerobic-anoxic experiments with PHA-depleted conditions.

Parameter	Scenario 2.3: PHA-absent conditions				
	unit	ST1		ST2	
Electron acceptor		NO ₃ ⁻	NO ₂ ⁻	NO ₃ ⁻	NO ₂ ⁻
NUR	mg N /(gMLVSS·h)	0.014	-	0.3	-
NiUR	mg N /(gMLVSS·h)	-	0.003	-	0.3
COD _{anoxic}		6.7	1.9	17.3	18.5
COD:N	g COD /g N	33.87	163.5	41.75	45.5
Carbon source		anaerobic-acetate, an anoxic-glucose addition			

4.3.3 Denitrification share by microbial groups based on NURs and NiUR

The modified anoxic denitrification activities under three distinct scenarios were assessed for two trials (ST1 and ST2) by evaluating **NUR** and **NiUR**. The experimental findings are summarized in **Table 4-9**. **Table 4-10** presents the computed microbial percentage shares derived from NUR and NiUR (**Equations 1** and **2**), together with the rate component breakdown illustrated in **Figure 3-5**. This applied to both trials of the experiment (ST1 and ST2) across modified anoxic scenarios (2.1, 2.2, and 2.3).

Under the reference condition (**Scenarios 2.1**), both trials recorded the highest NUR and NiUR values, with **ST1** showing slightly higher activity (NUR = 1.40 mg N /(gMLVSS·h), NiUR = 1.79 mg N /(gMLVSS·h)) compared to **ST2** (NUR = 1.03, NiUR = 1.29) mg N /(gMLVSS·h)). This confirms the optimal metabolic activity and availability of intracellular storage compounds under standard conditions.

In **scenario 2.2** (PO_4^{3-} precipitated), both NUR and NiUR values dropped drastically. ST1 showed a negative NiUR ($-0.46 \text{ mg N / (gMLVSS}\cdot\text{h)}$), indicating potential inhibition or absence of nitrite reduction pathways, possibly due to the removal of phosphorus, which may have affected the activity of PAOs. A similar trend was observed for ST2 (NiUR = -0.30), although its NUR (0.42) was slightly higher than that of ST1 (0.39).

Scenario 2.3 (PHA-depleted) showed the lowest NUR and NiUR in ST1, with values nearing zero (NUR = 0.01 , NiUR = 0.03), implying strong metabolic limitation due to carbon unavailability. However, ST2 performed relatively better under the same conditions (NUR = 0.27 , NiUR = 0.28), suggesting more robust utilization of alternative carbon sources or more efficient carbon management by the microbial community as in **Table 4-9**.

Table 4-9: NUR and NiUR rates and estimated microbial group contributions under modified anoxic conditions for Trial 1 (ST1) and Trial 2 (ST2).

Scenario	Condition	NUR (ST1) (mg N /(gMLVSS·h))	NiUR (ST1) (mg N /(gMLVSS·h))	NUR (ST2) (mg N /(gMLVSS·h))	NiUR (ST2) (mg N /(gMLVSS·h))
2.1	Reference /standard	1.40	1.79	1.03	1.29
2.2	PO_4^{3-} - precipitated	0.39	0	0.42	0
2.3	PHA- depleted	0.01	0.03	0.27	0.28

The estimated microbial group contributions to total denitrification activity (based on NUR data) revealed notable differences between trials. DPAOs contributed significantly under reference

conditions, with 40.72% (ST1) and 31.37% (ST2), showing their active role when intracellular PHA and P were available. Their activity sharply decreased under modified conditions. Compared to the HET which had the highest proportional contribution under ST2 in all scenarios, particularly in Scenario 2.2 (55.28%), indicating their dominant role when PAO activity was compromised. NiUR-based share proportions were not evaluated due to zero or negligible uptake values in some scenarios, particularly under phosphate-precipitated conditions.

Table 4-10: Estimated microbial group share proportions in total NUR and their corresponding percentage contributions to denitrification activity (ST1 and ST2).

Microbial group	% Contribution (ST1)	% Contribution (ST2)
DPAOs	26.00%	32.31%
Heterotrophs (HET)	74.00%	67.69%

The share contribution values presented in **(Figure 4-14)** are calculated excluding unidentified denitrifying microorganisms, potentially utilizing stored lipids or other internal carbon reserves. As such, the percentage contributions reflect only the relative proportions of DPAOs and HET within the denitrifying community.

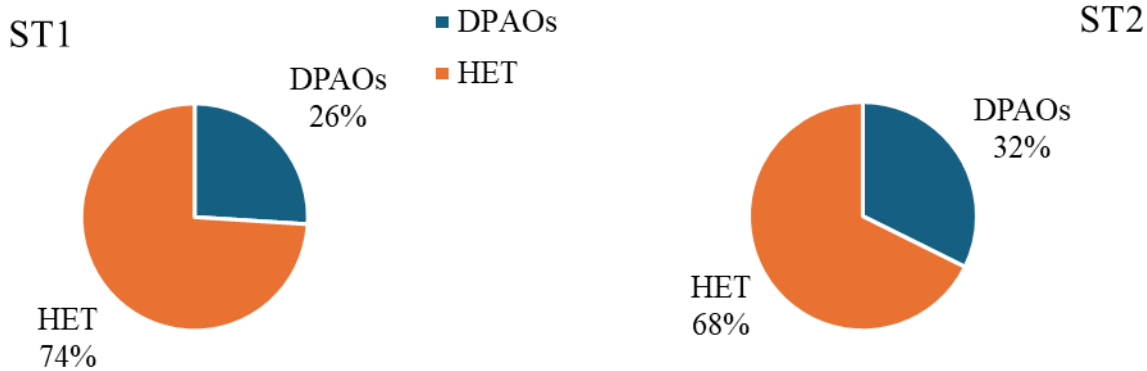


Figure 4-14:Percentage contribution of DPAOs and HET to NUR under modified anoxic conditions.

4.4 N₂O production and DPAO activities

This section presents the key findings from experimental investigations aimed at evaluating the dynamics of N₂O production and the activity of DPAOs under varying anoxic conditions in enhanced biological phosphorus removal (EBPR) systems. The experiments were conducted in two main phases—**series I** and **series II**—each designed to assess the influence of specific operational parameters including electron acceptor type (NO₂⁻ vs. NO₃⁻), carbon source (acetate vs. glucose), COD:N and COD:P ratios, and microbial community composition on N₂O emissions and denitrification performance.

Series I focused on evaluations under control of COD-limiting and COD-non-limiting conditions, allowing for direct observation of N₂O profiles in response to changes in substrate availability and electron acceptor. Series II further explored the effects of three distinct Scenarios -reference conditions (**Scenario 2.1**), PO₄³⁻ precipitated conditions (**Scenario 2.2**), and PHA-depleted conditions (**Scenario 2.3**) applied across two experimental trials (**ST1** and **ST2**). Data is provided for **series I**, **Scenario 1.2** (COD non-limiting conditions), and for **series II** (**Scenarios 2.1, 2.2,**

and 2.3) under two trials (ST1 and ST2). Unfortunately, data for **Series I, Scenario 1.1**, could not be included due to experimental complications and subsequent data processing issues. Nevertheless, the remaining dataset is robust and sufficient to meet the study's objectives, particularly concerning the evaluation of N₂O production patterns under controlled operational variables.

4.4.1 N₂O production under COD non-limiting conditions :Series I

In **Series I, Scenario 1.2**, with COD non-limiting, the impact of electron acceptor and carbon source type on N₂O emissions was clearly evident. **Figures 4-15** and **Figure 4-16** illustrate production of N₂O under various combinations of substrates (acetate and glucose) and electron acceptors (NO₂⁻ and NO₃⁻). The results reveal a strong dependency of N₂O accumulation on the nature of the electron acceptor. When NO₃⁻ was used, N₂O emissions were negligible across both carbon sources (**Figure 4-15**). This indicates complete denitrification and effective reduction of N₂O to N₂, likely due to uninhibited activity of the N₂O reductase enzyme (NosZ). In both acetate – NO₃⁻ and glucose – NO₃⁻ conditions, N₂O concentrations remained close to zero throughout the anoxic phase, confirming the low emission potential of nitrate-reducing pathways under these conditions.

In contrast, when NO₂⁻ was used as the electron acceptor (**Figure 4-16**), significant N₂O accumulation was observed. In the acetate – NO₂⁻ condition with pulse dosing, N₂O concentration rapidly increased during the first five hours of the anoxic phase, reaching a peak of approximately 0.6 mg N₂O-N/L, before declining to near-zero levels. This suggests a transient inhibition or limitation of NosZ activity, resulting in temporary N₂O accumulation. The rapid decline in N₂O thereafter may be due to the depletion of nitrite or the recovery of N₂O reductase function. This

result is consistent with previous findings by (C. Li et al., 2013) , which noted that NO_2^- can stimulate N_2O accumulation under conditions of high carbon availability.

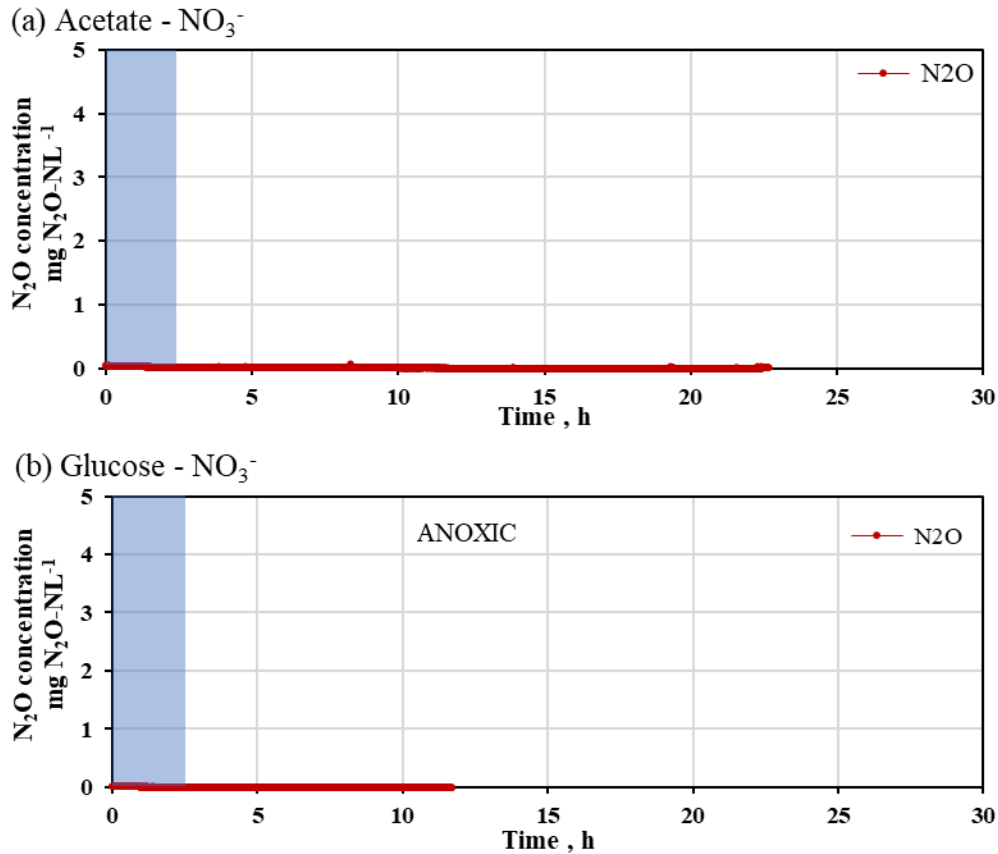
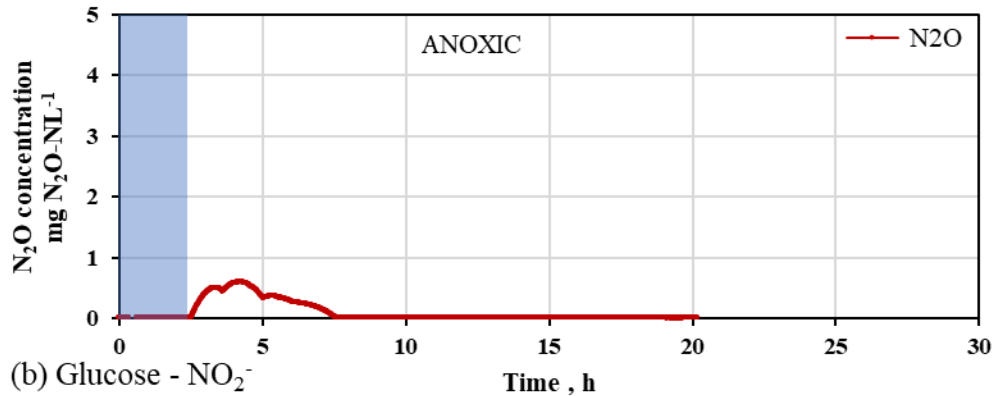


Figure 4-15: N_2O production profiles in experimental series I , scenario 1.2 COD non-limiting conditions under NO_3^- as the electron acceptor.

The glucose - NO_2^- condition displayed a markedly different N_2O profile (**Figure 4-16b**). A steady and prolonged increase in N_2O was observed, with the concentration peaking at approximately 2.9 mg N_2O -N/L after around 15 hours of anoxic operation. This prolonged accumulation suggests slower denitrification kinetics or lower enzymatic efficiency in the glucose-fed system, possibly due to differences in metabolic pathways or microbial community structure. Compared to acetate,

glucose may promote the growth of heterotrophic denitrifiers but less efficient at reducing N_2O production.

(a) Acetate - NO_2^- Pulse dosage



(b) Glucose - NO_2^-

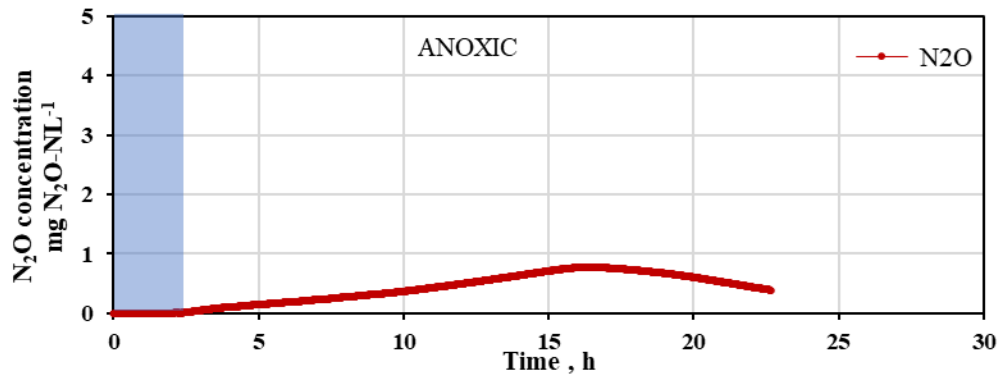


Figure 4-16: N_2O production profiles in experimental series I , scenario 1.2 COD non-limiting conditions with NO_2^- as the electron acceptor.

These observations collectively demonstrate that NO_2^- as an electron acceptor has a higher tendency to cause N_2O accumulation than NO_3^- , particularly in the presence of excess carbon. This is likely due to NO_2^- -induced inhibition of the NosZ enzyme, which catalyzes the final step of denitrification reduction of N_2O to N_2 . The presence of NO_2^- , especially in combination with high carbon availability, may cause imbalance and metabolic bottlenecks that lead to incomplete

denitrification. This finding aligns with (Pan et al., 2024), who also reported increased N_2O emissions under NO_2^- fed conditions in EBPR systems.

Furthermore, the N dosing strategy played a critical role in determining the extent of N_2O accumulation. In the acetate – NO_2^- condition, pulse dosing of the electron acceptor (**Figure 4-16a**) resulted in a lower and shorter N_2O emission peak compared to the glucose – NO_2^- full-dosage setup (**Figure 4-16b**). While the peak concentration in the pulse-dosed condition was only 0.6 mg N_2O -N/L (**Figure 4-16a**), the full-dosage scenario reached 2.9 mg N_2O -N/L, five times higher, and maintained elevated N_2O levels for a longer period. This suggests that gradual or pulse input of the electron acceptor can mitigate N_2O production by preventing the overloading of denitrifying pathways and ensuring better redox balance. The implication is that careful control of NO_2^- availability and carbon dosing patterns may help minimize N_2O production in practical WWTP operations. Since DPAOs are known to play a significant role in denitrifying P removal under anoxic conditions, their metabolic performance can be inferred from the N_2O patterns. The relatively low N_2O accumulation under acetate – NO_3^- and acetate – NO_2^- conditions with pulse dosing may reflect efficient DPAO-mediated denitrification and complete N_2O reduction, especially when acetate (a preferred carbon source for DPAOs) was provided in a controlled manner. On the other hand, higher N_2O production in glucose-fed systems suggests that HETs, rather than DPAOs, dominated the microbial activity, possibly due to substrate preferences and slower kinetics associated with glucose metabolism.

4.4.2 N_2O production in dynamic anoxic conditions - Series II

The N_2O production profiles obtained under dynamic anoxic conditions in **Series II** revealed distinct trends associated with the type of electron acceptor, availability of intracellular storage

compounds, and operational trials (ST1 and ST2). **Figures 4-17** and **4-18** represent trial 1 (ST1), while **Figures 4-19** and **4-20** correspond to trial 2 (ST2), each under NO_2^- and NO_3^- conditions across three experimental scenarios: **Scenario 2.1** – reference condition (serving as a standard for comparison), **Scenario 2.2** – PO_4^{3-} -precipitated condition (a chemically induced limitation of P availability) and **Scenario 2.3** – PHA-depleted condition, representing a biological limitation in intracellular carbon reserve. The specific electron acceptors used are indicated in each of the tests.

4.4.2.1 N_2O production profiles under series II, Trial 1 (ST1)

Figures 4-17 and **4-18** provide N_2O production profiles for Trial 1 (ST1) with NO_2^- and NO_3^- electron acceptors respectively. Under the reference condition (**Figure 4-17a**), a steep and rapid rise in N_2O concentration was observed shortly after the transition from anaerobic to anoxic phases, stabilizing between 2.5–3.0 mg N_2O -N/L, which indicates efficient and sustained denitrifying activity likely fueled by sufficient internal reserves of PHA and polyphosphate. In the phosphate-precipitated condition (**Figure 4-17b**), although the final N_2O concentration was similar to the reference. N_2O concentrations peaked at comparable levels (= 3.0 mg N_2O -N/L) but were sustained for a longer duration, nearly 20 hours, indicating a shift in metabolic response likely influenced by the chemical removal of PO_4^{3-} and a reduced capacity for energy generation and storage.

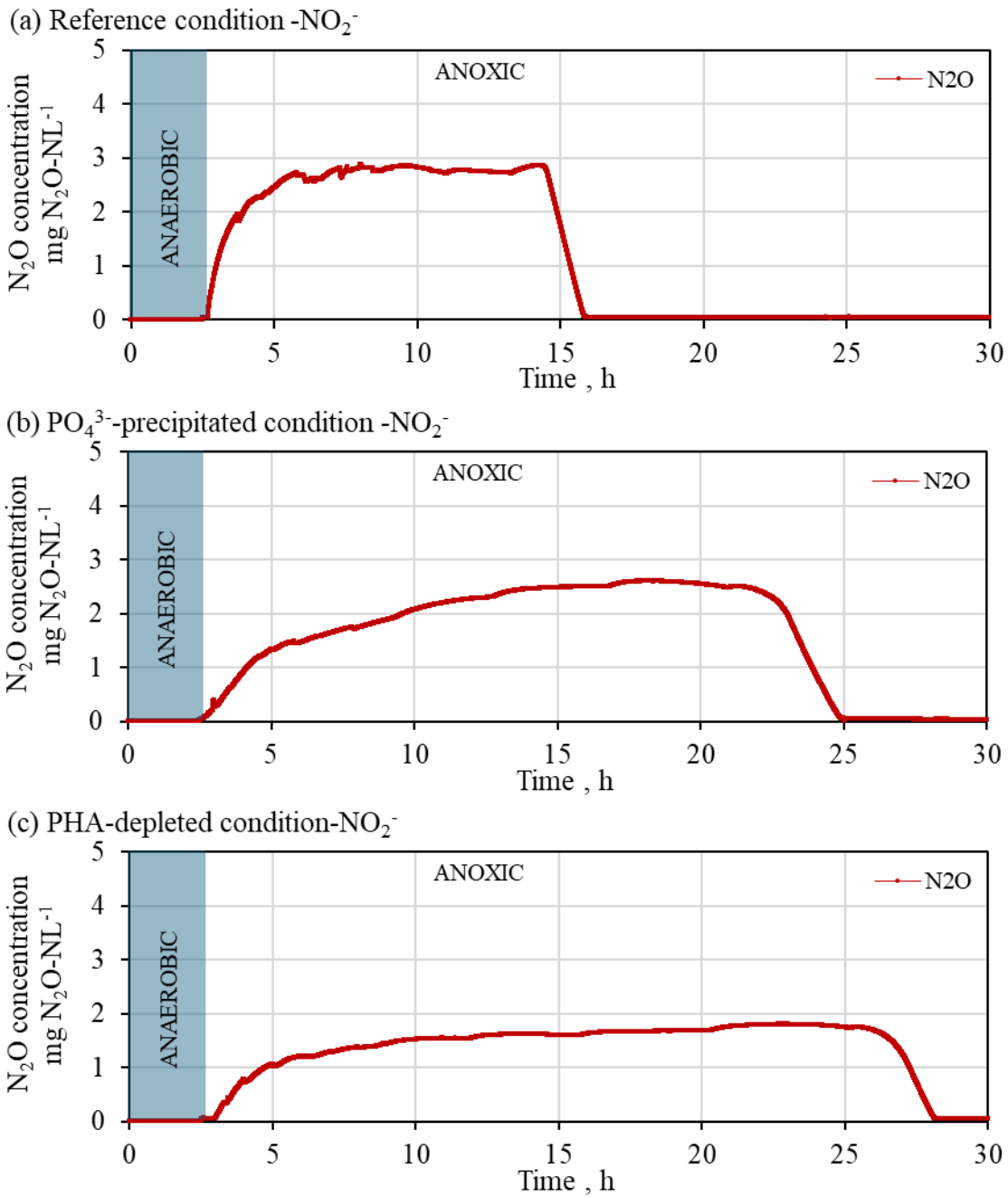
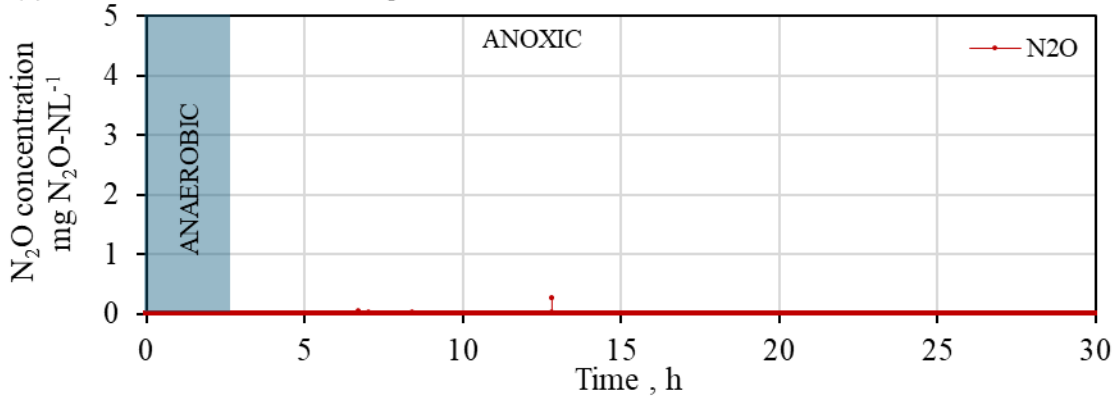


Figure 4-17: N₂O production profiles under dynamic anoxic conditions in series II – Trial 1 (ST1) using NO₂⁻ as electron acceptor across scenarios (a) 2.1 (reference) ,(b) 2.2 (PO₄³⁻-precipitated), and (c) 2.3 (PHA-depleted)

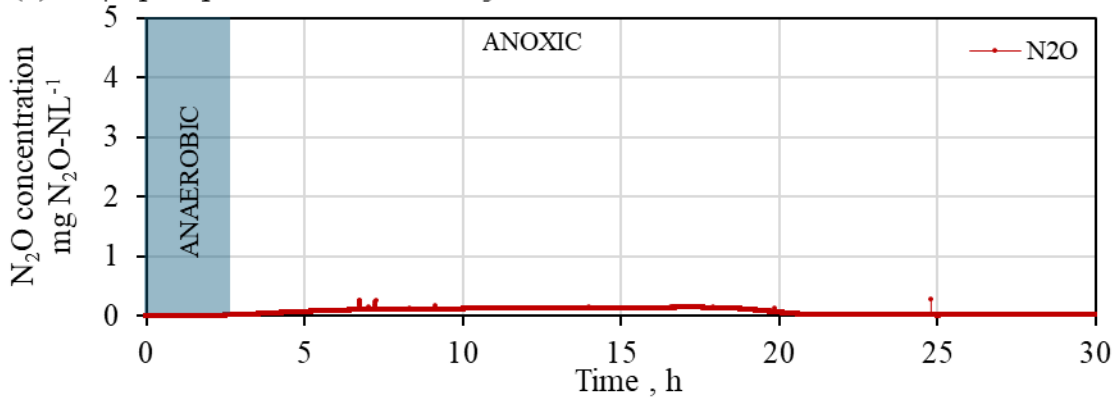
Meanwhile, the PHA-depleted condition (**Figure 4-17c**) resulted in significantly lower N_2O production, with concentrations barely exceeding 2.0 mg N_2O -N/L and displaying a flatter accumulation profile. The suppressed N_2O emissions in this scenario highlight the critical role of PHA as a key internal carbon source driving DPAOs.

In **Figure 4-18** tests under NO_3^- , across all three scenarios, N_2O production was negligible, with recorded concentrations remaining close to zero throughout the entire anoxic phase. In the reference condition (**Figure 4-18a**), only trace levels of N_2O were detected sporadically, with no significant accumulation observed, indicating a highly efficient denitrification pathway with minimal N_2O production. Similarly, in the PO_4^{3-} -precipitated conditions (**Figure 4-18b**), no N_2O production was recorded, suggesting that the removal of polyphosphate reserves did not stimulate incomplete denitrification or increase N_2O emissions when NO_3^- was the electron acceptor. The PHA-depleted condition (**Figure 4-18c**) followed the similar trend, with negligible and stable N_2O levels, further supporting the notion that nitrate reduction in these conditions proceeds through complete denitrification, even under carbon-limited scenarios. These results contrast sharply with those from NO_2^- -based conditions (**Figure 4-17**), where substantial N_2O production occurred, underscoring the key role of the electron acceptor type in governing gaseous intermediate emissions. Collectively, The use of NO_3^- as an electron acceptor promoted complete reduction to N_2 with minimal N_2O production, regardless of the internal storage status.

(a) Reference condition - NO_3^-



(b) PO_4^{3-} -precipitated condition - NO_3^-



(c) PHA-depleted condition - NO_3^-

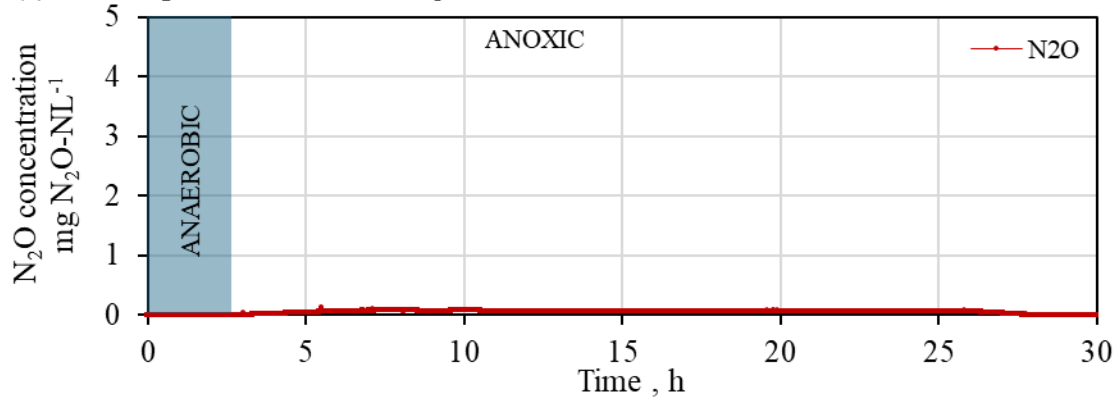


Figure 4-18: N_2O production profiles under dynamic anoxic conditions in series II – Trial 1 (ST1) using NO_3^- as electron acceptor across scenarios (a) 2.1 (reference) ,(b) 2.2 (PO_4^{3-} -precipitated), and (c) 2.3 (PHA-depleted)

4.4.2.2 N_2O production profiles under series II , Trial 2 (ST2)

Figures 4-19 and **4-20** illustrate the N_2O production profiles under dynamic anoxic conditions in Series II – Trial 2 (ST2) with NO_2^- and NO_3^- electron acceptors respectively.

When NO_2^- was used as the electron acceptor , production of the N_2O was observed across all three scenarios: (a) reference condition (**Scenario 2.1**), (b) PO_4^{3-} -precipitated condition (**Scenario 2.2**), and (c) PHA-depleted condition (**Scenario 2.3**). In the reference condition (**Figure 4-19a**), the N_2O production was minimal and short-lived, with a slight peak observed early in the anoxic phase, reaching approximately 0.7 mg N_2O -N/L. This brief peak was followed by a rapid decline in N_2O levels, indicating efficient denitrification activity and minimal intermediate accumulation. This performance can be attributed to the balanced availability of PHA and PO_4^{3-} , which supported optimal metabolic functioning of DPAOs. In contrast, under PO_4^{3-} precipitated conditions (**Figure 4-19b**), where intracellular phosphorus cycling was disrupted, a continuous and linear increase in N_2O concentration was observed throughout the anoxic phase, ultimately exceeding 3 mg N_2O -N/L by the end of the 24-hour test. The absence of PO_4^{3-} likely impaired the normal functioning of DPAOs, leading to an imbalance in electron flow and accumulation of N_2O as a by-product of incomplete denitrification. Similarly, in the PHA-depleted scenario (**Figure 4-19c**), the initial N_2O levels remained low; however, a noticeable increase in N_2O production occurred in the latter part of the anoxic phase, peaking at around 2.5 mg N_2O -N/L. This delayed rise suggests that the absence of readily available intracellular carbon limited the energy supply needed for complete denitrification, forcing microorganisms to rely on slower, less efficient pathways. . The lowest productions were observed under balanced conditions (**Scenario 2.1**), while disturbances to either

carbon or P availability (**Scenarios 2.2** and **2.3**) significantly increased N₂O accumulation, even though with differing patterns.

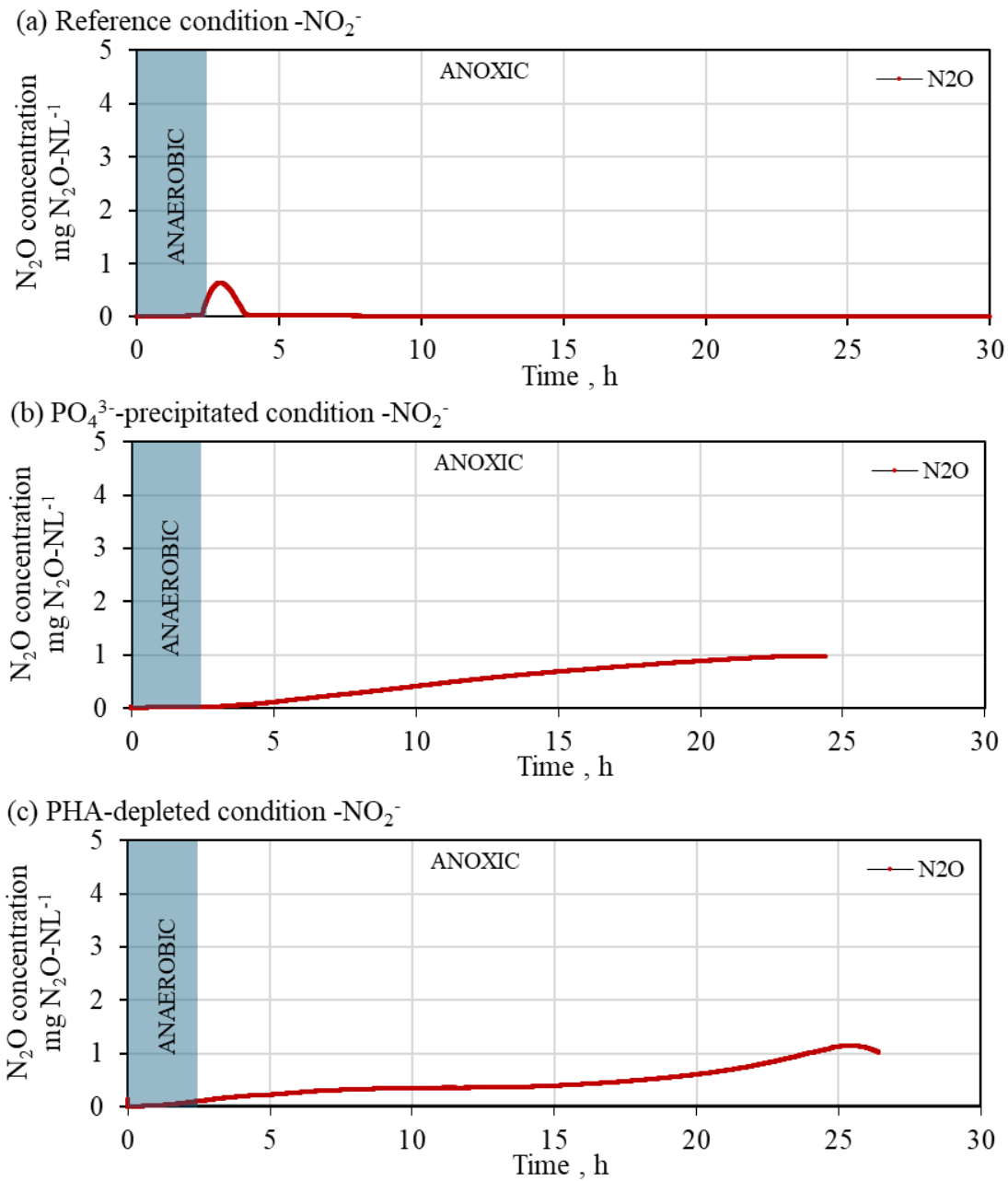


Figure 4-19: N₂O production profiles under dynamic anoxic conditions in series II – Trial 2 (ST2) using NO₂⁻ as electron acceptor across scenarios (a) 2.1 (reference), (b) 2.2 (PO₄³⁻-precipitated), and (c) 2.3 (PHA-depleted)

In **Figure 4-20**, N₂O production under anoxic conditions using NO₃⁻ as the electron acceptor. Across all scenarios, N₂O concentrations remained consistently low, with values near or at zero throughout the 30-hour experimental period. Under reference conditions (**Figure 4-20a**), a stable profile with no detectable N₂O production was recorded, suggesting complete and efficient denitrification supported by sufficient intracellular PHA and polyphosphate reserves. Even in the PO₄³⁻-precipitated scenario (**Figure 4-20b**), where energy storage via polyphosphate was compromised, N₂O emissions remained nearly undetectable. Similarly, under the PHA-depleted condition (**Figure 4-20c**), despite carbon availability through glucose, N₂O levels did not rise, indicating sustained denitrifying activity and electron transfer efficiency. These observations demonstrate that microbial communities retained their capacity for full NO₃⁻ reduction to N₂ gas, even under resource-constrained conditions, and suggest minimal risk of N₂O when NO₃⁻ is used.

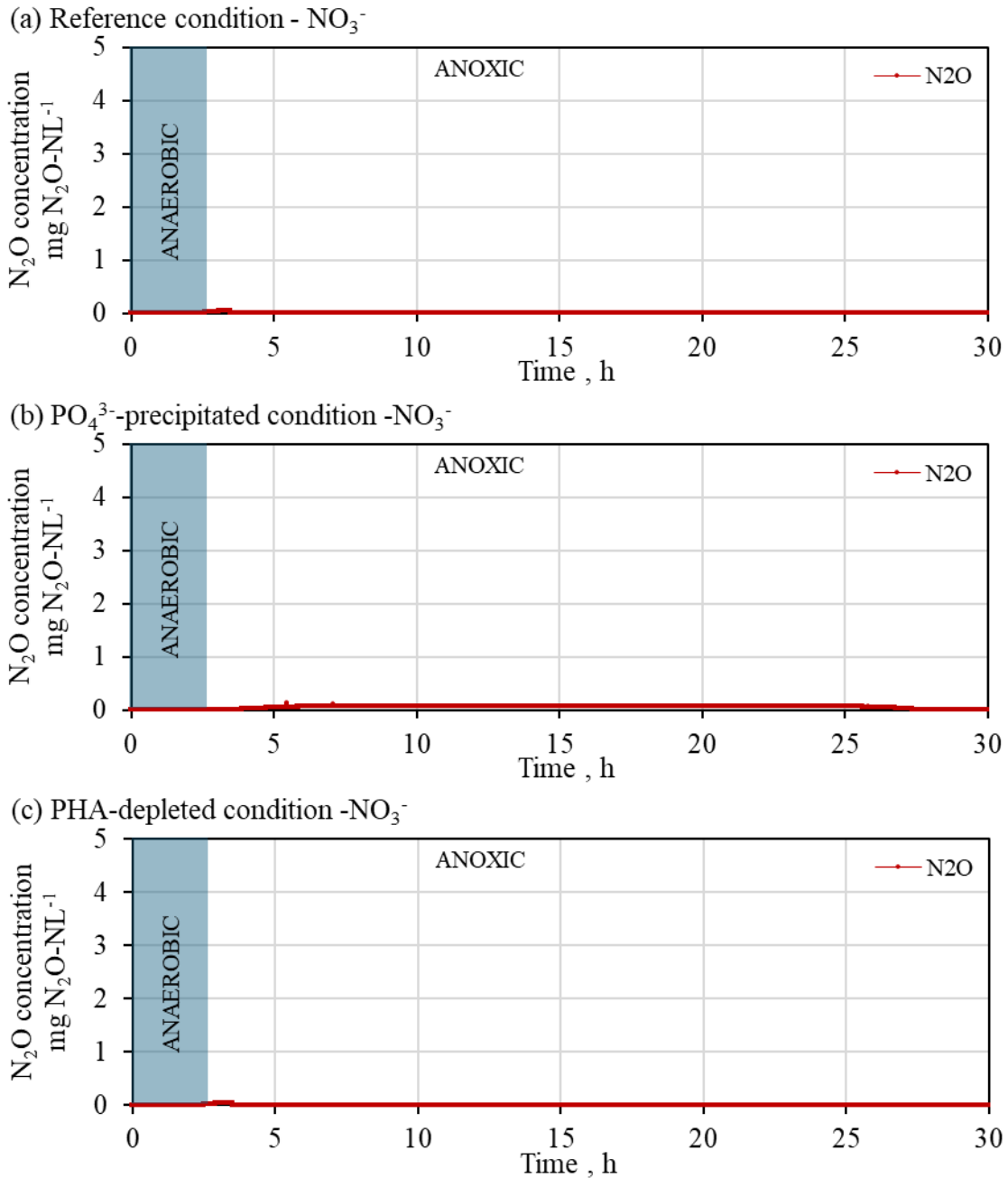


Figure 4-20: N_2O production profiles under dynamic anoxic conditions in series II – Trial 2 (ST2) using NO_3^- as electron acceptor across scenarios (a) 2.1 (reference) ,(b) 2.2 (PO_4^{3-} -precipitated), and (c) 2.3 (PHA-depleted)

Compared to **Figure 4-18** (of ST1) and **Figure 4-20** (of ST2) in both trials resulted in negligible N_2O production across all scenarios, highlighting the robustness of NO_3^- -based denitrification in minimizing N_2O production regardless of intracellular storage limitations.

Series I (tests under COD non-limiting conditions - **Figure 4-15**, **Figure 4-16**) and **Series II** (tests under modified anoxic phase - **Figure 4-17** to **Figure 4-20**) highlights similarities and differences in the N_2O production. In both series, the use of NO_3^- as the electron acceptor resulted in negligible N_2O emissions across all scenarios, regardless of internal resource limitations, confirming its role in promoting complete denitrification and minimizing N_2O production. In contrast, NO_2^- led to substantial N_2O accumulation, especially under PHA-depleted and PO_4^{3-} -precipitated conditions. However, the pattern of N_2O differed: Series I exhibited rapid but relatively short lived N_2O peaks due to the abundance of readily available COD, while **Series II** (Trial 1 and 2) showed a slower, more prolonged N_2O production due to fluctuating or declining carbon availability under dynamic conditions with NO_2^- electron acceptor. These differences highlight how COD dynamics influence microbial denitrification performance and N_2O production. In both trials, the reference conditions characterized by sufficient PHA and polyphosphate reserves consistently resulted in the lowest N_2O production when NO_2^- was used. Overall, the results underscore that while both internal storage compounds and the type of electron acceptor significantly affect N_2O dynamics, operational context particularly carbon availability plays a critical role in shaping the timing and amount of production in EBPR systems.

5. DISCUSSION

5.1 Microbial Community Structure the four WWTPs in the Pomeranian region, Poland

The outcome of the microbial community as presented in **Figure 4-1** aimed to determine the WWTP with highest *Tetrasphaera*- enrichment highlights distinct variations in the abundance and composition of DPAOs across the four full-scale EBPR plants in Pomeranian region of Poland. The range of relative abundance of total PAOs and DPAOs, including *Tetrasphaera*, measured between (11.0 – 12.4%) with higher abundance realized in Gdynia Debogórze (GD). Such values agree with those reported for other full-scale EBPR systems, where DPAO abundances typically range between 8–15% of total bacterial populations (Camejo et al., 2016; Oehmen et al., 2010), indicating that these organisms occupy a stable niche in the activated sludge microbial community. Among the microbial populations identified apart from *Tetrasphaera*, included *Candidatus* *Microthrix*, *Dechloromonas* and *Halomonas* and *Ca. Accumulibacter* which align with findings by Nielsen et al., (2019) who reported the presence of other bacteria genus, including *Dechloromonas*, *Ca. Holomonas* and *Ca. Microthrix* with substantial poly-P reserves with emphasis on their collaborative nature of in P removal processes.

5.1.1 *Dominance of Tetrasphaera*

As shown in the **Figure 4-1**, *Tetrasphaera* consistently accounted for the largest fraction of overall microbial community with average abundance of $7.0\% \pm 2.2\%$. Gdynia Debogórze (GD) and Swarzewo (SW) WWTPs being among the two with highest individual percentage of *Tetrasphaera* at about 6% and 7% respectively. These findings are in agreement with the growing body of literature that report *Tetrasphaera* as a key and often dominant DPAO in full-scale EBPR systems (R. Liu et al., 2019a; Sun et al., 2021b; Y. Zhang & Kinyua, 2020). Herbst et al. (2019) and

Muszyński et al. (2015) documented *Tetrasphaera* abundances ranging from 20-30% in Danish and Polish WWTPs based on 16S rRNA gene sequencing and FISH analyses. The MIDAS global survey (Dueholm et al., 2024) further supports these findings, identifying *Tetrasphaera* as the most prevalent PAO across 32 EBPR plants worldwide, with relative abundances ranging from 1.3-11.9% and an average of 4.6%, surpassing traditional PAOs, such as *Ca. Accumulibacter* (1.19%) and *Dechloromonas* (2.84%). Comparatively, the relatively low reported proportions of *Ca. Accumulibacter* at $(0.51\% \pm 0.15\%)$ and *Dechloromonas* at $(0.05\% \pm 0.01\%)$, depart from expectations based on laboratory-scale enrichment studies that favored these taxa under acetate-rich conditions (Bond et al., 1995; Crocetti et al., 2000; Kong et al., 2004). The slightly higher *Tetrasphaera* abundance in the current study compared to the MIDAS average could be attributed to regional factors, process configurations, or environmental conditions specific to Polish WWTPs.

As noted by Ong et al. (2014) and Stokholm-Bjerregaard et al. (2017), the relative dominance between *Tetrasphaera* and *Ca. Accumulibacter* can shift depending on the carbon source availability, anaerobic retention time, and NO_3^- exposure, which influence microbial competition and niche selection. The strong representation of *Tetrasphaera* in Polish WWTPs validates global observations of its importance in WWTPs in line with the growing recent literature (Liu et al., 2019b; Sun et al., 2021; Zhang & Kinyua, 2020). However, unlike *Ca. Accumulibacter* which primarily take up VFAs like acetate, *Tetrasphaera* utilizes more diverse carbon substrates including glucose and can switch flexibly between aerobic respiration and denitrification (Liu et al., 2019; Zhao et al., 2022). Roy et al. (2021) equally reported the ability of *Tetrasphaera* to metabolize complex carbon compounds, such as glucose which in this study hasn't proven viable

preferable substrate to the EBPR process based on the low activities realised with the use of glucose for instance in **Figure 4-6**.

5.1.2 *Abundance of *Ca. Microthrix**

An outstanding observation is the relatively high abundance of *Ca. Microthrix* across all four WWTPs, ranging between 4% and 6%, with particularly elevated levels in GD and SL (**Figure 4-1**). While *Ca. Microthrix* is not conventionally categorized as a PAO, its role in EBPR systems cannot be overlooked. Traditionally, it has been linked to filamentous bulking and poor sludge settleability, posing serious operational challenges (Nierychlo et al., 2021). However, emerging evidence demonstrates its capacity to store polyphosphate granules, suggesting that it may contribute in a supplementary and less dynamic manner to P removal (Nierychlo et al., 2021). This duality underscores its complex ecological role. On one hand, its persistence within activated sludge communities may enhance resilience and structural stability process. On the other hand, its slower metabolic activity and filamentous morphology risk displacing functionally active PAOs, such as *Tetrasphaera* and *Ca. Accumulibacter*, which are directly responsible for efficient denitrifying P removal.

5.1.3 *Low abundance of *Ca. Accumulibacter* and *Dechloromonas**

In contrast to the high abundance of *Tetrasphaera* and *Ca. Microthrix*, *Ca. Accumulibacter* was consistently detected at very low levels ($0.5\% \pm 0.1\%$), with *Dechloromonas* showing even lower abundance at ($0.14\% \pm 0.1\%$). The results contradicts Chen et al., (2021) who observed significant dominance of *Dechloromonas* despite being identified as members of the DPAO group (Zhao et al., 2022). Moreover, this observation contrasts with the long-standing view of *Ca. Accumulibacter*

as the “conventional PAO” in EBPR systems (Bond et al., 1995; Seviour & McIlroy, 2008). While *Ca. Accumulibacter* has been widely reported in lab-scale acetate-fed reactors and full-scale WWTPs (Hesselmann et al., 1999; Kong et al., 2004), its diminished presence in these Polish WWTPs may reflect influent variability, operational conditions, or the competitive advantage of *Tetrasphaera* under temperate climates. Similarly, the low detection of *Dechloromonas* recently identified as an important DPAO group (Petriglieri et al., 2021), suggests that its ecological niche is less prominent in some systems. In contrast to the moderate levels of *Ca. Accumulibacter* detected in this study ($0.51\% \pm 0.15\%$), earlier work consistently reported *Ca. Accumulibacter* as the dominant PAO in EBPR systems. For instance, quantitative fluorescence in situ hybridization (FISH) analyses revealed that *Ca. Accumulibacter* could account for more than 80% of the bacterial community, with only low levels of *Competibacter* and other GAOs present barely at 15% of all bacteria (Seviour & McIlroy, 2008). Such dominance highlights its traditionally recognized role as the central driver of P removal, especially in acetate- or propionate-enriched environments (Bond et al., 1995; Hesselmann et al., 1999; Kong et al., 2004).

Whereas earlier studies emphasized *Ca. Accumulibacter* as the key PAO members, more other recent surveys highlight *Tetrasphaera* as a dominant and versatile genus across multiple regions (Dueholm et al., 2024; Stokholm-Bjerregaard et al., 2017). These findings fit the updated narrative, yet also emphasize the complicated role of *Ca. Microthrix*, whose high abundance introduces potential imbalance between P removal and sludge settleability. The consistently low levels of *Dechloromonas* and *Halomonas* further illustrate that not all reported DPAOs play equivalent roles across different locations. Further, microbial characteristics of the individual DG WWTPs based on their phylum and affiliation to specific taxonomic level are discussed below (see **section 5.2**).

5.2 Microbial characterization of the case study WWTPs - GD

The Illumina sequencing analysis of 16S rRNA gene fragments from the case study WWTP (**Figure 4-2**) revealed diverse microbial community typical of full-scale EBPR systems. At the phylum level, the microbial community was dominated by Proteobacteria (23.27%), Actinobacteriota (21.70%), Chloroflexi (15.28%), and Bacteroidota (14.98%). Phyla present at lower abundance included Patescibacteria (7.15%), Acidobacteriota (4.10%), and Firmicutes (2.95%), while others accounted for less than 2% of the total community. This composition of phylum is typical for activated sludge in line with the global study of diversity and biogeography of activated sludge bacterial communities reported by (L. Wu et al., 2019) which revealed diverse microorganisms from across 269 WWTPs in 23 countries on 6 continents. Equally Dueholm et al.,(2024) and R. Liu et al.,(2019a) observed a wide range of functionally significant organisms at phylum including members of PAOs or DPAOs and GAOs. Specific members such as *Ca. Accumulibacter* have been reported by (Qiu et al., 2019), *Halomonas* (H. Nguyen et al., 2012) , *Tetrasphaera* (Liu et al., 2019; Zhao et al., 2022), *Dechloromonas* (Petriglieri et al., 2021) and *Ca. Microthrix* (Nierychlo et al., 2021).

In the case study GD ,WWTP , the overall dominance of PAOs and DPAOs in the community ($9.4\% \pm 0.02\%$),with *Tetrasphaera* ($4.73\% \pm 0.69\%$) and *Ca. Microthrix* ($4.08\% \pm 1.06\%$) **Figure 4-2**, underscores their increasing significance in EBPR systems. Similar observation was reported the findings by (Liu et al. 2019b; Sun et al., 2021; Zhang & Kinyua, 2020). Additionally, these findings are in strong agreement with global surveys such as the MIDAS project, which reported *Tetrasphaera* to be the most abundant PAO in many full-scale plants worldwide, averaging 4.6% of the microbial community and often surpassing *Ca. Accumulibacter* (Dueholm et al., 2024).

Earlier investigations also identified high abundances of *Tetrasphaera* using FISH and high-throughput sequencing, with values of up to 30–35% in some Danish and European WWTPs (F.-A. Herbst et al., 2019; Muszyński et al., 2015; Stockholm-Bjerregaard et al., 2017). Unlike *Tetrasphaera* and *Ca. Accumulibacter*, which are well-established PAOs, the substantial presence of *Ca. Microthrix* highlights a different ecological contribution. Although primarily linked to bulking issues (Nierychlo et al., 2021), its capacity to accumulate poly-P (not fully understood) indicates a supplementary role in P dynamics, although less dynamic than conventional PAOs.

In contrast, the relatively low abundances of *Ca. Accumulibacter* ($0.51\% \pm 0.15\%$) and *Dechloromonas* ($0.05\% \pm 0.01\%$) contradicts long standing assumptions in literature which traditionally, placed *Ca. Accumulibacter* as the dominant PAO in EBPR, in most acetate-fed laboratory reactors and full-scale plants (Bond et al., 1995; Kong et al., 2004; Seviour & McIlroy, 2008). Nevertheless, recent molecular surveys and single-cell analyses have shown that its role is highly plant-specific, with *Tetrasphaera* often dominating under conditions with more diverse influents (Fernando et al., 2019b). Similarly, the very low representation of *Dechloromonas* contrasts with recent work identifying it as an important DPAO with denitrification and P-removal potential (Petriglieri et al., 2021; W. Zhao et al., 2022a). This contrast suggests other possible operational influences shaping microbial community assembly in Baltic EBPR, WWTPs.

On the other hand, the GAOs, represented by *Ca. Competibacter* at ($1.4\% \pm 0.01\%$) compared the microbial communities of PAOs and DPAOs at ($9.4\% \pm 0.02\%$), suggests stable EBPR performance since carbon limitation due to carbon competition (GAOs vs PAOs/DPAOs) impedes EBPR performance (Ma et al., 2024). Fundamentally presence of GAOs at higher proportions essentially compete with PAOs for carbon sources, while not contributing to P removal (Izadi et

al., 2021). Similar set back of GAO presence in EBPR activity was also reported by (Meng et al., 2020). Other studies in contrast have reported higher GAO levels in full-scale plants, where *Defluviicoccus* and *Ca. Competibacter* accounted to 36.0 – 42.6% and 15.3–24.9%, respectively (Maszenan et al., 2022; Song et al., 2022). Higher GAO proportion has been linked to propionate-rich influent (Song et al., 2022), shifts in solids retention time (Onnis-Hayden et al., 2020), and changes in COD:P ratios and carbon source type (J. Li, Zhu, Lv, Tan, et al., 2024; Shen et al., 2017; W. Tian et al., 2010). Even though some literature have reported GAOs' possible overestimation under acetate-based laboratory enrichments (Aghilinasrollahabadi et al., 2024; Nielsen et al., 2019), GAOs lack of poly-P removal capacity and reliance on PHA metabolism, emphasis on their suppression over the PAO is reliable for P removal processes (Roy et al., 2021).

5.3 Impact of COD:P ratios on the DPAO metabolism (glucose and acetate as substrates and NO_3^- or NO_2^- as electron acceptors).

The experimental findings on DPAOs performance in *Tetrasphaera*-enriched activated sludge under various substrate and electron acceptor conditions from **Series I (Section 4.2)** demonstrated the critical role of COD:P ratios in shaping DPAO metabolism, particularly under COD-limiting conditions (**Scenario 1.1**) compared to COD-non-limiting conditions (**Scenario 1.2**). Moreover, the results in **Series II** experimental tests (**Section 4.3**) under modified anoxic conditions, reinforced these observations by showing that not only COD availability but also the type of carbon source and electron acceptor strongly influenced process dynamics in EBPR systems. These effects were evaluated through key process rates, such as PRR, PUR, NUR, NiUR, and COD consumption, calculated from equations (1–5) in **Section 3.11**. Each of these process rate are discussed in detail in **Section 5.3.1** and subsequent sections. Generally, acetate significantly

enhances DPAO activity especially in *Tetrasphaera*- enriched activated sludge, while glucose exhibits lower and more variable performance.

5.3.1 Phosphorus release and uptake rate (PRR and PUR)

The measured anaerobic PRRs values in experimental tests in **series I**, COD-limiting conditions with glucose (0.3 ± 0.02 and 0.4 ± 0.05) mg P/(gMLVSS·h) and acetate (7.3 ± 1.1 and 6.3 ± 0.4) mg P/(gMLVSS·h) (**Table 4-1**) were comparable to those under COD non-limiting conditions with glucose (0.4 ± 0.01 and 0.5 ± 0.02) mg P/(gMLVSS·h) and acetate (6.7 ± 0.4 , 7.4 ± 0.9 and 6.3 ± 1.0) mg P/(gMLVSS·h) (**Table 4-3**). Moreover, **series II** where acetate was the only external carbon source used revealed comparable trend of anaerobic PRR values of 6.2 ± 0.1 mg P/(gMLVSS·h) and 7.2 ± 0.02 mg P/(gMLVSS·h) in trial 1 (**ST1**) and trial 2 (**ST2**), **Figure 4-10 (a and b)** respectively. In all these tests with acetate an immediate PO_4^{3-} release was realized as seen in (**Figures 4-3**, **4-5**, **4-7** and **4-10**), with the corresponding range of COD consumption range between 19.1 – 33.2 mg COD/(gMLVSS·h). The highest COD consumption rate with acetate realized was at 32.1 ± 3.2 mg COD/(gMLVSS·h) to the anaerobic PRR values of 7.3 ± 1.1 mg P/(gMLVSS·h) (**Table 4-1**). In **series II**, $\text{PO}_4\text{-P}$ concentration eventually reached a level of 23.8 mg P/L (ST1) and 24.8 mg P/L (ST2) (**Figure 4-10**). Similar results were recently reported by Tuszynska et al.(2019) who found that after addition of acetate in the anaerobic phase, PO_4^{3-} release reached 4.4 ± 0.4 mg P/(gMLVSS·h) with maximum P concentration of 38.8 ± 2.6 mgP/L. This finding equally aligns to the M. Zhang et al. (2016) who reported P concentration of between 25.0 – 34.0 mg P/L by the COD consumption of $84.0 \pm 2.0\%$. Moreover, comparable findings were realized with anaerobic PO_4^{3-} release up to 5 mg P/(gMLVSS·h) and 4.7 mg P/(gMLVSS·h) by Monclús et al. (2010) and (Z. Wang et al., 2015) respectively. The results revealed that PAOs

/ DPAOs can release up to $7.3 \pm 1.1 \text{ mg P / (gMLVSS} \cdot \text{h)}$ in response to the addition of acetate (**Figure 4-3a**) compared to those in glucose the $0.3 \pm 0.02 \text{ mg P / (gMLVSS} \cdot \text{h)}$ (**Figure 4-4a**) with glucose. Similar findings was reported by Yu et al., (2023), who found that acetate was the most effective carbon source, leading to superior P removal compared to glucose and glycerol. This stronger acetate performance was also reported by (Chen et al., 2015) who recognised acetate as one of the most prevalent VFA and the typical carbon source for EBPR in laboratory studies and full-scale WWTPs. Oehmen, Yuan, et al. (2005) findings on acetate as an effective carbon to P removal also support this finding. While He et al. (2024) observed glucose uptake and activity by *Tetrasphaera*, in this study minimal effect of glucose on anaerobic PO_4^{3-} release was observed despite the presence of *Tetrasphaera* - enriched sludge aligning with Wang et al.,(2010), where glucose as the primary carbon source led to sub optimal EBPR performance. The dismal performance by glucose as observed is comparable use of other substrates reported in literature such as like fusel oil (Tuszynska et al., 2019) and ethanol reported in (Swinarski et al., 2012) and as well as study by (Puig et al.2008). Tuszynska et al.(2019) found that the addition of fusel oil had only a minor effect on PO_4^{3-} release (PRR $0.65 \pm 0.08 \text{ mg P / (gMLVSS} \cdot \text{h)}$) and COD consumption in the anaerobic phase $24.7 \pm 2.5 \text{ mg COD / (gMLVSS} \cdot \text{h)}$. This was comparable to the COD consumption in anaerobic phase with glucose was at $13.1 \pm 0.1 \text{ mg COD / (gMLVSS} \cdot \text{h)}$ (**Table 4-1** , **Figure 4-4**).Moreover, Swinarski et al. (2012) found that ethanol insignificantly induced anaerobic PO_4^{3-} release. Similarly, low anaerobic PO_4^{3-} release profile trend was reported by Puig et al.(2008) ranging between $0.9 - 1.5 \text{ mg P / (gMLVSS} \cdot \text{h)}$ compared to the glucoses' $0.3 \pm 0.02 \text{ mg P / (gMLVSS} \cdot \text{h)}$ in this case study. Despite the presence of *Tetrasphaera* enriched

sludge, glucose use as alternative carbon source was not effective even in the anaerobic PO_4^{3-} release.

PUR

The anoxic phase the PUR values as in **series I**, COD-limiting conditions indicates significant anoxic PO_4^{3-} uptake with acetate at $(0.9 \pm 0.1$ and $0.8 \pm 0.2)$ mg P / $(\text{gMLVSS} \cdot \text{h})$ while none is realized under glucose (**Table 4-2**). Compared to PUR values under COD non-limiting conditions, tests with acetate showed a stronger PO_4^{3-} uptake of $(1.5 \pm 0.6$, 0.7 ± 0.5 and $0.6 \pm 0.1)$ mg P / $(\text{gMLVSS} \cdot \text{h})$ (**Table 4-4**). Likewise, as in the case of glucose, no PO_4^{3-} uptake occurred under COD non-limiting conditions. Moreover, **series II** tests recorded PUR ranged between 0.5 – 1.4 mg P / $(\text{gMLVSS} \cdot \text{h})$ (**Table 4-6**) with initial anaerobic acetate addition. It should be noted that the PUR values in series II tests of modified anoxic conditions were only measured under the reference test (**Scenario 2.1**) while other **scenarios (2.2 and 2.3)** had PO_4^{3-} precipitated out. Generally, the PO_4^{3-} release was more pronounced compared to PO_4^{3-} uptake. The low PO_4^{3-} release and negligible or no PO_4^{3-} uptake in glucose confirms that indeed glucose is not a suitable carbon source for EBPR in activated sludge. The maximum PUR of 1.5 ± 0.6 mg P / $(\text{gMLVSS} \cdot \text{h})$ reported by tests under COD non-limiting conditions with acetate, affirming its viability as carbon source. These results are in line with the findings by (Zhao et al., 2024) which state that DPAOs particularly Type I perform efficient NO_3^- and NO_2^- reduction during P uptake when powered by intracellular PHA reserves formed from acetate. (Zekker et al., 2021) observed that NO_3^- generally supports more stable anoxic P uptake, while NO_2^- may cause partial inhibition. Comparatively, the zero PUR in glucose fed systems suggest that glucose does not support denitrification-P uptake pathways, possibly due to poor compatibility with DPAO metabolism despite possible

anaerobically fermented and stored as glycogen in *Tetrasphaera* (Kong et al., 2004; Kristiansen et al., 2013b).

The corresponding PUR anoxic values showed trends of DPAOs under anoxic dependence on the carbon and the type of electron acceptor. The specific anoxic values for PUR of 0.9 ± 0.1 mg P / (gMLVSS·h) (with NO_3^-) and 0.8 ± 0.2 mg P / (gMLVSS·h), (NO_2^-) (**Table 4-2**) was measured. DPAOs are not implicitly capable of using glucose, and any negligible PO_4^{3-} uptake observed could also be related to the use of their intracellular storage compounds. The negligible PO_4^{3-} -release and -uptake rates would confirm that glucose was not a suitable carbon source for EBPR. These observations confirmed the conclusion of Guerrero et al. (2011) and Tuszynska et al. (2019) that the availability of VFA is the key factor in triggering EBPR activity and the complex compound like glucose must be fermented to VFAs to maintain the EBPR activity. The superior performance of acetate supports long established evidence that acetate is the most readily metabolized carbon source for DPAOs, particularly *Ca. Accumulibacter* and acetate-type *Tetrasphaera* strains (Kristiansen et al., 2013b; Maszenan et al., 2000). This observation is equally in line with the finding that acetate can anaerobically assimilate and stored as intracellular PHA as seen in **Figure 4-9**, and are subsequently used in P uptake during anoxic phase (Oehmen et al., 2007b; Y. Zhao et al., 2024a). It is worth noting that even under COD-limiting conditions, the availability of a favorable substrate such as acetate supports conventional EBPR metabolism by prioritizing storage overgrowth, thereby maintaining functionality. Furthermore, glucose is more likely to be consumed by heterotrophic competitors for instance GAOs, such as *Defluviicoccus* and *Ca. Competibacter*, which do not contribute to P removal (Izadi et al., 2021a; Ma et al., 2024). This

makes glucose a less selective carbon source, especially under COD limitation, where competition for electron donors intensifies.

COD:P non-limiting condition and prolonged PO_4^{3-} release phenomenon

The prolonged PO_4^{3-} release into the anoxic phase observed with acetate under COD-non-limiting conditions at 6.7 ± 0.4 mg P / (gMLVSS·h) (**Figure 4-5a**) compared to COD-limiting conditions, (**Figure 4-3a**), at 7.3 ± 1.1 mg P / (gMLVSS·h) reflects influence of excess external carbon presence, where DPAOs continue carbon storage before initiating PO_4^{3-} uptake. COD availability in non-limiting amounts suppressed P uptake. The outcome aligns to findings (Z. Li et al., 2024; Y. Zhao et al., 2024a), on COD in higher dosages impairs DPAOs carbon consumption and storage. Additionally, non-limiting COD may stimulate heterotrophs, leading to competition for NO_3^-/NO_2^- , which are essential for DPAO metabolism (Ma et al., 2024) and a stable EBPR. As noted in (Tuszynska et al., 2019), a COD:P ratio above optimal thresholds can promote GAO proliferation, especially when slowly biodegradable organics like (glucose) are present.

On the other hand, as observed COD-limited conditions (COD:P ratio below 2.5) was characterized by absence of prolonged PO_4^{3-} release. According (Li et al., 2024), maintaining an optimal COD:P ratio ensures that PAOs and DPAOs can perform carbon uptake and phosphate removal without being outcompeted by GAOs. A low but balanced COD:P prevents excessive carbon competition while still supplying enough energy for phosphate release and uptake. Studies have shown that EBPR performance begins to decline either under carbon limitation or under carbon overload, where heterotrophs consume excess substrate (T. Xie et al., 2017). Henceforth, a ratio of less than 2.5 ensures that DPAOs i.e. *Tetrasphaera*, which can operate under low-COD conditions maintain dominance in the microbial community (F.-A. Herbst et al., 2019). In contrary

, while low COD:P prevents overgrowth of GAOs and supports stable EBPR, it may not allow full denitrification (complete $\text{NO}_3^-/\text{NO}_2^-$ reduction) if the carbon is too limiting (Zekker et al., 2021). Also, not all DPAOs perform equally well under COD constraints. *Ca. Accumulibacter* with preference to acetate and may underperform if COD levels drop too low (Schuler & Jenkins, 2002b).

5.3.2 Nitrate and nitrite utilization rates (NUR and NiUR)

The rates of the experimental NUR rates of series I as summarized in the tests under COD-limiting conditions (0.9 ± 0.1 and 0.6 ± 0.0) $\text{mg N}/(\text{gMLVSS}\cdot\text{h})$ (**Table 4-2**) compared to COD non-limiting conditions (2.9 ± 0.9 with acetate) and 0.5 ± 0.2 with glucose)) $\text{mg N}/(\text{gMLVSS}\cdot\text{h})$ (**Table 4-4** , **Figure 4-5**). Compared to the values of NUR under dynamic anoxic conditions, **Series II** , in standard reference conditions ($1.3 \text{ mg N}/(\text{gMLVSS}\cdot\text{h})$ in ST1 and $1.0 \text{ mg N}/(\text{gMLVSS}\cdot\text{h})$ in ST2 respectively (**Table 4.7, Figure 4-11**) were achieved without chemical precipitation of $\text{PO}_4\text{-P}$. In $\text{PO}_4\text{-P}$ precipitated conditions NUR increased by $0.4 \text{ mg N}/(\text{gMLVSS}\cdot\text{h})$ in each of the trials (**Table 4-8**) after chemical precipitation of $\text{PO}_4\text{-P}$. Moreover, a further increase of NUR (0.01 and 0.3) $\text{mg N}/(\text{gMLVSS}\cdot\text{h})$ in ST1 and in ST2 respectively in the PHA depleted conditions combine with chemical precipitation of $\text{PO}_4\text{-P}$ (**Table 4-9**).The maximum NUR was observed the experiment with COD non-limiting conditions followed the addition of acetate in the anaerobic phase.

Among the standard tests , those of **Series I** and **Scenario 2.1** of the **Series II**, the maximum NUR rate reached was $2.9 \pm 0.9 \text{ mg N}/(\text{gMLVSS}\cdot\text{h})$ (**Figure 4-5**) by the average net NO_3^- removal of $17 \pm 3 \text{ mgN/L}$ (**Figure 4-5a**). Tuszynska et al.(2019) reported similar findings with the addition of fusel oil in the anoxic phase followed the addition of acetate in the anaerobic phase. In that study,

the maximum NUR reached was 1.40 ± 0.07 mg N / (gMLVSS·h) and corresponding average net NO_3^- removal -16.4 ± 0.7 mgN/L . In the similar study , NURs increased by 0.60 ± 0.08 mg N / (gMLVSS·h) in comparison with the reference test without chemical precipitation of $\text{PO}_4\text{-P}$ and subsequently by 0.30 ± 0.06 mg N / (gMLVSS·h) after chemical precipitation of $\text{PO}_4\text{-P}$. It can be postulated that as a result of the chemical precipitation of $\text{PO}_4\text{-P}$, DPAOs reduced their metabolism, resulting in lower NURs which were necessary for respiration and intracellular transformation. Accordingly, it can be assumed that the difference between the N removal values before and after chemical precipitation of $\text{PO}_4\text{-P}$ could be related to the activity of DPAOs (storage of $\text{PO}_4\text{-P}$ at the expense of PHA, which was approximately 26% and 32.31% of the total NUR in ST1 and ST2 respectively (**Table 4-11**). This was slightly higher compared to the values reported approximately 20% of the total NUR by (Tuszynska et al.2019). Also (Swinarski et al., 2012) with tests with ethanol observed NUR from 1.5 to about 3.7 ± 0.1 mg N / (gMLVSS·h).

NO₂⁻ pulse dosing effect

The application of NO_2^- pulse dosing saw an improved PUR from 0.6 to 0.7 mg P / (gMLVSS·h), suggesting that some DPAOs can respond positively to NO_2^- availability, especially under non-limiting COD conditions as seen in (**Table 4-6; Figure 4-7**).Oehmen et al. (2010) confirms that Type II DPAOs or NO_2^- adapted *Tetrasphaera* strains which specialize in using NO_2^- as their terminal electron acceptor may be stimulated under NO_2^- rich conditions, contributing to P uptake .The slight increase in PUR with NO_2^- pulse dosing may therefore reflect the activation of a DPAO subpopulation, or enhanced electron flow through partial denitrification steps as reported in (Rubio-Rincón et al., 2019b). Moreover, *Tetrasphaera* species have demonstrated flexible responses to NO_3^- and NO_2^- availability, supporting the possibility of selective stimulation (F.-A.

Herbst et al., 2019). However, the improvement was modest and may be insufficient to justify reliance on NO_2^- dosing alone. NO_2^- is known to inhibit some denitrifiers and can accumulate to toxic levels if not properly managed (Zhao et al., 2024). While NO_2^- can serve as an effective electron acceptor, its effectiveness varies by strain and redox potential, and its overuse may impair overall EBPR performance if not precisely controlled.

5.3.3 *Polyhydroxyalkanoates (PHA) production*

The results presented in (**Figure 4-9**) highlight the differential synthesis of polyhydroxyalkanoates (PHAs), specifically polyhydroxybutyrate (3PHB) and polyhydroxyvalerate (3PHV), in response to two distinct carbon sources acetate and glucose and their link with NO_3^- or NO_2^- as electron acceptors. The clear accumulation of PHAs in the acetate-fed systems and the negligible response under glucose-fed conditions underscore the substrate specificity in DPAO-mediated phosphorus removal pathways.

The PHA accumulation with acetate - NO_3^- **Figure 4-9(a)**, was significant during the 2.5-hour anaerobic phase with the maximum peak reached just before the onset of the anoxic phase suggesting effective carbon uptake and storage. Both 3PHB and 3PHV were present, with 3PHB dominating, aligning with previous findings by (Bauhs et al., 2022), who identified 3PHB as the major polymer in acetate-driven EBPR systems. This PHA production coincides with the luxury uptake mechanism of PAOs, where hydrolysis of intracellular polyphosphate provides the energy (ATP) for acetate assimilation and PHA storage, an essential step for subsequent anoxic phosphorus uptake (Oehmen et al., 2007b; Y. Zhao et al., 2024a).

Similarly, the test with acetate- NO_2^- pulse **Figure 4-9(b)** experienced PHA accumulation is primarily dependent on the carbon source and not the electron acceptor used in the anoxic phase. This finding is consistent with which affirms that while NO_2^- or NO_3^- influences PO_4^{3-} uptake dynamics, PHA synthesis occurs anaerobically and is driven by the substrate's metabolic compatibility with PAOs. Even under NO_2^- addition, the sustained presence of 3PHB suggests that DPAOs can adapt and maintain storage under diverse anoxic conditions when fed with acetate.

In contrast, the results presented in **Figure 4-9(c)** (glucose with NO_2^-) showed negligible PHA production, with near-zero concentrations of both 3PHB and 3PHV. This absence of PHA synthesis underlines the poor suitability of glucose for anaerobic EBPR. Despite *Tetrasphaera's* known ability to ferment glucose and produce intracellular glycogen (Kristiansen et al., 2013b; H. T. T. Nguyen et al., 2015b), this pathway does not result in PHA formation, especially not in the absence of an aerobic phase.

The comparative stability of PHA levels in both acetate scenarios also suggests a metabolic readiness of DPAOs to utilize the stored carbon during the subsequent anoxic phase, regardless of the electron acceptor. This observation supports the notion from Oehmen et al. (2010) and (J. Li, Zhu, Lv, Tan, et al., 2024) that PHA storage is a preparatory phase for denitrifying phosphorus uptake and is essential for the efficient coupling of nitrogen and phosphorus removal in DPAO-enriched systems.

5.4 DPAO metabolism under modified anoxic conditions.

While the results of the anaerobic process rates (PRR, PUR and COD) as seen in **Figure 4-10** were consistent in reference to those of series I (**Tables 4-1** and **4-3**) as discussed in section **5.3.1**, modified anoxic condition showed dynamic trend with PO_4^{3-} precipitated and PHA depleted conditions in terms of NUR, NiUR and PUR values (**Table 4-6**, **4.7** and **4-8**).

5.4.1 *DPAOs metabolism under anoxic standard conditions*

The findings of **Scenario 2.1** (**Table 4-6** and **Figure 4-11**) under modified anoxic reference conditions highlight the continued metabolic activity of DPAOs in the absence of external carbon feeding during the anoxic phase. Both ST1 and ST2 used acetate exclusively in the anaerobic phase, followed by NO_3^- or NO_2^- addition in the anoxic phase, with no glucose supplementation. This setup was designed to evaluate DPAO performance under realistic COD-limited conditions without stimulating heterotrophic competitors.

The PURs under NO_3^- were measured at 1.4 mg P /($\text{gMLVSS}\cdot\text{h}$) for ST1 and 1.1 mg P /($\text{gMLVSS}\cdot\text{h}$) for ST2. These values are comparable to those obtained in Series I Scenario 1.1 under COD-limited conditions (PUR = 0.9 mg P /($\text{gMLVSS}\cdot\text{h}$)) (**Table 4-2**), suggesting that pre-acclimated DPAOs in Scenario 2.1 (**Table 4-6**) maintained effective anoxic phosphate uptake using internally stored carbon. Conversely, PUR under NO_2^- varied more distinctly between ST1 (0.5 mg P /($\text{gMLVSS}\cdot\text{h}$)) and ST2 (1.2 mg P /($\text{gMLVSS}\cdot\text{h}$)), indicating possible variability in microbial acclimation or NO_2^- reduction pathways between the two strategies. These findings align with (Oehmen et al., 2010), who classified DPAOs into Type I and Type II, depending on their electron acceptor reduction capabilities - where NO_2^- specific DPAOs (Type II) can dominate under certain conditions.

On the other hand, the NUR also followed a similar pattern. Under NO_3^- , NUR was $1.3 \text{ mg N}/(\text{gMLVSS}\cdot\text{h})$ in ST1 and $1.0 \text{ mg N}/(\text{gMLVSS}\cdot\text{h})$ in ST2, slightly lower than in **Series I** non-limiting acetate conditions ($2.9 \text{ mg N}/(\text{gMLVSS}\cdot\text{h})$), likely due to the absence of external carbon input in the anoxic phase. Importantly, NO_2^- uptake rates (NiUR) reached $1.8 \text{ mg N}/(\text{gMLVSS}\cdot\text{h})$ and $1.3 \text{ mg N}/(\text{gMLVSS}\cdot\text{h})$ for ST1 and ST2, respectively, exceeding the NO_3^- NURs (**Table 4-6**). This suggests an enhanced capacity for denitrification via NO_2^- , reinforcing literature findings that NO_2^- can be a more efficient electron acceptor for some DPAOs (Y. Zhao et al., 2024a). Furthermore, the strong NO_2^- reduction activity may reflect a microbial community rich in *Tetrasphaera* or other Type II DPAOs, which confirms to be metabolically adaptable under fluctuating substrate conditions (Kristiansen et al., 2013b; Marques et al., 2018b). In contrast to Series I, glucose was intentionally excluded in **Scenario 2.1** due to its poor performance as a P-release substrate (**Series I**, PRR: $0.3 - 0.5 \text{ mg P}/(\text{gMLVSS}\cdot\text{h})$). Glucose can stimulate HETs at the expense of DPAO activity (Kong et al., 2004; X. Wang et al., 2019). The absence of glucose in **Scenario 2.1** ensured that DPAO-driven P uptake processes were not competitively suppressed, contributing to relatively stable performance metrics despite the COD-limited anoxic conditions.

5.4.2 *PO_4^{3-} anoxic precipitation on DPAO metabolism*

The application of chemical PO_4^{3-} precipitation in **Scenario 2.2** significantly impaired denitrification performance across both strategies (ST1 and ST2), as evidenced by the notably reduced NO_3^- uptake rates (NUR) of $0.4 \text{ mg N}/(\text{gMLVSS}\cdot\text{h})$ (**Table 4-8**) compared to **Scenario 2.1**, where NUR values ranged from $1.0\text{--}1.3 \text{ mg N}/(\text{gMLVSS}\cdot\text{h})$ (**Table 4-7**) under similar electron acceptor conditions. As discussed in **section 5.3.2** this substantial drop reflects a major

inhibition of DPAO activity following the removal of freely available phosphate in the anoxic phase.

The suppressed NO_3^- uptake in the absence of PO_4^{3-} is biologically significant. DPAOs rely on polyphosphate accumulation as a terminal step during anoxic respiration using internal PHAs to drive phosphorus uptake while reducing $\text{NO}_3^- / \text{NO}_2^-$. By chemically precipitating PO_4^{3-} , the terminal sink for intracellular electron flow is removed, thereby decoupling the respiration-P uptake synergy, and leading to energy limitation (Oehmen et al., 2010; R. J. Zeng et al., 2003). DPAO-mediated denitrification and P-uptake are tightly coupled, with polyphosphate serving both as an energy source and a redox buffer during anoxic respiration (H. Li et al., 2020b; Y. Zhao et al., 2024). This is visually supported by **Figure 4-12**, which shows stagnated PO_4^{3-} profiles and depressed $\text{NO}_3^- / \text{NO}_2^-$ depletion during the anoxic phase.

In contrast, **Scenario 2.1** maintained moderate DPAO performance (NUR: 1.0 –1.3 mg N / (g MLVSS·h)) (**Table 4-6**) without glucose addition, indicating that internal carbon reserves and PO_4^{3-} presence was sufficient for denitrification and P uptake. However, in **Scenario 2.2**, glucose was supplemented in the anoxic phase, yet the performance deteriorated further. Clearly, even though glucose was added during the anoxic phase in this scenario, it did not offset the impaired DPAO activity. This observation is consistent with previous **Series I** results and existing literature, which emphasize that glucose favors HETs rather than DPAOs (Rosas-Echeverría et al., 2023; X. Wang et al., 2019). This suggests that external glucose may have induced competition from GAOs or heterotrophs, without benefiting DPAOs. The very high COD:N ratios in ST2 (up to 491.3 and 249.8 g COD/g N (**Table 4-8**)) further emphasize this imbalance, indicating that the available COD was excessive relative to nitrogen, but likely inefficiently utilized due to impaired DPAO activity.

This confirms that the carbon source alone cannot sustain DPAO metabolism in the absence of phosphate, undermining the intended dual nutrient removal.

Additionally, NiUR were 0.5 mg N / (gMLVSS·h) and 0.3 mg N / (gMLVSS·h) in ST1 and ST2 respectively both markedly lower than in Scenario 2.1 (1.8 and 1.3 mg N / (gMLVSS·h)), again affirming the inhibitory role of PO_4^{3-} removal on NO_2^- reducing DPAOs, possibly of Type II, as discussed in previous literature (Kristiansen et al., 2013b). Furthermore, the COD_{anoxic} rates (5.8 and 6.8 mg O_2 / (gMLVSS·h)) in ST1 and (14.1 and 21.6 mg O_2 / (gMLVSS·h)) in ST2 which were in the range between 14.1 to 21.6 mg O_2 / (gMLVSS·h) in **Scenario 2.2 (Table 4-8)** remained moderate to high, especially in ST2, indicating that carbon oxidation did occur, but likely due to glucose-stimulated activity of non-PAO organisms. The mismatch between high COD consumption and low nitrogen removal efficiency further supports the idea that glucose failed to promote DPAO metabolism, and instead favored heterotrophic pathways unrelated to phosphorus removal, potentially even increasing N_2O emissions due to incomplete denitrification (as reported by Shen & Zhou, 2016).

This scenario demonstrates that chemical PO_4^{3-} removal disrupts DPAO metabolism, even in the presence of external carbon sources. Without PO_4^{3-} as an electron sink, the link between P uptake and $\text{NO}_3^-/\text{NO}_2^-$ respiration is broken, severely compromising nutrient removal efficiencies. Moreover, the data show that additional glucose under these disrupted conditions is not beneficial and may lead to EBPR process setbacks.

5.4.3 *PHA depleted anoxic on DPAO metabolism*

As seen in the results of the anoxic phase in **Scenario 2.3 (Table 4-9)**, the NUR and NiUR rates discussed in **section 5.3.2**, DPAOs were functionally suppressed, evidenced by extremely low NUR values ($0.014 \text{ mg N}/(\text{gMLVSS}\cdot\text{h})$ in ST1 and $0.3 \text{ mg N}/(\text{gMLVSS}\cdot\text{h})$ in ST2), and similarly poor NiUR performance (0.003 and $0.1 \text{ mg N}/(\text{gMLVSS}\cdot\text{h})$). These findings confirm that DPAO-mediated denitrification is not merely dependent on external electron acceptors, but more crucially on the availability of internal energy carriers like PHAs.

These outcomes support the notion that DPAOs rely on intracellular PHAs mainly 3-hydroxybutyrate (3PHB) to generate reducing equivalents under anoxic conditions (Kristiansen et al., 2013b; R. Liu et al., 2019a). Without PHA reserves, key DPAO functions such as anoxic phosphate uptake and denitrification are impaired. Although glucose was added during the anoxic stage, its role was insufficient in reactivating DPAO performance. This agrees with previous findings (Marques et al., 2018; Wang et al., 2019), where glucose favored heterotrophic organisms rather than DPAOs, and provided minimal support for PHA replenishment under EBPR operational conditions.

Interestingly, COD consumption persisted, with ST2 showing $17.3\text{--}18.5 \text{ mg O}_2 /(\text{g MLVSS}\cdot\text{h})$, yet no associated improvement in NUR. This suggests that glucose-fueled metabolism occurred but was mostly directed toward non-DPAO populations. High COD:N ratios (33.9 and 163) g COD /g N in ST1 and (41.75 and 45.5) g COD /g N in ST2) (**Table 4-9**) further indicate inefficient carbon utilization, confirming that in the absence of PHA, denitrification becomes uncoupled from EBPR performance. This finding demonstrates that PHA presence is indispensable for efficient EBPR. Even when external COD is available (via glucose), the lack of stored intracellular carbon

impedes the respiratory potential of DPAOs. This has practical implications for process design, emphasizing the need for a robust anaerobic phase where acetate or suitable VFAs can stimulate sufficient PHA synthesis before initiating denitrification.

Under normal EBPR conditions, PAOs such as *Tetrasphaera* and *Ca. Accumulibacter* produce PHAs in anaerobic environments by converting acetate or other volatile fatty acids (VFAs) into intracellular carbon granules (Kong et al., 2005; Kristiansen et al., 2013). These are then utilized during anoxic conditions to drive PO_4^{3-} uptake and electron transport for NO_3^- or NO_2^- reduction. In **Scenario 2.3**, the absence of this PHA pool essentially immobilized DPAO activity, even in the presence of added glucose.

The elevated $\text{COD}_{\text{anoxic}}$ rates (17.3–18.5 $\text{mg O}_2 / (\text{gMLVSS} \cdot \text{h})$) and the staggering COD:N ratios (up to 163.5 $\text{g COD} / \text{g N}$) suggest that the added glucose stimulated metabolism, but not in a direction beneficial for EBPR. Instead, as noted by Rosas-Echeverría et al. (2023), such conditions often favor fermentative or aerobic heterotrophs, which compete with DPAOs for carbon but do not contribute to phosphorus removal. The inability of glucose to generate PHA rapidly, and its preferential uptake by generalist bacteria, limits its usefulness in supporting EBPR under PHA-depleted scenarios (H. T. T. Nguyen et al., 2015b).

In contrast to **Scenario 2.1**, which supported balanced anoxic uptake and respiration via retained PHA ($\text{NUR} = 1.0 - 1.3 \text{ mg N} / (\text{gMLVSS} \cdot \text{h})$, $\text{COD:N} = 15 \text{ g COD} / \text{g N}$), **Scenario 2.3** reveals how metabolic uncoupling occurs when PAOs are deprived of their primary energy reserves. Even compared to the PO_4^{3-} -precipitated Scenario 2.2, where limited DPAO activity persisted ($\text{NUR} = 0.4 \text{ mg N} / (\text{gMLVSS} \cdot \text{h})$), PHA depletion had a more profound impact, confirming that carbon storage, not just electron acceptor availability, is significant to the DPAO-driven nutrient removal.

5.5 N₂O production and denitrifying PAO activity

5.5.1 *Electron acceptor type on N₂O production*

Across **series I** (COD non-limiting conditions) (**Figure 4-15** and **Figure 4-16**) and **series II** (dynamic anoxic, ST1 & ST2), NO₃⁻ (**Figure 4-18** and **Figure 4-20**) consistently produced negligible N₂O, whereas NO₂⁻ (**Figure 4-17** and **Figure 4-19**) promoted substantial accumulation. This finding is in line (Kampschreur et al., 2009; Schulthess et al., 1995) which reported NO₂⁻ effect on inhibiting microbial growth and increasing N₂O production during denitrification. Equally, Schulthess et al. (1995) observed that during denitrification with NO₃⁻ as the first electron acceptor neither NO nor N₂O is accumulated in significant amounts. The results consistently demonstrated that the type of electron acceptor exerted the most pronounced influence on N₂O production. In **series I**, under NO₃⁻ (**Figure 4-15**), both acetate- and glucose-fed systems maintained N₂O concentrations near zero throughout the anoxic phase, indicating complete denitrification with no significant intermediate accumulation. This observation agrees with findings from Campos et al. (2016) and Vieira et al. (2018), who showed that NO₃⁻ reduction tends to proceed to completion under stable anoxic conditions, avoiding the build-up of N₂O. In contrast, when NO₂⁻ was used as electron acceptor, rapid and substantial N₂O peaks were observed, with acetate plus pulse-dosing (**Figure 4-16a**) producing a short-lived peak of 0.6 mg N₂O-N/L, and glucose plus full-dosing resulting in prolonged accumulation up to 2.9 mg N₂O-N/L. The higher and more sustained emissions under glucose-fed conditions suggest slower denitrification kinetics and possible shifts in microbial community activity toward heterotrophic denitrifiers less efficient at N₂O reduction. This observation supports prior reports by Marques et al. (2018) and Nielsen et al. (2019), which linked glucose-rich conditions to the activity of *Tetrasphaera* and other

heterotrophs possessing partial denitrification pathways that may terminate in N_2O , particularly under NO_2^- stress.

5.5.2 *Pulse dosage of NO_2^- strategy effect on N_2O*

The effect of electron dosing strategy observed here provides a practical operational insight. Pulse-dosing of NO_2^- in acetate-fed systems (**Figure 4-16a**) led to much lower and shorter N_2O peaks than full dosing in glucose-fed systems (**Figure 4-16b**). This suggests that controlled, gradual electron acceptor supply allows for better redox balance and avoids overloading denitrification pathways, thereby minimizing N_2O emissions. Similar conclusions were drawn by C. Li et al. (2013) and Ribera-Guardia et al. (2016), who demonstrated that step-feed or pulse-feed of nitrite could significantly reduce N_2O accumulation in EBPR configurations. These findings indicate that beyond simply choosing the right electron acceptor, the strategy dosage is critical to minimizing N_2O production in the EBPR.

5.5.3 *Internal reserves (PHA, poly-P) on N_2O production*

In **series II**, the availability of intracellular storage compounds PHA and poly-P was a key determinant of the pattern of N_2O production under NO_2^- -driven denitrification. Under reference conditions (**Scenario 2.1**) (**Figure 4-17a** and **Figure 4-19 a**), where both PHA and poly-P reserves were present, NO_2^- exposure produced the lower and shorter N_2O peaks in both trials, particularly in ST2 where peak concentrations were around 0.7 mg N_2O -N/L, where production were minimal and rapidly diminished. In contrast, (**Scenario 2.2**) (**Figure 4-17b** and **Figure 4-19 b**), N_2O production was both higher up to 3.0 mg N_2O -N/L in ST1 and over 3.0 mg N_2O -N/L in ST2 and sustained for longer, indicating that $P0_4^{3-}$ depletion conditions impaired the ATP generation

required for complete denitrification . Similarly, under PHA depletion (**Scenario 2.3**)(**Figure 4-17c** and **Figure 4-19 c**) a delayed but substantial N_2O production suggested that the absence of readily available internal carbon initially suppressed denitrification rates but later forced microorganisms into slower, less efficient pathways with greater intermediate accumulation. These patterns are consistent with the bioenergetic roles of these reserves in DPAO metabolism. PHA oxidation supplies reducing power for denitrification, while poly-P cycling supports ATP generation and electron transport. Limiting either pathway constrains electron flow to N_2O reductase (NosZ), thereby increasing the likelihood of incomplete N_2O reduction under NO_2^- stress (Hou et al., 2022; Marques et al., 2018c; Ribera-Guardia et al., 2016). Notably, even under severe storage limitation, NO_3^- driven denitrification consistently maintained near zero N_2O levels across all scenarios, again reinforcing that electron acceptor type remains the primary determinant of N_2O production risk. The magnitudes of N_2O emissions observed here fall within the ranges previously reported for EBPR systems. Y. Liu et al. (2015) documented that denitrifying P removal could generate N_2O equivalent to 2.3 – 21.6% of the influent nitrogen load, while Asadi & McPhedran. (2021) and Maktabifard et al. (2023) estimated that N_2O from WWTPs contributes 3.3 –10% of total plant greenhouse gas emissions, with EBPR processes representing a significant fraction of that total. The clear suppression of N_2O under NO_3^- , however, demonstrates that process configuration and control can greatly influence the greenhouse gas in the EBPR.

The patterns observed in this study also align with the growing recognition of the role of *Tetrasphaera* in EBPR-related N_2O emissions. Molecular studies have shown that *Tetrasphaera* possesses partial denitrification pathways, reducing NO_3^- to NO_2^- and in some strains further to N_2O , but lacking the full complement of enzymes for complete N_2 reduction (Marques et al.,

2018a; Nielsen et al., 2019) This metabolic profile, coupled with its ability to use diverse carbon sources including glucose, may explain the higher N_2O observed in glucose-fed NO_2^- systems in the present work. In contrast, acetate is a preferred substrate for *Ca. Accumulibacter*, which is generally associated with more complete denitrification and lower N_2O production when NO_2^- exposure is limited (Bond et al., 1995; Kong et al., 2004; Kristiansen et al., 2013a) . The interplay between substrate type, dominant DPAO genus, and electron acceptor thus emerges as a key determinant of N_2O emissions in EBPR systems.

5.5.4 *Effect of carbon source on N_2O production*

The type of carbon source available to DPAOs had a clear influence on N_2O production dynamics in this study. Across both **Series I** (COD non-limiting conditions) and **Series II** (dynamic anoxic conditions), the use of acetate consistently resulted in lower and shorter N_2O peaks compared to glucose when NO_2^- was the electron acceptor. In **Series I**, acetate with pulse-dosed NO_2^- produced a modest, short-lived peak (0.6 mg N_2O -N/L) (**Figure 4-16a**), whereas glucose with full NO_2^- dosing led to prolonged accumulation, reaching 2.9 mg N_2O -N/L after 15 hours (**Figure 4-16b**). . These differences were observed despite both systems maintaining anoxic PO_4^{3-} uptake, indicating that N_2O production can be driven by metabolic pathway differences rather than by gross P removal performance.

The superior performance of acetate-fed systems in limiting N_2O production can be attributed to the substrate preferences and metabolic efficiency of *Ca. Accumulibacter*, a dominant PAO known for efficient uptake and oxidation of VFAs such as acetate (Bond et al., 1995; Kong et al., 2004; Kristiansen et al., 2013b). Acetate is rapidly converted to PHA during the anaerobic phase, which can then be oxidized during anoxic denitrification to provide a stable and sufficient supply of

electrons for the complete reduction of NO_3^- or NO_2^- species, including N_2O , to N_2 (Hou et al., 2022; Ribera-Guardia et al., 2016). The ready availability of electrons from acetate-derived PHA likely ensures that nitrous oxide reductase (NosZ) responsible for the final reduction step from N_2O to N_2 remains competitively supplied, reducing the chance of intermediate production.

In contrast, glucose-fed systems often promote the growth of heterotrophic denitrifiers such as *Tetrasphaera* spp., which possess partial denitrification pathways and, in many strains, lack the complete enzymatic machinery for N_2O reduction (Close et al., 2021; Marques et al., 2018b; Nielsen et al., 2019). As a result, N_2O can be produced and accumulate even when NO_2^- or NO_3^- reduction rates remain relatively high. Additionally, glucose metabolism proceeds through more complex pathways that may generate transient metabolic imbalances and slower electron release compared to VFAs (Fernando et al., 2019b), which can disadvantage NosZ in the electron competition hierarchy. This is consistent with the sustained N_2O accumulation observed under glucose – NO_2^- conditions in this study.

The interplay between carbon source and dosing strategy was also notable. Under acetate – NO_2^- conditions, pulse dosing of the electron acceptor led to lower N_2O peaks than full dosing, suggesting that controlled nitrite supply can prevent overload of denitrification pathways and reduce the risk of NosZ inhibition (C. Li et al., 2013; Ribera-Guardia et al., 2016). In glucose-fed systems, however, even with reduced nitrite exposure, the structural limitations of the microbial community dominated by partial denitrifiers may still lead to higher N_2O yields.

These findings align with previous reports that carbon source quality, in addition to quantity, plays a decisive role in N_2O emissions from EBPR systems. Pan et al. (2024) observed higher N_2O accumulation in glucose-fed EBPR reactors compared to acetate-fed ones under identical nitrite

loading, attributing the difference to shifts in the active denitrifying population. Similarly, Wisniewski et al. (2018) found that acetate-enriched DPAO communities maintained higher *NosZ* expression and lower N_2O yields than those enriched with more complex carbon substrates.

6. CONCLUSIONS

Based on the literature review and experimental work conducted in this doctoral dissertation, it can be concluded that DPAOs play a critical role in optimizing EBPR by providing a sustainable pathway for simultaneous N and P removal. This study focused on glucose as a potential alternative carbon source for the *Tetrasphaera*-rich DPAOs, comparing its effects with acetate under different electron acceptor conditions (nitrate and nitrite).

The main conclusions are summarized as follows:

1. Impact of COD:P ratios and electron acceptor type

- Optimizing COD:P ratios and maintaining sufficient carbon availability are crucial for both DPAO-driven P removal and minimizing N₂O production. COD:P ratios below 2.5 (limiting conditions) enhanced DPAO activity, leading to more complete denitrification, effective PO₄³⁻ uptake without prolonged PO₄³⁻ release, and reduced N₂O production. In contrast, COD:P non-limiting conditions (>2.5) scenarios resulted in prolonged PO₄³⁻ release.
- Acetate with NO₃⁻ proved to be the most favorable combination for DPAO activity, achieving PRRs 25-times higher compared to glucose. This emphasizes the key role of acetate as a carbon source in enhancing DPAO activity in *Tetrasphaera*-rich sludge.
- Higher NURs were obtained with acetate than those with glucose under both NO₃⁻ and NO₂⁻ electron-acceptor conditions.

2. Contribution shares to P removal

- The estimated contribution of *Tetrasphaera*-rich DPAOs to the total P removal ranged between 26.0–32.3%, while OHOs contributed between 67.7-74.0%.

3. N₂O Production

- COD:P non-limiting conditions ratios provided sufficient carbon for complete denitrification, reducing N₂O accumulation under anoxic conditions.
- N₂O production was predominantly governed by the presence of NO₂⁻.
- Under modified anoxic conditions (chemical PO₄³⁻ precipitation and PHA-depleted sludge), incomplete denitrification occurred, leading to elevated N₂O production.
- A single (full) dosage of NO₂⁻ strongly induced N₂O accumulation compared to intermittent (pulse) dosing.

4. Microbial community

- DPAOs represented approximately 12.4% of the total bacterial community, with high enrichment of *Tetrasphaera*.
- DPAOs contributed primarily to NO₃⁻ reduction, while OHOs were mainly responsible for N₂O production. Despite the promising abundance and diversity of DPAOs (particularly *Tetrasphaera*), the role of glucose as a carbon source for denitrification and P removal remains uncertain and only partially understood, indicating the need for further research.

6.1 Challenges and future research directions

Several challenges were encountered during this study. Under *Tetrasphaera*-enriched sludge higher and prolonged N_2O production was realized under NO_2^- conditions when PO_4^{3-} precipitation occurred and intracellular PHA reserves were depleted during the anoxic phases as a sign of incomplete denitrification. The limited availability of carbon under these conditions disrupted the denitrification pathway, especially the critical reduction step from NO_2^- to N_2O and N_2 , leading to elevated N_2O production, contributing to increased potential of greenhouse gas emissions.

Secondly, despite the detection of abundant DPAOs in the *Tetrasphaera*-enriched activated sludge, their actual specific utilization of glucose and contribution to overall denitrification and P removal remains only partially understood. While molecular analyses showed the presence of DPAO-related genera, distinguishing their precise activity from denitrifying OHOs remains methodologically challenging. Monitoring of intracellular storage compounds, such as PHA, can serve as an early indicator for the risk of incomplete denitrification and N_2O production.

Future research should prioritize the development of advanced tools and methodologies that can accurately differentiate between DPAO- and OHO-driven denitrification with diverse carbon including glucose at a metabolic level, such as the use of isotopic labeling, single-cell analyses, or real-time molecular markers. Additionally, it will be critical to explore how environmental factors, such as fluctuating influent loads, carbon source variation, and dissolved oxygen levels in the aerobic compartments, affect the competition between DPAOs i.e. *Tetrasphaera* and OHOs. COD:P ratios should be optimized in real-time operation to minimize N_2O production while enhancing simultaneous N and P removal. Operational strategies (e.g., intermittent carbon dosing) should be

explored to stimulate DPAO i.e. *Tetrasphaera*'s specific activity. Addressing these aspects will enhance the design and control of EBPR systems, maximizing both nutrient removal efficiency and environmental sustainability.

REFERENCES

- Abdoli, S., Asgari Lajayer, B., Dehghanian, Z., Bagheri, N., Vafaei, A. H., Chamani, M., Rani, S., Lin, Z., Shu, W., & Price, G. W. (2024). A Review of the Efficiency of Phosphorus Removal and Recovery from Wastewater by Physicochemical and Biological Processes: Challenges and Opportunities. *Water*, *16*(17), Article 17. <https://doi.org/10.3390/w16172507>
- Acelas, N. Y., López, D. P., Brilman, D. W. F. (Wim), Kersten, S. R. A., & Kootstra, A. M. J. (2014). Supercritical water gasification of sewage sludge: Gas production and phosphorus recovery. *Bioresource Technology*, *174*, 167–175. <https://doi.org/10.1016/j.biortech.2014.10.003>
- Achilleos, P., Roberts, K. R., & Williams, I. D. (2022). Struvite precipitation within wastewater treatment: A problem or a circular economy opportunity? *Heliyon*, *8*(7), e09862. <https://doi.org/10.1016/j.heliyon.2022.e09862>
- Aghilinasrollahabadi, K., Kjellerup, B. V., Nguyen, C., Saavedra, Y., & Li, G. (2024). Impact of Carbon Sources Application in Enhanced Biological Phosphorous Removal (EBPR) Improvement: A Review. *Water, Air, & Soil Pollution*, *235*(8), 543. <https://doi.org/10.1007/s11270-024-07350-8>
- Akinnawo, S. O. (2023). Eutrophication: Causes, consequences, physical, chemical and biological techniques for mitigation strategies. *Environmental Challenges*, *12*, 100733. <https://doi.org/10.1016/j.envc.2023.100733>
- Alasino, N., Mussati, M., Scenna, N., & Aguirre, P. (2008). Combined nitrogen and phosphorus removal. Model-based process optimization. *Computer Aided Chemical Engineering*, *25*, 163–168. [https://doi.org/10.1016/S1570-7946\(08\)80032-6](https://doi.org/10.1016/S1570-7946(08)80032-6)
- Al-Hazmi, H. E., Grubba, D., Majtacz, J., Ziemińska-Buczyńska, A., Zhai, J., & Mąkinia, J. (2023). Combined partial denitrification/anammox process for nitrogen removal in wastewater treatment. *Journal of Environmental Chemical Engineering*, *11*(1), 108978. <https://doi.org/10.1016/j.jece.2022.108978>
- Andersen, J., Laamanen, M., Aigars, J., Axe, P., Blomqvist, M., Carstensen, J., Claussen, U., Josefson, A., Fleming, V., Järvinen, M., Kaartokallio, H., Kaitala, S., Kauppila, P., Knuutila, S., Korovin, L., Korpinen, S., Kotilainen, P., Kubiliute, A., Kuuppo, P., &

- Villnäs, A. (2009). *HELCOM (2009): Eutrophication in the Baltic Sea. An integrated thematic assessment of the effects of nutrient enrichment in the Baltic Sea region. Balt. Sea. Env. Proc. No. 115. Helsinki Commission. 148 pp.*
<https://doi.org/10.13140/RG.2.1.2669.0400>
- Asadi, M., & McPhedran, K. (2021). Estimation of greenhouse gas and odour emissions from a cold region municipal biological nutrient removal wastewater treatment plant. *Journal of Environmental Management*, 281. Scopus. <https://doi.org/10.1016/j.jenvman.2020.111864>
- Bai, M., Zhao, W., Wang, Y., Bi, X., Su, S., Qiu, H., & Gao, Z. (2024). Towards low carbon demand and highly efficient nutrient removal: Establishing denitrifying phosphorus removal in anaerobic/anoxic/oxic + nitrification system. *Bioresource Technology*, 395, 130385. <https://doi.org/10.1016/j.biortech.2024.130385>
- Bai, X., McKnight, M. M., Neufeld, J. D., & J. Parker, W. (2023). Simultaneous nitrification, denitrification, and phosphorus removal from municipal wastewater at low temperature. *Bioresource Technology*, 368, 128261. <https://doi.org/10.1016/j.biortech.2022.128261>
- Bali, M., & Gueddari, M. (2019). Removal of phosphorus from secondary effluents using infiltration–percolation process. *Applied Water Science*, 9(3), 54. <https://doi.org/10.1007/s13201-019-0945-5>
- Bannert, J. A., Bannert, J. A., Brad, A. A., Brad, A. A., Klöden, J. A., Klöden, J. A., Gebauer, A. A., Gebauer, A. A., Tent, N. A., Tent, N. A., Hernández, A. A. A., & Hernández, A. A. A. (2021). A review of the challenges and strategies of delivering services of general interest in European rural areas. [Http://195.187.71.2/Ipac20/Ipac.Jsp?profile=geogpan&index=BOCLC&term=bb99159581](http://195.187.71.2/Ipac20/Ipac.Jsp?profile=geogpan&index=BOCLC&term=bb99159581). <https://doi.org/10.7163/Eu21.2021.41.4>
- Barnard, J. (1974). *CUT P AND N WITHOUT CHEMICALS*. <http://pascal-francis.inist.fr/vibad/index.php?action=getRecordDetail&idt=PASCAL7588501407>
- Barnard, J. (1975). *Nutrient removal in biological systems*. 74, 143–154.
- Barnard, J. (2006). Biological NUTRIENT removal: Where we have been where we are going? *Proceedings of the Water Environment Federation*, 2006, 1–25. <https://doi.org/10.2175/193864706783710578>

- Barnard, J. L., Dunlap, P., & Steichen, M. (2017a). Rethinking the Mechanisms of Biological Phosphorus Removal. *Water Environment Research*, 89(11), 2043–2054. <https://doi.org/10.2175/106143017X15051465919010>
- Bauhs, K. T., Gagnon, A. A., & Bott, C. B. (2022). Investigating the use of anaerobically stored carbon in post-anoxic denitrification. *Water Environment Research: A Research Publication of the Water Environment Federation*, 94(6), e10749. <https://doi.org/10.1002/wer.10749>
- Begum, S., & Batista, J. (2012). Begum SA, Batista JR. Microbial selection on enhanced biological phosphorus removal systems fed exclusively with glucose. *World J Microbiol Biotechnol* 28: 2181-2193. *World Journal of Microbiology & Biotechnology*, 28, 2181–2193. <https://doi.org/10.1007/s11274-012-1024-3>
- Bertanza, G., Menoni, L., Capoferri, G. U., & Pedrazzani, R. (2020). Promoting biological phosphorus removal in a full scale pre-denitrification wastewater treatment plant. *Journal of Environmental Management*, 254, 109803. <https://doi.org/10.1016/j.jenvman.2019.109803>
- Bi, J., Marques, R., Wang, D., Qin, L., Close, K., Li, G., Wang, Z. L., Tooker, N. B., Srinivasan, V., Onnis-Hayden, A., Oehmen, A., & Gu, A. Z. (2025). Phenotypic discrimination and characterization of microbial populations in enhanced biological phosphorus removal using single-cell raman spectroscopy-based methods. *Water Research*, 281, 123577. <https://doi.org/10.1016/j.watres.2025.123577>
- Bond, P. L., Hugenholtz, P., Keller, J., & Blackall, L. L. (1995). Bacterial community structures of phosphate-removing and non-phosphate-removing activated sludges from sequencing batch reactors. *Applied and Environmental Microbiology*, 61(5), 1910–1916. <https://doi.org/10.1128/aem.61.5.1910-1916.1995>
- Bond, P. L., Keller, J., & Blackall, L. L. (1999). Bio-P and non-bio-P bacteria identification by a novel microbial approach. *Water Science and Technology*, 39(6), 13–20. [https://doi.org/10.1016/S0273-1223\(99\)00118-3](https://doi.org/10.1016/S0273-1223(99)00118-3)
- Broman, E., Jawad, A., Wu, X., Christel, S., Ni, G., Lopez-Fernandez, M., Sundkvist, J. E., & Dopson, M. (2017). Low temperature, autotrophic microbial denitrification using

- thiosulfate or thiocyanate as electron donor. *Biodegradation*, 28(4), 287–301. <https://doi.org/10.1007/s10532-017-9796-7>
- Camejo, P. Y., Owen, B. R., Martirano, J., Ma, J., Kapoor, V., Santo Domingo, J., McMahon, K. D., & Noguera, D. R. (2016). *Candidatus* Accumulibacter phosphatis clades enriched under cyclic anaerobic and microaerobic conditions simultaneously use different electron acceptors. *Water Research*, 102, 125–137. <https://doi.org/10.1016/j.watres.2016.06.033>
- Campos, J. L., Valenzuela-Heredia, D., Pedrouso, A., Val del Río, A., Belmonte, M., & Mosquera-Corral, A. (2016). Greenhouse Gases Emissions from Wastewater Treatment Plants: Minimization, Treatment, and Prevention. *Journal of Chemistry*, 2016, e3796352. <https://doi.org/10.1155/2016/3796352>
- Carrillo, V., Castillo, R., Magrí, A., Holzapfel, E., & Vidal, G. (2024). Phosphorus recovery from domestic wastewater: A review of the institutional framework. *Journal of Environmental Management*, 351, 119812. <https://doi.org/10.1016/j.jenvman.2023.119812>
- Carvalho, G., Lemos, P. C., Oehmen, A., & Reis, M. A. M. (2007). Denitrifying phosphorus removal: Linking the process performance with the microbial community structure. *Water Research*, 41(19), 4383–4396. <https://doi.org/10.1016/j.watres.2007.06.065>
- Chan, C., Guisasola, A., & Baeza, J. A. (2020). Living on the edge: Prospects for enhanced biological phosphorus removal at low sludge retention time under different temperature scenarios. *Chemosphere*, 258, 127230. <https://doi.org/10.1016/j.chemosphere.2020.127230>
- Chen, H., Wang, D., Li, X., Yang, Q., Luo, K., Zeng, G., Tang, M., Xiong, W., & Yang, G. (2014). Effect of dissolved oxygen on biological phosphorus removal induced by aerobic/extended-idle regime. *Biochemical Engineering Journal*, 90, 27–35. <https://doi.org/10.1016/J.BEJ.2014.03.004>
- Chen, H., Wang, D., Li, X., Yang, Q., & Zeng, G. (2015). Enhancement of post-anoxic denitrification for biological nutrient removal: Effect of different carbon sources. *Environmental Science and Pollution Research*, 22(8), 5887–5894. <https://doi.org/10.1007/s11356-014-3755-1>
- Chen, J., Tao, A., Li, Q., Chen, Z., Wu, Z., Liu, X., Chen, S., Lu, Y., Mo, Y., & Su, C. (2025). Effects of different influent carbon-to-phosphorus ratios on phosphorus transformation,

- microbial community structure and metabolic functions in an upflow anaerobic sludge bed reactor. *Biochemical Engineering Journal*, 220, 109740. <https://doi.org/10.1016/j.bej.2025.109740>
- Chen, L., Chen, H., Hu, Z., Tian, Y., Wang, C., Xie, P., Deng, X., Zhang, Y., Tang, X., Lin, X., Li, B., Wei, C.-H., & Qiu, G. (2022). Carbon Uptake Bioenergetics of PAOs and GAOs in Full-scale Enhanced Biological Phosphorus Removal Systems. *Water Research*, 216, 118258. <https://doi.org/10.1016/j.watres.2022.118258>
- Chen, P., Wu, J., Lu, X., & Yu, R. (2021). Denitrifying phosphorus removal and microbial community characteristics of two-sludge DEPHANOX system: Effects of COD/TP ratio. *Biochemical Engineering Journal*, 172, 108059. <https://doi.org/10.1016/j.bej.2021.108059>
- Chen, X., Hao, K., Zhao, L., Zong, Y., & Chen, J. (2023). Carbon, nitrogen, and phosphorus metabolic relationships and reaction mechanisms in SBBR processes in the plateau habitat. *Environmental Monitoring and Assessment*, 195. <https://doi.org/10.1007/s10661-023-11961-9>
- Chen, Y., Chen, J., Xia, R., Li, W., Zhang, Y., Zhang, K., Tong, S., Jia, R., Hu, Q., Wang, L., & Zhang, X. (2023). Phosphorus – The main limiting factor in riverine ecosystems in China. *Science of The Total Environment*, 870, 161613. <https://doi.org/10.1016/j.scitotenv.2023.161613>
- Chen, Y., Lan, S., Wang, L., Dong, S., Zhou, H., Tan, Z., & Li, X. (2017). A review: Driving factors and regulation strategies of microbial community structure and dynamics in wastewater treatment systems. *Chemosphere*, 174, 173–182. <https://doi.org/10.1016/j.chemosphere.2017.01.129>
- Cheng, M., Guisasola, A., & Baeza, J. A. (2024). Leveraging side-stream sludge fermentation for phosphorus recovery in wastewater treatment systems. *Chemical Engineering Journal*, 500, 156637. <https://doi.org/10.1016/j.cej.2024.156637>
- Close, K., Marques, R., Carvalho, V. C. F., Freitas, E. B., Reis, M. A. M., Carvalho, G., & Oehmen, A. (2021). The storage compounds associated with Tetrasphaera PAO metabolism and the relationship between diversity and P removal. *Water Research*, 204, 117621. <https://doi.org/10.1016/j.watres.2021.117621>

- Coma, M., Verawaty, M., Pijuan, M., Yuan, Z., & Bond, P. L. (2012). Enhancing aerobic granulation for biological nutrient removal from domestic wastewater. *Bioresource Technology*, *103*(1), 101–108. <https://doi.org/10.1016/j.biortech.2011.10.014>
- Comeau, Y., Oldham, W. K., & Hall, K. J. (1987). DYNAMICS OF CARBON RESERVES IN BIOLOGICAL DEPHOSPHATATION OF WASTEWATER. In R. Ramadori (Ed.), *Biological Phosphate Removal from Wastewaters* (pp. 39–55). Pergamon. <https://doi.org/10.1016/B978-0-08-035592-4.50010-9>
- Conidi, D., Andalib, M., Andres, C., Bye, C., Umble, A., & Dold, P. (2018). Modeling quaternary ammonium compound inhibition of biological nutrient removal activated sludge. *Water Science and Technology*, *79*(1), 41–50. <https://doi.org/10.2166/wst.2018.449>
- Council Directive of 21 May 1991 Concerning Urban Waste Water Treatment (91/271/EEC) (2014). <http://data.europa.eu/eli/dir/1991/271/2014-01-01/eng>
- Crocetti, G. R., Hugenholtz, P., Bond, P. L., Schuler, A., Keller, J., Jenkins, D., & Blackall, L. L. (2000). Identification of polyphosphate-accumulating organisms and design of 16S rRNA-directed probes for their detection and quantitation. *Applied and Environmental Microbiology*, *66*(3), 1175–1182. <https://doi.org/10.1128/AEM.66.3.1175-1182.2000>
- Daebeler, A., Herbold, C. W., Vierheilig, J., Sedlacek, C. J., Pjevac, P., Albertsen, M., Kirkegaard, R. H., de la Torre, J. R., Daims, H., & Wagner, M. (2018). Cultivation and genomic analysis of ‘*Candidatus Nitrosocaldus islandicus*,’ an obligately thermophilic, ammonia-oxidizing thaumarchaeon from a hot spring biofilm in Graendalur valley, Iceland. *Frontiers in Microbiology*, *9*(FEB), 1–16. <https://doi.org/10.3389/fmicb.2018.00193>
- Di Capua, F., de Sario, S., Ferraro, A., Petrella, A., Race, M., Pirozzi, F., Fratino, U., & Spasiano, D. (2022). Phosphorous removal and recovery from urban wastewater: Current practices and new directions. *Science of The Total Environment*, *823*, 153750. <https://doi.org/10.1016/j.scitotenv.2022.153750>
- Diaz, R., Mackey, B., Chadalavada, S., kainthola, J., Heck, P., & Goel, R. (2022). Enhanced Bio-P removal: Past, present, and future – A comprehensive review. *Chemosphere*, *309*, 136518. <https://doi.org/10.1016/j.chemosphere.2022.136518>
- Dueholm, M. K. D., Andersen, K. S., Korntved, A.-K. C., Rudkjøbing, V., Alves, M., Bajón-Fernández, Y., Batstone, D., Butler, C., Cruz, M. C., Davidsson, Å., Erijman, L., Holliger,

- C., Koch, K., Kreuzinger, N., Lee, C., Lyberatos, G., Mutnuri, S., O'Flaherty, V., Oleskowicz-Popiel, P., ... Nielsen, P. H. (2024). MiDAS 5: Global diversity of bacteria and archaea in anaerobic digesters. *Nature Communications*, *15*(1), 5361. <https://doi.org/10.1038/s41467-024-49641-y>
- Egle, L., Rechberger, H., Krampe, J., & Zessner, M. (2016). Phosphorus recovery from municipal wastewater: An integrated comparative technological, environmental and economic assessment of P recovery technologies. *The Science of the Total Environment*, *571*, 522–542. <https://doi.org/10.1016/j.scitotenv.2016.07.019>
- Erdal, U. G., Erdal, Z. K., & Randall, C. W. (2006). The Mechanism of Enhanced Biological Phosphorus Removal Washout and Temperature Relationships. *Water Environment Research*, *78*(7), 710–715. <https://doi.org/10.2175/106143006X101737>
- Farmer, M., Rajasabhai, R., Tarpeh, W., Tyo, K., & Wells, G. (2023). Meta-omic profiling reveals ubiquity of genes encoding for the nitrogen-rich biopolymer cyanophycin in activated sludge microbiomes. *Frontiers in Microbiology*, *14*, 1287491. <https://doi.org/10.3389/fmicb.2023.1287491>
- Fernandes, H., Jungles, M. K., Hoffmann, H., Antonio, R. V., & Costa, R. H. R. (2013). Full-scale sequencing batch reactor (SBR) for domestic wastewater: Performance and diversity of microbial communities. *Bioresource Technology*, *132*, 262–268. <https://doi.org/10.1016/j.biortech.2013.01.027>
- Fernando, E. Y., McIlroy, S. J., Nierychlo, M., Herbst, F.-A., Petriglieri, F., Schmid, M. C., Wagner, M., Nielsen, J. L., & Nielsen, P. H. (2019a). Resolving the individual contribution of key microbial populations to enhanced biological phosphorus removal with Raman-FISH. *The ISME Journal*, *13*(8), 1933–1946. <https://doi.org/10.1038/s41396-019-0399-7>
- Filipe, C. D. M., Daigger, G. T., & Grady Jr., C. P. L. (2001). pH as a Key Factor in the Competition Between Glycogen-Accumulating Organisms and Phosphorus-Accumulating Organisms. *Water Environment Research*, *73*(2), 223–232. <https://doi.org/10.2175/106143001X139209>
- Fuhs, G. W., & Chen, M. (1975). Microbiological basis of phosphate removal in the activated sludge process for the treatment of wastewater. *Microbial Ecology*, *2*(2), 119–138. <https://doi.org/10.1007/BF02010434>

- Gao, M., Sun, S., Qiu, Q., Zhou, W., & Qiu, L. (2023). Enrichment denitrifying phosphorus-accumulating organisms in alternating anoxic-anaerobic/aerobic biofilter for advanced nitrogen and phosphorus removal from municipal wastewater. *Journal of Water Process Engineering*, 55, 104089. <https://doi.org/10.1016/j.jwpe.2023.104089>
- Gebremariam, S. Y., Beutel, M. W., Christian, D., & Hess, T. F. (2011). Research Advances and Challenges in the Microbiology of Enhanced Biological Phosphorus Removal—A Critical Review. *Water Environment Research*, 83(3), 195–219.
- Gong, L., Huo, M., Yang, Q., Li, J., Ma, B., Zhu, R., Wang, S., & Peng, Y. (2013). Performance of heterotrophic partial denitrification under feast-famine condition of electron donor: A case study using acetate as external carbon source. *Bioresource Technology*, 133, 263–269. <https://doi.org/10.1016/j.biortech.2012.12.108>
- Graziani, M. (2006). *Phosphorus Treatment and Removal Technologies*.
- Green, S. J., Prakash, O., Gihring, T. M., Akob, D. M., Jasrotia, P., Jardine, P. M., Watson, D. B., Brown, S. D., Palumbo, A. V., & Kostka, J. E. (2010). Denitrifying bacteria isolated from terrestrial subsurface sediments exposed to mixed-waste contamination. *Applied and Environmental Microbiology*, 76(10), 3244–3254. <https://doi.org/10.1128/AEM.03069-09>
- Guerrero, J., Guisasola, A., & Baeza, J. A. (2011). The nature of the carbon source rules the competition between PAO and denitrifiers in systems for simultaneous biological nitrogen and phosphorus removal. *Water Research*, 45(16), 4793–4802. <https://doi.org/10.1016/j.watres.2011.06.019>
- Guisasola, A., Qurie, M., Vargas, M. d. M., Casas, C., & Baeza, J. A. (2009). Failure of an enriched nitrite-DPAO population to use nitrate as an electron acceptor. *Process Biochemistry*, 44(7), 689–695. Scopus. <https://doi.org/10.1016/j.procbio.2009.02.017>
- Gujer, W., Henze, M., Mino, T., & van Loosdrecht, M. (1999). Activated Sludge Model No. 3. *Water Science and Technology*, 39(1), 183–193. <https://doi.org/10.2166/wst.1999.0039>
- Guo, G., Wu, D., Ekama, G. A., Hao, T., Mackey, H. R., & Chen, G. (2018). Denitrifying sulfur conversion-associated EBPR: Effects of temperature and carbon source on anaerobic metabolism and performance. *Water Research*, 141, 9–18. <https://doi.org/10.1016/j.watres.2018.04.028>

- Guo, G., Wu, D., Hao, T., Mackey, H. R., Wei, L., & Chen, G. (2017). Denitrifying sulfur conversion-associated EBPR: The effect of pH on anaerobic metabolism and performance. *Water Research*, 123, 687–695. <https://doi.org/10.1016/j.watres.2017.07.020>
- Hallin, S., Philippot, L., Löffler, F. E., Sanford, R. A., & Jones, C. M. (2018). Genomics and Ecology of Novel N₂O-Reducing Microorganisms. *Trends in Microbiology*, 26(1), 43–55. <https://doi.org/10.1016/j.tim.2017.07.003>
- Harry R. Beller et al., 2006. (1977). The Genome Sequence of the Obligately Chemolithoautotrophic, Facultatively Anaerobic Bacterium *Thiobacillus denitrificans*. *British Journal of Venereal Diseases*, 53(1), 12–18. <https://doi.org/10.1128/JB.188.4.1473>
- He, C., Wu, H., Wei, G., Zhu, S., Qiu, G., & Wei, C. (2024). Simultaneous decarbonization and phosphorus removal by *Tetrasphaera elongata* with glucose as carbon source under aerobic conditions. *Bioresource Technology*, 393, 130048. <https://doi.org/10.1016/j.biortech.2023.130048>
- Henze, M., Gujer, W., Mino, T., Matsuo, T., Wentzel, M. C., Marais, G. v. R., & Van Loosdrecht, M. C. M. (1999). Activated Sludge Model No.2d, ASM2D. *Water Science and Technology*, 39(1), 165–182. <https://doi.org/10.2166/wst.1999.0036>
- Herbst, F. A., Dueholm, M. S., Wimmer, R., & Nielsen, P. H. (2019). The proteome of *Tetrasphaera elongata* is adapted to changing conditions in wastewater treatment plants. *Proteomes*, 7(2), 16. <https://doi.org/10.3390/proteomes7020016>
- Hesselmann, R. P. X., Werlen, C., Hahn, D., van der Meer, J. R., & Zehnder, A. J. B. (1999). Enrichment, Phylogenetic Analysis and Detection of a Bacterium That Performs Enhanced Biological Phosphate Removal in Activated Sludge. *Systematic and Applied Microbiology*, 22(3), 454–465. [https://doi.org/10.1016/S0723-2020\(99\)80055-1](https://doi.org/10.1016/S0723-2020(99)80055-1)
- Hou, R., Liu, J., Yang, P., Liu, H., Yuan, R., Ji, Y., Zhao, H., Chen, Z., Zhou, B., & Chen, H. (2024). Metabolomic reveals the responses of sludge properties and microbial communities to high nitrite stress in denitrifying phosphorus removal systems. *Environmental Research*, 252, 118924. <https://doi.org/10.1016/j.envres.2024.118924>
- Hou, R., Yuan, R., Chen, R., Zhou, B., & Chen, H. (2022). Metagenomic analysis of denitrifying phosphorus removal in SBR system: Comparison of nitrate and nitrite as electron

- acceptors. *Chemical Engineering Journal*, 446, 137225.
<https://doi.org/10.1016/j.cej.2022.137225>
- Hu, X., Sobotka, D., Czerwionka, K., Zhou, Q., Xie, L., & Makinia, J. (2018). Effects of different external carbon sources and electron acceptors on interactions between denitrification and phosphorus removal in biological nutrient removal processes. *Journal of Zhejiang University. Science. B*, 19(4), 305–316. <https://doi.org/10.1631/jzus.B1700064>
- Hu, Z., Wentzel, M., & Ekama, G. (2002). The significance of denitrifying polyphosphate accumulating organisms in biological nutrient removal activated sludge systems. *Water Science and Technology: A Journal of the International Association on Water Pollution Research*, 46, 129–138. <https://doi.org/10.2166/wst.2002.0468>
- Huser, B. J., Futter, M., Lee, J. T., & Perniel, M. (2016). In-lake measures for phosphorus control: The most feasible and cost-effective solution for long-term management of water quality in urban lakes. *Water Research*, 97, 142–152. <https://doi.org/10.1016/j.watres.2015.07.036>
- Izadi, P., & Andalib, M. (2023). Anaerobic zone Functionality, Design and Configurations for a Sustainable EBPR process: A Critical Review. *Science of The Total Environment*, 870, 162018. <https://doi.org/10.1016/j.scitotenv.2023.162018>
- Izadi, P., Izadi, P., & Eldyasti, A. (2020). Design, operation and technology configurations for enhanced biological phosphorus removal (EBPR) process: A review. *Reviews in Environmental Science and Bio/Technology*, 19(3), 561–593. <https://doi.org/10.1007/s11157-020-09538-w>
- Izadi, P., Izadi, P., & Eldyasti, A. (2021a). A review of biochemical diversity and metabolic modeling of EBPR process under specific environmental conditions and carbon source availability. *Journal of Environmental Management*, 288, 112362. <https://doi.org/10.1016/j.jenvman.2021.112362>
- Jenkins, D., & Wanner, J. (2014). Activated Sludge – 100 Years and Counting. *Water Intelligence Online*, 13. <https://doi.org/10.2166/9781780404943>
- Ji, B., Yang, K., Zhu, L., Jiang, Y., Wang, H., Zhou, J., & Zhang, H. (2015). Aerobic denitrification: A review of important advances of the last 30 years. *Biotechnology and Bioprocess Engineering*, 20(4), 643–651. <https://doi.org/10.1007/s12257-015-0009-0>

- Kacprzak, M. J., & Kupich, I. (2023). The specificities of the circular economy (CE) in the municipal wastewater and sewage sludge sector—Local circumstances in Poland. *Clean Technologies and Environmental Policy*, 25(2), 519–535. <https://doi.org/10.1007/s10098-021-02178-w>
- Kampschreur, M. J., Temmink, H., Kleerebezem, R., Jetten, M. S. M., & van Loosdrecht, M. C. M. (2009). Nitrous oxide emission during wastewater treatment. *Water Research*, 43(17), 4093–4103. Scopus. <https://doi.org/10.1016/j.watres.2009.03.001>
- Kang, A. J., Munz, G., & Yuan, Q. (2019). Influence of pH control on material characteristics, bacterial community composition and BNR performance of mature aerobic granules. *Process Safety and Environmental Protection*, 124, 158–166. <https://doi.org/10.1016/j.psep.2019.02.014>
- Keegan, K. P., Glass, E. M., & Meyer, F. (2016). MG-RAST, a Metagenomics Service for Analysis of Microbial Community Structure and Function. *Methods in Molecular Biology (Clifton, N.J.)*, 1399, 207–233. https://doi.org/10.1007/978-1-4939-3369-3_13
- Khalil, M., AlSayed, A., Elsayed, A., Sherif Zaghoul, M., Bell, K. Y., Al-Omari, A., Laqa Kakar, F., Houweling, D., Santoro, D., Porro, J., & Elbeshbishy, E. (2024). Advances in GHG emissions modelling for WRRFs: From State-of-the-Art methods to Full-Scale applications. *Chemical Engineering Journal*, 494, 153053. <https://doi.org/10.1016/j.cej.2024.153053>
- Kong, Y., Nielsen, J. L., & Nielsen, P. H. (2004). Microautoradiographic study of Rhodocyclus-related polyphosphate-accumulating bacteria in full-scale enhanced biological phosphorus removal plants. *Applied and Environmental Microbiology*, 70(9), 5383–5390. <https://doi.org/10.1128/AEM.70.9.5383-5390.2004>
- Kong, Y., Nielsen, J. L., & Nielsen, P. H. (2005). Identity and ecophysiology of uncultured actinobacterial polyphosphate-accumulating organisms in full-scale enhanced biological phosphorus removal plants. *Applied and Environmental Microbiology*, 71(7), 4076–4085. <https://doi.org/10.1128/AEM.71.7.4076-4085.2005>
- Koutsou, O. P., Gatidou, G., & Stasinakis, A. S. (2018). Domestic wastewater management in Greece: Greenhouse gas emissions estimation at country scale. *Journal of Cleaner Production*, 188, 851–859. <https://doi.org/10.1016/j.jclepro.2018.04.039>

- Kowal, P., Mehrani, M.-J., Sobotka, D., Ciesielski, S., & Małkinia, J. (2022). Rearrangements of the nitrifiers population in an activated sludge system under decreasing solids retention times. *Environmental Research*, 214, 113753. <https://doi.org/10.1016/j.envres.2022.113753>
- Kristiansen, R., Nguyen, H. T. T., Saunders, A. M., Nielsen, J. L., Wimmer, R., Le, V. Q., McIlroy, S. J., Petrovski, S., Seviour, R. J., Calteau, A., Nielsen, K. L., & Nielsen, P. H. (2013). A metabolic model for members of the genus *Tetrasphaera* involved in enhanced biological phosphorus removal. *The ISME Journal*, 7(3), 543–554. <https://doi.org/10.1038/ismej.2012.136>
- Kuba, T., Murnleitner, E., Van Loosdrecht, M. C. M., & Heijnen, J. J. (1996). A metabolic model for biological phosphorus removal by denitrifying organisms. *Biotechnology and Bioengineering*, 52(6), 685–695. Scopus. [https://doi.org/10.1002/\(SICI\)1097-0290\(19961220\)52:6<685::AID-BIT6>3.3.CO;2-M](https://doi.org/10.1002/(SICI)1097-0290(19961220)52:6<685::AID-BIT6>3.3.CO;2-M)
- Law, Y., Kirkegaard, R. H., Cokro, A. A., Liu, X., Arumugam, K., Xie, C., Stokholm-Bjerregaard, M., Drautz-Moses, D. I., Nielsen, P. H., Wuertz, S., & Williams, R. B. H. (2016). Integrative microbial community analysis reveals full-scale enhanced biological phosphorus removal under tropical conditions. *Scientific Reports*, 6(1), 25719. <https://doi.org/10.1038/srep25719>
- Lemley, D. A., Lakane, C. P., Taljaard, S., & Adams, J. B. (2022). Inorganic nutrient removal efficiency of a constructed wetland before discharging into an urban eutrophic estuary. *Marine Pollution Bulletin*, 179, 113727. <https://doi.org/10.1016/j.marpolbul.2022.113727>
- Levin, G. V., & Sala, U. D. (1987). PHOSTRIP® PROCESS — A VIABLE ANSWER TO EUTROPHICATION OF LAKES AND COASTAL SEA WATERS IN ITALY. In R. Ramadori (Ed.), *Biological Phosphate Removal from Wastewaters* (pp. 249–259). Pergamon. <https://doi.org/10.1016/B978-0-08-035592-4.50027-4>
- Levin, G. V., & Shapiro, J. (1965). Metabolic Uptake of Phosphorus by Wastewater Organisms. *Journal (Water Pollution Control Federation)*, 37(6), 800–821.
- Li, C., Zhang, J., Liang, S., Ngo, H. H., Guo, W., Zhang, Y., & Zou, Y. (2013). Nitrous oxide generation in denitrifying phosphorus removal process: Main causes and control measures.

- Environmental Science and Pollution Research*, 20(8), 5353–5360.
<https://doi.org/10.1007/s11356-013-1530-3>
- Li, D., Li, W., Zhang, K., Zhang, G., Zhang, H., Zhang, D., Lv, P., & Wu, J. (2020). Nutrient removal by full-scale Bi-Bio-Selector for nitrogen and phosphorus removal process treating urban domestic sewage at low C/N ratio and low temperature conditions. *Process Safety and Environmental Protection*, 140, 199–210.
<https://doi.org/10.1016/j.psep.2020.05.011>
- Li, H., Zhong, Y., Huang, H., Tan, Z., Sun, Y., & Liu, H. (2020). Simultaneous nitrogen and phosphorus removal by interactions between phosphate accumulating organisms (PAOs) and denitrifying phosphate accumulating organisms (DPAOs) in a sequencing batch reactor. *Science of The Total Environment*, 744, 140852.
<https://doi.org/10.1016/j.scitotenv.2020.140852>
- Li, J., Zhu, Z., Lv, X., Hu, X., Tan, H., Liu, W., & Luo, G. (2024). Influence of carbon to phosphorus ratio on the performance of single-stage aerobic simultaneous nitrogen and phosphorus removal by bioflocs. *Aquacultural Engineering*, 107, 102467.
<https://doi.org/10.1016/j.aquaeng.2024.102467>
- Li, J., Zhu, Z., Lv, X., Tan, H., Liu, W., & Luo, G. (2024). Optimizing carbon sources on performance for enhanced efficacy in single-stage aerobic simultaneous nitrogen and phosphorus removal via biofloc technology. *Bioresource Technology*, 411, 131347.
<https://doi.org/10.1016/j.biortech.2024.131347>
- Li, W., Liu, N., Wang, H., Hou, Y., Wang, Y., Chen, Y., & Gao, Y. (2022). Enhancement of denitrifying phosphorus removal and DPAOs identification in the anaerobic/anoxic sequencing batch reactor system. *Desalination and Water Treatment*, 253, 88–99.
<https://doi.org/10.5004/dwt.2022.28154>
- Li, X., Su, J., Wang, H., Boczkaj, G., Mahlkecht, J., Singh, S. V., & Wang, C. (2024). Bibliometric analysis of artificial intelligence in wastewater treatment: Current status, research progress, and future prospects. *Journal of Environmental Chemical Engineering*, 12(4), 113152.
<https://doi.org/10.1016/j.jece.2024.113152>
- Li, Z., Li, X., Wang, H., & Peng, Y. (2024). Achieving synchronous and highly efficient removal of nitrogen and phosphorus by rapid enrichment and cultivation denitrifying phosphorus

- accumulating organisms in anaerobic-oxic-anoxic operation mode. *Bioresource Technology*, 396, 130426. <https://doi.org/10.1016/j.biortech.2024.130426>
- Liu, R., Hao, X., Chen, Q., & Li, J. (2019a). Research advances of Tetrasphaera in enhanced biological phosphorus removal: A review. *Water Research*, 166, 115003. <https://doi.org/10.1016/j.watres.2019.115003>
- Liu, W.-T., Mino, T., Matsuo, T., & Nakamura, K. (1996). Biological phosphorus removal processes—Effect of pH on anaerobic substrate metabolism. *Water Science and Technology*, 34(1), 25–32. [https://doi.org/10.1016/0273-1223\(96\)00491-X](https://doi.org/10.1016/0273-1223(96)00491-X)
- Liu, Y., Peng, L., Chen, X., & Ni, B.-J. (2015). Mathematical Modeling of Nitrous Oxide Production during Denitrifying Phosphorus Removal Process. *Environmental Science & Technology*, 49(14), 8595–8601. <https://doi.org/10.1021/acs.est.5b01650>
- Long, X.-Y., Tang, R., Wang, T., Tao, G.-J., Wang, J.-Y., Zhou, H.-W., Xue, M., & Yu, Y.-P. (2021). Characteristics of enhanced biological phosphorus removal (EBPR) process under the combined actions of intracellular and extracellular polyphosphate. *Chemosphere*, 279, 130912. <https://doi.org/10.1016/j.chemosphere.2021.130912>
- Lopez-Vazquez, C. M., Hooijmans, C. M., Brdjanovic, D., Gijzen, H. J., & van Loosdrecht, M. C. M. (2009). Temperature effects on glycogen accumulating organisms. *Water Research*, 43(11), 2852–2864. <https://doi.org/10.1016/j.watres.2009.03.038>
- Lopez-Vazquez, C. M., Oehmen, A., Hooijmans, C. M., Brdjanovic, D., Gijzen, H. J., Yuan, Z., & van Loosdrecht, M. C. M. (2009). Modeling the PAO-GAO competition: Effects of carbon source, pH and temperature. *Water Research*, 43(2), 450–462. <https://doi.org/10.1016/j.watres.2008.10.032>
- Lu, X., Duan, H., Oehmen, A., Carvalho, G., Yuan, Z., & Ye, L. (2021). Achieving combined biological short-cut nitrogen and phosphorus removal in a one sludge system with side-stream sludge treatment. *Water Research*, 203, 117563. <https://doi.org/10.1016/j.watres.2021.117563>
- Luo, X., Guo, M., Zheng, X., Zheng, S., & Li, S. (2024). Distinguished denitrifying phosphorus removal in the high-rate anoxic/microaerobic system for sewage treatment. *Chemosphere*, 359, 142377. <https://doi.org/10.1016/j.chemosphere.2024.142377>

- Lv, T., Wang, D., Hui, J., Cheng, W., Ai, H., Qin, L., Huang, M., Feng, M., & Wu, Y. (2023). Effect of return activated sludge diversion ratio on phosphorus removal performance in side-stream enhanced biological phosphorus removal (S2EBPR) process. *Environmental Research*, 235, 116546. <https://doi.org/10.1016/j.envres.2023.116546>
- Ma, J., Guan, Z., Shen, G., Zhang, K., Zhang, X., Zhao, L., Zhou, Y., & Yu, Z. (2024). Substrate preference of *Tetrasphaera* in dual PAOs synergistic EBPR system and its phosphorus removal performance. *Journal of Water Process Engineering*, 67, 106269. <https://doi.org/10.1016/j.jwpe.2024.106269>
- Makinia, J., & Zaborowska, E. (2020). *Mathematical Modelling and Computer Simulation of Activated Sludge Systems—Second Edition*. <https://doi.org/10.2166/9781780409528>
- Maktabifard, M., Al-Hazmi, H. E., Szulc, P., Mousavizadegan, M., Xu, X., Zaborowska, E., Li, X., & Makinia, J. (2023). Net-zero carbon condition in wastewater treatment plants: A systematic review of mitigation strategies and challenges. *Renewable and Sustainable Energy Reviews*, 185, 113638. <https://doi.org/10.1016/j.rser.2023.113638>
- Mannina, G., Ekama, G., Caniani, D., Cosenza, A., Esposito, G., Gori, R., Garrido-Baserba, M., Rosso, D., & Olsson, G. (2016). Greenhouse gases from wastewater treatment—A review of modelling tools. *Science of The Total Environment*, 551–552, 254–270. <https://doi.org/10.1016/j.scitotenv.2016.01.163>
- Marques, R., Ribera-Guardia, A., Santos, J., Carvalho, G., Reis, M. A. M., Pijuan, M., & Oehmen, A. (2018a). Denitrifying capabilities of *Tetrasphaera* and their contribution towards nitrous oxide production in enhanced biological phosphorus removal processes. *Water Research*, 137, 262–272. <https://doi.org/10.1016/j.watres.2018.03.010>
- Marques, R., Santos, J., Nguyen, H., Carvalho, G., Noronha, J. P., Nielsen, P. H., Reis, M. A. M., & Oehmen, A. (2017). Metabolism and ecological niche of *Tetrasphaera* and *Ca. Accumulibacter* in enhanced biological phosphorus removal. *Water Research*, 122, 159–171. <https://doi.org/10.1016/j.watres.2017.04.072>
- Maszenan, A. M., Bessarab, I., Williams, R. B. H., Petrovski, S., & Seviour, R. J. (2022). The phylogeny, ecology and ecophysiology of the glycogen accumulating organism (GAO) *Defluviicoccus* in wastewater treatment plants. *Water Research*, 221, 118729. <https://doi.org/10.1016/j.watres.2022.118729>

- Maszenan, A. M., Seviour, R. J., Patel, B. K., Schumann, P., Burghardt, J., Tokiwa, Y., & Stratton, H. M. (2000). Three isolates of novel polyphosphate-accumulating gram-positive cocci, obtained from activated sludge, belong to a new genus, *Tetrasphaera* gen. Nov., and description of two new species, *Tetrasphaera japonica* sp. Nov. And *Tetrasphaera australiensis* sp. Nov. *International Journal of Systematic and Evolutionary Microbiology*, *50 Pt 2*, 593–603. <https://doi.org/10.1099/00207713-50-2-593>
- Meinhold, J., Arnold, E., & Isaacs, S. (1999). Effect of nitrite on anoxic phosphate uptake in biological phosphorus removal activated sludge. *Water Research*, *33*(8), 1871–1883. [https://doi.org/10.1016/S0043-1354\(98\)00411-4](https://doi.org/10.1016/S0043-1354(98)00411-4)
- Meng, Q., Zeng, W., Wang, B., Fan, Z., & Peng, Y. (2020). New insights in the competition of polyphosphate-accumulating organisms and glycogen-accumulating organisms under glycogen accumulating metabolism with trace Poly-P using flow cytometry. *Chemical Engineering Journal*, *385*, 123915. <https://doi.org/10.1016/j.cej.2019.123915>
- Mino, T., van Loosdrecht, M., & Heijnen, J. (1998). Microbiology and biochemistry of the enhanced biological phosphate removal process. *Water Research*, *32*(11), 3193–3207.
- Monclús, H., Sipma, J., Ferrero, G., Rodriguez-Roda, I., & Comas, J. (2010). Biological nutrient removal in an MBR treating municipal wastewater with special focus on biological phosphorus removal. *Bioresource Technology*, *101*(11), 3984–3991. <https://doi.org/10.1016/j.biortech.2010.01.038>
- Mukherjee, C., Chowdhury, R., Begam, M. M., Ganguli, S., Basak, R., Chaudhuri, B., & Ray, K. (2019). Effect of Varying Nitrate Concentrations on Denitrifying Phosphorus Uptake by DPAOs With a Molecular Insight Into Pho Regulon Gene Expression. *Frontiers in Microbiology*, *10*, 2586. <https://doi.org/10.3389/fmicb.2019.02586>
- Muszyński, A., Tabernacka, A., & Miłobędzka, A. (2015). Long-term dynamics of the microbial community in a full-scale wastewater treatment plant. *International Biodeterioration & Biodegradation*, *100*, 44–51. <https://doi.org/10.1016/j.ibiod.2015.02.008>
- Nadagouda, M., Varshney, G., Varshney, V., & Hejase, C. (2024). Recent Advances in Technologies for Phosphate Removal and Recovery: A Review. *ACS Environmental Au*, *4*. <https://doi.org/10.1021/acsenvironau.3c00069>
- National Recommended Water Quality Criteria: 2002*. (n.d.).

- Nguyen, H., Nielsen, J., & Nielsen, P. (2012). Candidatus Halomonas phosphatis', a novel polyphosphate-accumulating organism in full-scale enhanced biological phosphorus removal plants. *Environmental Microbiology*, *14*, 2826–2837. <https://doi.org/10.1111/j.1462-2920.2012.02826.x>
- Nguyen, H. T. T., Kristiansen, R., Vestergaard, M., Wimmer, R., & Nielsen, P. H. (2015a). Intracellular accumulation of glycine in polyphosphate-accumulating organisms in activated sludge, a novel storage mechanism under dynamic anaerobic-aerobic conditions. *Applied and Environmental Microbiology*, *81*(14), 4809–4818. https://doi.org/10.1128/AEM.01012-15/SUPPL_FILE/ZAM999116401SO1.PDF
- Nguyen, P. Y., Marques, R., Wang, H., Reis, M. A. M., Carvalho, G., & Oehmen, A. (2023). The impact of pH on the anaerobic and aerobic metabolism of Tetrasphaera-enriched polyphosphate accumulating organisms. *Water Research X*, *19*. Scopus. <https://doi.org/10.1016/j.wroa.2023.100177>
- Nielsen, P. H., McIlroy, S. J., Albertsen, M., & Nierychlo, M. (2019). Re-evaluating the microbiology of the enhanced biological phosphorus removal process. *Current Opinion in Biotechnology*, *57*, 111–118. <https://doi.org/10.1016/j.copbio.2019.03.008>
- Nierychlo, M., Singleton, C. M., Petriglieri, F., Thomsen, L., Petersen, J. F., Peces, M., Kondrotaitė, Z., Dueholm, M. S., & Nielsen, P. H. (2021). Low Global Diversity of Candidatus Microthrix, a Troublesome Filamentous Organism in Full-Scale WWTPs. *Frontiers in Microbiology*, *12*. <https://doi.org/10.3389/fmicb.2021.690251>
- Nittami, T., Oi, H., Matsumoto, K., & Seviour, R. J. (2011). Influence of temperature, pH and dissolved oxygen concentration on enhanced biological phosphorus removal under strictly aerobic conditions. *New Biotechnology*, *29*(1), 2–8. <https://doi.org/10.1016/j.nbt.2011.06.012>
- Oehmen, A., Lemos, P. C., Carvalho, G., Yuan, Z., Keller, J., Blackall, L. L., & Reis, M. A. M. (2007a). Advances in enhanced biological phosphorus removal: From micro to macro scale. *Water Research*, *41*(11), 2271–2300. <https://doi.org/10.1016/J.WATRES.2007.02.030>
- Oehmen, A., Lopez-Vazquez, C. M., Carvalho, G., Reis, M. A. M., & van Loosdrecht, M. C. M. (2010). Modelling the population dynamics and metabolic diversity of organisms relevant

- in anaerobic/anoxic/aerobic enhanced biological phosphorus removal processes. *Water Research*, 44(15), 4473–4486. <https://doi.org/10.1016/j.watres.2010.06.017>
- Oehmen, A., Teresa Vives, M., Lu, H., Yuan, Z., & Keller, J. (2005). The effect of pH on the competition between polyphosphate-accumulating organisms and glycogen-accumulating organisms. *Water Research*, 39(15), 3727–3737. <https://doi.org/10.1016/j.watres.2005.06.031>
- Oehmen, A., Yuan, Z., Blackall, L. L., & Keller, J. (2005a). Comparison of acetate and propionate uptake by polyphosphate accumulating organisms and glycogen accumulating organisms. *Biotechnology and Bioengineering*, 91(2), 162–168. <https://doi.org/10.1002/bit.20500>
- Ong, Y. H., Chua, A., Fukushima, T., Ngoh, G., Shoji, T., & Michinaka, A. (2014). High-temperature EBPR process: The performance, analysis of PAOs and GAOs and the fine-scale population study of *Candidatus “Accumulibacter phosphatis”*. *Water Research*, 64, 102–112. <https://doi.org/10.1016/j.watres.2014.06.038>
- Ong, Y. H., Chua, A. S. M., Huang, Y. T., Ngoh, G. C., & You, S. J. (2016). The microbial community in a high-temperature enhanced biological phosphorus removal (EBPR) process. *Sustainable Environment Research*, 26(1), 14–19. <https://doi.org/10.1016/j.serj.2016.04.001>
- Onnis-Hayden, A., Srinivasan, V., Tooker, N. B., Li, G., Wang, D., Barnard, J. L., Bott, C., Dombrowski, P., Schauer, P., Menniti, A., Shaw, A., Stinson, B., Stevens, G., Dunlap, P., Takács, I., McQuarrie, J., Phillips, H., Lambrecht, A., Analla, H., ... Gu, A. Z. (2020). Survey of full-scale sidestream enhanced biological phosphorus removal (S2EBPR) systems and comparison with conventional EBPRs in North America: Process stability, kinetics, and microbial populations. *Water Environment Research*, 92(3), 403–417. <https://doi.org/10.1002/wer.1198>
- Otieno, J., Kowal, P., & Maćkonia, J. (2022). The Occurrence and Role of Tetrasphaera in Enhanced Biological Phosphorus Removal Systems. *Water*, 14(21), Article 21. <https://doi.org/10.3390/w14213428>
- Owodunni, A. A., Ismail, S., Kurniawan, S. B., Ahmad, A., Imron, M. F., & Abdullah, S. R. S. (2023). A review on revolutionary technique for phosphate removal in wastewater using

- green coagulant. *Journal of Water Process Engineering*, 52, 103573. <https://doi.org/10.1016/j.jwpe.2023.103573>
- Pan, K., Guo, T., Liao, H., Huang, Z., & Li, J. (2024). Nitrous oxide emissions from aerobic granular sludge: A review. *Journal of Cleaner Production*, 434, 139990. <https://doi.org/10.1016/j.jclepro.2023.139990>
- Park, T., Ampunan, V., Lee, S., & Chung, E. (2016). Chemical behavior of different species of phosphorus in coagulation. *Chemosphere*, 144, 2264–2269. <https://doi.org/10.1016/j.chemosphere.2015.10.131>
- Pester, M., Rattei, T., Flechl, S., Gröngröft, A., Richter, A., Overmann, J., Reinhold-Hurek, B., Loy, A., & Wagner, M. (2012). AmoA-based consensus phylogeny of ammonia-oxidizing archaea and deep sequencing of amoA genes from soils of four different geographic regions. *Environmental Microbiology*, 14(2), 525–539. <https://doi.org/10.1111/j.1462-2920.2011.02666.x>
- Petriglieri, F., Singleton, C., Peces, M., Petersen, J. F., Nierychlo, M., & Nielsen, P. H. (2021). ‘Candidatus Dechloromonas phosphoritropha’ and ‘Ca. D. phosphorivorans’, novel polyphosphate accumulating organisms abundant in wastewater treatment systems. *The ISME Journal*, 15(12), 3605–3614. <https://doi.org/10.1038/s41396-021-01029-2>
- Poh, P., Ong, Y. H., Arumugam, K., Nittami, T., Yeoh, H. K., Bessarab, I., William, R., & Chua, A. (2021). Tropical-based EBPR Process: The Long-Term Stability, Microbial Community and Its Response Towards Temperature Stress. *Water Environment Research*, 93. <https://doi.org/10.1002/wer.1611>
- Preisner, M. (2020). Surface Water Pollution by Untreated Municipal Wastewater Discharge Due to a Sewer Failure. *Environmental Processes*, 7(3), 767–780. <https://doi.org/10.1007/s40710-020-00452-5>
- Preisner, M. (2023). Chapter 19—Phosphorus-driven eutrophication mitigation strategies. In M. N. Vara Prasad & M. Smol (Eds.), *Sustainable and Circular Management of Resources and Waste Towards a Green Deal* (pp. 257–268). Elsevier. <https://doi.org/10.1016/B978-0-323-95278-1.00013-9>

- Puig, S., Coma, M., Monclús, H., van Loosdrecht, M. C. M., Colprim, J., & Balaguer, M. D. (2008). Selection between alcohols and volatile fatty acids as external carbon sources for EBPR. *Water Research*, *42*(3), 557–566. <https://doi.org/10.1016/j.watres.2007.07.050>
- Qin, L., Wang, D., Zhang, Z., Li, X., Chai, G., Lin, Y., Liu, C., Cao, R., Song, Y., Meng, H., Wang, Z., Wang, H., Jiang, C., Guo, Y., Li, J., & Zheng, X. (2023). Impact of Dissolved Oxygen on the Performance and Microbial Dynamics in Side-Stream Activated Sludge Hydrolysis Process. *Water*, *15*(11), Article 11. <https://doi.org/10.3390/w15111977>
- Qiu, G., Law, Y., Zuniga-Montanez, R., Deng, X., Lu, Y., Roy, S., Thi, S. S., Hoon, H. Y., Nguyen, T. Q. N., Eganathan, K., Liu, X., Nielsen, P. H., Williams, R. B. H., & Wuertz, S. (2022). Global warming readiness: Feasibility of enhanced biological phosphorus removal at 35 °C. *Water Research*, *216*, 118301. <https://doi.org/10.1016/j.watres.2022.118301>
- Qiu, G., Zuniga-Montanez, R., Law, Y., Thi, S. S., Nguyen, T. Q. N., Eganathan, K., Liu, X., Nielsen, P. H., Williams, R. B. H., & Wuertz, S. (2019). Polyphosphate-accumulating organisms in full-scale tropical wastewater treatment plants use diverse carbon sources. *Water Research*, *149*, 496–510. <https://doi.org/10.1016/j.watres.2018.11.011>
- Ren, L., Wang, P., Wang, C., Chen, J., Hou, J., & Qian, J. (2017). Algal growth and utilization of phosphorus studied by combined mono-culture and co-culture experiments. *Environmental Pollution*, *220*, 274–285. <https://doi.org/10.1016/j.envpol.2016.09.061>
- Rey-Martínez, N., Merdan, G., Guisasola, A., & Baeza, J. (2021). Nitrite and nitrate inhibition thresholds for a glutamate-fed bio-P sludge. *Chemosphere*, *283*, 131173. <https://doi.org/10.1016/j.chemosphere.2021.131173>
- Ribera-Guardia, A., Marques, R., Arangio, C., Carvalheira, M., Oehmen, A., & Pijuan, M. (2016). Distinctive denitrifying capabilities lead to differences in N₂O production by denitrifying polyphosphate accumulating organisms and denitrifying glycogen accumulating organisms. *Bioresource Technology*, *219*, 106–113. <https://doi.org/10.1016/j.biortech.2016.07.092>
- Rosas-Echeverría, K., Fall, C., Gutiérrez-Segura, E., Romero-Camacho, M. P., & Ba, K. M. (2023). Mechanisms of persistence and impact of ordinary heterotrophic organisms in aerobic granular sludge. *Bioresource Technology*, *384*, 129346. <https://doi.org/10.1016/j.biortech.2023.129346>

- Roy, S., Guanglei, Q., Zuniga-Montanez, R., Williams, R. B., & Wuertz, S. (2021). Recent advances in understanding the ecophysiology of enhanced biological phosphorus removal. *Current Opinion in Biotechnology*, 67, 166–174. <https://doi.org/10.1016/j.copbio.2021.01.011>
- Roy, S., Petersen, J. F., Müller, S., Kondrotaite, Z., van Loosdrecht, M., Wintgens, T., & Nielsen, P. H. (2025). Wastewater biorefineries: Exploring biological phosphorus removal and integrated recovery solutions. *Current Opinion in Biotechnology*, 92, 103266. <https://doi.org/10.1016/j.copbio.2025.103266>
- Rubio-Rincón, F. J., Lopez-Vazquez, C. M., Welles, L., van Loosdrecht, M. C. M., & Brdjanovic, D. (2017). Cooperation between *Candidatus* Competibacter and *Candidatus* Accumulibacter clade I, in denitrification and phosphate removal processes. *Water Research*, 120, 156–164. <https://doi.org/10.1016/j.watres.2017.05.001>
- Rubio-Rincón, F. J., Weissbrodt, D. G., Lopez-Vazquez, C. M., Welles, L., Abbas, B., Albertsen, M., Nielsen, P. H., van Loosdrecht, M. C. M., & Brdjanovic, D. (2019). “*Candidatus* Accumulibacter delftensis”: A clade IC novel polyphosphate-accumulating organism without denitrifying activity on nitrate. *Water Research*, 161, 136–151. <https://doi.org/10.1016/j.watres.2019.03.053>
- Ruzhitskaya, O., & Gogina, E. (2017). Methods for Removing of Phosphates from Wastewater. *MATEC Web of Conferences*, 106, 07006. <https://doi.org/10.1051/mateconf/201710607006>
- Saito, T., Brdjanovic, D., & Van Loosdrecht, M. C. M. (2004). Effect of nitrite on phosphate uptake by phosphate accumulating organisms. *Water Research*, 38(17), 3760–3768. Scopus. <https://doi.org/10.1016/j.watres.2004.05.023>
- Sayi-Ucar, N., Sarioglu, M., Insel, G., Cokgor, E. U., Orhon, D., & van Loosdrecht, M. C. M. (2015). Long-term study on the impact of temperature on enhanced biological phosphorus and nitrogen removal in membrane bioreactor. *Water Research*, 84, 8–17. <https://doi.org/10.1016/j.watres.2015.06.054>
- Schuler, A. J., & Jenkins, D. (2002). Effects of pH on enhanced biological phosphorus removal metabolisms. *Water Science and Technology*, 46(4–5), 171–178. <https://doi.org/10.2166/WST.2002.0579>

- Schulthess, R. v., Kühni, M., & Gujer, W. (1995). Release of nitric and nitrous oxides from denitrifying activated sludge. *Water Research*, 29(1), 215–226. [https://doi.org/10.1016/0043-1354\(94\)E0108-I](https://doi.org/10.1016/0043-1354(94)E0108-I)
- Serralta, J., Ferrer, J., Borrás, L., & Seco, A. (2006). Effect of pH on biological phosphorus uptake. *Biotechnology and Bioengineering*, 95(5), 875–882. <https://doi.org/10.1002/bit.21040>
- Seviour, R. J., & McIlroy, S. (2008). The microbiology of phosphorus removal in activated sludge processes-the current state of play. *The Journal of Microbiology*, 46(2), 115–124. <https://doi.org/10.1007/s12275-008-0051-0>
- Shang, Z., Cai, C., Guo, Y., Huang, X., Peng, K., Guo, R., Wei, Z., Wu, C., Cheng, S., Liao, Y., Hung, C.-Y., & Liu, J. (2024). Direct and indirect monitoring methods for nitrous oxide emissions in full-scale wastewater treatment plants: A critical review. *Journal of Environmental Management*, 358, 120842. <https://doi.org/10.1016/j.jenvman.2024.120842>
- Shen, N., Chen, Y., & Zhou, Y. (2017). Multi-cycle operation of enhanced biological phosphorus removal (EBPR) with different carbon sources under high temperature. *Water Research*, 114, 308–315. <https://doi.org/10.1016/j.watres.2017.02.051>
- Shen, N., & Zhou, Y. (2016). Enhanced biological phosphorus removal with different carbon sources. *Applied Microbiology and Biotechnology*, 100(11), 4735–4745. <https://doi.org/10.1007/s00253-016-7518-4>
- Shoji, T., Satoh, H., & Mino, T. (2003). Quantitative estimation of the role of denitrifying phosphate accumulating organisms in nutrient removal. *Water Science and Technology*, 47(11), 23–29. <https://doi.org/10.2166/wst.2003.0582>
- Sin, G., Niville, K., Bachis, G., Jiang, T., Nopens, I., Van Hulle, S., & Vanrolleghem, P. A. (2008). Nitrite effect on the phosphorus uptake activity of phosphate accumulating organisms (PAOs) in pilot-scale SBR and MBR reactors. *Water SA*, 34(2), 249–260. Scopus. <https://doi.org/10.4314/wsa.v34i2.183646>
- Smol, M., Adam, C., & Preisner, M. (2020). Circular economy model framework in the European water and wastewater sector. *Journal of Material Cycles and Waste Management*, 22(3), 682–697. <https://doi.org/10.1007/s10163-019-00960-z>

- Smol, M., Kulczycka, J., & Kowalski, Z. (2016). Sewage sludge ash (SSA) from large and small incineration plants as a potential source of phosphorus – Polish case study. *Journal of Environmental Management*, 184. <https://doi.org/10.1016/j.jenvman.2016.10.035>
- Smolders, G. J. F., van der Meij, J., van Loosdrecht, M. C. M., & Heijnen, J. J. (1994). Model of the anaerobic metabolism of the biological phosphorus removal process: Stoichiometry and pH influence. *Biotechnology and Bioengineering*, 43(6), 461–470. <https://doi.org/10.1002/bit.260430605>
- Śniatała, B., Al-Hazmi, H. E., Sobotka, D., Zhai, J., & Małkinia, J. (2024). Advancing sustainable wastewater management: A comprehensive review of nutrient recovery products and their applications. *Science of The Total Environment*, 937, 173446. <https://doi.org/10.1016/j.scitotenv.2024.173446>
- Solís, B., Guisasola, A., Pijuan, M., Corominas, L., & Baeza, J. A. (2022). Systematic calibration of N₂O emissions from a full-scale WWTP including a tracer test and a global sensitivity approach. *Chemical Engineering Journal*, 435, 134733. <https://doi.org/10.1016/j.cej.2022.134733>
- Song, X., Yu, D., Qiu, Y., Qiu, C., Xu, L., Zhao, J., & Wang, X. (2022). Unexpected phosphorous removal in a *Candidatus_Cometibacter* and *Defluviicoccus* dominated reactor. *Bioresource Technology*, 345, 126540. <https://doi.org/10.1016/j.biortech.2021.126540>
- Srinath, E. G., Sastry, C. A., & Pillai, S. C. (1959). Rapid removal of phosphorus from sewage by activated sludge. *Experientia*, 15, 339–340. <https://doi.org/10.1007/BF02159818>
- Stewart, R. D., Myers, K. S., Amstadt, C., Seib, M., McMahon, K. D., & Noguera, D. R. (2024). Refinement of the “*Candidatus Accumulibacter*” genus based on metagenomic analysis of biological nutrient removal (BNR) pilot-scale plants operated with reduced aeration. *mSystems*, 9(3), e01188-23. <https://doi.org/10.1128/msystems.01188-23>
- Stokholm-Bjerregaard, M., McIlroy, S. J., Nierychlo, M., Karst, S. M., Albertsen, M., & Nielsen, P. H. (2017). A Critical Assessment of the Microorganisms Proposed to be Important to Enhanced Biological Phosphorus Removal in Full-Scale Wastewater Treatment Systems. *Frontiers in Microbiology*, 8, 718. <https://doi.org/10.3389/fmicb.2017.00718>
- Sun, H., Zhang, X., Zhang, F., Yang, H., Lu, J., Ge, S., Li, X., & Zhang, W. (2021). *Tetrasphaera*, rather than *Candidatus Accumulibacter* as performance indicator of free ammonia

- inhibition during the enhanced biological phosphorus removal processes. *Journal of Environmental Chemical Engineering*, 9(5), 106219. <https://doi.org/10.1016/j.jece.2021.106219>
- Swinarski, M., Makinia, J., Stensel, H. d., Czerwionka, K., & Drewnowski, J. (2012). Modeling External Carbon Addition in Biological Nutrient Removal Processes with an Extension of the International Water Association Activated Sludge Model. *Water Environment Research*, 84(8), 646–655. <https://doi.org/10.2175/106143012X13373550426670>
- Tang, Y., Wen, Q., & Chen, Z. (2023). Simultaneous removal of nitrogen and phosphorus nutrients from secondary effluent by magnetic resin containing two types of quaternary ammonium adsorption sites: Preparation, characterization, and application. *Chemical Engineering Journal*, 477, 147137. <https://doi.org/10.1016/j.cej.2023.147137>
- Tchobanoglous, G., & Burton, F. L. (with Metcalf & Eddy). (1991). *Wastewater engineering: Treatment, disposal, and reuse* (3rd ed). McGraw-Hill.
- Tian, W., Li, W., Zhang, H., & Yang, Z. (2010). Affecting factors and control strategies of the competition of phosphorus accumulating organisms (PAO) and glycogen accumulating organisms (GAO) in enhanced biological phosphorus removal. *2010 The 2nd Conference on Environmental Science and Information Application Technology*, 1, 626–628. <https://doi.org/10.1109/ESIAT.2010.5568854>
- Tian, Y., Chen, H., Chen, L., Deng, X., Hu, Z., Wang, C., Wei, C., Qiu, G., & Wuertz, S. (2022). Glycine adversely affects enhanced biological phosphorus removal. *Water Research*, 209, 117894. <https://doi.org/10.1016/j.watres.2021.117894>
- Tooker, N., Li, G., Bott, C., Dombrowski, P., Schauer, P., Menniti, A., Shaw, A., Barnard, J., Stinson, B., Stevens, G., Dunlap, P., Takács, I., Phillips, H., Analla, H., Russell, A., Ellsworth, A., Mcquarrie, J., Carson, K., Onnis-Hayden, A., & Gu, A. (2017). Rethinking and Reforming Enhanced Biological Phosphorus Removal (EBPR) Strategy – Concepts and Mechanisms of Side-Stream EBPR. *Proceedings of the Water Environment Federation*, 2017, 2547–2564. <https://doi.org/10.2175/193864717822153076>
- Tsertou, E., Caluwé, M., Goettert, D., Goossens, K., Seguel Suazo, K., Vanherck, C., & Dries, J. (2024). Impact of low and high temperatures on aerobic granular sludge treatment of

- industrial wastewater. *Water Science & Technology*, 89.
<https://doi.org/10.2166/wst.2024.024>
- Tuszynska, A., Kaszubowska, M., Kowal, P., Ciesielski, S., & Makinia, J. (2019). The metabolic activity of denitrifying microorganisms accumulating polyphosphate in response to addition of fusel oil. *Bioprocess and Biosystems Engineering*, 42(1), 143–155.
<https://doi.org/10.1007/s00449-018-2022-0>
- Valenzuela, E. I., Ortiz-Zúñiga, M. F., Carrillo-Reyes, J., Moreno-Andrade, I., & Quijano, G. (2021). Continuous anaerobic oxidation of methane: Impact of semi-continuous liquid operation and nitrate load on N₂O production and microbial community. *Chemosphere*, 278, 130441. <https://doi.org/10.1016/j.chemosphere.2021.130441>
- Vargas, M., Guisasola, A., Artigues, A., Casas, C., & Baeza, J. A. (2011). Comparison of a nitrite-based anaerobic–anoxic EBPR system with propionate or acetate as electron donors. *Process Biochemistry*, 46(3), 714–720. <https://doi.org/10.1016/j.procbio.2010.11.018>
- Venhauerova, P., Drahota, P., Strnad, L., & Matoušková, Š. (2022). Effects of a point source of phosphorus on the arsenic mobility and transport in a small fluvial system. *Environmental Pollution*, 315, 120477. <https://doi.org/10.1016/j.envpol.2022.120477>
- Vieira, A., Ribera-Guardia, A., Marques, R., Barreto Crespo, M. T., Oehmen, A., & Carvalho, G. (2018). The link between the microbial ecology, gene expression, and biokinetics of denitrifying polyphosphate-accumulating systems under different electron acceptor combinations. *Applied Microbiology and Biotechnology*, 102(15), 6725–6737.
<https://doi.org/10.1007/s00253-018-9077-3>
- Vlekke, G. J. F. M., Comeau, Y., & Oldham, W. K. (1988). Biological phosphate removal from wastewater with oxygen or nitrate in sequencing batch reactors. *Environmental Technology Letters*, 9(8), 791–796. <https://doi.org/10.1080/09593338809384634>
- Vollenweider, R. A. (1992). Coastal marine eutrophication: Principles and control. In R. A. Vollenweider, R. Marchetti, & R. Viviani (Eds.), *Marine Coastal Eutrophication* (pp. 1–20). Elsevier. <https://doi.org/10.1016/B978-0-444-89990-3.50011-0>
- Wagner, M., Amann, R., Kämpfer, P., Assmus, B., Hartmann, A., Hutzler, P., Springer, N., & Schleifer, K.-H. (1994). Identification and *in situ* Detection of Gram-negative Filamentous

- Bacteria in Activated Sludge. *Systematic and Applied Microbiology*, 17(3), 405–417.
[https://doi.org/10.1016/S0723-2020\(11\)80058-5](https://doi.org/10.1016/S0723-2020(11)80058-5)
- Wang, D., Tooker, N., Srinivasan, V., Li, G., Fernandez, L., Schauer, P., Menniti, A., Maher, C., Bott, C., Dombrowski, P., Barnard, J., Onnis-Hayden, A., & Gu, A. (2019). Side-stream enhanced biological phosphorus removal (S2EBPR) process improves system performance—A full-scale comparative study. *Water Research*, 167, 115109.
<https://doi.org/10.1016/j.watres.2019.115109>
- Wang, D., Zheng, W., Liao, D., Li, X., Yang, Q., & Zeng, G. (2013). Effect of initial pH control on biological phosphorus removal induced by the aerobic/extended-idle regime. *Chemosphere*, 90(8), 2279–2287. <https://doi.org/10.1016/j.chemosphere.2012.10.086>
- Wang, H., Chen, N., Feng, C., & Deng, Y. (2021). Insights into heterotrophic denitrification diversity in wastewater treatment systems: Progress and future prospects based on different carbon sources. *Science of The Total Environment*, 780, 146521.
<https://doi.org/10.1016/j.scitotenv.2021.146521>
- Wang, S., Li, Z., Wang, D., Li, Y., & Sun, L. (2020). Performance and population structure of two carbon sources granular enhanced biological phosphorus removal systems at low temperature. *Bioresource Technology*, 300, 122683.
<https://doi.org/10.1016/j.biortech.2019.122683>
- Wang, X., Zhang, G., Ding, A., Xie, E., Tan, Q., Xing, Y., Wu, H., Tian, Q., Zhang, Y., & Zheng, L. (2024). Distinctive species interaction patterns under high nitrite stress shape inefficient denitrifying phosphorus removal performance. *Bioresource Technology*, 394, 130269.
<https://doi.org/10.1016/j.biortech.2023.130269>
- Wang, X., Zhao, J., Yu, D., Chen, G., Du, S., Zhen, J., & Yuan, M. (2019). Stable nitrite accumulation and phosphorous removal from nitrate and municipal wastewaters in a combined process of endogenous partial denitrification and denitrifying phosphorus removal (EPDPR). *Chemical Engineering Journal*, 355, 560–571.
<https://doi.org/10.1016/j.cej.2018.08.165>
- Wang, Y., Jiang, F., Zhang, Z., Xing, M., Lu, Z., Wu, M., Yang, J., & Peng, Y. (2010). The long-term effect of carbon source on the competition between polyphosphorus accumulating organisms and glycogen accumulating organism in a continuous plug-flow

- anaerobic/aerobic (A/O) process. *Bioresource Technology*, 101(1), 98–104.
<https://doi.org/10.1016/j.biortech.2009.07.085>
- Wang, Z., Meng, Y., Fan, T., Du, Y., Tang, J., & Fan, S. (2015). Phosphorus removal and N₂O production in anaerobic/anoxic denitrifying phosphorus removal process: Long-term impact of influent phosphorus concentration. *Bioresource Technology*, 179, 585–594.
<https://doi.org/10.1016/j.biortech.2014.12.016>
- Weissbrodt, D. G., Holliger, C., & Morgenroth, E. (2017). Modeling hydraulic transport and anaerobic uptake by PAOs and GAOs during wastewater feeding in EBPR granular sludge reactors. *Biotechnology and Bioengineering*, 114(8), 1688–1702.
<https://doi.org/10.1002/bit.26295>
- Winkler, M.-K. H., Bassin, J. P., Kleerebezem, R., de Bruin, L. M. M., van den Brand, T. P. H., & van Loosdrecht, M. C. M. (2011). Selective sludge removal in a segregated aerobic granular biomass system as a strategy to control PAO–GAO competition at high temperatures. *Water Research*, 45(11), 3291–3299.
<https://doi.org/10.1016/j.watres.2011.03.024>
- Wisniewski, K., Kowalski, M., & Makinia, J. (2018). Modeling nitrous oxide production by a denitrifying-enhanced biologically phosphorus removing (EBPR) activated sludge in the presence of different carbon sources and electron acceptors. *Water Research*, 142, 55–64.
<https://doi.org/10.1016/j.watres.2018.05.041>
- Wu, L., Ning, D., Zhang, B., Li, Y., Zhang, P., Shan, X., Zhang, Q., Brown, M. R., Li, Z., Van Nostrand, J. D., Ling, F., Xiao, N., Zhang, Y., Vierheilig, J., Wells, G. F., Yang, Y., Deng, Y., Tu, Q., Wang, A., ... Zhou, J. (2019). Global diversity and biogeography of bacterial communities in wastewater treatment plants. *Nature Microbiology*, 4(7), 1183–1195.
<https://doi.org/10.1038/s41564-019-0426-5>
- Wu, Z., Ji, S., Li, Y.-Y., & Liu, J. (2023). A review of iron use and recycling in municipal wastewater treatment plants and a novel applicable integrated process. *Bioresource Technology*, 379, 129037. <https://doi.org/10.1016/j.biortech.2023.129037>
- Xie, T., Mo, C., Li, X., Zhang, J., An, H., Yang, Q., Wang, D., Zhao, J., Zhong, Y., & Zeng, G. (2017). Effects of different ratios of glucose to acetate on phosphorus removal and microbial community of enhanced biological phosphorus removal (EBPR) system.

- Environmental Science and Pollution Research International*, 24(5), 4494–4505.
<https://doi.org/10.1007/s11356-016-7860-1>
- Xie, X., Deng, X., Chen, L., Yuan, J., Chen, H., Wei, C., Liu, X., Wuertz, S., & Qiu, G. (2024). Integrated genomics provides insights into the evolution of the polyphosphate accumulation trait of *Ca. Accumulibacter*. *Environmental Science and Ecotechnology*, 20, 100353. <https://doi.org/10.1016/j.es.2023.100353>
- Yu, X., Tian, W., Deng, Y., Cai, Y., Wang, Y., Wang, Z., Li, J., & Ma, J. (2021). Nutrient removal and phosphorus recovery performance of an anaerobic side-stream extraction based enhanced biological phosphorus removal subjected to low dissolved oxygen. *Journal of Water Process Engineering*, 42, 101861. <https://doi.org/10.1016/j.jwpe.2020.101861>
- Yu, Z., Xu, S., Wang, P., Liu, D., & Lu, H. (2023). Phosphorus Removal and Storage Polymer Synthesis by Tetrasphaera-Related Bacteria with Different Carbon Sources. *ACS ES&T Water*, 3(5), 1374–1384. <https://doi.org/10.1021/acsestwater.3c00046>
- Zekker, I., Mandel, A., Rikmann, E., Jaagura, M., Salmar, S., Ghangrekar, M. M., & Tenno, T. (2021). Ameliorating effect of nitrate on nitrite inhibition for denitrifying P-accumulating organisms. *Science of The Total Environment*, 797, 149133. <https://doi.org/10.1016/j.scitotenv.2021.149133>
- Zeng, R. J., Saunders, A. M., Yuan, Z., Blackall, L. L., & Keller, J. (2003). Identification and comparison of aerobic and denitrifying polyphosphate-accumulating organisms. *Biotechnology and Bioengineering*, 83(2), 140–148. <https://doi.org/10.1002/bit.10652>
- Zeng, W., Li, B., Wang, X., Bai, X., & Peng, Y. (2016). Influence of nitrite accumulation on ‘*Candidatus Accumulibacter*’ population structure and enhanced biological phosphorus removal from municipal wastewater. *Chemosphere*, 144, 1018–1025. <https://doi.org/10.1016/j.chemosphere.2015.08.064>
- Zeng, W., Li, B., Yang, Y., Wang, X., Li, L., & Peng, Y. (2014). Impact of nitrite on aerobic phosphorus uptake by poly-phosphate accumulating organisms in enhanced biological phosphorus removal sludges. *Bioprocess and Biosystems Engineering*, 37(2), 277–287. Scopus. <https://doi.org/10.1007/s00449-013-0993-4>

- Zhang, B., Mao, W., Chen, S., & Wang, X. (2024). Characteristics and key driving factors of nitrous oxide emissions from a full-scale landfill leachate treatment system. *Science of The Total Environment*, 931, 172821. <https://doi.org/10.1016/j.scitotenv.2024.172821>
- Zhang, C., Guisasola, A., & Baeza, J. A. (2023). Exploring the stability of an A-stage-EBPR system for simultaneous biological removal of organic matter and phosphorus. *Chemosphere*, 313, 137576. <https://doi.org/10.1016/j.chemosphere.2022.137576>
- Zhang, J., Zeng, W., Meng, Q., Liu, H., Lu, S., & Peng, Y. (2023). Denitrifying phosphorus removal (DPR) performance and metabolic mechanisms of Tetrasphaera at long-term nitrite exposure. *Chemical Engineering Journal*, 475, 146249. <https://doi.org/10.1016/j.cej.2023.146249>
- Zhang, M., Wang, Y., Fan, Y., Liu, Y., Yu, M., He, C., & Wu, J. (2020). Bioaugmentation of low C/N ratio wastewater: Effect of acetate and propionate on nutrient removal, substrate transformation, and microbial community behavior. *Bioresource Technology*, 306, 122465. <https://doi.org/10.1016/j.biortech.2019.122465>
- Zhang, M., Yang, Q., Zhang, J., Wang, C., Wang, S., & Peng, Y. (2016). Enhancement of denitrifying phosphorus removal and microbial community of long-term operation in an anaerobic anoxic oxic–biological contact oxidation system. *Journal of Bioscience and Bioengineering*, 122(4), 456–466. <https://doi.org/10.1016/j.jbiosc.2016.03.019>
- Zhang, Y., & Kinyua, M. (2020). Identification and classification of the Tetrasphaera genus in enhanced biological phosphorus removal process: A review. *Reviews in Environmental Science and Bio/Technology*, 19, 1–17. <https://doi.org/10.1007/s11157-020-09549-7>
- Zhang, Y., Qiu, X., Luo, J., Li, H., How, S.-W., Wu, D., He, J., Cheng, Z., Gao, Y., & Lu, H. (2024). A review of the phosphorus removal of polyphosphate-accumulating organisms in natural and engineered systems. *Science of The Total Environment*, 912, 169103. <https://doi.org/10.1016/j.scitotenv.2023.169103>
- Zhao, W., Bi, X., Peng, Y., & Bai, M. (2022). Research advances of the phosphorus-accumulating organisms of Candidatus Accumulibacter, Dechloromonas and Tetrasphaera: Metabolic mechanisms, applications and influencing factors. *Chemosphere*, 307, 135675. <https://doi.org/10.1016/j.chemosphere.2022.135675>

- Zhao, Y., Zhu, Z., Chen, X., & Li, Y. (2024). Discovery of a novel potential polyphosphate accumulating organism without denitrifying phosphorus uptake function in an enhanced biological phosphorus removal process. *Science of The Total Environment*, *912*, 168952. <https://doi.org/10.1016/j.scitotenv.2023.168952>
- Zheng, X., Sun, P., Han, J., Song, Y., Hu, Z., Fan, H., & Lv, S. (2014). Inhibitory factors affecting the process of enhanced biological phosphorus removal (EBPR) – A mini-review. *Process Biochemistry*, *49*(12), 2207–2213. <https://doi.org/10.1016/j.procbio.2014.10.008>
- Zhou, Y., Ganda, L., Lim, M., Yuan, Z., & Ng, W. J. (2012). Response of poly-phosphate accumulating organisms to free nitrous acid inhibition under anoxic and aerobic conditions. *Bioresource Technology*, *116*, 340–347. Scopus. <https://doi.org/10.1016/j.biortech.2012.03.111>
- Zhu, G., Wang, X., Wang, S., Yu, L., Armanbek, G., Yu, J., Jiang, L., Yuan, D., Guo, Z., Zhang, H., Zheng, L., Schwark, L., Jetten, M. S. M., Yadav, A. K., & Zhu, Y.-G. (2022). Towards a more labor-saving way in microbial ammonium oxidation: A review on complete ammonia oxidization (comammox). *Science of The Total Environment*, *829*, 154590. <https://doi.org/10.1016/j.scitotenv.2022.154590>
- Zuthi, M. F. R., Guo, W. S., Ngo, H. H., Nghiem, L. D., & Hai, F. I. (2013). Enhanced biological phosphorus removal and its modeling for the activated sludge and membrane bioreactor processes. *Bioresource Technology*, *139*, 363–374. <https://doi.org/10.1016/J.BIORTECH.2013.04.038>

APPENDICES

The following appendices provide supplementary information to support the findings of this thesis. These include detailed raw and experimental data. All appendices are stored on the accompanying CD.

APPENDIX 1 : Raw data from batch experiments under **series I** - scenario 1.1: COD limiting conditions (COD:P ratio >2.5)

APPENDIX 2 : Raw data from batch experiments under **series I** - scenario 1.2: COD non-limiting conditions (COD:P ratio >2.5)

APPENDIX 3 : **Raw data from batch experiment with dynamics anoxic conditions**

Series II: Trial 1 (ST1)

- (a) Scenario 2.1: *Reference batch tests with nitrate (Reactor 1) and nitrite (Reactor 2)*
- (b) Scenario 2.2: *P₀₄⁻³ precipitated tests with nitrate (Reactor 1) and nitrite (Reactor 2)*
- (c) Scenario 2.3: *PHA depleted tests with nitrate (Reactor 1) and nitrite (Reactor 2)*

APPENDIX 4 : **Raw data from series batch experiment with dynamics anoxic conditions**

Series II: Trial 2 (ST2)

- (a) Scenario 2.1: *Reference batch tests with nitrate (Reactor 1) and nitrite (Reactor 2)*
- (b) Scenario 2.2: *P₀₄⁻³ precipitated tests with nitrate (Reactor 1) and nitrite (Reactor 2)*
- (c) Scenario 2.3: *PHA depleted tests with nitrate (Reactor 1) and nitrite (Reactor 2)*

APPENDIX 1 : Raw data from batch experiment under Series I - scenario 1.1: COD limiting conditions (COD:P ratio < 2.5)

(a) **Glucose vs acetate with nitrate (Series I, scenario 1.1)**

(i) Glucose with nitrate and PHA results

Glucose vs NO3(G.L.NO3)						
Time	NO ₃ -N	COD	PO ₄ -P	3PHB	3PHV	3PHB+3PHV
[h]	[mg N/dm ³]	[mg COD/dm ³]	[mg P/dm ³]	[mg /g DM]	[mg /g DM]	[mg /g DM]
0.0		151.0	1.5			
0.3		109.0	1.6	3.2	2.1	5.4
0.7		99.8	2.2	3.5	4.0	7.5
1.0		91.0	2.2	3.6	7.1	10.8
1.5		77.4	2.4	3.9	3.6	7.5
2.0		77.2	2.6	3.5	3.6	7.1
2.5		77.0	2.6	4.6	2.6	7.3
2.8	20.1	64.7	2.6			
3.0	19.4	64.7	2.6			
3.3	19.3					
3.5	19.2					
4.0	19.2	64.6	2.6			
4.5	18.5					
5.0	17.8					
5.5	17.0	64.6	2.6			
6.0						
6.5	16.3					
7.0	15.8	64.6	3.0			
8.0	14.1		3.1			
9.0	12.0	64.6	3.7			

(ii) Acetate with nitrate and PHA results

Acetate vs NO3 (A.L.NO3)						
Time	NO ₃ -N	COD	PO ₄ -P	3PHB	3PHV	3PHB+3PHV
[h]	[mg N/dm ³]	[mg COD/dm ³]	[mg P/dm ³]	[mg /g DM]	[mg /g DM]	[mg /g DM]
0.0		195.0	3.9			
0.3		144.0	14.1	10.1	2.6	12.7
0.7		102.0	20.0	13.2	3.8	17.0
1.0		85.0	24.0	14.4	3.0	17.4
1.5		71.0	25.0	13.4	3.4	16.9
2.0		67.5	25.7	11.5	3.0	14.5
2.5	21.7	64.6	25.9			
2.8	21.3	63.1	25.9			
3.0	19.6					
3.3	18.6					
3.5	18.3	62.6	25.5			
4.0	17.2					
4.5	16.4	61.8	23.5			
5.0	15.2					
6.0	14.5					
6.0	13.8	61.3	20.1			
6.5						
7.0						
8.0	12.3	61.3	17.6			
9.0		61.1	16.3			
10.0						

(b) Glucose vs acetate with nitrite (Series I, scenario 1.1)

(i) Glucose with nitrite and PHA results

(ii) Acetate with nitrite and PHA results

Glucose vs NO ₂ (G.L.NO ₂)						
ne	NO ₂ -N	COD	PO ₄ -P	3PHB	3PHV	3PHB+3PHV
i]	[mg N/dm ³]	[mg COD/dm ³]	[mg P/dm ³]	[mg /g DM]	[mg /g DM]	[mg /g DM]
0.0		200.0	3.5			
0.3		110.0	3.4	2.2	3,42	5,57
0.7		99.6	3.9	2.2	3,74	5,90
1.0		92.9	4.1	1.9	3,57	5,43
1.5		96.8	4.4	2.9	1,54	4,47
2.0		93.3	5.0	4.7	1,97	6,72
2.5		92.0	5.1	3.4	1,46	4,82
2.8	19.0	92.5	5.6	7.2	3,11	10,36
3.0	18.9	92.5	5.6			
3.3	18.8					
3.5	18.6					
4.0	18.1	88.8	5.4			
4.5	17.0					
5.0	16.7	87.9	6.1			
5.5						
6.0						
6.5	14.9	87.5	6.4			
7.0	14.5	86.6	7.5			
8.0	14.1	85.7	6.6			
9.0	13.7	84.8	6.8			

Acetate vs NO ₂ (A.L.NO ₂)			
Time	NO ₂ -N	COD	PO ₄ -P
[h]	[mg N/dm ³]	[mg COD/dm ³]	[mg P/dm ³]
0.0		198.0	4.9
0.3		121.0	12.7
0.7		106.0	18.9
1.0		87.3	20.1
1.5		84.9	23.4
2.0		82.5	23.2
2.5	19.0	81.5	23.0
2.8	18.9	81.2	22.3
3.0	18.8		
3.3	18.6		
3.5	18.1	81.2	21.0
4.0	17.0		
4.5	16.7	80.3	19.7
5.0			
5.5			
6.0	14.9	80.3	18.0
6.5	14.5	80.0	17.0
7.0	14.1	79.7	16.0
8.0	13.7	79.4	15.0
9.0	13.3	79.1	14.0

APPENDIX 2 : Raw data from batch experiment under Series I, scenario 1.2: COD non- limiting conditions (COD:P ratio >2.5)

a) Glucose vs acetate with nitrite (Series I, scenario 1.2)

(i) Glucose with nitrite and PHA results

Glucose vs NO2(G.nL.NO2)						
Time	NO2-N	COD	PO ₄ -P	3PHB	3PHV	3PHB+3PHV
[h]	[mg N/dm ³]	[mg COD/dm ³]	[mg P/dm ³]			
0.0		251.0	2.4			0.0
0.3			2.9	3.0	0.2	3.2
0.7		185.0	3.1			
1.0			3.2			
1.5		180.0	3.5	3.6	0.4	4.0
2.0			3.5			
2.5	25.1	176.0	3.6			
2.8	25.8	174.0	3.8	3.6	0.9	4.5
3.0						
3.3	25.0	169.0	4.2			
3.5						
4.0	24.7		4.6	3.0	1.6	4.6
4.5						
5.0	24.3	169.0	5.4			
5.5						
6.0	24.3		5.3	4.3	0.4	4.7
6.5						
7.0	24.3	135.0	6.4			
8.0	24.0		7.5			
9.0	23.5	124.0	6.9			

(ii) Acetate with nitrite

Acetate vs NO2(A.nL.NO2)			
Time	NO2-N	COD	PO ₄ -P
[h]	[mg N/dm ³]	[mg COD/dm ³]	[mg P/dm ³]
0.0		219.0	6.1
0.3		164.0	14.5
0.7		139.0	22.6
1.0		124.0	24.4
1.5		94.2	27.4
2.0		86.3	29.0
2.5	20.1	77.1	28.9
2.8	18.5	77.1	29.1
3.0	18.4		28.6
3.3	18.0	73.7	28.2
3.5	17.5		28.1
4.0	17.4	72.0	27.0
4.5			26.8
5.0	16.4	72.0	26.5
5.5	15.6		24.8
6.0	14.5	68.9	24.6
6.5	13.0		24.3
7.0	12.8	66.2	22.8
8.0	12.3	60.0	20.6
9.0			

b) *Glucose vs acetate with nitrate (Series I, scenario 1.2)*

(i) Glucose with nitrate

Glucose vs NO ₃ (G.n.L.NO ₃)			
Time	NO ₃ -N	COD	PO ₄ -P
[h]	[mg N/dm ³]	[mg COD/dm ³]	[mg P/dm ³]
0.0		291.0	3.1
0.3		244.0	3.3
0.7		233.0	3.6
1.0		225.0	3.7
1.5		208.0	3.9
2.0		201.0	4.0
2.5	24.5	185.0	4.2
2.8	24.6	183.0	4.2
3.0	23.6		4.3
3.3	24.2	176.0	4.3
3.5	24.1		4.3
4.0	23.6	136.0	4.4
4.5			
5.0	22.1	105.0	4.8
5.5			
6.0	22.6	62.1	4.9
6.5	21.1	61.0	4.5
7.0	20.2	56.0	4.1
8.0	18.9	55.9	3.2
9.0			

(ii) Acetate with nitrate and PHA results

Test 1A						
Acetate vs NO ₃ (A.n.L.NO ₃)						
e	NO ₃ -N	COD	PO ₄ -P	3PHB	3PHV	3PHB+3PHV
i0]	[mg N/dm ³]	[mg COD/dm ³]	[mg P/dm ³]			
0.0		270.0	3.0	4.2	0.7	4.9
0.3		234.0	12.5			
0.7		206.0	21.5			
1.0		192.0	26.4	40.9	6.7	47.6
1.5		168.0	28.3			
2.0		150.0	29.3			
2.5	20.6		31.0	64.8	10.6	75.4
2.8	19.8		29.9			
3.0	18.3	115.0	31.9			
3.3	17.7		32.5			
3.5	15.9		32.0	64.8	10.6	75.4
4.0	14.7		31.9			
4.5	11.9		32.7			
5.0	7.0	50.0	30.7			
5.5	4.1	23.0	29.0	64.8	10.6	75.4
6.0	2.0		24.7			
6.5	0.4		20.0	30.1	4.9	35.1
7.0						
8.0						
9.0						

c) *Acetate vs pulse- dosage nitrite (Series I, scenario 1.2)*

(i) Acetate with pulse dosage of nitrite and PHA results

Acetate vs NO ₂ - PULSE dosage (A.nLNO ₂)						
Time	NO ₂ -N	COD	PO ₄ -P	3PHB	3PHV	3PHB+3PHV
[h]	[mg N/dm ³]	[mg COD/dm ³]	[mg P/dm ³]			
0.0		212.0	1.5			0.0
0.3		159.0	9.2	4.2	1.1	5.3
0.7		139.0	18.2			
1.0		136.0	21.8			
1.5		132.0	23.9	49.0	5.0	54.0
2.0		124.0	25.4			
2.5	4.7	121.0	25.3			
2.8	4.0	112.0	25.6	90.2	7.2	97.4
3.0	3.1		26.1			
3.3	2.1	102.0	25.6			
3.5	1.2		25.8			
4.0	4.6	88.8	25.2	88.3	8.7	97.0
4.5	2.6		25.9			
5.0	0.8	76.3	23.9	77.8	7.0	84.9
5.5	4.8		23.5			
6.0	3.1	62.9	22.8	78.2	6.8	84.9
6.5	2.2		21.6			
7.0	1.2	57.8	21.0			
8.0	0.0		20.2	82.7	7.5	90.2
9.0						

APPENDIX 3 : Raw data from Series II batch experiments with dynamics anoxic conditions
Trial 1 (ST1):

 a) **Scenario 2.1: Reference batch test with nitrate (Reactor 1) and nitrite (Reactor 2)**
(Series II , ST1, scenario 2.1)

CLASSICAL R1 (NO3)			
Time	NO ₃ -N	COD	PO ₄ -P
[h]	[mg N/dm ³]	[mg COD/dm ³]	[mg N/dm ³]
0.0		145.0	3.3
0.3		114.0	17.4
0.7		90.3	22.6
1.0		89.9	22.7
1.5		87.7	23.0
2.0		87.4	23.8
2.5	20.6	87.9	23.6
2.8	18.0	90.7	22.1
3.0	16.2	88.4	20.6
3.3			
3.5			
4.0	13.5	86.5	19.3
4.5			
5.0	11.3	81.4	17.6
5.5			
6.0	9.6	81.8	12.7
6.5			
7.0	8.0	52.2	10.9
8.0	6.4	47.8	9.0
9.0			
10.0			

CLASSICAL R2 (NO2)			
Time	NO ₂ -N	COD	PO ₄ -P
[h]	[mg N/dm ³]	[mg COD/dm ³]	[mg N/dm ³]
0.0		145.0	3.3
0.3		114.0	17.4
0.7		90.3	22.6
1.0		89.9	22.7
1.5		87.7	23.0
2.0		87.4	23.8
2.5	20.0	86.5	23.6
2.8	16.3	85.2	21.0
3.0	13.2	84.2	19.3
3.3			
3.5			
4.0	9.6	70.7	16.7
4.5			
5.0	5.8	69.9	15.9
5.5			
6.0	3.3	63.6	14.0
6.5			
7.0	0.9	56.7	13.0
8.0	0.5	59.7	11.7
9.0			
10.0			

b) **Scenario 2.2:** PO_4^{3-} precipitated tests with nitrate (Reactor 1) and nitrite (Reactor 2)

(Series II, ST1, scenario 2.2)

No -PO4 NO3(NO3)			
Time	NO ₃ -N	COD	PO ₄ -P
[h]	[mg N/dm ³]	[mg COD/dm ³]	[mg N/dm ³]
0.0		145.0	3.3
0.3		114.0	17.4
0.7		90.3	22.6
1.0		89.9	22.7
1.5		87.7	23.0
2.0		87.4	23.8
2.5	21.0	62.3	23.6
2.8	19.6	61.5	
3.0	18.9	60.1	
3.3			
3.5			
4.0	18.2	59.9	
4.5			
5.0	17.0		
5.5		58.0	
6.0	16.6	106.0	
6.5	16.1	108.0	
7.0	17.5	136.0	
8.0	16.2	111.0	
9.0	14.7	108.0	
10.0			

No PO4 (NO2)			
Time	NO ₂ -N	COD	PO ₄ -P
[h]	[mg N/dm ³]	[mg COD/dm ³]	[mg N/dm ³]
0.0		145.0	3.3
0.3		114.0	17.4
0.7		90.3	22.6
1.0		89.9	22.7
1.5		87.7	23.0
2.0		87.4	23.8
2.5	20.1	77.7	23.6
2.8	19.3	76.0	
3.0	18.0	70.0	
3.3			
3.5			
4.0	16.5	69.0	
4.5			
5.0	17.0		
5.5		67.0	
6.0	16.5	129.0	
6.5	15.8	131.0	
7.0	15.6	151.0	
8.0	14.9	140.0	
9.0	13.0	135.0	

c) **Scenario 2.3:** PHA depleted tests with nitrate (Reactor 1) and nitrite (Reactor 2)

(Series II, ST1, scenario 2.3)

No -PHA NO3			
Time	NO ₂ -N	COD	PO ₄ -P
[h]	[mg N/dm ³]	[mg COD/dm ³]	[mg N/dm ³]
0.0		145.0	3.3
0.3		114.0	17.4
0.7		90.3	22.6
1.0		89.9	22.7
1.5		87.7	23.0
2.0		85.0	23.8
2.5	17.6	63.0	23.6
2.8	15.4	62.1	
3.0	16.8	61.0	
3.3			
3.5			
4.0	16.2	60.7	
4.5			
5.0	16.5	60.0	
5.5		60.0	
6.0	17.3	135.0	
6.5	17.2	113.0	
7.0	17.0	108.0	
8.0	15.6	108.0	
9.0	15.5	102.0	

No -PHA NO ₂ (NO ₂)			
Time	NO ₃ -N	COD	PO ₄ -P
[h]	[mg N/dm ³]	[mg COD/dm ³]	[mg N/dm ³]
0.0		145.0	3.3
0.3		114.0	17.4
0.7		90.3	22.6
1.0		89.9	22.7
1.5		87.7	23.0
2.0		87.4	23.8
2.5	16.2	76.2	23.8
2.8	16.1	79.2	
3.0	15.6	76.7	
3.3			
3.5			
4.0	15.2	83.6	
4.5			
5.0	14.9	86.4	
5.5		86.4	
6.0	15.9	159.0	
6.5	15.0	157.0	
7.0	15.1	147.0	
8.0	16.1	159.0	
9.0	15.4	155.0	
10.0			

APPENDIX 4 : Raw data from series II batch experiment with dynamics anoxic conditions
Trial 2 (ST2)

d) **Scenario 2.1:** Reference batch tests with nitrate (Reactor 1) and nitrite (Reactor 2)

(Series II , ST2, scenario 2.1)

CLASSICAL R1 (NO3)			
Time	NO ₃ -N	COD	PO ₄ -P
[h]	[mg N/dm ³]	[mg COD/d m ³]	[mg P/dm ³]
0.0		92.6	2.5
0.3		65.6	17.0
0.7		45.4	23.1
1.0		37.9	24.8
1.5		35.0	24.6
2.0		30.1	24.2
2.5	19.5	27.4	24.2
2.8	18.1	26.5	23.0
3.0	16.4	25.9	21.9
3.3			
3.5			
4.0	14.6	23.6	20.0
4.5			
5.0	13.0	21.8	19.1
5.5			
6.0	12.6	21.5	17.0
6.5			
7.0	9.9	20.8	14.5
8.0	7.3	19.5	12.4
9.0			
10.0			

CLASSICAL R2 (NO2)			
Time	NO ₂ -N	COD	PO ₄ -P
[h]	[mg N/dm ³]	[mg COD/d m ³]	[mg P/dm ³]
0.0		92.6	2.5
0.3		65.6	17.0
0.7		45.4	23.1
1.0		37.9	24.8
1.5		35.0	24.6
2.0		30.1	24.2
2.5	18.7	27.4	24.2
2.8	17.5	28.8	24.0
3.0	16.0	27.0	23.0
3.3			
3.5			
4.0	14.5	26.3	21.0
4.5			
5.0	10.0	25.8	19.0
5.5	9.0		
6.0	7.5	24.0	16.0
6.5			
7.0	7.0	21.4	14.0
8.0	6.0	20.1	12.0
9.0			
10.0			

a) **Scenario 2.2:** PO_4^{3-} precipitated test with nitrate (Reactor 1) and nitrite (Reactor 2)

(Series II, ST2, scenario 2.2)

No -PO4 NO3(NO3)			
Time	NO ₃ -N	COD	PO ₄ -P
[h]	[mg N/dm ³]	[mg COD/d m ³]	[mg P/dm ³]
0.0		92.6	2.5
0.3		65.6	17.0
0.7		45.4	23.1
1.0		37.9	24.8
1.5		35.0	24.6
2.0		30.1	24.2
2.5	21.0	27.4	24.2
2.8	20.6	68.7	
3.0	20.2	87.5	
3.3			
3.5		88.0	
4.0	19.4	98.0	
4.5			
5.0	17.9		
5.5		145.0	
6.0	17.7	195.0	
6.5	17.6	214.0	
7.0	17.5	215.0	
8.0	16.9	209.0	
9.0	14.9	208.0	
10.0			

No PO4 (NO2)			
Time	NO ₂ -N	COD	PO ₄ -P
[h]	[mg N/dm ³]	[mg COD/d m ³]	[mg P/dm ³]
0.0		92.6	2.5
0.3		65.6	17.0
0.7		45.4	23.1
1.0		37.9	24.8
1.5		35.0	24.6
2.0		30.1	24.2
2.5	18.9	27.4	24.2
2.8	18.6	72.9	
3.0	18.2	88.3	
3.3		126.0	
3.5			
4.0	17.2	153.0	
4.5			
5.0	19.3		
5.5		170.0	
6.0	20.3	229.0	
6.5	19.1	229.0	
7.0	21.3	231.0	
8.0	19.5	245.0	
9.0	18.0	250.0	

b) **Scenario 2.3:** PHA depleted tests with nitrate (Reactor 1) and nitrite (Reactor 2)

(Series II, ST2, scenario 2.3)

No -PHA NO3			
Time	NO ₃ -N	COD	PO ₄ -P
[h]	[mg N/dm ³]	[mg COD/d m ³]	[mg P/dm ³]
0.0		92.6	2.5
0.3		65.6	17.0
0.7		45.4	23.1
1.0		37.9	24.8
1.5		35.0	24.6
2.0		30.1	24.2
2.5	18.2	27.4	24.2
2.8	17.8	102.0	
3.0	18.6	114.0	
3.3			
3.5			
4.0	17.6	127.0	
4.5			
5.0	17.2	146.0	
5.5		148.0	
6.0	16.4	207.0	
6.5	16.5	206.6	
7.0	15.6	208.0	
8.0	15.6	190.0	
9.0	15.3	176.0	
	14.3		

No -PHA NO ₂ (NO ₂)			
Time	NO ₂ -N	COD	PO ₄ -P
[h]	[mg N/dm ³]	[mg COD/d m ³]	[mg P/dm ³]
0.0		92.6	2.5
0.3		65.6	17.0
0.7		45.4	23.1
1.0		37.9	24.8
1.5		35.0	24.6
2.0		30.1	24.2
2.5	18.2	27.4	24.2
2.8	18.2	128.0	
3.0	19.5	135.0	
3.3		153.0	
3.5			
4.0	17.0	161.0	
4.5			
5.0	17.8		
5.5		175.0	
6.0	17.2	230.0	
6.5	16.3	229.0	
7.0	15.8	226.0	
8.0	16.2	228.0	
9.0	15.1	226.0	
10.0			